LATE GLACIAL PALAEOMAGNETIC SECULAR VARIATIONS FROM FRANCE

Graeme Smith

Doctor of Philosophy
University of Edinburgh
1985

ABSTRACT

The first part of this thesis describes the development of a control system for the departmental CCL cryogenic magnetometer using a Sirius microcomputer. This controls the operation of the magnetometer, the calculation of the remanent magnetisation and provides for the transfer of results directly to the mainframe computer. It allows the rapid, accurate measurement of up to 100 samples per hour and has been used extensively to measure not only lake sediment samples studied in this project but also the bulk of the palaeomagnetic measurements made within the department.

The main part of the project describes the measurement of the remanent magnetisation carried by sediment deposited in Lac du Bouchet, (Haute Loire), France. These were obtained using pneumatically operated corers (**Mackereth (1958)**) up to 12m long. The NRM records reveal secular variations of the declination, inclination and intensity of the geomagnetic field during the last 30,000 years and possibly up to 42,000 years ago.

The dating has been performed on samples taken from two of the cores. Conventional radiocarbon and palynological methods have been used on one set of samples and a new technique on the other. This technique is the use of an accelerator as a high energy mass spectrometer to count the number of radiocarbon atoms and hence determine the age.

Other pilot samples have been subjected to a variety of magnetic experiments. These have revealed that the NRM is remarkably stable and that the carrier is a coarse grained, (multi domain) magnetite with a small titanium impurity. Further experiments show that the grain size of the carrier remains uniform throughout the late glacial period.

A detailed series of spectral analyses have been performed upon a stack of the records from eight of the cores. These reveal that periods of 5,000, 3,300 and 2,000 years appear regularly, despite the apparent non-stationarity of the records. The relation between the sources of these variations and their resulting records are examined.

The variation of the relative intensity of the geomagnetic field during the late glacial has been estimated. This has been achieved by a normalisation using both ARM and SIRM and by a theoretical model. The results obtained that are estimated to extend back to 42,000 years ago fail to reveal a reversal in their inclination records despite Lac du Bouchet being less than 150 km from the sites for which the Laschamp and Olby events have been described.

ACKNOWLEDGEMENTS

I would like to thank my supervisor Prof. K.M. Creer for introducing me to the subject of palaeomagnetism of lake sediments and his help and guidance throughout the project. Alan Pike has provided most of the technical assistance in all aspects of coring and upkeep of the magnetometer. Without him the project would have been much more difficult and less enjoyable.

I am also grateful to Roy Thompson, Piotr Tucholka and Barbara Maher for many useful discussions and much advice.

Various people helped me with fieldwork. In particular N. Thouveny, E. Truze, R. Woods and A. Carruthers helped in France, as did E. Bonifay who also made me very welcome at the CNRS in Marseille.

Dr. R. E. M. Hedges made the HEMS measurements for which I am grateful and allowed me to prepare my samples at his laboratory.

I would also like to thank N. Stroud, M. Robinson and M. Brown of the ERCC advisory who have helped with computing problems and to K. Currie who provided an introduction to the UCSD operating system.

Finally I would like to thank my parents, grandparents and friends for all their help and encouragement.

CONTENTS

List of Abbreviations

ADC	analogue to digital converter
af	alternating field
AR	auto regressive
ARM	anhysteretic remanent magnetisation
α_{95}	alpha 95
bp	before present (radiocarbon years).
C(s)	graphite
C^{14}	radiocarbon
C_2H_2	acetylene
CCL	Cryogenic Consultants Limited
cm	centimetres
$CO_2(g)$	gaseous carbon dioxide
CVMSE	cross validation mean square error
D.C.	direct current
DFT	discrete Fourier transform
DRM	detrital remanent magnetisation
FFT	fast Fourier transform
g	grammes
H_{CR}	coercivity of remanence
HEMS	high energy mass spectrometer
H_{sat}	Field required to produce SIRM
IRM	isothermal remanent magnetisation
K-Ar	Potassium - Argon
Kbyte	1000 bytes
kyrs	1000 years
m	metres
mA	milliamperes
MD	multi domain
MDF	median destructive field
MEM	maximum entropy method
mg	milligrammes
mm	millimetres
M_{sat}	saturation remanence of magnetisation
mT	milliteslas
µm	microns
$N_2(l)$	liquid nitrogen
nA	nanoamperes
NRM	Natural remanent magnetisation
PDRM	post detrital remanent magnetisation
pef	prediction error filter
PSD	pseudo single domain
RD	radial dipole
r.f.	radio frequency
RM	remanent magnetisation
S_{100}	magnetisation when back IRM field = 100 mT
SD	single domain
SIRM	Saturated isothermal remanent magnetisation
SQUID	Superconducting Quantum Interference Device
SV	secular variation
TL	thermoluminescence
TRM	thermoremanent magnetisation
VGP	virtual geomagnetic pole
UCSD(-P)	University of California; San Diego (Pascal)

List of tables

Table 6.1 The main periods obtained from an examination of the correlation functions. The minus sign indicates that the correlation is negative; the order given is the order of relative strengths of the correlations.

Table 6.2a The main periods obtained from an examination of the Fourier transform spectra for the merged stack. Note that periods found in the spectra of the same order as the length of the data set have been ignored.

Table 6.2b The main periods obtained from an examination of the Fourier transform spectra for the Gaussian stack. Note that periods found in the spectra of the same order as the length of the data set have been ignored.

Table 6.3 The main periods found from an examination of the MEM spectra for the two stacks.

Table 6.4 The main periods found from a complex MEM analysis of the two stacks.

Table 8.1 The variation of the MDF and α_{95} down core B63 from an analysis of pilots taken at different depths.

Table 8.2 The main periods obtained from a Fourier spectral analysis of the merged stack.

Table 8.3 The main periods obtained from a MEM spectral analysis of the merged stack.

Table 8.4 Palaeomagnetic excursions that have been reported for the last 50,000 years.

Table 8.5 The different ages that have been obtained for the Laschamp and Olby reversals.

Table 8.6 The averages of the ages obtained for the Laschamp and Olby flows by different methods indicating that they are not contemporaneous and that the 'event' must therefore last at least 4,000 years.

List of figures

that the units for the intensity and the Q ratio scales are mA m^{-1}.

Figure 3.2 The records for the eight cores described in the text in (a) declination, (b) inclination, (c) intensity (mA m^{-1}) and (d) susceptibility. Each core is presented on its own depth scale.

Figure 3.3 The records for the eight minicores described in the text in (a) declination, (b) inclination, (c) intensity (mA m^{-1}) and (d) susceptibility. Each core is presented on its own depth scale.

Figure 3.4 The NRM records for core B49 after af demagnetisation in a peak field of 10mT showing the variations in declination, inclination, intensity (mA m^{-1}), susceptibility and Q ratio.

Figure 3.5 The B49 depth transform functions for the long cores.

Figure 3.6 The records for the eight cores described in the text in (a) declination, (b) inclination, (c) intensity (mA m^{-1}) and (d) susceptibility after transformation to the B49 depth scale.

Figure 3.7 The records for the eight minicores described in the text in (a) declination, (b) inclination, (c) intensity (mA m^{-1}) and (d) susceptibility after transformation to the B49 depth scale.

Figure 4.1 The step af demagnetisation of six typical pilots from core B49 showing (a) the normalised Zijderveldt plot, (b) the variation of normalised NRM intensity and (c) the stereographic projection for each of the pilots.

Figure 4.2 The step demagnetisation of the SIRM given to six typical pilots down core B49; the intensity has been normalised.

Figure 4.3 The step demagnetisation of the ARM acquired in five different peak fields for the six typical pilots from core B49.

Figure 4.4 The variation of the MDF found during demagnetisation of the NRM, the SIRM and five different ARMs for the six typical pilots from core B49.

Figure 4.5 A direct comparison of the step demagnetisations of the NRM, the SIRM and three of the ARMs given to the six typical pilots from core B49.

Figure 4.6 A least squares comparison of the step demagnetisations of the NRM, the SIRM and three of the ARMs given to the six typical pilots from core B49.

Figure 4.7 The growth of IRM and back IRM for the six typical pilots taken from core B49.

Figure 4.8 The incremental coercivity spectra for the six typical pilots taken from core B49 during the growth of IRM.

Figure 4.9 The remanent hysteresis loop found for two samples from core B49.

Figure 4.10 The incremental coercivity spectra for the six typical pilots taken from core B49 during the growth of ARM.

Figure 4.11 The variation of saturation magnetisation with temperature for a typical pilot sample taken from core B49 from the translation balance, showing the slightly different results for the raw sediment to the magnetic extract.

Figure 4.12 (a) A photograph of a part of the magnetic extract taken from pilot S121 showing the variation in the grain sizes and (b) the five grains and the assemblage that have been subjected to an EDAX analysis.

Figure 4.13 The EDAX spectra for the grains shown in figure 12b.

Figure 4.14 The EDAX spectra for three grains taken from assemblage 6 in figure 12b.

Figure 4.15 Grain size spectra for (a,b) low intensity samples, (c,d) average intensity samples and (e,f) high intensity samples.

Figure 5.1 Schematic diagram of the beam handling arrangement for the Oxford High Energy Mass Spectrometer. (after **Hedges (1981)**).

Figure 5.2 The graphite preparation rig for the Oxford high energy mass spectrometer. (after **Wand et al (1984)**).

Figure 5.3 The depth time transform function defined by the ages obtained from the dating of core B49 using the Oxford high energy mass spectrometer.

Figure 5.4 The palynological and radiocarbon dates obtained for samples taken

from core B5 after adjustment to a B49 depth scale.

Figure 5.5 The dates available from the cores from Lac du Bouchet that have been used to define the depth time transform function.

Figure 5.6a The declination records for eight cores taken from Lac du Bouchet after transformation to the time domain.

Figure 5.6b The inclination records for eight cores taken from Lac du Bouchet after transformation to the time domain.

Figure 5.6c The intensity records for eight cores taken from Lac du Bouchet after transformation to the time domain.

Figure 5.7 A comparison of the Lac du Bouchet records with the U.K. records defined by **Turner and Thompson (1981).**

Figure 5.8 A comparison of the Lac du Bouchet records with the Black Sea records defined by **Creer et al (1974).**

Figure 6.1a The merged records of eight of the cores taken from Lac du Bouchet with the errors calculated by averaging over a period of 15 years.

Figure 6.1b The merged records of eight of the cores taken from Lac du Bouchet after a 50 knot cubic spline smoothing.

Figure 6.1c The stacked records of eight of the cores taken from Lac du Bouchet with the errors calculated by averaging all the cores at each level.

Figure 6.2 The results for the CVSME analysis for the two stacks.

Figure 6.3 The secular variation records produced by (i) a radial dipole drifting westwards at a rate of one revolution every 5,000 years, (ii) a stationary radial dipole whose strength varies sinusoidally with a period of 2,000 years, and (iii) the combination of (i) and (ii). Each plot shows the effect of adding 10% random noise.

Figure 6.4 a) autocorrelation and b) cross correlation results for model (i) (see text).

Figure 6.4 a) autocorrelation and b) cross correlation results for model (ii) (see text).

Figure 6.5 The result of a) autocorrelation and b) cross correlation for the merged stack of eight Lac du Bouchet cores.

Figure 6.6 The Fourier transform spectra for model (i).

Figure 6.6 The Fourier transform spectra for model (ii).

Figure 6.7a The Fourier transform spectra for the merged stack.

Figure 6.7b The Fourier transform spectra for Gaussian stack.

Figure 6.8 The MEM spectra for the model (i) declinations showing the effect of varying the pef length.

Figure 6.8 The MEM spectra for the model (ii) declinations showing the effect of varying the pef length.

Figure 6.9 The MEM spectra for a pef length of 67 for a) the merged stack and b) the Gaussian stack.

Figure 6.10 The complex MEM spectra for model (i).

Figure 6.11 The complex MEM spectra for a) the merged stack and b) the Gaussian stack.

Figure 6.12 The VGP path of a) model (i) showing open clockwise looping, b) the stationary pulsing model showing a linear path and c) model (ii) which combines pulsing and drift and produces a 'petal' pattern. The latitude is 90° at the centre and marked in 10° increments.

Figure 6.13 The VGP paths for the 50 knot smoothed merged stack in 2,500 year increments. a) 12,500 - 10,000 years bp b) 15,000 - 12,500 years bp c) 17,500 - 15,000 years bp d) 20,000 - 17,500 years bp

Figure 6.13 The VGP paths for the 50 knot smoothed merged stack in 2,500 year increments. e) 22,500 - 20,000 years bp f) 25,000 - 22,500 years bp g) 27,500 - 25,000 years bp h) 30,000 - 27,500 years bp

Figure 6.14 The definition of the curvature angle A for the two VGP path points (x_t,y_t), (x_{t-1},Y_{t-1}) after (x_{t+1},y_{t+1}).

Figure 6.15 The curvature plot for the merged stack after smoothing using a 50 knot cubic spline.

Figure 6.16 The effects of smoothing on the curvature plot. a) Smoothing using a high pass Fourier filter with the low cut off frequency in cycles per 1000 years and b) smoothing using cubic splines with the number of knots as specified.

Figure 6.17 The curvature spectrum for the merged stack with a bandpass filter with a bandwidth of a) 1 years and b) 10 years.

Figure 6.18 The curvature spectra for a) Western Europe and b) North America for two bandwidths (1 and 10 years).

Figure 6.19 The possible period combinations that can be derived from a source that is drifting whilst changing in magnitude (at fixed rates). The periods are as defined in the text.

Figure 7.1 Variation of ARM with depth for five of the Lac du Bouchet cores.

Figure 7.2 Variation of SIRM with depth for five of the Lac du Bouchet cores.

Figure 7.3 Variation of susceptibility with depth for five of the Lac du Bouchet cores.

Figure 7.4 The ARM/susceptibility ratio for five cores taken from Lac du Bouchet.

Figure 7.5 The ARM/SIRM ratio for five cores taken from Lac du Bouchet.

Figure 7.6 The NRM after normalisation using a) ARM and b) SIRM.

Figure 7.7 The variation of intensity during the late glacial showing a) the NRM b) NRM/susceptibility, c) NRM/ARM and d) NRM/SIRM. All the variations have been produced using a merged stack.

Figure 7.8 The stacked intensity record after deconvolution of the exponential fixing function with half fixing times of 50, 100, 200, 500 and 1000 years.

Figure 8.1 The NRM records for core B64 showing the variations in declination, inclination and intensity (mA m^{-1}).

Figure 8.2 The step af demagnetisation of two samples from core B64 showing a) the Zijderveldt diagram, b) the step demagnetisation plot and c) the stereographic projection.

Figure 8.3 A comparison of the long core records in a) declination and b) inclination.

Figure 8.3 A comparison of the long core records in c) intensity and d) susceptibility.

Figure 8.4 The Fourier transform spectra for the merged stack.

Figure 8.5 The MEM spectra for a pef length of 90 for the merged stack.

Figure 8.6 The VGP paths for the 50 knot smoothed merged stack in 3,000 year increments. a) 33,000 - 30,000 years bp b) 36,000 - 33,000 years bp c) 39,000 - 36,000 years bp d) 42,000 - 39,000 years bp.

Figure 8.7 The variation of a) ARM and b) SIRM for the three long cores.

Figure 8.8 The NRM for the long cores after normalisation using a) ARM and b) SIRM.

Figure A1.1 A schematic diagram of the Mackereth pneumatic corer.

Figure A1.2 A schematic diagram of the new main piston for the Mackereth corer which incorporates both the piston and the fixing of the core tube.

Figure A1.3 The collar for the lower end of the core tube which forces the sediment slightly away from the walls of the tube, improving recovery.

Figure A2.1 The hydraulic pump system for subsampling the minicores.

Figure A4.1 The response of the exponential fixing function in the frequency domain. As T decreases the amplification decreases and the phase increases.

CHAPTER 1
THE APPLICATION OF MICROCOMPUTER CONTROL TO NRM MEASUREMENTS

1.1 Introduction

The subject of palaeomagnetism has mushroomed since the development of magnetometers capable of accurately measuring the magnetisation of samples in a short time. The astatic instruments, although very accurate, required a great deal of time to make measurements but have the advantage of being simple to operate and maintain. Fluxgate magnetometers, less sensitive than the astatic systems allow much more rapid measurement of samples, most commonly in the form of a spinner magnetometer. (e.g. **Molyneux (1971)**). These are more complicated to operate but for relatively strong samples are excellent for rapid, accurate measurements.

More recently the cryogenic magnetometer has been developed (**Goree and Fuller (1976)**). This is much more complicated to operate but has the advantage of being capable of accurately measuring very weak samples. The cryogenic magnetometer is also potentially capable of very rapid measurement. This requires that most of the operation of the magnetometer is under computer control.

Described below is the program developed to control the Edinburgh University cryogenic magnetometer using a Sirius microcomputer. This has been written so that all sample positioning and measurement is performed by the computer, the results being written to a floppy disc for subsequent transfer to the University mainframe computer. The program has been designed to be "user friendly", that is, to be easily operated by any new user. This involves the extensive use of detailed screen prompts and help information incorporated into the program.

There follows a brief description of reasons why it was deemed necessary to use a microcomputer to perform these tasks, descriptions of the Sirius microcomputer and the operating system used, the Cryogenic Consultants Ltd. (CCL) cryogenic magnetometer and the program itself. A full listing of the program is given in appendix 5.

1.1.1 Instrument Control

A microcomputer can be used to control or to monitor the output from a range of instruments. It can provide speed, accuracy (in both calculation and sample orientation) and reliability. An 8 bit Digital M16E microcomputer had been used to control the measurement of the magnetisation of samples by the cryogenic magnetometer. It was felt however, that a number of benefits could be gained by changing the controlling microcomputer. These include

(i) the ease of loading the program (this used to be achieved by using paper tape).

(ii) The ability to output results to a floppy disc which can be transferred directly to the mainframe computer. (Results used to be output to paper tape that had to be read by computing staff).

(iii) The generation of a program that is straightforward to use. This means that commands should be succinct and easily remembered (not involving strings of escape sequences) and the text of the program should be readily understandable. (The original program was written in assembler).

(iv) The chance to improve the facilities offered by the controlling program to make the operation of the magnetometer possible in a wider range of circumstances and with a wider range of samples. This involves programming alternative calculation sequences for when only one SQUID is functioning and including methods of improving the signal to noise ratio.

The Sirius microcomputer was chosen for two reasons; it was supported by the University and it could also provide a powerful range of facilities at a reasonable cost.

1.1.2 The Sirius microcomputer

The departmental Sirius microcomputer, manufactured by ACT computers Ltd., is a 16 bit, 128 Kbyte (RAM) microcomputer with twin $5^1/_4$ inch, 512 Kbyte floppy disc drives. It has excellent communications facilities incorporating two RS232C compatible serial communication ports and one IEEE488 compatible, "Centronics" parallel port.

There is only a small amount of ROM in the Sirius. The operating system is loaded from disc after switching on. This means that any operating system can be used allowing a great versatility. Despite the availability of many BASIC operating systems Edinburgh Regional computing centre has supported the development of the UCSD-P operating system, this system was chosen for the work described here.

1.1.3 The UCSD-P Operating System

This operating system was written at the University of California in San Diego in the Pascal language. The design of the system is based on the premise of portability. This is so that programs written and compiled on one machine can be run on any machine under the same operating system. In order to do this programs are not compiled to the host machine language but to a "pseudo"-machine language - the "P-code" - which is then interpreted by the host machine at run time. The programs therefore take slightly longer to run but the advantage is that they can be used on many different computers.

A full range of languages are supported by the UCSD-P system but as the system itself is written in Pascal this offers the fastest programs and the widest range of accessible facilities. Another advantage of the Pascal language is that it is very easy to read (making debugging more straightforward) and this was the language chosen in which to write the magnetometer control program.

1.1.4 The Analogue 1208 A-D converter

A drawback of the Sirius is that it does not have an inbuilt analogue to digital converter (ADC). In order to access the output from the magnetometer it

was necessary to interface an ADC with the Sirius. The Analogue 1208 is a multichannel converter manufactured by EDC Photonic Ltd. and provides either a 16 channel single end multiplexed facility or an 8 channel differential multiplexor which has the advantage of eliminating ground loops. The conversion time is very small being between 20 and 40 µsecs and there are 4 different range scales of plus or minus 5V, 0.5V, 50mV and 5mV. In the work described here it is used in the eight channel mode, with the program controlling the range automatically.

The ADC is controlled by the program. This can be achieved either at the high level of the Pascal program or by using the Sirius assembler language. As the assembler language provides much more rapid access this method was chosen. Many more conversions can thus be performed in a given length of time allowing a larger "window" of the output to be averaged (and hence increasing the accuracy of the result).

1.2 The cryogenic magnetometer

1.2.1 Description

The CCL magnetometer used in this work is shown schematically in **figure 1.1**. Since the operation of the sensors requires a superconducting environment the magnetometer requires substantial heat shielding. This is achieved using radiation shields and vaccua. One vaccuum separates the liquid helium chamber from the insert cavity and another protects the liquid nitrogen dewar from both the helium chamber and the outside. The pick up coils and the SQUID sensors (see next section) are submerged in liquid helium to provide the superconducting environment. The original magnetometer was 3 component (3 pick up coils and 3 SQUIDs). As these SQUIDs failed two new SQUIDs have been purchased resulting in a 2 component magnetometer however, the program has been written so that it is easily adapted to allow for a third SQUID.

1.2.2 Principle of Operation

The operation of the magnetometer is based upon the properties of a superconducting ring. The current induced within this ring by the magnetic field of a sample is measured using Superconducting QUantum Interference Devices.

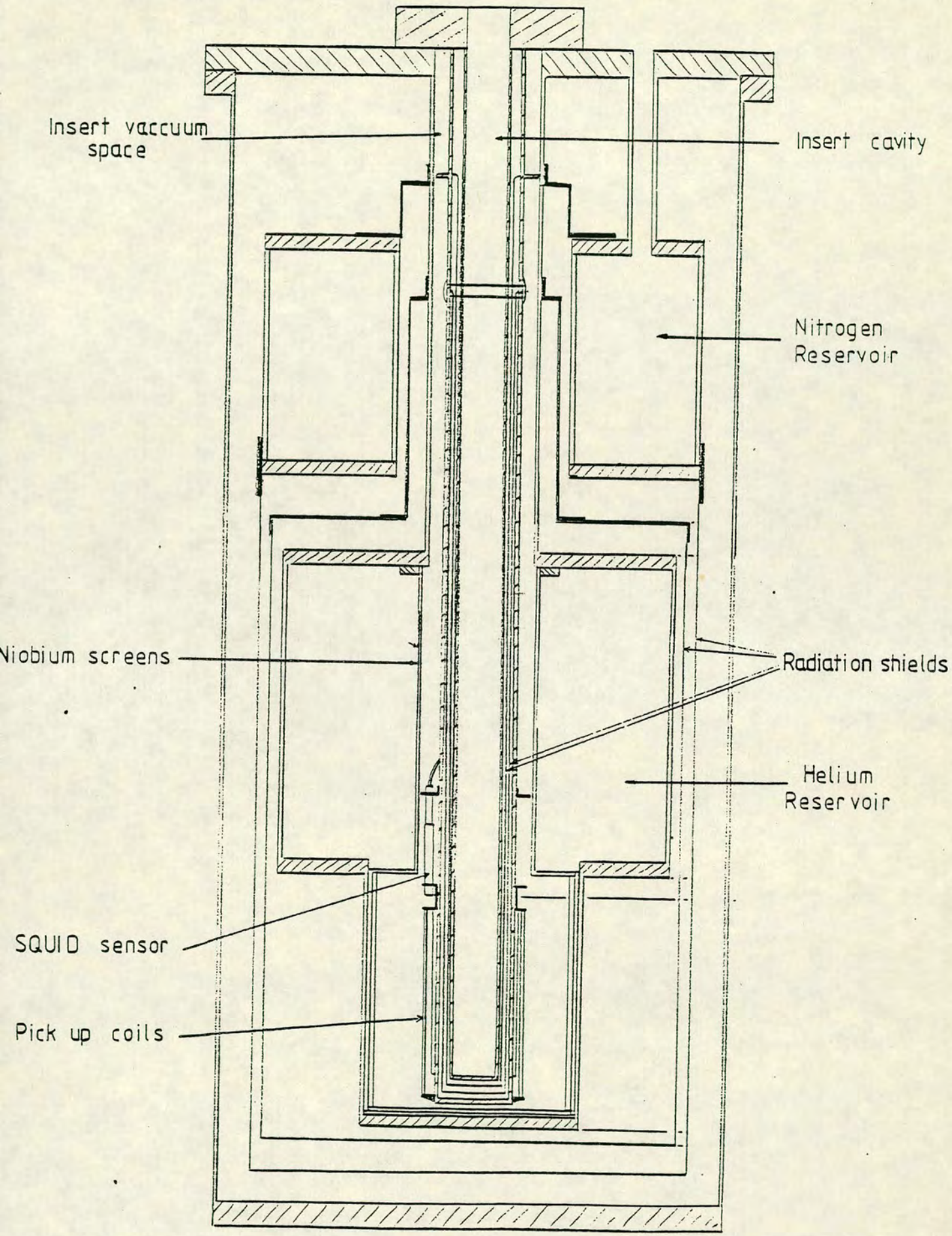

Figure 1.1 A schematic diagram of the CCL cryogenic magnetometer.

Any magnetic flux within a body when it falls below the critical temperature (T_c) for superconductivity will be expelled by the action of the "Cooper pairs" of electrons (**Bardeen, Cooper & Schreiffer (1957)**) which constitute the superconducting "particle". (The superconducting state is such that if there is an energy level with a wavenumber σ and spin 1/2 that is occupied then the level with wavenumber $-\sigma$ and spin $-1/2$ is also occupied, the pair then being superimposed in phase).

If the body is a ring then although the magnetic field within the body is expelled, the flux threading the hole is trapped. This occurs due to the action of the persistent supercurrent (I) that flows through the ring as long as the field (B_e) is less than the critical field (B_c) that suppresses superconductivity in the ring. As the supercurrent is sustained by the quantised Cooper pairs it follows that the flux threading the ring (Φ_t) is also quantised (**Meissner and Ochsenfeld (1933)**); the basic quantity of flux being the flux quantum, Φ_o. That is

$$\Phi_t = n\Phi_o \qquad (1.1)$$

were, if h is Plancks constant and e, the charge of an electron

$$\Phi_o = {}^{h}/_{2e} = 2.07 \times 10^{-15}\ \text{Wb} \qquad (1.2)$$

If B_e changes then the supercurrent changes to exactly match the change in flux, until a critical current (I_c) is reached. (where $B_e' = B_c$). At this point the supercurrent is suppressed and the ring becomes resistive. Up to the point where the ring becomes resistive the supercurrent provides a measure of the flux through the hole. In order to measure the flux the size of the current must be evaluated.

To interrogate the current a "weak link" (**Josephson (1962)**) is built into the ring. This is a point contact with an area of about $1nm^2$. The critical current of the ring will now depend upon the critical current through the point contact and this is designed to be of the order of Φ_o.

The SQUID consists of a loop with such a junction with a geometry which determines the self-inductance and capacitance. The loop is loosely coupled inductively with a tuned circuit with a very high Q factor. The tuned circuit is driven at its resonant frequency and the voltage across it (10-100μV) is amplified and detected (**figure 1.2**). The response of the tuned circuit is stepwise (**figure 1.3a**). The initial rise is determined by the tuned circuit

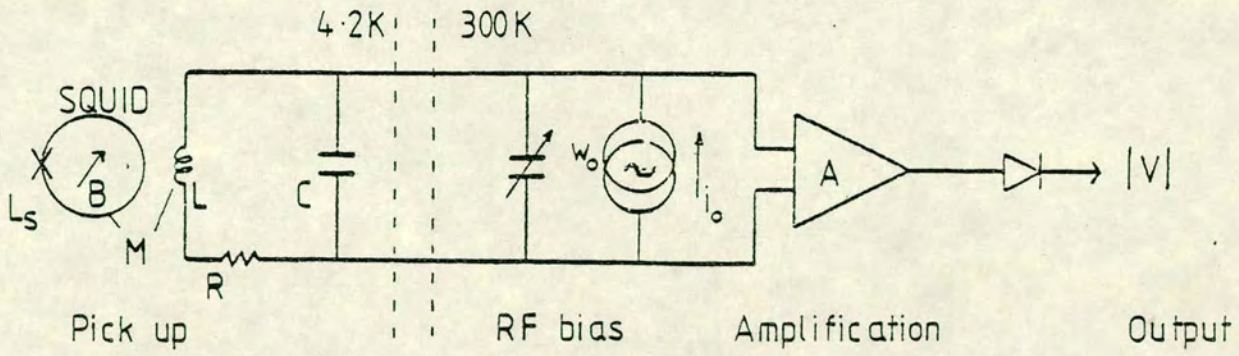

Figure 1.2 A schematic diagram of the CCL r.f. biased SQUID circuit.

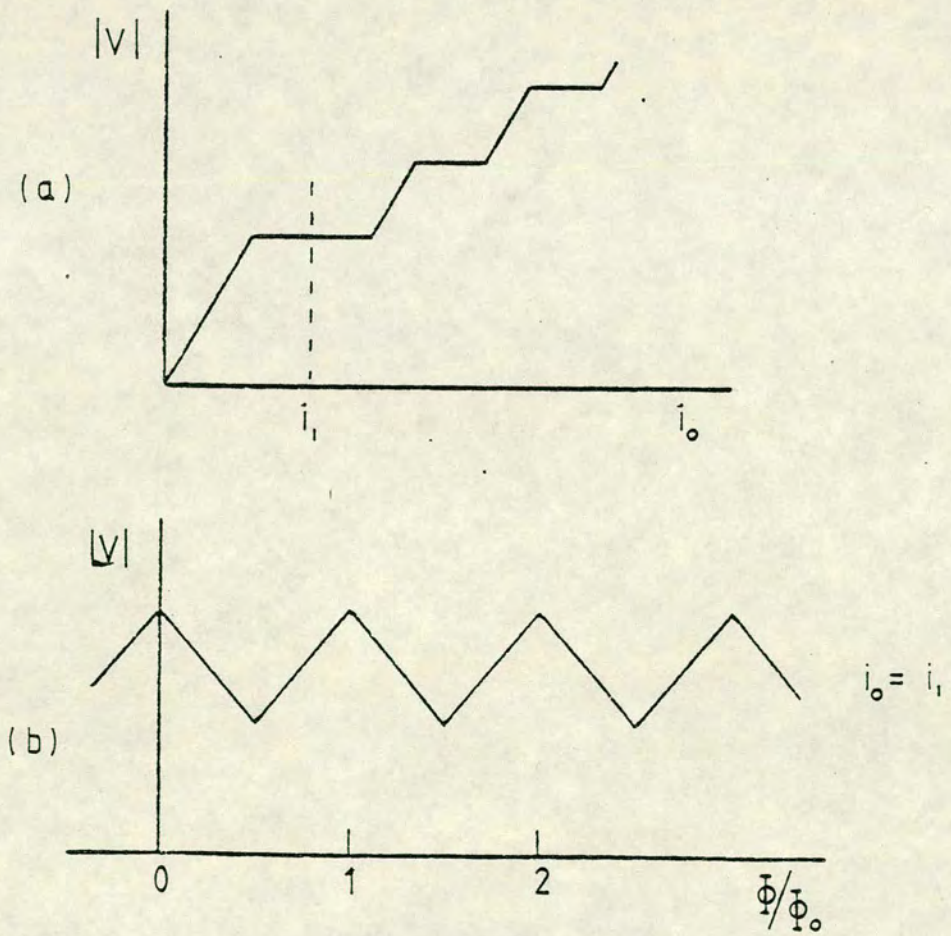

Figure 1.3 The idealised response characteristics of a typical r.f. detection circuit. (a) The stepwise voltage response with increasing current. (b) The detected output from the SQUID sensor.

impedance with the first step occuring when, during one cycle of the driving frequency the supercurrent in the loop just reaches its critical value, twice. This causes a loss of energy from the tuned circuit reducing the voltage. A relaxation oscillation process results, as, a few cycles later the voltage recovers and again transitions occur. Increasing the frequency, the voltage moves along the step and the probability of a transition increases from 0 to 1. As the frequency increases after the probability of a transition reaches 1 the voltage in the tuned circuit increases again (with one transition each cycle) until the point is reached where it is possible for there to be two transitions in each cycle and the second step is reached.

If there is an external field threading the loop then the combined effect is to cause the onset of transitions to shift. This will cause a change in the height of a step. The external field can also be varied by passing a d.c or low frequency current through the tuned circuit. The detected output (**figure 1.3b**) will be triangular, the period corresponding to a change of Φ_o and the amplitude to the r.f excitation level of the tuned circuit. By the means of a feedback circuit the flux in the SQUID is held at a fixed level then, the external field is matched by the d.c. field (c.f. a null detector) and the current required to keep the flux constant is an accurate measure of the external flux. (to a precision of the order $10^{-3}\Phi_o$).

The detected current is amplified and output as a voltage which can be measured by the ADC and input to the microcomputer.

1.3 Requirements of the Magnetometer Control Program

The previous section has outlined how the SQUIDs of the cryogenic magnetometer will produce an output voltage which is proportional to the change in the field at the pick up coil caused by the insertion of the sample. The control program needs, therefore, to be able to accurately locate the sample in the pick up coils and then measure the output voltage produced. From a knowledge of the sensitivity of the SQUIDs, the program should be able to convert the voltage to a magnetic moment and, by allowing for the volume, to a magnetisation.

As the magnetometer has two SQUID sensors it will be possible to obtain a value for the total remanent magnetisation of the sample from a single insertion into the pick up coil if the sample is rotated through an angle of 90°. The

minimum requirements for the control program therefore are

(i) Location of the sample in the pick up coils

(ii) Measurement of the output voltage

(iii) Rotation of the sample and remeasurement

(iv) Calculation and output of the sample magnetisation.

In order to be worthwhile the program must also locate the sample for removal or reorientation, check that the SQUIDs have remained at the flux position at which they started ("flux locked") and store the result.

1.4 The program CONTROL

A listing of the major structure of the program is given in appendix 5. CONTROL has been written predominantly in UCSD Pascal except for short sections to read the ADC and to affect positional changes of the carriage system which have been written in UCSD 8086 assembler. The cryogenic magnetometer should be cooled and then the components connected up as shown in **figure 1.4**. The location of the sample is then controlled by the CCL sample handler.

1.4.1 Carriage Control

The sample handler operates in two modes "local" and "remote". The local mode allows the user to define the positions for sample insertion, sample measurement and a position between the two (termed "background") where the background value of the flux within the SQUIDs can be determined. In addition all movement of the carriage system can be operated in this mode. In remote mode the sample handler is operated by signals input to the 25-way connector at the rear. Signals are generated by the assembler subroutine MOVE. This addresses the peripheral interface adaptor, the chip controlling the parallel port of the Sirius, and sends an integer to the output port. The signal is about +5 volts for a one and less than 0 volts for a zero; their combination making up a binary number. The actual integer required obviously depends upon the wiring between the parallel port and the sample handler. **Table 1.1a** illustrates the

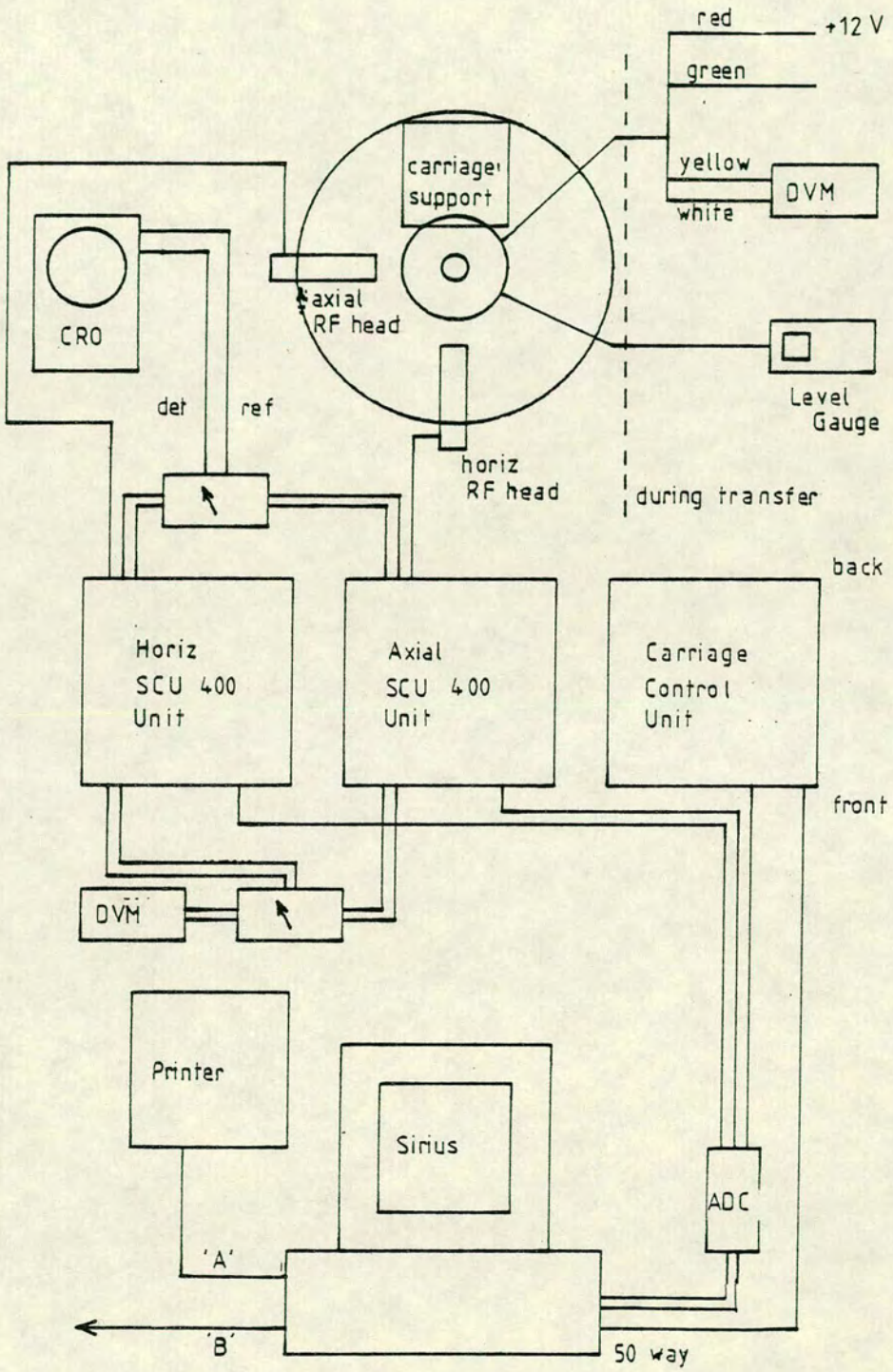

Figure 1.4 A schematic diagram of the wiring required for the CCL cryogenic magnetometer under the control of the Sirius microcomputer.

wiring used and **table 1.1b** gives the integers, their binary values and their effect on the carriage mechanism.

Whilst the sample is in motion, pin 14 of the 25-way connector on the sample handler is set to a positive voltage. On completion of the movement the signal drops negative. This is monitored using channel 0 of the ADC in the subroutine HIGH TO LOW.

1.4.2 The measurement sequence

The sample is inserted and the program starts to make a measurement by the following sequence

(i) Move sample to background position. Measure field. (X_{b1},Z_{b1}).

(ii) Move to measure position. Rotate to 270° and measure. (X_{270},Z_{270})

(iii) Rotate to 0° and measure. (X_0,Z_0)

(iv) Rotate to 90° and measure. (X_{90},Z_{90})

(v) Rotate to 180° and measure. (X_{180},Z_{180})

(vi) Return to background and rotate to 0°. (X_{b2},Z_{b2})

(vii) Return sample to insert position.

The program performs these movements using MOVE as outlined in section 1.4.1. The SQUID output is monitored using channels 3 and 7 of the ADC and the assembler subroutine GET READING. For each measurement a user controlled number of conversions are performed and averaged on each channel. This is achieved by using two "words" (i.e. 4 bytes) for each sum of the conversions performed. As the Sirius is a 16-bit (i.e. 2 byte) machine this means that a 4 byte integer must be carefully controlled by the software using two variables instead of one. The first variable is used as a store for the sum of the conversions. When this becomes full (i.e. its value exceeds 32767) the second variable is incremented. Thus the second variable acts as a counter. It follows that when the two variables are passed back to the main program (on the stack) the average can be calculated by multiplying the counter by 32767

Table 1.1 The connections and communications to facilitate the control of the sample handling mechanism for the cryogenic magnetometer.

a) Connections for carriage controller

Sirius (parallel port)	Sample Handler (25 way connector)	Colour
2	22	Red
3	24	Brown
4	25	Blue
5	23	White
6	20	Yellow
7	21	Green
8	19	Orange
	14	ADC (channel 0)

b) Movement of carriage

Position	Decimal	Binary
		Pin 876 5432
Insert	8	0000 1000
Background	0	0000 0000
Measure 0	1	0000 0001
Measure 90	3	0000 0011
Measure 180	69	0100 0101
Measure 270	7	0000 0111

and adding the result to the other. The resulting number can then be divided by the number of conversions to give the digital representation of the input voltage. This method increases the accuracy of the measurement without sacrificing the amount of time taken. (The default value of 2048 conversions per channel takes less than 1.5 seconds).

The results of the measurements from the four rotated positions allow the average for three components of the magnetisation to be calculated. From the nomenclature above these are

$$Z = 0.25 \times (Z_{270} + Z_0 + Z_{90} + Z_{180}) \quad (1.3)$$

$$X = 0.5 \times (X_{180} - X_0) \quad (1.4)$$

$$Y = 0.5 \times (X_{270} - X_{90}) \quad (1.5)$$

These are calculated after the voltages have been converted to magnetisations within the subroutine CALC MAGNETIC VECTOR which proceeds to convert the cartesian values of the magnetisation to the more standard form of presentation namely declination, inclination and intensity.

1.4.3 Other facilities

Various extra routines have been provided to allow the user to improve the accuracy of a measurement, to increase the rate at which the measurements are made or to simplify the operation of the magnetometer.

1.4.3.1 Improving the accuracy of measurements

There are three ways of improving the accuracy of a measurement of the magnetisation

(i) Repeat the measurement in up to 6 different orientations. These are illustrated in **figure 1.5** for cubic samples and allow the program to compute the magnetisation after 2, 3, 4 or 6 reorientations.

(ii) Remove the holder magnetisation. This is particularly useful when the

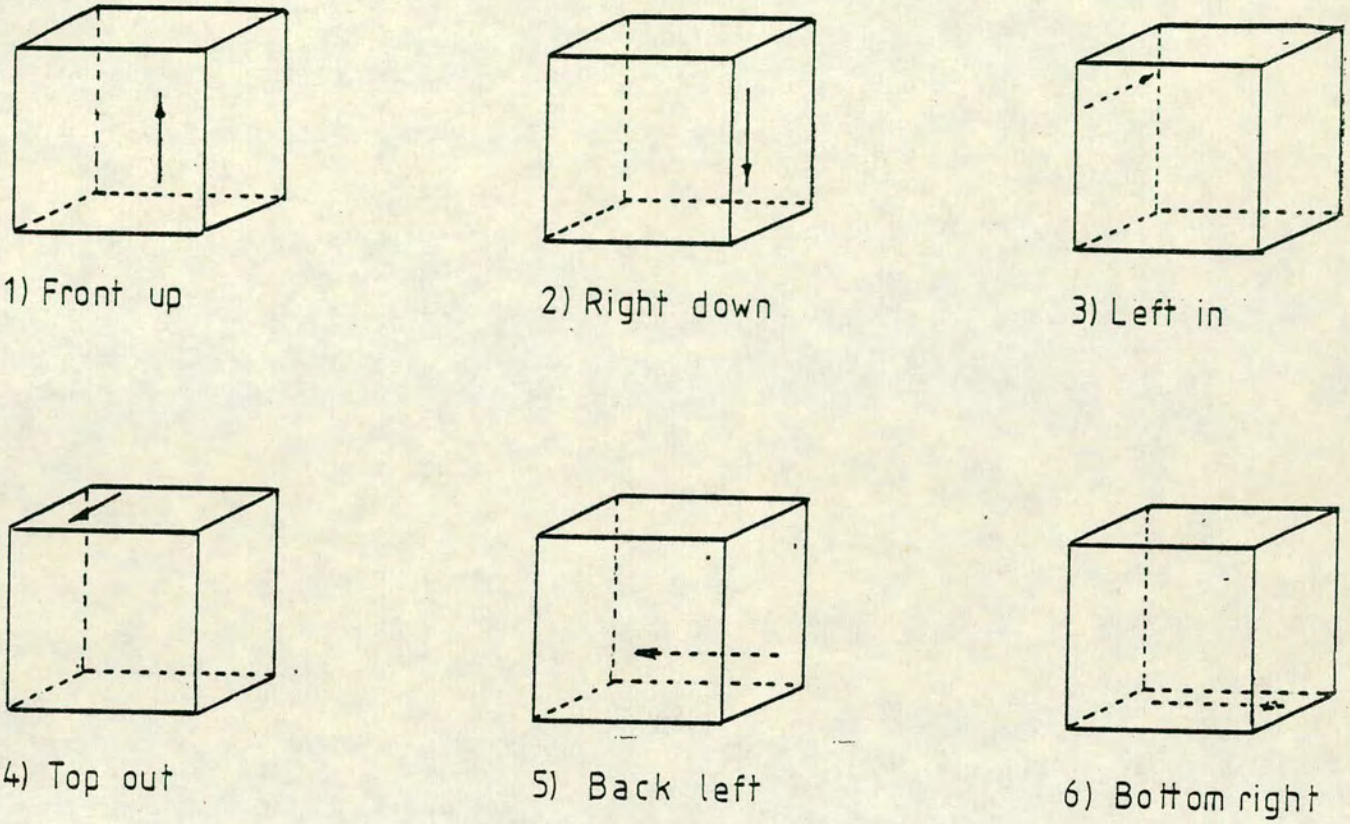

Figure 1.5 The orientation sequence used for cubes of sediment (the arrow points to the top of the core).

magnetisation of the sample is of the same order of magnitude as that of the holder and less than 6 measurements are being made.

(iii) Increase the number of ADC conversions made at each measure position. Although this increases the time taken for a measurement it reduces the measurement error of the output voltage. (Note that although the time taken from insertion to insertion changes from 21 seconds for 100 conversions to about 140 seconds for 10,000 conversions the accuracy of the result does not seem to be substantially increased after 5,000 conversions. The default value of 2048 is chosen to optimise the accuracy gained by a substantial number of conversions with the comparatively short time (29 seconds) taken to make the measurement.)

1.4.3.2 Simplifying the use of the program

The following facilities simplify the use of the program and speed up the rate of measurement.

(i) All commands are called by single keystrokes. If the user presses a key that is incorrect a "beep" sounds. Any user input of real or integer numbers is monitored by the procedures READ REAL and READ INT in the GENERAL unit. These will not accept the input value unless the number is a true integer or real number. This means that the user cannot inadvertently crash the program by mistyping their input.

(ii) All prompts are as detailed as possible.

(iii) "Function" keys are labelled using the non scrolling 25th line of the screen to help the user locate frequently used commands.

(iv) There are two levels of help information. One provides a command summary (see **table 1.2**) and the other provides a detailed account of the commands available. (Procedure HELP in the GENERAL unit).

(v) Measurements can be repeated in three ways; same sample, same orientation; same sample, a previous orientation and a previous sample. (Procedure REPEAT MEASUREMENTS).

(vi) The results can be output with or without a hard copy on the printer and

Table 1.2 A summary of the single key commands available for the operation of the CONTROL program for the cryogenic magnetometer.

Prompt	Reply	Result
Go?:	'A'	: switch Autoname on or off
	'B'	: switch result Bell on or off
	'C'	: Calculate magnetic vector (=2 measurements)
	'D'	: switch printer on/off for harDcopy
	'E'	: print Extra values - cartesian components (N,E,Z)
	'F'	: change output File name
	'G'	: change amplifier or ADC Gain
	'H'	: get Help information
	'I'	: output useful program Information
	'K'	: user exchanged Kalibration of squids
	'L'	: print Last result
	'M'	: calculate holder Magnetisation
	'N'	: get new sample Name
	'P'	: Print result
	'Q'	: sQuid calibration with known sample
	'R'	: Repeat measurement
	'S'	: Squid down switch
	'V'	: change the sample Volume
	'W'	: shows What each key does - these pages (or '?')
	'X'	: eXchange the number of ADC reads per measurement
	'Z'	: switch off auto ranging gain
	' '	: start measurement (or <CR>)

with or without the north, east and down components. (Procedures PRINT RESULTS, LAST RESULTS and SAVE RESULTS).

(vii) An automatic naming facility allows the user to automatically increment the number of a name (made up of a prefix and a suffix surrounding a number) by a given amount. (Procedure SET AUTONAME).

(viii) The mainframe computer can be called from within the program and used independently or to transfer results stored on disc. (Procedure TTY in the XTALK unit).

(ix) There is a page of information accessible from the main command level to indicate the current state of the program parameters. (Procedure OUTPUT DATA).

(x) If one of the SQUIDs fails the output from that SQUID can be neglected and the magnetometer still used. Note that this necessitates more than one orientation per measurement. (Procedures SQUID FAILURE and CALC NEW VECTOR).

(xi) Calibration routines are provided to allow calibration of the SQUIDs with either a standard sample or a current in a coil. (Procedures SQUID CALIBRATION and SET UP CALS).

1.5 Operation

A full description of the operation of the CONTROL program and the magnetometer itself has been written for internal use. The magnetometer is calibrated before operation using a 10 turn coil wound on a permalloy former which is enclosed within a standard sample box. This has been found to give extremely consistent results and can be used to calibrate any of the three operating ranges of the magnetometer by changing the current within the coil. Standard samples of known magnetic moment are used for more frequent checks on instrumental drift and for obtaining the optimum measure position.

The program has been successfully used by several different people. The operation has been shown to be generally straightforward and easy to understand. Most of the results presented in the rest of this work have been obtained using the magnetometer under the control of this version of the

program.

Direct comparison with the original program is difficult. The most immediate advantage is the ability to transfer the results quickly and easily to the mainframe computer, the other advantages of speed, accuracy and simplicity will only become apparent as users get used to the operation and scope of the program.

The noise level is currently less than 10^{-11} A turns m^2. This is the noise level that remains when the empty sample holder is measured with the holder magnetisation being removed, (the sample holder itself has a moment of about 0.1 nA turns m^2), and making 2 measurements at 2048 conversions per channel. If more conversions are made the noise level is reduced very slightly but as mentioned above the measurement time increases.

T. M. M. Clube has measured particularly weak (chalk) samples from Cyprus and Turkey. These have magnetic moments of less than 10 nA m^2; some of less than 1 nA (of the same order as the sample holder). **Figure 1.6** shows the step alternating field demagnetisation of sample CYBM63A. The original moment of the sample was 2.74 nA turns m^2; equivalent to a magnetisation of 0.27 mA m^{-1} since the sample volume is approximately 10 cm^3. This has been reduced to a moment of 0.97 nA turns m^2 (0. 1 mA m^{-1}) after demagnetisation in a peak field of 60 mT. Despite these very small moments the diagrams clearly show that the remanent magnetisation direction can be easily found and shown to be the primary remanent direction.

Up to 100 measurements can now be made in an hour. The number of samples depends upon the number of orientations used. For symmetrical samples with a moment greater than about 500 nA turns m^2 a single measurement is sufficient. This measurement will be repeated to a 98% accuracy if the sample is remeasured. For weaker or asymmetrical samples at least two orientations will be required. In addition for very weak samples the output SQUID voltage should be amplified using the SCU 400 control units. (As long as the user tells the program that the gain has been changed - using the 'G'ain command - the units will be maintained).

The final test of the program is time. If it can cope with many different users measuring different types of samples then it performs its task. To date this has been achieved.

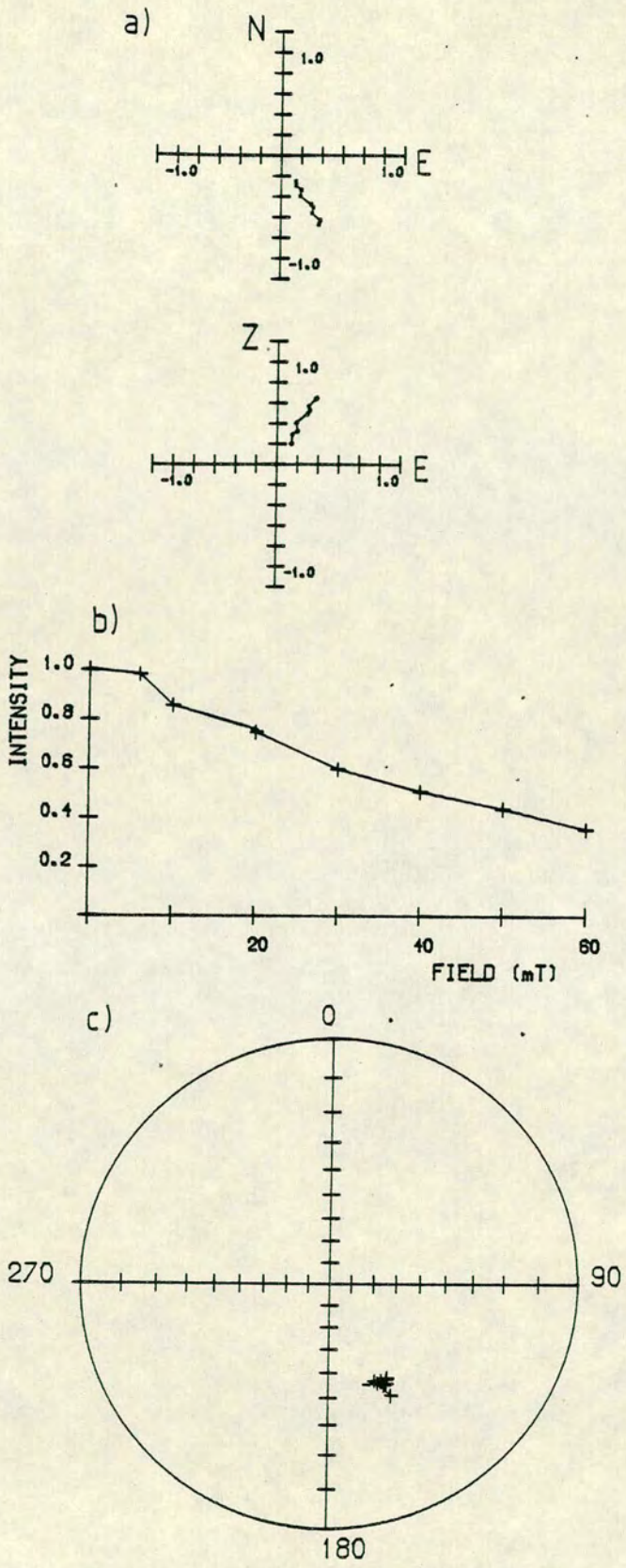

Figure 1.6 The demagnetisation of sample CYBM63A, a chalk from Cyprus. a) The Zijderveld plot, b) step demagnetisation of the normalised intensity and c) a stereographic projection of the declinations and inclinations. (See chapter 4 for more details of such plots).

CHAPTER 2
GEOMAGNETISM, LAKE SEDIMENTS AND LAC DU BOUCHET

2.1 The geomagnetic spectrum

That the earth acts as a magnet was probably known to the Chinese as early as the first century A.D. and natural magnets were known to the ancient Greeks. However, it was not until the end of the sixteenth century that Gilbert first compared the terrestrial magnetic field to that of a uniformly magnetised sphere in what is regarded as the first scientific treatise, 'De Magnete'. Since that time measurements have shown that instead of being a constant dipole field, (as would be expected for a uniformly magnetised sphere), the geomagnetic field is neither purely dipolar nor non-varying. **Gauss (1839)** showed, by a spherical harmonic analysis, that the geomagnetic field was essentially dipolar, time varying and could be analysed in terms of sources of internal and external origin. External effects can cause time variations of the field of a period less than a second and yet studies of deep sea sediments and lava flows have shown that the dipole aspect of the field is capable of reversing over periods of millions of years. It is apparent therefore that there is a large spectral content to the variations of the geomagnetic field.

Due, in part, to the different techniques that are available to measure the magnetic field of the earth, there has developed a gap in our knowledge of the geomagnetic spectrum. Observatory and maritime records have given information about the directional variations of the field, especially in Europe and around the coasts of the other continents, for, at most, the last 400 years. Variations with periods less than this length of time have therefore been subject to detailed study. The techniques of archaeomagnetism have extended this period to about 5,000 years before present (bp - 'present' is usually taken to be 1950 - all dates in this work will be in radiocarbon years). Palaeomagnetic studies on deep sea sediments in particular have given a quite detailed knowledge of the reversal spectrum (of periods of the order 10^4 to 10^7 years). The gap in our knowledge of the spectrum thus lies in the range of periods

between 10^3 and 10^4 years. The aim of this project is to add to the information available about the variations of the geomagnetic field at periods of this order.

2.2 Lake sediments as recorders of the geomagnetic field

The ability of rocks to acquire a remanent magnetisation in the direction of the ambient field at the time of cooling, for those containing a thermoremanent magnetisation (TRM), and at or soon after being deposited for those acquiring a detrital or post-detrital remanent magnetisation (DRM or PDRM), is now well established. It is the ability to determine the primary remanent direction of the rock upon which the subject of palaeomagnetism, the study of the prehistoric variations of the geomagnetic field, is founded.

Lake sediments were amongst the first rocks to be studied palaeomagnetically (**McNish and Johnson (1938), Johnson et al. (1948), Ising (1943), King (1955)**), but were found initially to be unreliable recorders of the ambient field at the time of deposition. The effect of 'bedding errors' (**King (1955), Rees (1965)**), caused by elongate particles and the effects of high energy depositional environments swamped the primary remanence. It required the demonstration by **Mackereth (1971)**, that the variation in declination (the angle between true north and the east vector of the recorded magnetic field), for sediments taken from Lake Windermere, could be correlated directly with observatory records for the last 400 years, to show the potential of sediments. His work was followed by other investigations in Britain (**Creer et al. (1972), Turner and Thompson (1979,1981)**), Europe (**Creer (1974), Thompson and Kelts (1974), Creer et al. (1979,1980,1981)**), North America (**Creer et al. (1976a,1976b), Dodson and Fuller (1977), Verosub (1977), Vitorello and Van der Voo (1977), Banerjee et al. (1979), Mothersill (1979,1981), Turner et al. (1982)**) and the rest of the world (**Barton and McElhinny (1981), Creer et al. (1983), Constable and McElhinny (1985)**). These have been reviewed most recently by **Creer (1985)**.

The results of these investigations reveal certain characteristic features of the geomagnetic field as recorded by lake sediments. Variations in the declination and inclination (the dip - the angle between the horizontal component and the total vector), show changes in direction of as much as 100° peak to peak in the former and 50° in the latter, although around 40° and 10-15° respectively seems to be more typical. These changes in direction have been shown to arise from the secular variation of the geomagnetic field, due to variations in both the dipole and non-dipole fields. Attempts have been made to

correlate these variations over large areas (**Creer and Tucholka (1982)**).

The sediments have also revealed changes in the recorded intensities and some attempts have been made to obtain relative palaeointensities from lake sediments. This is discussed in more detail in chapter 7. However, the nature of the sediment is very important and some general criteria have emerged about what makes a sediment 'reliable' for palaeomagnetic investigation.

2.2.1 Features required for a 'reliable' sediment

Early workers found difficulty obtaining the variations of the geomagnetic field from lake sediments, so that the plethora of results now being published indicates that some sediments are suitable for palaeomagnetic investigation whilst others are not. The major features required of a sediment before it can be accepted as accurately recording the geomagnetic field variations are summarized below.

(i) Grain size. **Tucker (1979,1980)** has shown that the distribution of grain sizes within a sediment affects its ability to record the direction of the ambient field. The important grains are those which carry the natural remanent magnetisation (NRM), which he found could be quite different in size from the general sediment matrix. In general, larger grains will give less reliable results (these will be moreoften irrecoverably affected by forces other than the magnetic field e.g. gravity, bioturbation). Smaller grains being able to reorient post-depositionally in the water filled interstices will give better results, but with a small 'phase' lag between the time of deposition and the field they record.

(ii) Grain shape. The shape of the grain will effect the non magnetic forces upon the grain during deposition. e.g. elongated grains will tend to align with their long axes horizontal irrespective of the ambient field direction. **(King (1955), Rees (1965))**.

(iii) Type of grains. The source of the sediment will affect the type of grains and hence, the proportion of magnetic grains to non magnetic grains. In general, igneous sources will tend to give a higher proportion of magnetic grains than a sediment source and thus a stronger signal.

(iv) Stability. There are two stability factors that are important. The carrier of

the NRM signal must be of a large enough size that the relaxation time of the grain is great enough for the NRM to be measured, (this is directly associated with the size of the grain - see chapter 4). Also, the environment in which the sediment is laid down must be stable. The more 'quiet' the environment the smaller the errors caused by realignments due to slumping, turbidity currents, inflow, exflow etc.

(v) Depositional rates. To be useful as a recorder of the geomagnetic field variations, the sediment must be continuously deposited (with no breaks). The rate of sedimentation must allow between 1,000 and 50,000 years of sediment to be accessible with relatively cheap, (and therefore simple), coring techniques.

(vi) Organic content. It has been found in this work, that the organic matter content of the sediment is inversely related to the NRM intensity. The 'ideal' organic content of a sediment in this work, to be useful for palaeomagnetic work is small, but sufficient for a reliable radiocarbon date to be made. This will be a content of about 8-15% for conventional techniques but could drop to less than 5% for the new accelerator techniques (see chapter 5).

The early workers tended to use sediments laid down in 'high energy' environments e.g. varves, which will give depositional alignment errors of the type proposed by **King (1955)**. More recent workers have been able to obtain more reliable records by using sediments that satisfy all or most of the criteria suggested above. The work described here is an account of results taken from Lac du Bouchet, a crater lake in France, whose properties have been found to satisfy the above criteria exceptionally well, especially for the period covering the late glacial in western Europe.

2.3 Lac du Bouchet

Lac du Bouchet is located in the Massif Central in the Haute Loire region of southern central France (Lat. 44° 57'N, long. 3° 47'E). It is situated about 16 km south west of the town of Le Puy in the crater of a strombolian type volcano. (**figures 2.1 and 2.2**). The volcano is part of the Quaternary sequence of eruptions that have characterised this region and which have resulted in the formation of a number of scoriacious (cinder) cones that typify the landscape of the area. Many of these craters have had lakes within them at some time, but

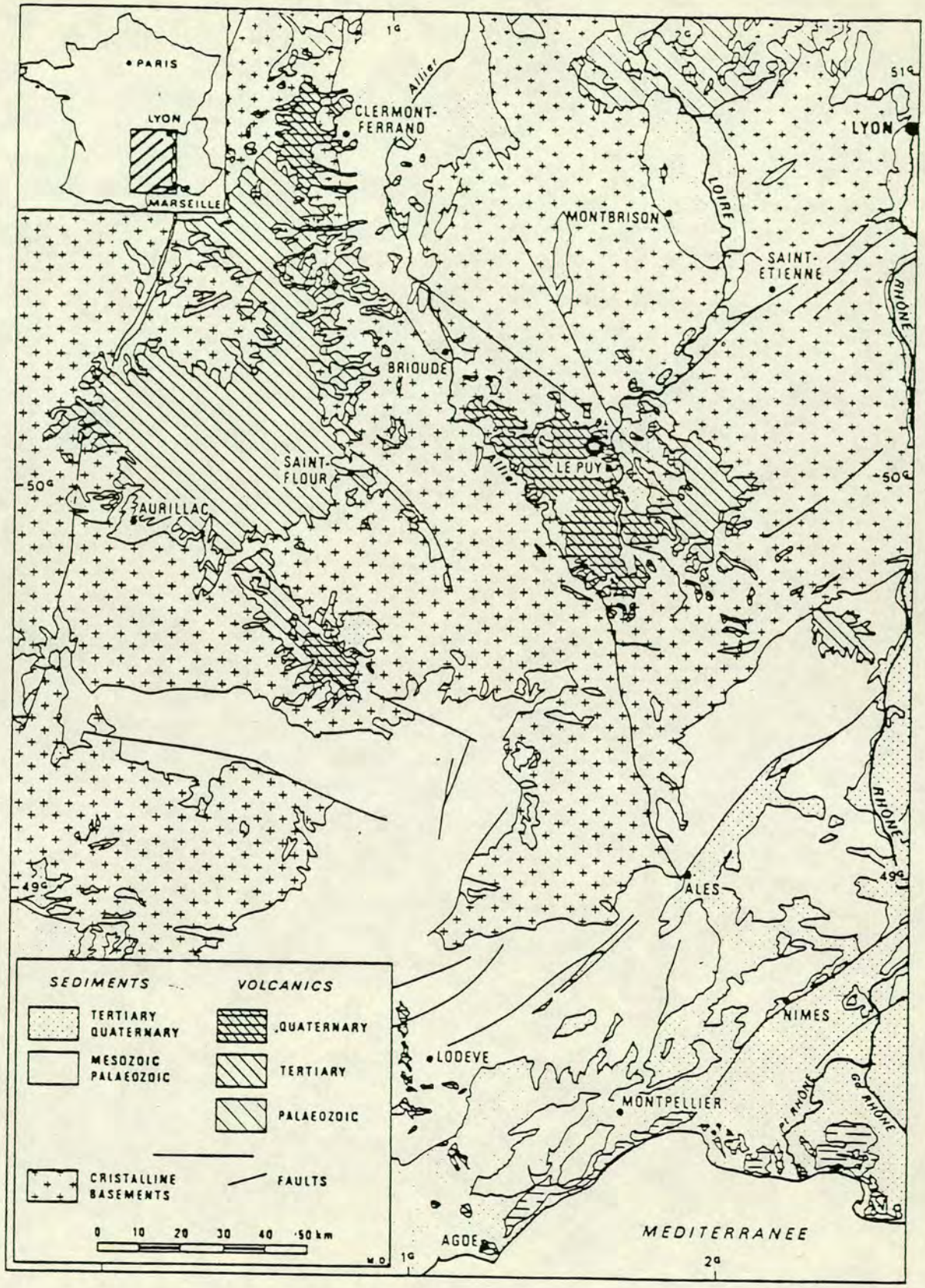

Figure 2.1 The location of Lac du Bouchet in the Massif Central region of France and the local geology.

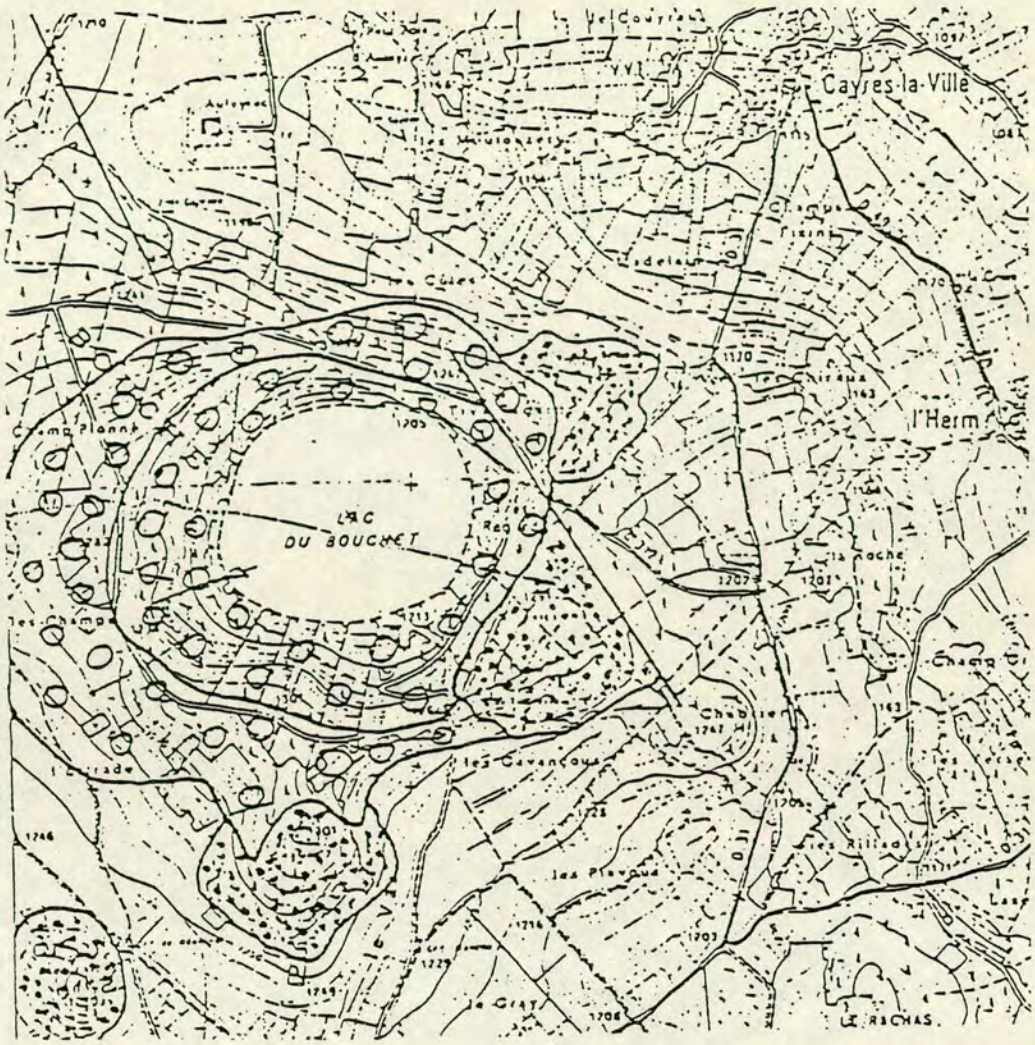

Explosion crater

fault

Strombolien (cinder) cone

Figure 2.2 Lac du Bouchet. Situated about 4 km southwest of the village of Cayres. Note the approximately circular shape of the lake, its crater and the associated cinder cones. The scale is 1:25,000.

the majority have already been infilled.

2.3.1 Description

The lake is almost perfectly circular with a diameter of about 800m. It lies at an altitude of 1206m in the crater of the volcano formed by a 'maar' type phreatomagmatic explosion (**Bout (1978), Truze (1983)**), almost a million years ago. Two K-Ar dates for the lava, taken from the side of the crater, reveal ages of 870,000 ± 60,000 years and 800,000 ± 40,000 years respectively (**Mitchell (pers. comm)**). A seismic survey of the lake (**Carruthers (1984)**) and measurements with a depth gauge, reveal that the lake has a narrow littoral prism of sediment, between 10-30m in width and about 3m depth, around the edge, which drops to a very flat bottom found to be between 25 and 27m in depth. The depth of water indicates that there must be a great thickness of sediment (about 50-60 m according to the reflection profile) and that the rate of deposition has been very slow (<0.1mm per year over the whole 800,000 year period).

The reason for the very slow depositional rate can be found by an inspection of the sides of the crater. There are no streams flowing either into or out of the lake indicating that the main mode of mass transport is by the wind and rain. The littoral prism is built up from the detritus washed down into the lake from the slopes of the crater. When the angle of the slope of the prism exceeds some critical angle a slump occurs, depositing the larger grained material near the edge of the lake and allowing the very fine grained material to be slowly deposited in the centre of the lake (**Bonifay and Truze (1984a,1984b)**). Examination of the sediments taken from the cores has revealed that the sedimentation has been essentially continuous and the rate has been low, especially during the Holocene period.

2.4 Coring campaigns

The sediment from Lac du Bouchet has been sampled in continuous sequences to successively greater depths, by means of a series of coring campaigns between April 1982 and April 1985. Details of the palaeomagnetic measurements made on these cores are given later. The corer used was an adaptation of the pneumatic piston corer designed for shallow lake sediments by **Mackereth (1958)** which is described in appendix 1.

2.5 The Lac du Bouchet sediments

Examination of the sedimentology of the Bouchet cores is described in detail by **Truze (1983)** and **Bonifay and Truze (1984)**, and was performed in Marseille. The different cores reveal a sequence of different lithologies of predominantly fine grained clays, silts and muds, resulting from the decantation process described above. (This is because most of the cores taken from Lac du Bouchet, and all those used for palaeomagnetism, were taken from the centre of the lake, well away from the edges of the littoral prism). The coarser fractions found in the cores were associated with the edges of the prism.

The stratigraphy for the top 9m of sediment, with which this project is predominantly associated, can be summarized into 6 main assemblages. These are described below in general terms, the detailed analysis being performed in France. **Figure 2.3** indicates the positions of the major assemblages in some typical cores; **figure 2.4** shows the variation in water content down one of these cores, B49. The positions of the boundaries vary from core to core but can be correlated and described.

2.5.1 Assemblage A

This is the uppermost organic gyttja layer containing the very wet sediment close to the sediment/water interface. It is generally about 1 - 2.5 m thick but has been found to be severely disturbed in some cores (due to the coring mechanism). The organic matter content is high (20-40%), which causes the very brown appearance of the sediment. The colour changes from a light reddish brown to a very dark brown from the top of the assemblage to the bottom. It has a gelatinous consistency (though the compaction reduces substantially towards the top), and there is a weak stratification with alternating light and dark bands. These bands are found to be of the order 2-8 cm in thickness and are assumed to be caused by varying amounts of organic matter. The dating (presented in chapter 5), reveals an estimated depositional rate of about 0.15mm per year.

2.5.2 Assemblage B

This layer is readily identifiable from core to core and varies appreciably in thickness. Some cores (e.g. B7, B12) have a very thin layer (around 5cm) and

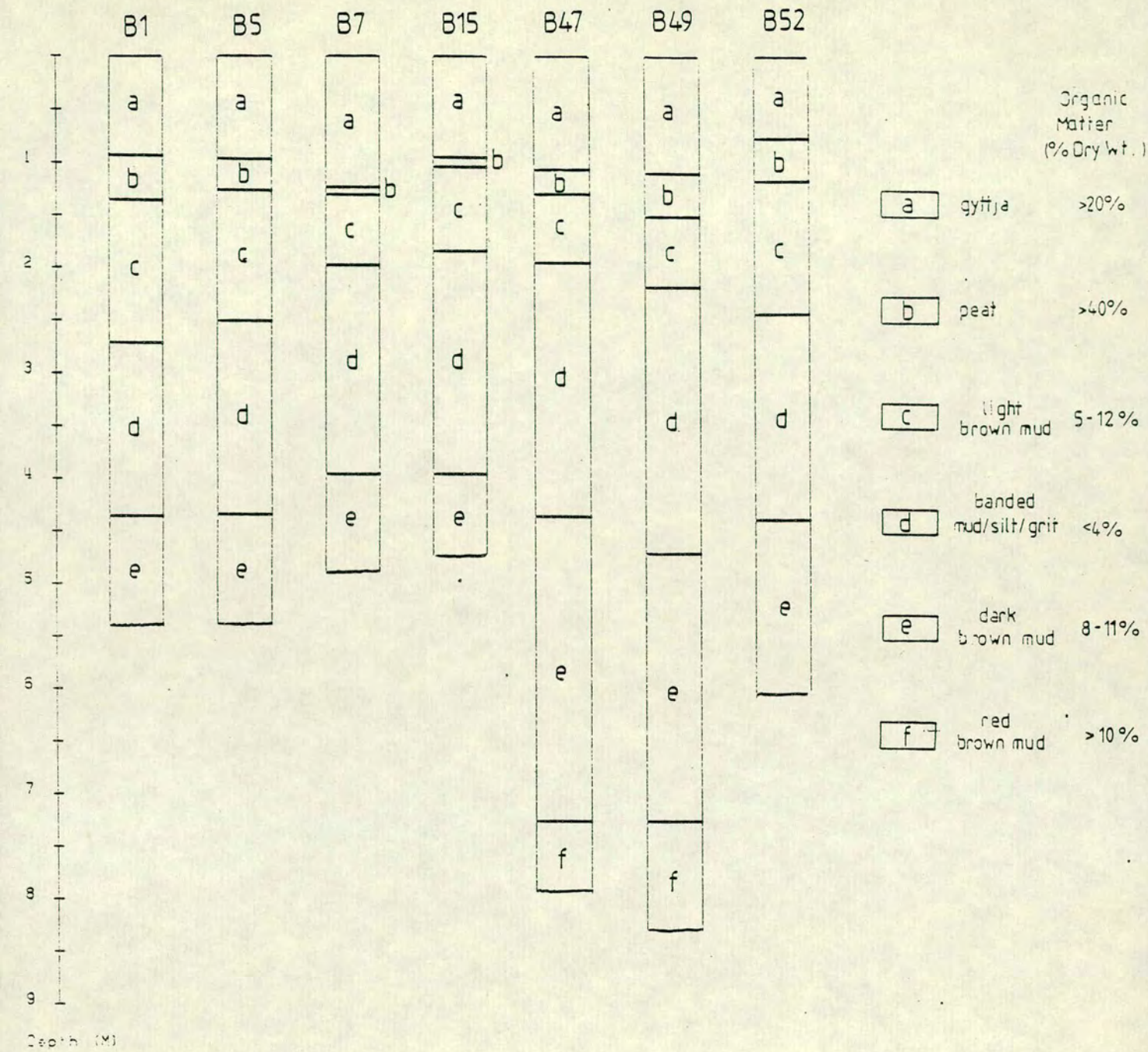

Figure 2.3 The general stratigraphy of some of the cores taken from Lac du Bouchet.

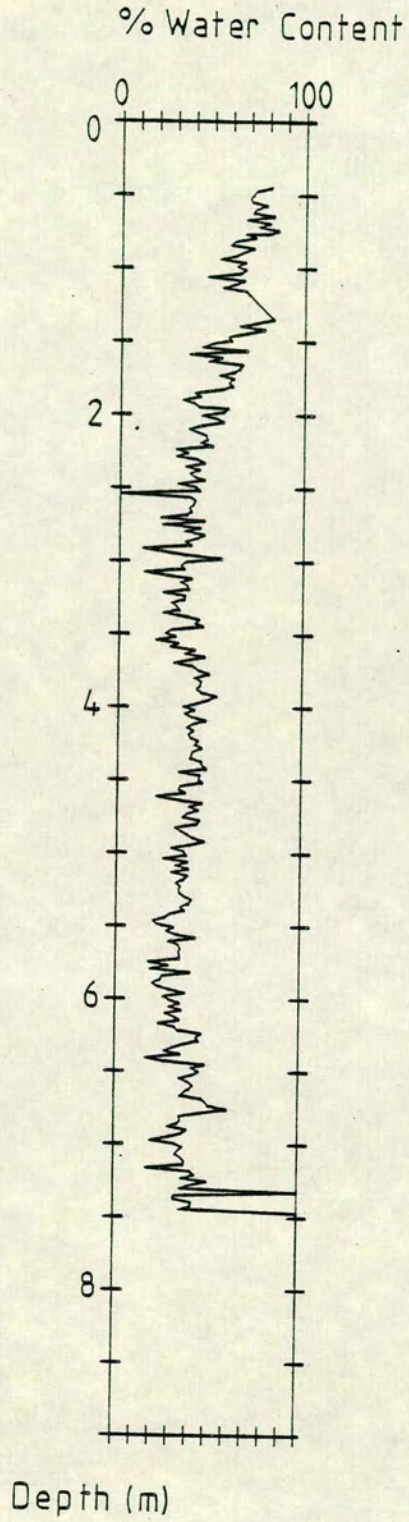

Figure 2.4 The variation of water content down core B49.

others have a layer of 30-40 cm (e.g. B5, B49). The colour is very dark, almost black, caused by the extremely high content of organic material (>40%). This highly fibrous material is impossible to subsample accurately for palaeomagnetic measurements, which has resulted in there being gaps in most of the cores measured. (see chapter 3). The inorganic matrix is very fine silt and clay of the same nature as in assemblages A and C but in much lower proportions.

2.5.3 Assemblage C

Below the organic rich 1-2 metres of assemblages A and B there is an abrupt change of character (marked in some cores by a very thin red, oxidised band). The character change reflects the boundary between the warmer post-glacial climate, conducive to the growth of flora and fauna, and the much harsher late glacial climate. The colour lightens from the dark brown organic rich clay, through a very light brown to a light grey inorganic (5-12% organic matter) clay. The assemblage is characterised by thick sections of homogeneous clay of very uniform size and composition, sometimes intersperced with thin layers of sandy and gritty layers (about 1cm thick), caused by very occasional slumping. There are also a few thin black cinder layers, micaceous layers and yellow clay layers. The sediment is still quite damp but well compacted and the assemblage varies in thickness between 1.3 and 1.7m. Dating has shown that the rate of deposition is higher than in the post glacial sediments, though still less than 0.4mm a year.

2.5.4 Assemblage D

The boundary between assemblages C and D is not as clearly noticeable as those between the earlier assemblages. The nature of the sediment is still essentially similar to assemblage C consisting of grey, inorganic (2-4% organic matter), clay. In addition to the same kind of thin layers as appear in C, there are some thin blue/grey layers consisting of coalesced particles of iron phosphates.

Some of the gravelly layers are sorted, indicating that there were some violent slumpings during this period. They are more common towards the lower part of the assemblage. Occasionally, these layers are hydraulic in the sense that water is trapped by them. This results in very wet sediment for about 5cm either side, and great care must be taken during subsampling. The actual

thickness of the assemblage is difficult to determine accurately because of the poorly defined boundaries but is usually around 2m. The colour darkens towards the lower end to a dark green/grey.

2.5.5 Assemblage E

The 6m cores all have this more organic rich assemblage as their maximum extent. It is darker in colour and more compact than the previous layers, possibly due to the increasing organic nature (8-12% organic matter). The brown, predominantly silts and clays, are intersperced with very thin (1-2mm) green and yellow bands and some thin black cinder layers. It is about 1 - 1.5 m long in the 9m cores and reveals a much more compact and dry nature when being subsampled. Again there are one or two layers with large grits or stony particles. These could have been the layers that caused the corer to be unable to penetrate to deeper sediment on some occasions.

2.5.6 Assemblage F

This layer, found at the bottom of the 9m cores, is characterised by a chestnut brown appearance and a slight increase in water content. Again the boundary between it and the assemblage above is unclear, with the thin layers of yellow and green continuing to be observed. The numbers of these layers decreases though towards the bottom of the assemblage and the grain sizes increase, from predominantly muds to clays and silts. The organic content of this layer has not been accurately determined in France; the results from work done on the sediment here as part of the dating revealed that this layer has a slightly increased proportion of organic matter (10-15%?) and may indicate the beginning of an amelioration of the climate.

2.5.7 Other aspects of the sediments

The results of the pollen analyses (from which some dates were estimated and used in chapter 5) and the diatom analyses have been described in detail in **Bonifay et al. (1985)**.

2.6 The approach for this work

The work performed upon the sediments taken from Lac du Bouchet is described in six stages. Chapter 3 presents the results of measurements of the NRM and susceptibility of the 1m, 6m and 9m cores, taken for palaeomagnetic study and the way in which the results can be compared and correlated.

Chapter 4 describes some of the experiments performed to identify the carrier of the remanent magnetisation of the sediments: chapter 5 the dating of the sediment and chapter 6, some analyses of the spectral content of the records after establishing the time scale.

In chapter 7 the effect of normalising the DRM by laboratory induced remanent magnetisations is investigated to try to establish estimates of the variations of the geomagnetic intensity through the Late glacial period.

Chapter 8 describes the results obtained from some 12m cores taken in April 1985 and extending the record back to about 40,000 years bp. This introduces questions pertaining to the existence of the Laschamp event, which is not found recorded within these sediments.

A major portion of the time spent during this project has been towards the improvement of facilities used to analyse lake sediments. One aspect has been discussed in chapter 1 which describes the improvements made to the control of the cryogenic magnetometer operation. Other changes include modifications to the Mackereth corer (described in appendix 1). Others are the control of measurements using the translation balance and the suite of programs developed to organise, analyse and present the results of palaeomagnetic measurements on lake sediments in particular, but any rocks in general (appendix 3).

CHAPTER 3
MEASUREMENTS OF NATURAL REMANENT MAGNETISATION

3.1 Introduction

The cores taken from Lac du Bouchet during the six coring campaigns varied in length from 1m to 12m. The first campaign, in April 1982, obtained five 6m cores of which three were measured palaeomagnetically (**Thouveny (1983)**; **Creer et al. (1985)**). The results obtained from these cores indicated that Lac du Bouchet had great potential for palaeomagnetic work because of its very low rate of sedimentation (giving a larger time window for a given length of core) and because the sediments themselves exhibited a strong and seemingly stable remanent magnetisation. The second campaign (in September 1982), attempted to obtain 12m cores using a two piece Mackereth type corer (**Mackereth (1958)**). This failed to obtain more than 6m of sediment (due to a combination of the nature of the sediment and the join in the corer). The third campaign was designed to obtain "mini" (1m) cores (November 1982), that preserve the sediment/water interface. The fourth and fifth campaigns (August, November 1983) used a single piece 9m corer specially designed and built to produce a greater coring pressure (see appendix 1). The fourth campaign was unsuccessful as the corer failed under the stress of coring and broke. The fifth campaign successfully obtained 9m cores.

This chapter describes the results obtained from these campaigns, notably the results from the minicorer and the successful 6m and 9m cores. The results obtained from the final field campaign (April 1985), which used a specially constructed single piece 12m corer, are described in chapter 8.

3.2 NRM results from 6m and 9m cores

This section describes the results from the 6m and 9m cores obtained in the second and fourth field seasons. There is a brief account of subsampling and

storage followed by the results of the NRM measurements on a typical core, and a comparison of the results from the other cores.

3.2.1 Sampling, storage and measurement

Table 3.1 shows a summary of the long cores that have been measured. During this work eleven 6m and, five 9m and three 12m cores have been examined. Cores B1, B3 and B5 were those measured as part of the first campaign by N. Thouveny. The eight cores between B7 and B26 were taken in the second field season and the others in the fourth and fifth. As indicated in **table 3.1** some were subsampled in Marseille and some in Edinburgh. The method used for subsampling such cores is described in detail in appendix 2; it consists essentially of splitting the PVC core tubes lengthwise and continuously sampling the sediment down the core, by carefully inserting small plastic sample boxes.

To reduce the effects of viscous remanent magnetisation the subsamples were stored in a zero field environment (produced by a set of Helmholtz coils), for a period of not less than one week prior to the measurement of the NRM. All measurements presented in this chapter (except those for B5 and B7) were measured on the cryogenic magnetometer under the control of the program described in chapter 1. After measurement on the magnetometer the results were transferred to the university mainframe computer for subsequent analysis and plotting. The programs used for the analysis and plotting have been developed specifically for this type of work and a user library has been created for multi access. The program library produced is described in appendix 3.

Magnetic volume susceptibility was measured on the Bartington bridge susceptibility meter and the results written on to the mainframe. These were measured between the measurements of NRM and bulk demagnetised RM to reduce the possibility of viscous effects due to the instrument. A copper sulphate or ammonium ferrous sulphate standard sample was used to calibrate the meter.

3.2.2 Typical results - Core B49

The results obtained from the measurement of the NRM of each subsample down core B49 are shown in **figure 3.1**. The corresponding susceptibilities and

Table 3.1 Long cores taken from Lac du Bouchet between April 1982 and April 1985 for palaeomagnetic analysis.

Core	Date Taken	Attempted Length(m)	Actual Length(m)	Where Subsampled	No. of Subsamples
B1	Apr 82	6	5.40	Edinburgh	225
B3	Apr 82	6	5.55	Edinburgh	199
B5	Apr 82	6	5.50	Edinburgh	442
B7	Sep 82	6	4.95	Edinburgh	205
B12	Sep 82	6	5.30	Marseille	214
B15	Sep 82	6	4.98	Edinburgh	198
B16	Sep 82	12	5.69	Marseille	220
B23	Sep 82	12	4.66	Edinburgh	400
B24	Sep 82	6	5.71	Edinburgh	352
B25	Sep 82	6	5.29	Edinburgh	298
B26	Sep 82	6	5.36	Edinburgh	270
B42	Aug 83	9	6.90	Marseille	287
B46	Oct 83	9	6.73	Marseille	278
B47	Oct 83	9	7.75	Marseille	309
B49	Oct 83	9	8.20	Marseille	322
B52	Oct 83	9	5.86	Marseille	244
B61	Apr 85	12	11.25	Edinburgh	406
B63	Apr 85	12	10.57	Edinburgh	405
B64	Apr 85	12	11.18	Edinburgh	463
				Total	5737

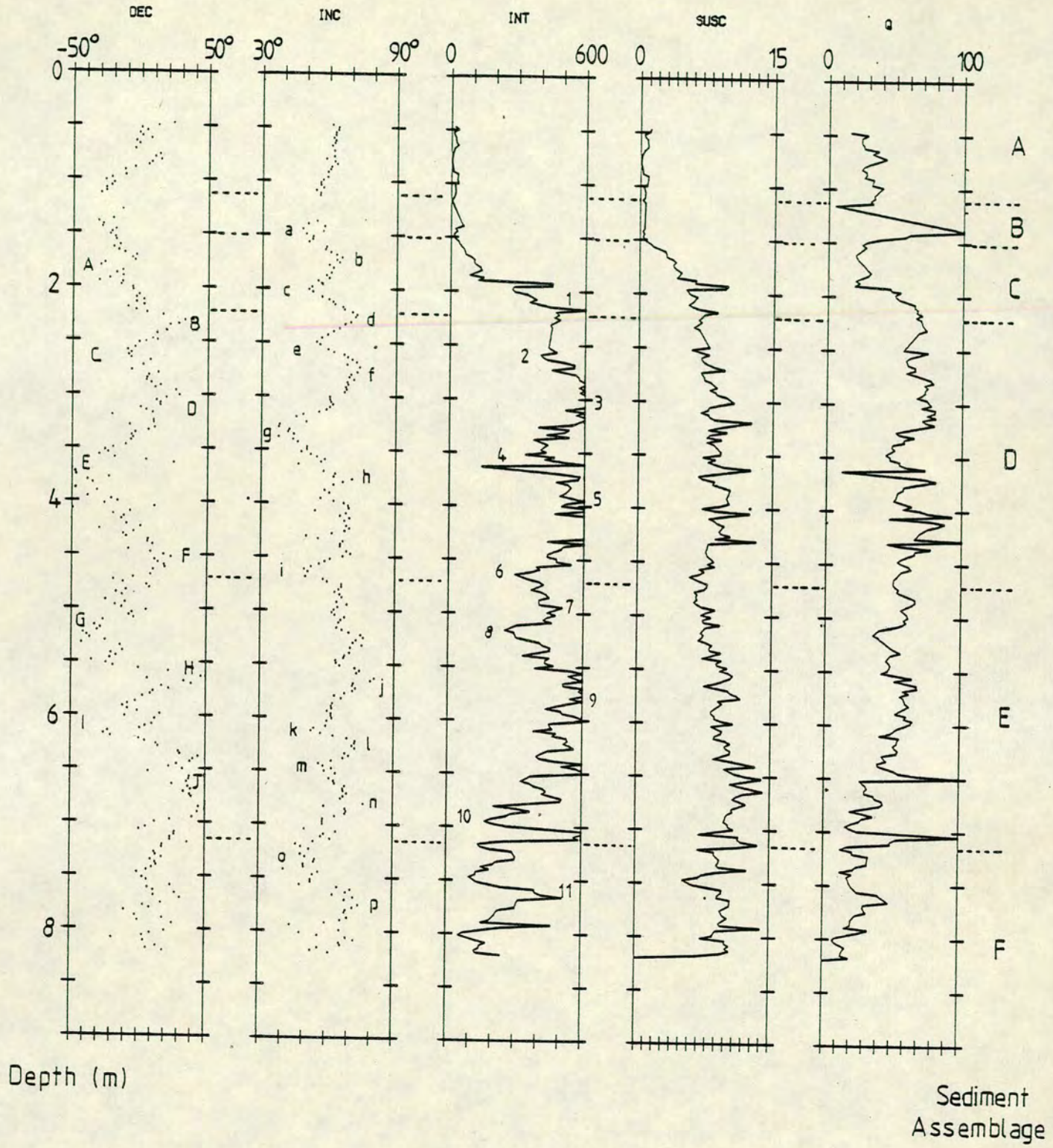

Figure 3.1 The NRM records for core B49 showing the variations in declination inclination and intensity. The variation of susceptibility and Q ratio are also shown as are the different sediment assemblages as outlined in chapter 1. Note that the units for the intensity and the Q ratio scales are mA m^{-1}.

Q-ratio (**Konigsberger (1938)**), (defined as the ratio between the NRM and volume susceptibility) are also shown. This core has been chosen for several experiments and analyses because, for the greater part of the time spent on this project, it was the longest core available. Declinations have been averaged and then reduced to a zero mean and the inclinations averaged and set to that inclination that would be expected due to a geocentric axial dipole field at the site of Lac du Bouchet. The "raw" results - those obtained before averaging - are summarized in **table 3.2**.

3.2.2.1 NRM Intensity

Throughout the sediment assemblages A and B (and the top part of C), the NRM intensity is very low (< 80 mA m^{-1}) and begins to increase at a depth of about 1.75m. The highly organic sediment of assemblage B was not subsampled due to the large quantities of fibrous material that causes severe disturbance of the rest of the sediment matrix during subsampling. This leaves a gap in the record between 1.16 and 1.37 metres.

Between 2.00 and 5.50 metres (i.e. through assemblages D and the top of E), the record shows an oscillatory pattern as the intensity varies between peaks (approximately 600mA m^{-1}) and troughs (approximately 250mA m^{-1}). Eleven such turning points are labelled (numerically), on **figure 3.1**, showing a "period" of about 1 metre. Superimposed upon this longer "period" variation are numerous "spikes" (of both high and low intensity), some of which are labelled in Roman numerals. These spikes are easily recognized from core to core and can be identified with specific layers of sediment within the cores. These spikes have been found (in chapter 4), to contain a greater proportion of magnetic minerals than most of the sediment.

Below 5.50 metres the intensity appears to decay from about 550mA m^{-1} to about 150mA m^{-1} although, again, superimposed upon this decay is an apparent oscillatory pattern.

In general, the variation of intensity follows, inversely, the amount of organic material within the sediment. The sediment rich in organic matter has a low intensity of magnetisation (e.g. A, B and F) and the layers with little organic matter have a much greater intensity.

Table 3.2 "Raw" declination and inclination data as measured on the cryogenic magnetometer, before standardisation. Data for the long cores taken from Lac du Bouchet.

Core	Average Dec	Average Inc	Minimum Inc
B1	74.26	51.25	10.34
B3	287.42	63.64	9.66
B5	60.47	60.65	2.20
B7	94.60	65.39	5.21
B12	118.70	53.60	31.10
B15	264.59	59.62	8.08
B16	171.78	61.03	-36.55
B23	194.37	62.26	3.83
B24	234.41	55.40	6.01
B25	185.55	63.58	45.40
B26	73.68	50.02	26.97
B42	82.70	62.26	8.58
B46	142.92	55.49	17.62
B47	66.20	65.29	12.27
B49	89.29	64.72	3.21
B52	229.34	61.72	12.09
B61	304.69	53.87	-42.90
B63	302.24	54.70	3.93
B64	97.61	62.43	-70.07
		Average 59.31 (Axial dipole 63.43)	

3.2.2.2 Inclination

The variation in inclination with depth shows quasi-periodicity especially in the sediment assemblages C and D. Due to the nature of the sediment (which is very wet) and to the coring mechanism the top metre of the record, assemblage A, reveals little information. The nature of the variation can be seen a little more clearly in the results from the minicores described in the next section. At depths between 1.50 and 4.00 metres the record is remarkably smooth and shows oscillations with a peak to peak amplitude of up to 40°, and a "period" of approximately 1m. These extrema have been labelled using lower case letters starting from the top of assemblage C (1.50m). The amplitude of the variations is reduced by a factor of about 2 through the lower part of assemblage D and the upper part of assemblage E (4.00 to 5.50 metres) where only one notable minimum (i) has been identified. Below this level, to the bottom of the core, the larger amplitude variations are again apparent, although the amount of scatter is seen to increase slightly also.

3.2.2.3 Declination

The declination record is also not clear in the very wet sediment at the top of the core. The quasi-periodicity (labelled using upper case letters) apparent in this core is of a slightly longer "period" (about 2m), and the peak to peak variation is much greater (up to 90°). It is also noticeable that there is a greater amount of scatter in this record than in the inclination record, probably as the result of the greater force on the magnetic particles in the vertical plane than in the horizontal. This scatter is also more noticeable towards the bottom of the core although the general shape of the variation is clearly visible. There seems to be little change in the character of the variation below 1.50 metres, the variations appearing to be relatively continuous.

3.2.2.4 Susceptibility

The general form of the susceptibility record is similar to the intensity log. There are low susceptibilities below 1.50 metres followed by a rise. However, there does not seem to be the periodic variation that is so apparent in the intensity log, although there is a very long period trend and several spikes that

correlate well with the spikes in intensity. Another feature is that there appears to be a steady increase in the susceptibility with depth up to about 7 metres, in contrast to the general shape of the intensity log, especially between 5.50 and 7.00 metres.

A comparison of the susceptibility log with the down core water content (**figure 1.4**) reveals a remarkable inverse correlation. This agreement indicates that the changes in the susceptibility are likely to be directly reflecting the changes in the concentration of magnetic minerals in the sediment. This is discussed more in chapter 4.

3.2.2.5 Q-Ratio

The Q ratio was one of the first parameters used in the attempt to obtain the variation of geomagnetic intensity from sediment records (**Konigsberger (1938)**). It is an attempt to normalise the NRM values obtained from the sediment relative to the sediments ability to record the field. As such it does provide a loose idea of how the geomagnetic field is likely to have varied.

The Q ratio log is very similar to the intensity log. There are two noticeable features. There is a clear decrease in the ratio below 4.00 metres (despite the corresponding increase in susceptibility) and the amplitude of the variations are not as great. Another less apparent feature is that the the record is somewhat noisier than either of the 'parent' records.

3.2.2.6 General features

Several other features are apparent in a study of **figure 3.1**. There appears to be a correlation between the oscillations in intensity and in inclination i.e. both logs show peaks at similar depths (e.g. "d" and "1", "e" and "2" etc.) although there seems to be a slight lag between them (of about 10cm). In contrast a comparison of the variations in the declinations and inclinations indicates an approximately 90° phase lag between the records between 2.00 and 3.50 metres. In particular peak "c" occurs as "A" to "B" passes through zero, "e" as "B" to "C" does and "f" as "C" to "D" is zero. Lower down the core inclination features "h" and "i" appear almost to be in antiphase to declination features "E" and "F". Below 5.50 metres the declination and inclination features appear to be in phase although the increase in scatter does make this less immediately

apparent. The implications of these phase relations are discussed in chapter 6 when the depth scale has been transformed into a time scale.

3.2.3 Results from other 6m and 9m cores

Of the sixteen 6 and 9 metre cores taken and measured, eight are presented here and subsequently analysed. The other cores have not been used for a number of reasons. B1 and B3 were part of the initial field campaign and the samples were not measured for susceptibility. These two cores have however been analysed as part of the work presented in **Creer et al. (1985)**. Core B52 was found to have separated within the core tube, resulting in severe movement of pieces of sediment and a large scatter of results, particularly in the declination record. Of the remaining cores subsampled and measured B16, B23, B24, B25 and B26 were subsampled using smaller cylindrical subsample boxes in an attempt to get an increased density of sampling. Unfortunately this led to a great increase in the scatter due to the difficulty in orienting the subsample accurately and the increased disturbance at the sides of the core tube where the sediment was necessarily sampled. (The samples were taken at overlapping depths). All these cores show the same features as the cores analysed but have been rejected as the potential error especially in depth and orientation is considered too great.

The eight cores remaining are shown in **figure 3.2** (a to d). Each core is plotted on the depth scale estimated from the position of the sediment in the core tube. Few long cores retain the sediment/water interface. The five parameters discussed in the previous section are plotted side by side and the features labelled in **figure 3.1** can be seen for the other cores in **figures 3.2**. All the records have had any linear trends removed, these being assumed to be the result of the corer not entering vertically. Note the similarity of the records from the different cores, the varying degrees of smoothness and scatter and the variation in the downcore depths of the major features of each record.

In order to examine the magnetic features in more detail it is important to establish that the depth scales presented in **figure 3.2** can be adjusted to a common lake depth scale. To do this the stratigraphy down each has been examined and a comparison of the cores made. The down core correlations are discussed in section 3.5.

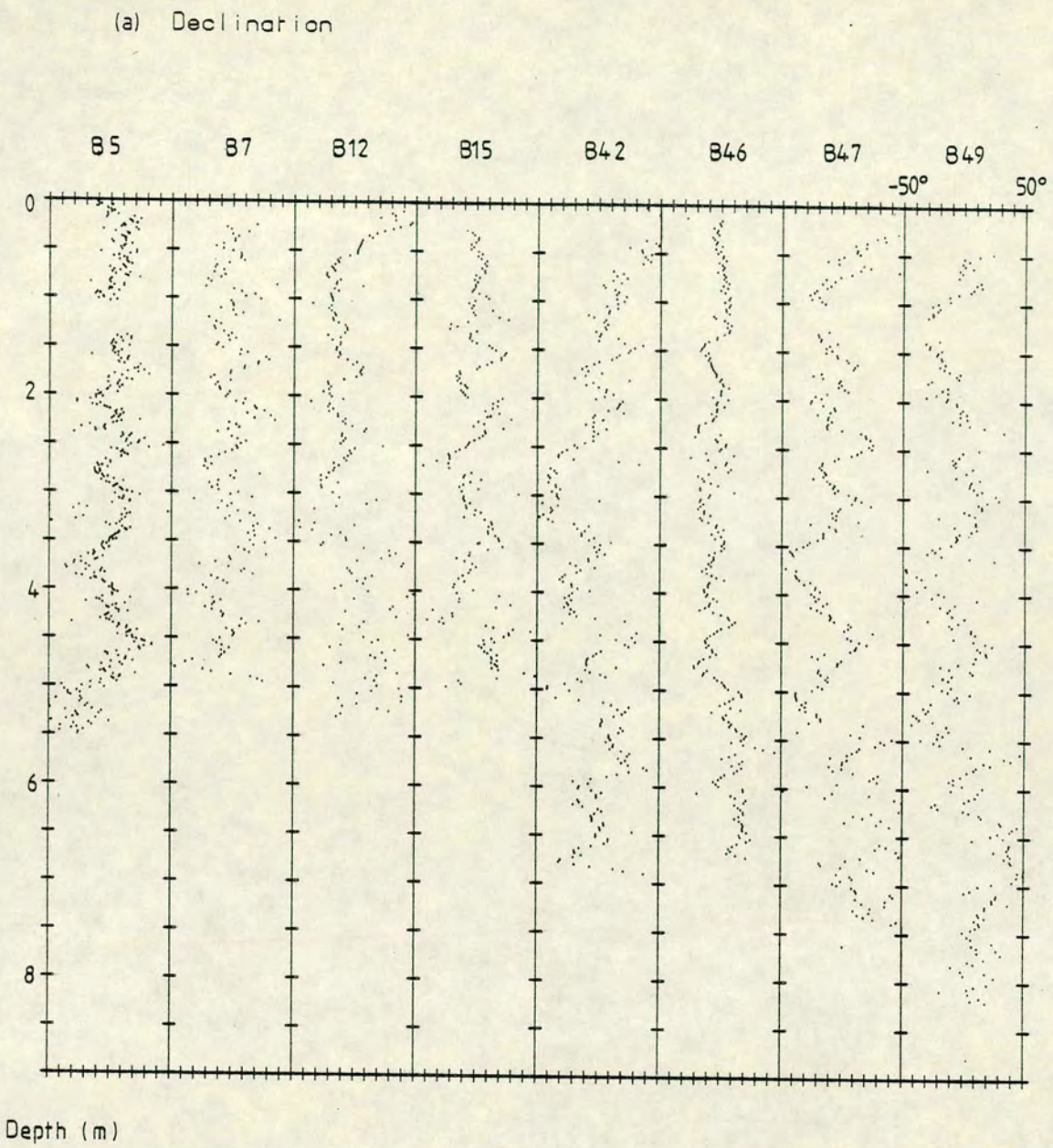

Figure 3.2 The records for the eight cores described in the text in (a) declination, (b) inclination, (c) intensity (mA m^{-1}) and (d) susceptibility. Each core is presented on its own depth scale.

(b) Inclination

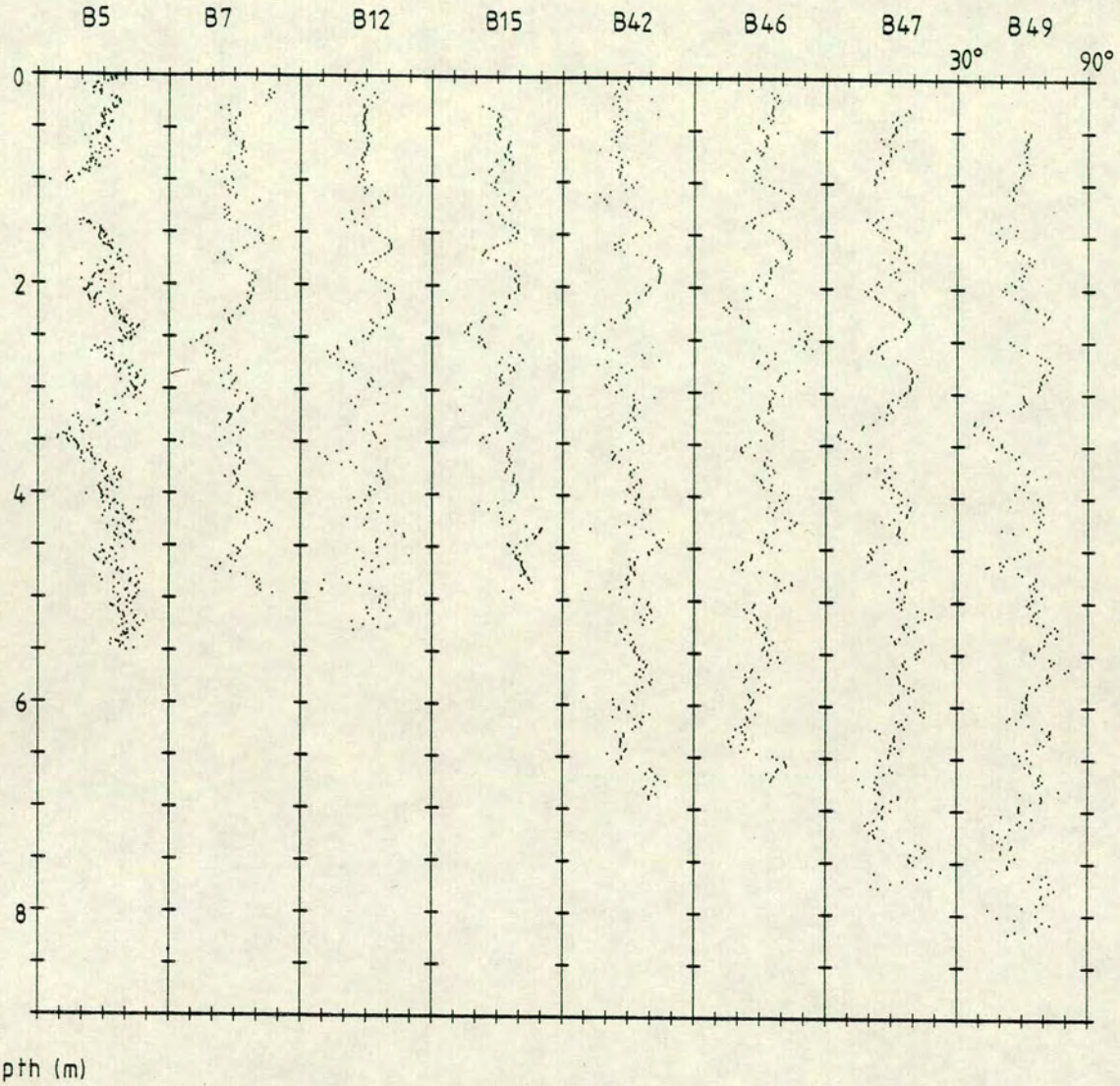

(c) Intensity

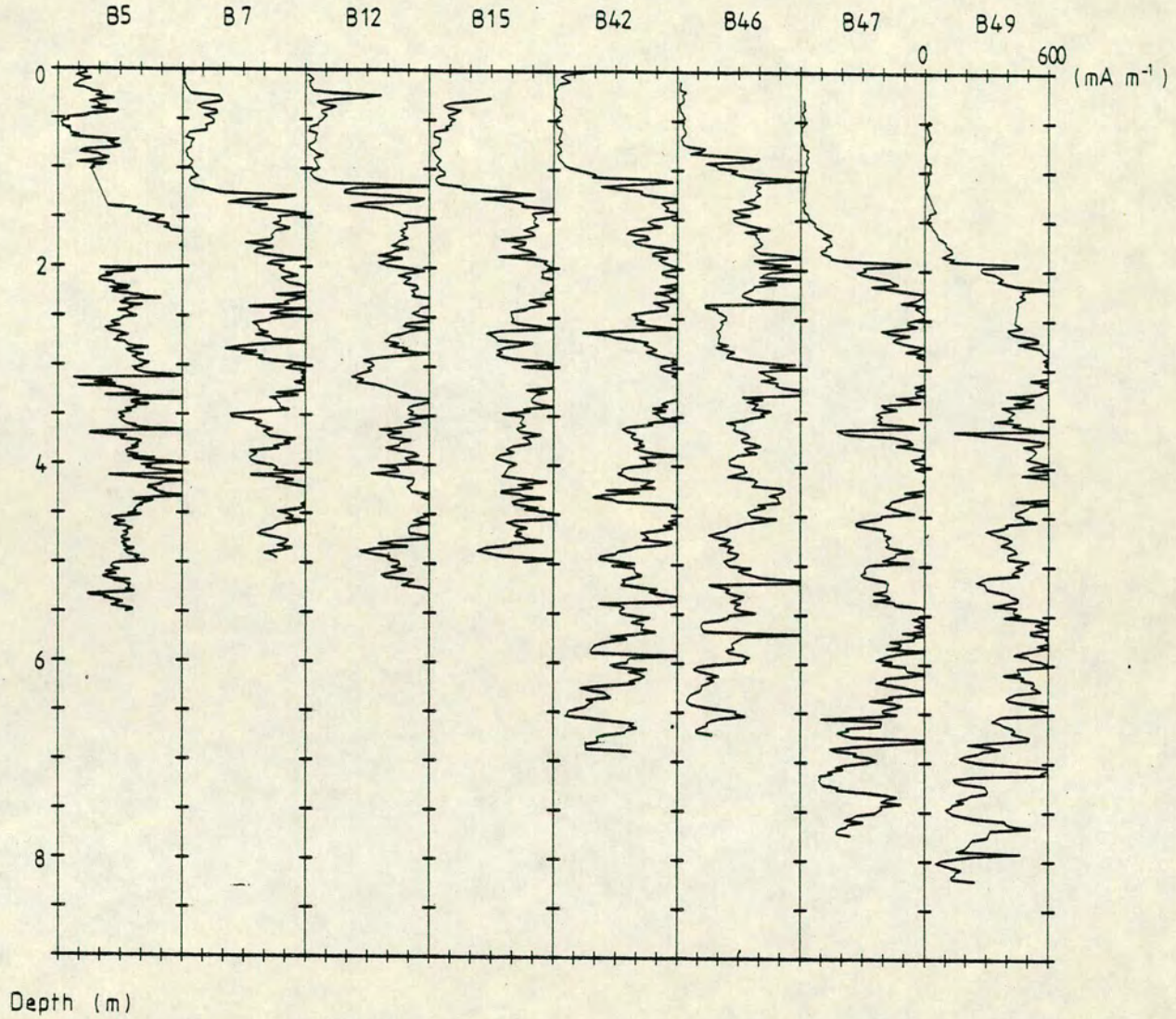

(d) Susceptibility

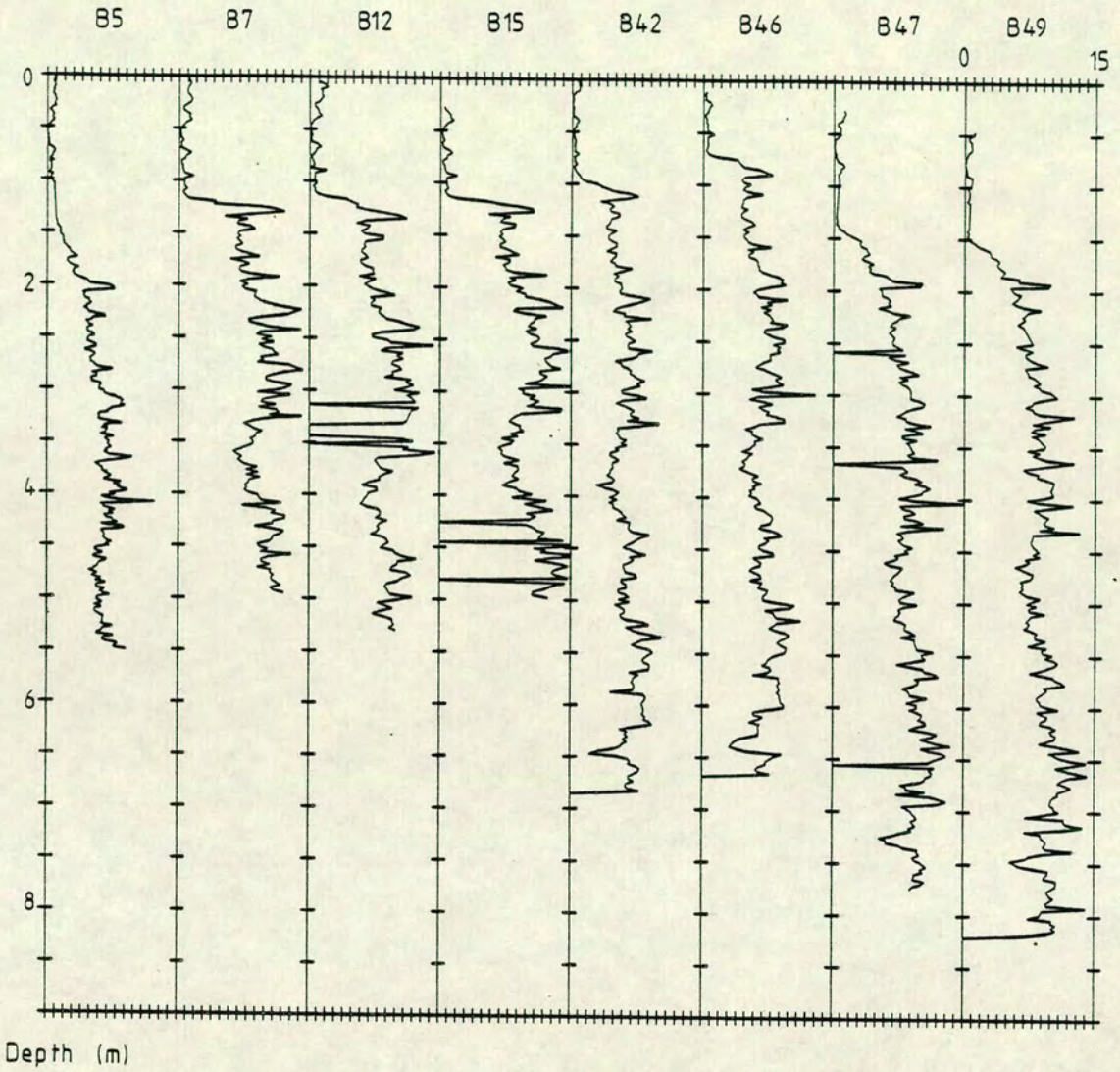

3.3 Results from the mini cores

In the third field campaign in November 1982 eleven mini cores were taken and then subsampled in Marseille. The method of subsampling these cores is different from that for the long cores and is described in detail in appendix 2. Essentially it consists of pneumatically pushing the sediment out of the top of the core tube, approximately 2cm at a time and subsampling this portion into a plastic sample box. The corer is designed to preserve the sediment/water interface and so the sediment subsampled is extremely wet and easily disturbed.

The results obtained for the first 8 of the 11 minicores for both NRM and susceptibility are shown in **figure 3.3** (a - d). These are described in the following sections. Again, the declinations are centred on zero and the inclinations on the expected value of a geocentric dipole field. The results of the "raw" measurements are given in **table 3.3.**

3.3.1 NRM Intensity

All the minicores have a much lower intensity of magnetisation than the samples from the long cores. They all reveal a similar variation with depth; that is an initial low intensity ($< 50 mA\ m^{-1}$) followed by a section with a higher intensity sometimes reaching more than $200 mA\ m^{-1}$ then another fall and rise. The similarity of the records is readily apparent. The grouping of the records so that sets BM1 and BM2; BM3, BM4 and BM5; and BM6, BM7 and BM8; have almost identical records is brought about by the fact that each set is from a single location within the lake. Each area however, can clearly be seen to have the same features, labelled M1 to M5.

3.3.2 Inclination

The inclination records for the minicores show very small variations. The maximum peak to peak variation of all of the cores is less than 20°. These features have been labelled using lower case Greek letters. The correlation from core to core is much less clear from these records although the scatter does appear to be very small.

Table 3.3 Pre standardisation data for the minicores taken from Lac du Bouchet in November 1982.

Core	Length (m)	No. Subsamples	Average Dec	Average Inc	Minimum Inc
BM1*	0.90	44	259.85	66.16	56.50
BM2	0.97	48	223.86	65.19	55.30
BM3	1.27	57	197.22	57.04	46.50
BM4	1.27	58	105.37	48.27	41.40
BM5	1.27	59	318.62	55.33	38.60
BM6	1.27	61	324.17	68.83	54.60
BM7	1.15	51	251.86	60.66	53.90
BM8	1.27	56	151.09	64.58	51.00
BM9	1.22	50	272.01	75.64	66.30
BM10	1.21	52	97.29	67.83	62.10
BM11	1.20	50	50.99	64.90	57.10

Average 63.13 (Axial dipole 63.43)

Table 3.4 Transform functions to the B5 depth scale for the minicores

B5	BM1	BM2	BM3	BM4	BM5	BM6	BM7	BM8
0.00	0.0	0.0	0.0	0.0	0.0	0.0	0.0	0.0
10.13	13.5	21.0	11.5	13.0	13.0	11.0	7.0	15.0
24.02	23.5	31.0	27.5	25.0	27.0	33.0	25.0	37.0
33.34	31.5	39.0	35.5	33.0	37.0	39.0	33.0	45.0
42.57	43.5	49.0	47.5	45.0	47.0	49.0	43.0	55.0
54.13	53.5	59.0	61.5	57.0	61.0	61.0	55.0	67.0
72.68	71.5	79.0	79.5	77.0	79.0	83.0	75.0	91.0
83.17	81.5	87.0	89.5	85.0	87.0	93.0	87.0	101.0
94.73	92.5	95.8	103.5	99.0	101.0	109.0	101.0	117.0

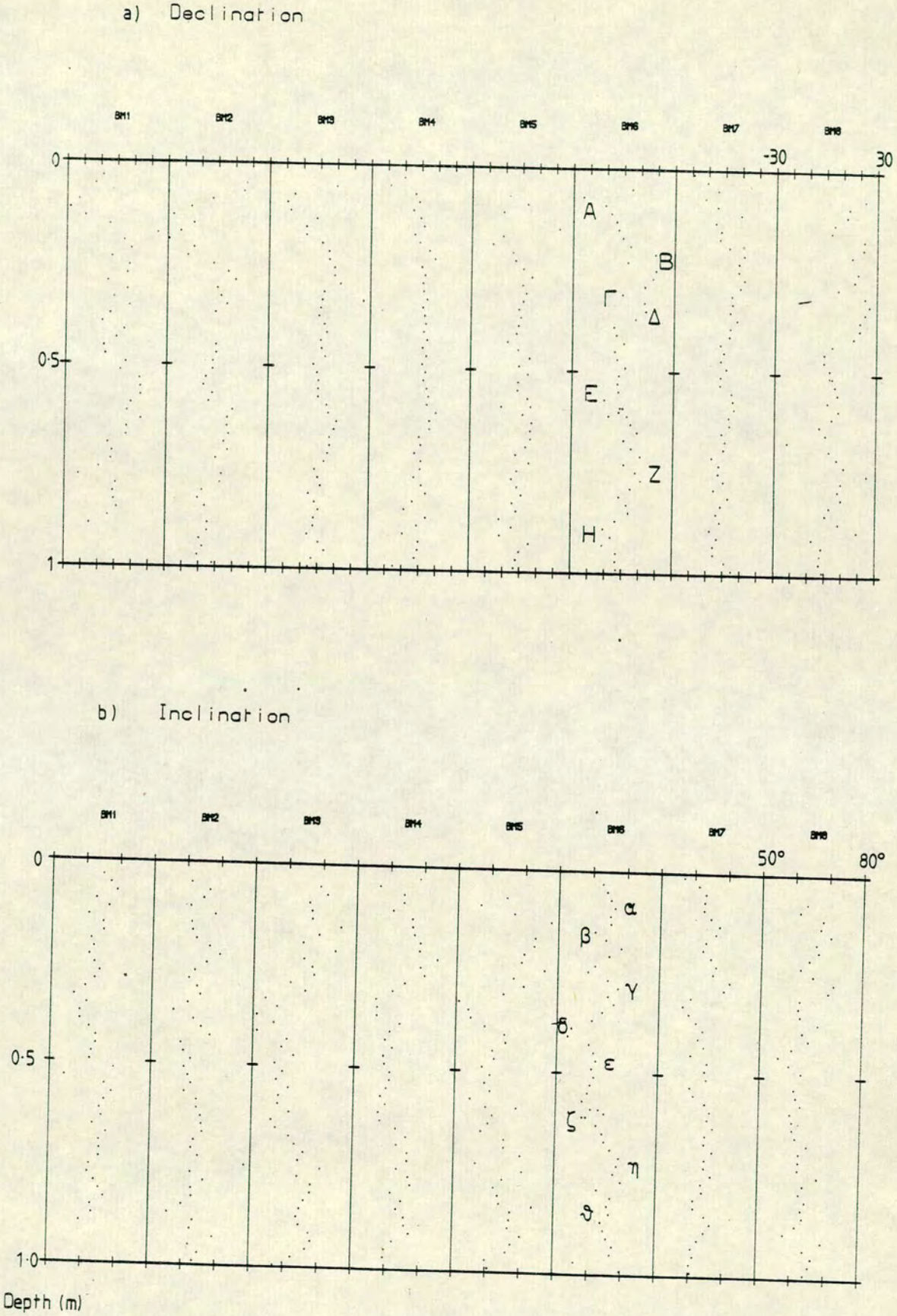

Figure 3.3 The records for the eight minicores described in the text in (a) declination, (b) inclination, (c) intensity (mA m^{-1}) and (d) susceptibility. Each core is presented on its own depth scale.

c) Intensity

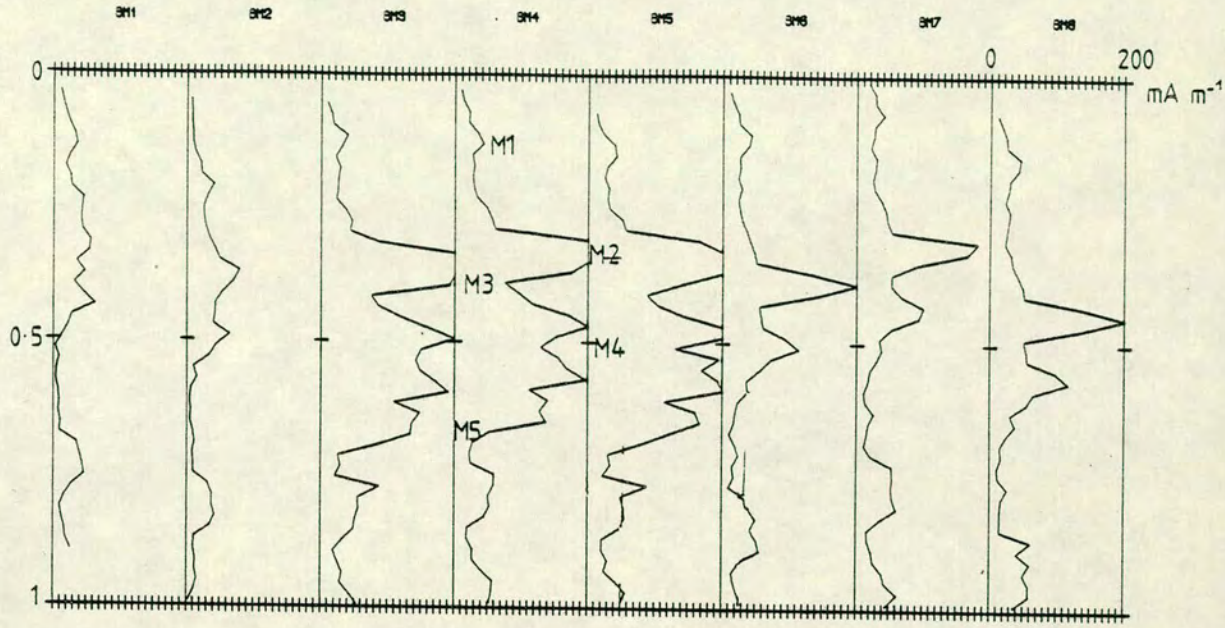

Depth (m)

d) Susceptibility

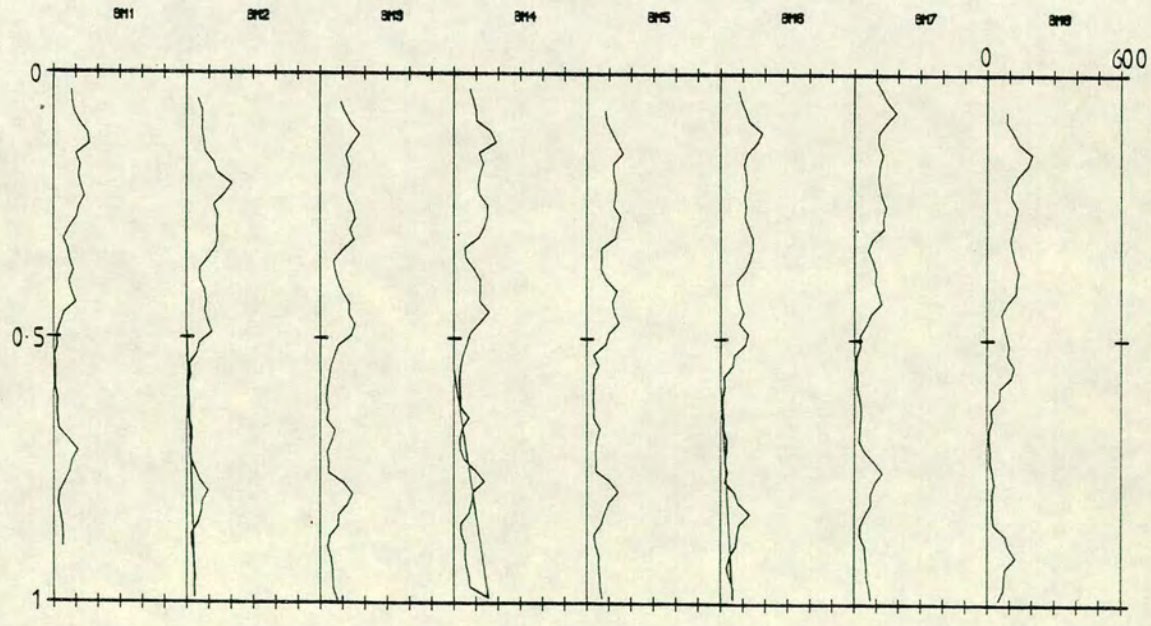

Depth (m)

3.3.3 Declination

The declination features, labelled using upper case Greek letters, also show very little detail. The similarity of the cores from the same location is again apparent though not as readily as in the intensity results. The records also show a larger apparent scatter than either the intensity or the inclination records.

3.3.4 Susceptibility

The susceptibility records of the minicores are very similar to the intensity logs and can be clearly correlated from core to core. The most striking feature once again is the remarkable similarity of the records from a single location.

3.3.5 Q-ratio

The Q ratios emphasize the agreement of the minicores. A short period of steadily rising values is followed by a strong peak and fall. The longer minicores then reveal another short increase followed by a fall which can be correlated from core to core.

3.4 Stability of remanent magnetisation

In order to allow the remanent magnetisation directions to be interpreted, usefully, it is necessary to remove any magnetisations that have been acquired since the sediment was deposited i.e. any secondary magnetisation. Ten per cent of the samples of the 9m cores B47 and B49 and of the minicores BM1, BM3 and BM8 have been step demagnetised in increasing peak alternating fields. The method and results for B49 are presented in chapter 4. These reveal that there are 2 magnetisations within each of the samples, a weak viscous component which could be removed by the application of a peak alternating field greater than 8mT and a magnetisation stable in all fields up to the maximum peak field used (usually 60mT). This is interpreted as the primary remanent direction reflecting the direction of the geomagnetic field when the magnetisation was "fixed" into the sediment.

The viscous remanence was found to have no preferred direction so all of the samples have been demagnetised in a peak field of 10mT. This produced, on average, a 25% reduction in the intensity of magnetisation. The record for core B49 after af demagnetisation in a peak field of 10mT is shown in **figure 3.4** which illustrates both the reduction in intensity and the stability of the directional components. It is this directional data that will be analysed in the work presented later.

3.5 The creation of a common depth scale

As the rate of sedimentation within the lake will not be constant over the whole lake floor, the features that are equivalent in time may appear at different depths within different cores. To compare the results obtained for the RM measurements it would be best to transform each of the cores to a common depth scale, ideally one that has been dated. To perform this transform it was decided not to assume, *a priori*, that the variations in the recorded directions of magnetisation occured at the same time from core to core. Instead the depth transform was performed using the stratigraphical correlations based upon sedimentology, susceptibility and intensity.

The transform functions were initially determined by a combination of the positions of the sediment assemblages and the variation of susceptibility. On discovering that these transforms produced a matching of the longer "period" features of the intensity records the detailed transformations were produced by correlating the spikes in intensity discussed above. (Section 3.2.2.1).

The core selected to be the base core for the common depth scale was B49. For the reasons stated in chapter 5 this core had been selected for dating. However, since core B5 had been intensively dated palynologically in the top 1.5 metres it was decided to transform the minicores to a B5 depth scale. The transform functions for the long cores are shown in **figure 3.5** and those for the minicores are given in **table 3.4**. These functions can be seen to be essentially linear indicating that the rate of sedimentation is constant (but may be different) at different locations within the lake. The result of applying these transform functions to the individual cores can be seen in **figures 3.6** and **3.7**. These show respectively, the results of the af demagnetised remanent magnetisations of the long cores and the minicores on their common depth scales. Note the excellent agreement produced between the various cores.

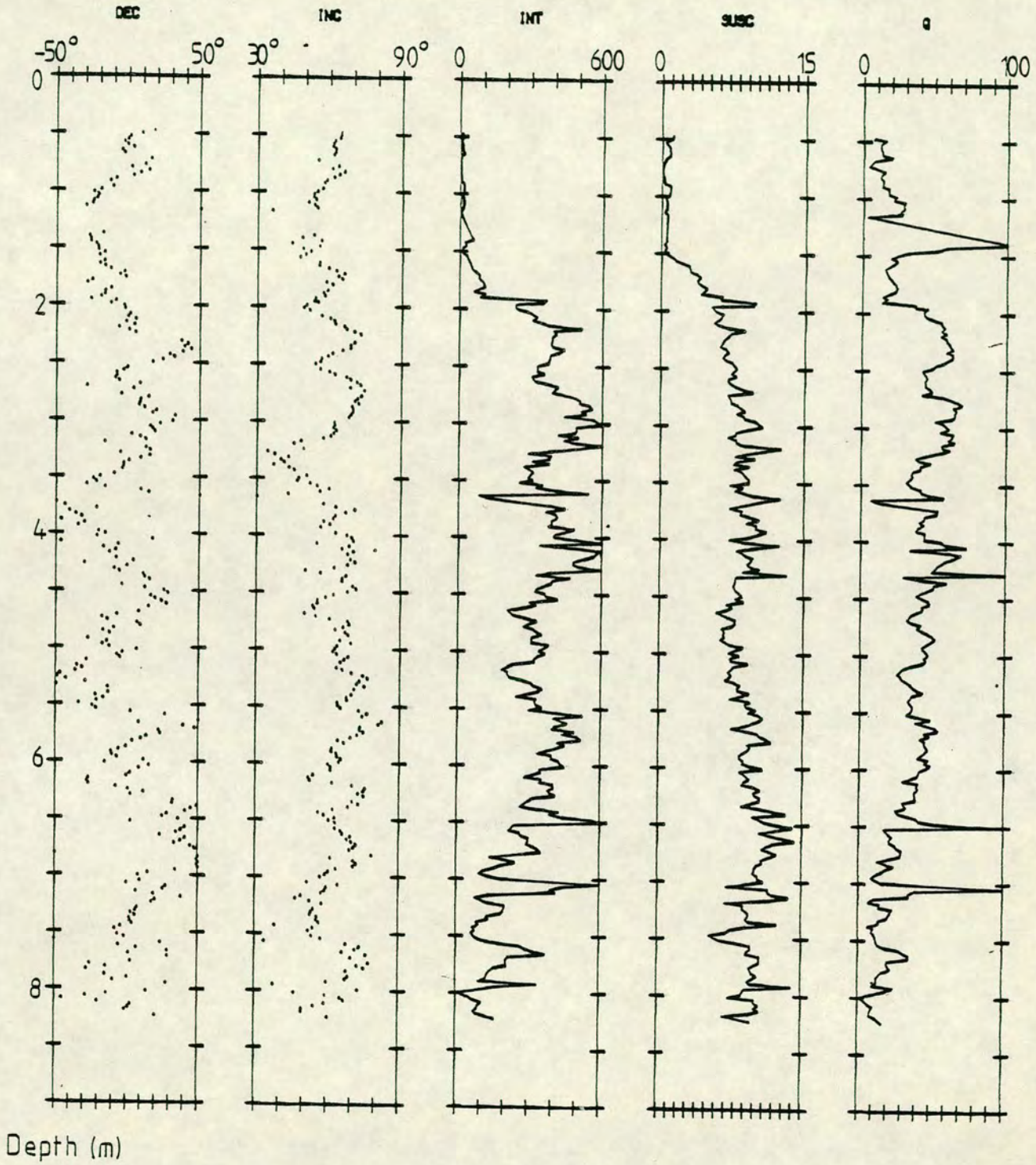

Figure 3.4 The NRM records for core B49 after af demagnetisation in a peak field of 10mT showing the variations in declination, inclination, intensity (mA m^{-1}), susceptibility and Q ratio.

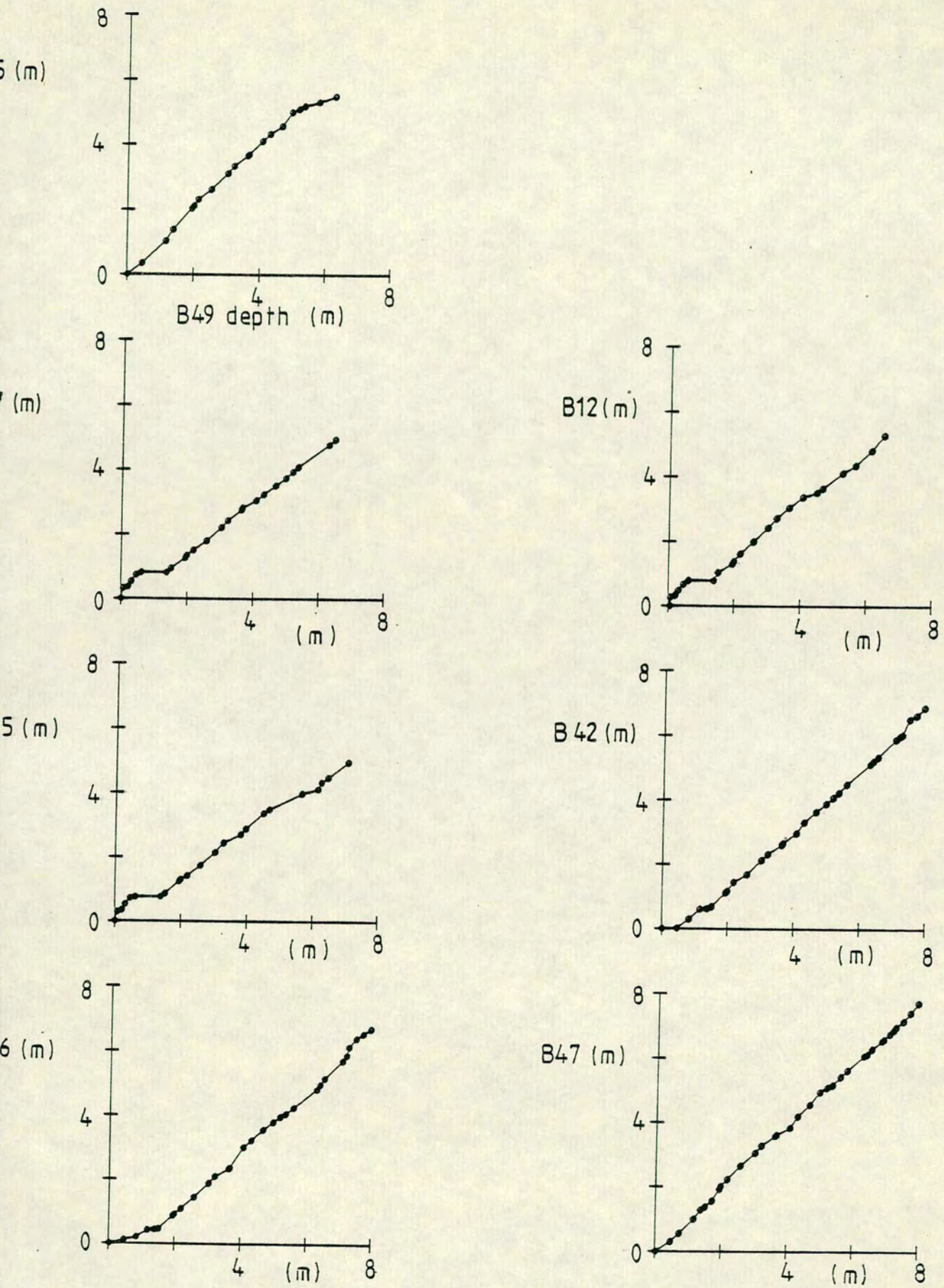

Figure 3.5 The B49 depth transform functions for the long cores.

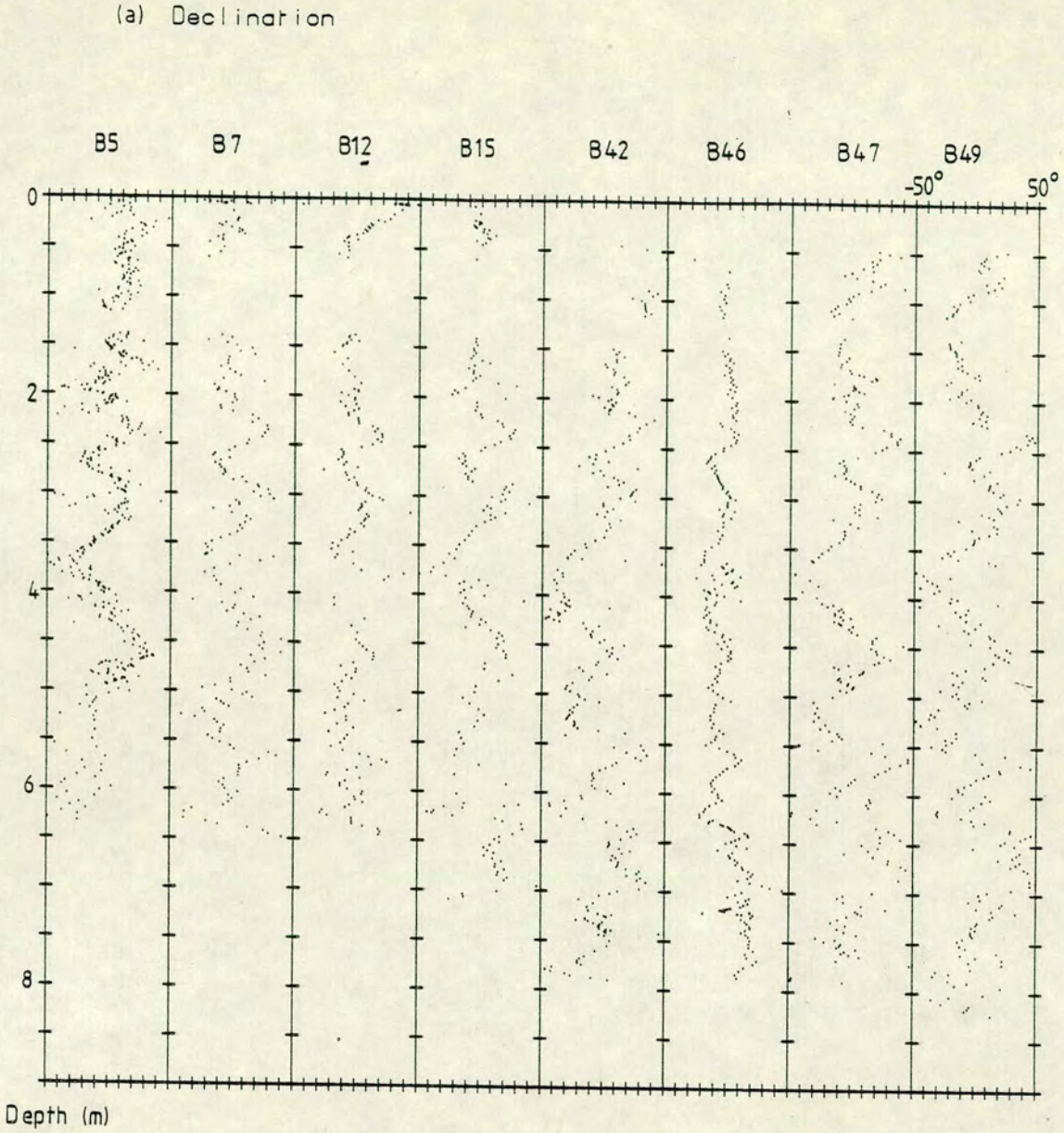

Figure 3.6 The records for the eight cores described in the text in (a) declination, (b) inclination, (c) intensity (mA m^{-1}) and (d) susceptibility after transformation to the B49 depth scale.

(b) Inclination

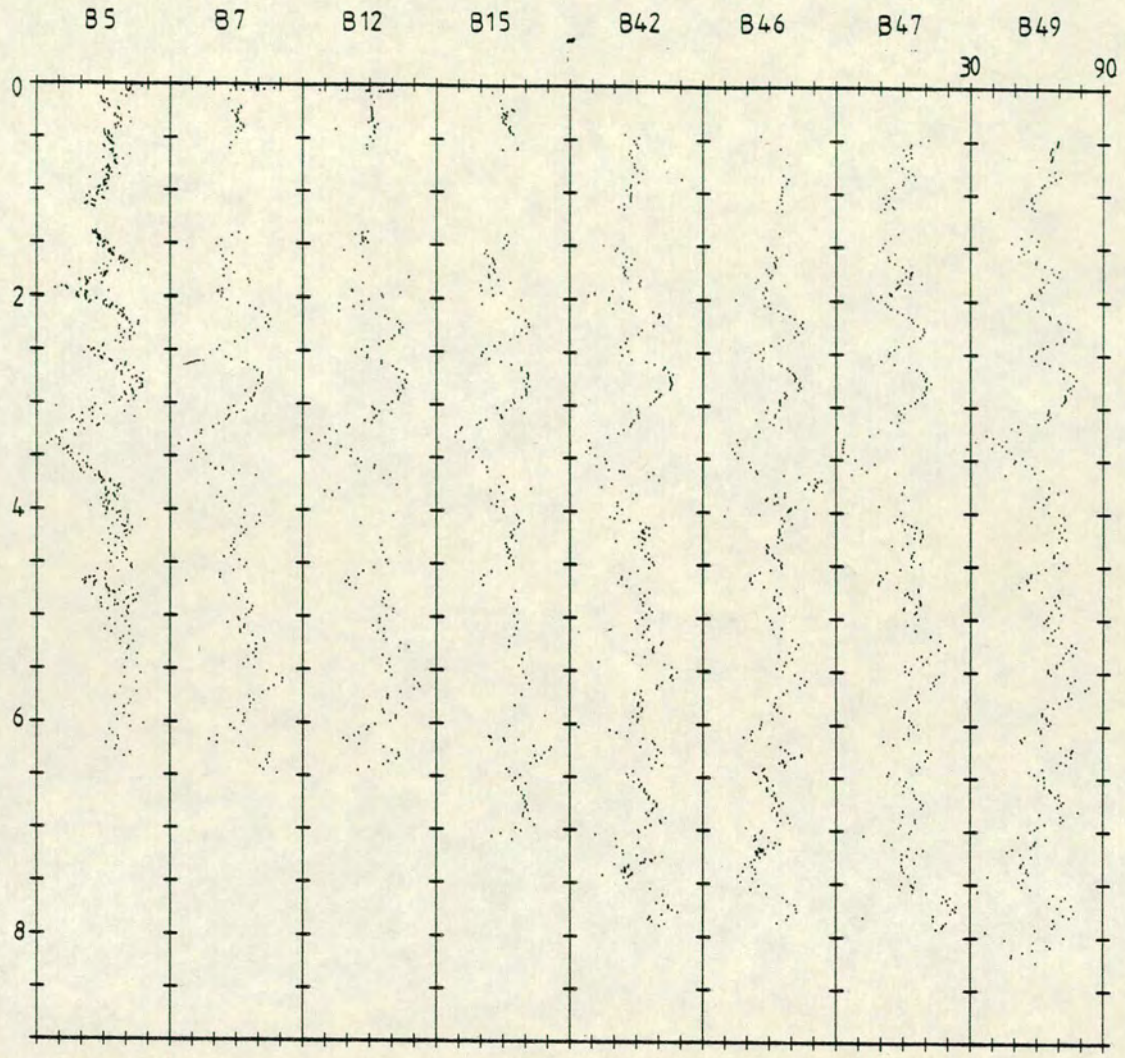

(c) Intensity

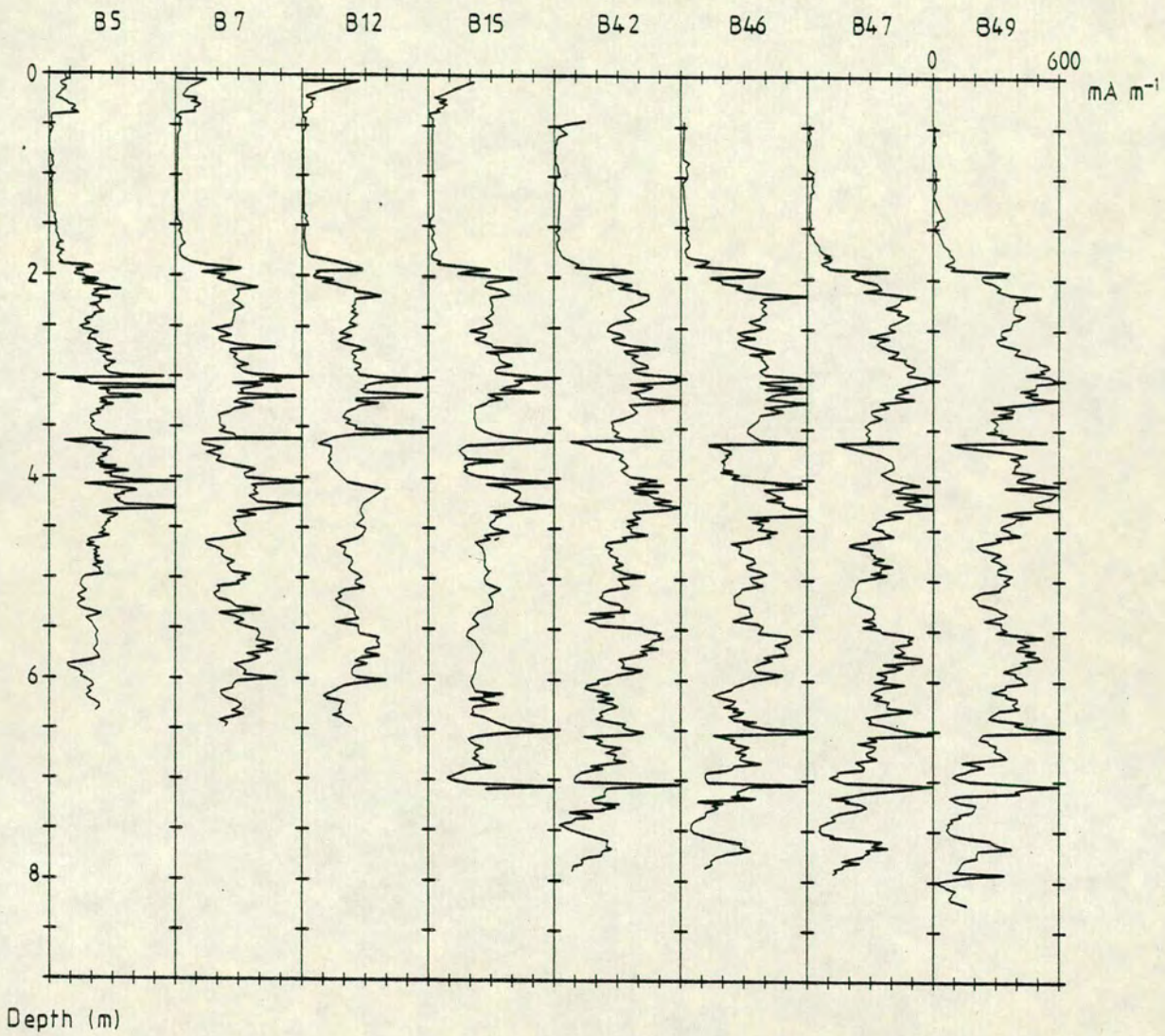

(d) Susceptibility

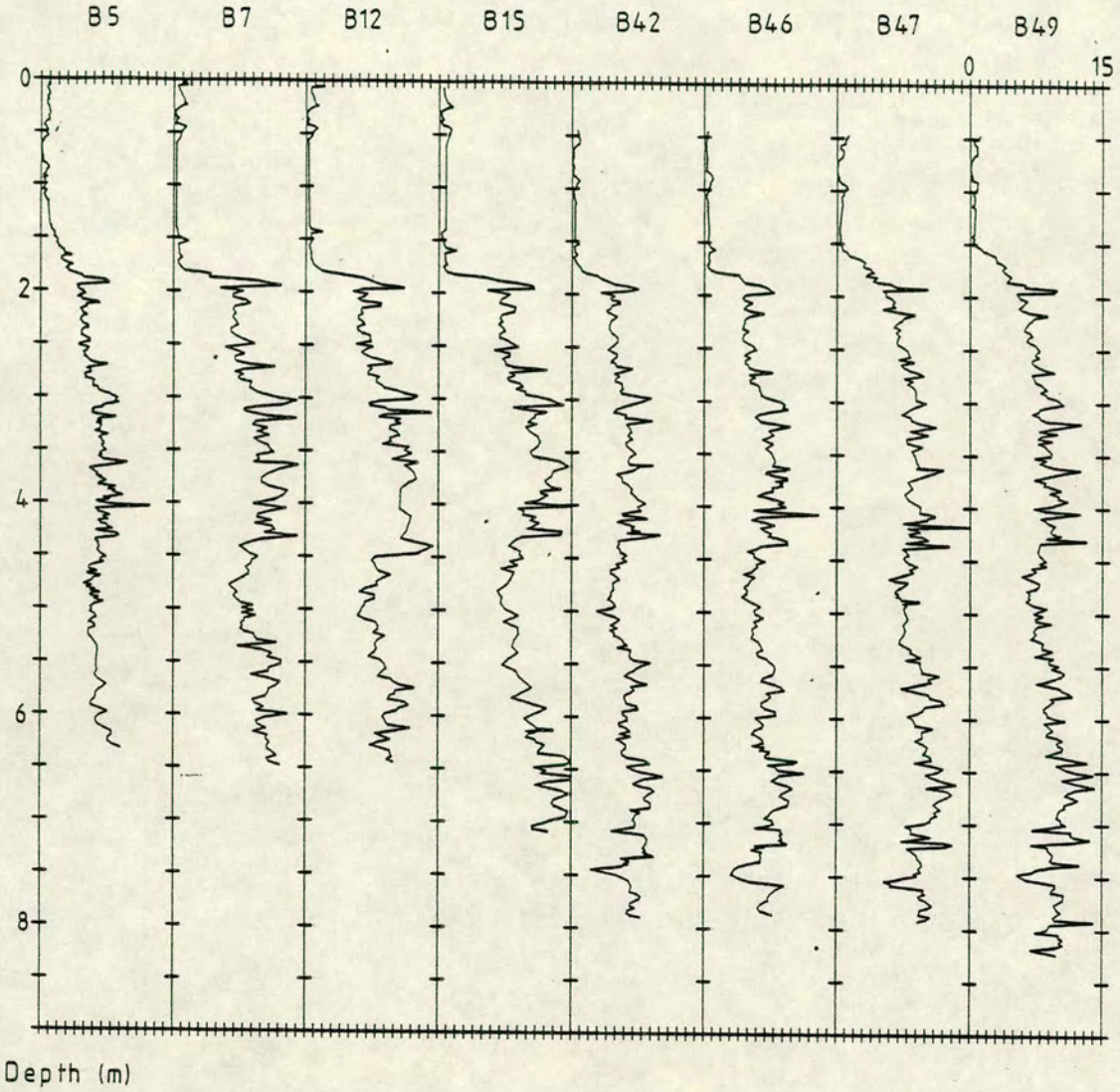

a) Declination

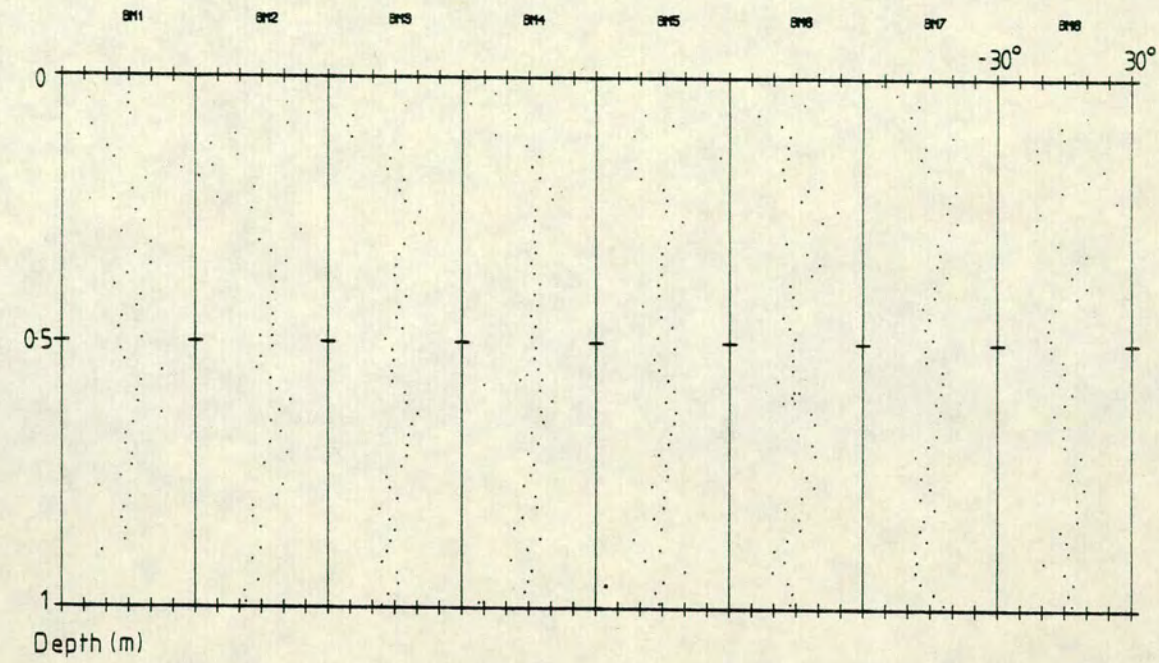

b) Inclination

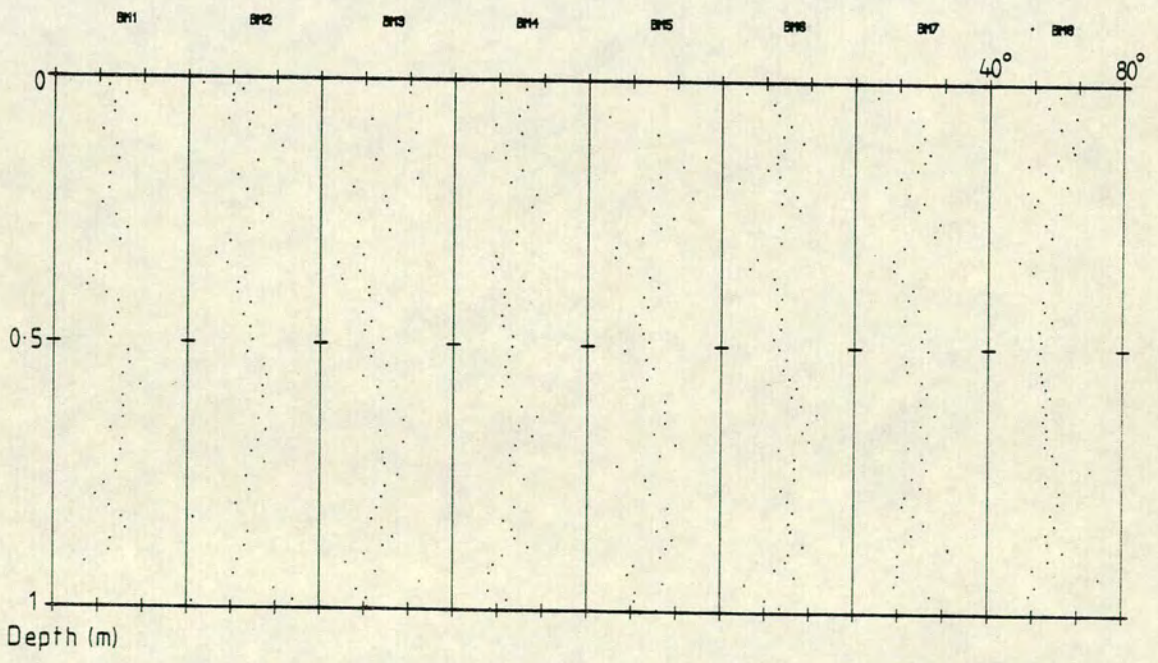

Figure 3.7 The records for the eight minicores described in the text in (a) declination, (b) inclination, (c) intensity (mA m^{-1}) and (d) susceptibility after transformation to the B49 depth scale.

c) Intensity

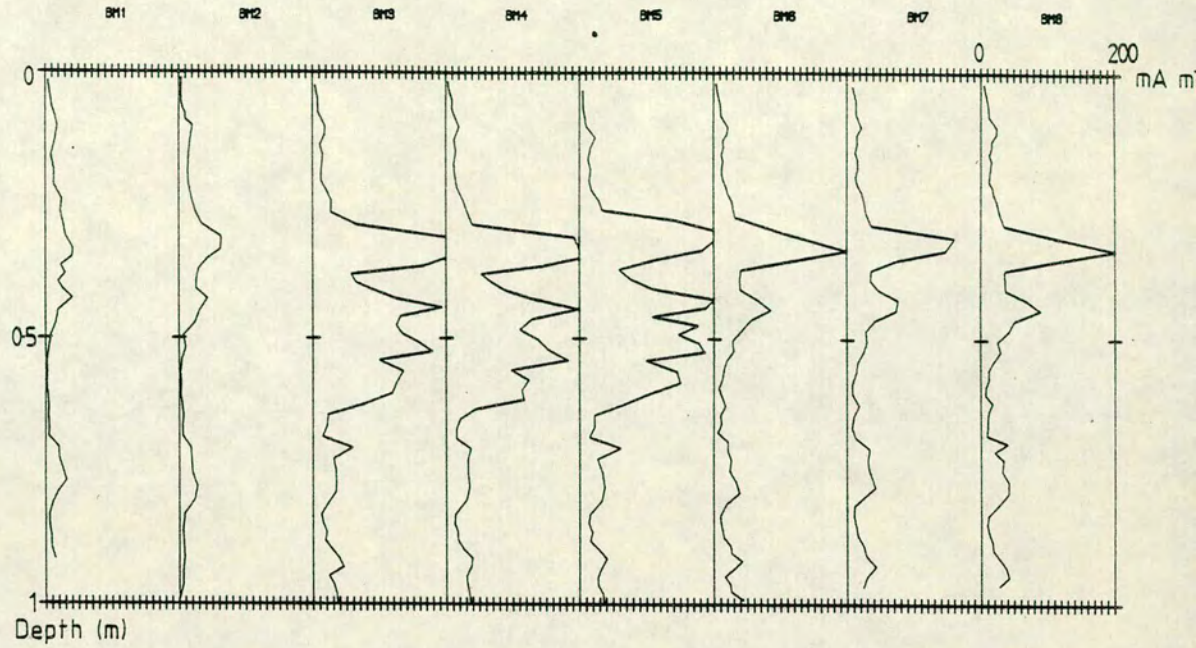

d) Susceptibility

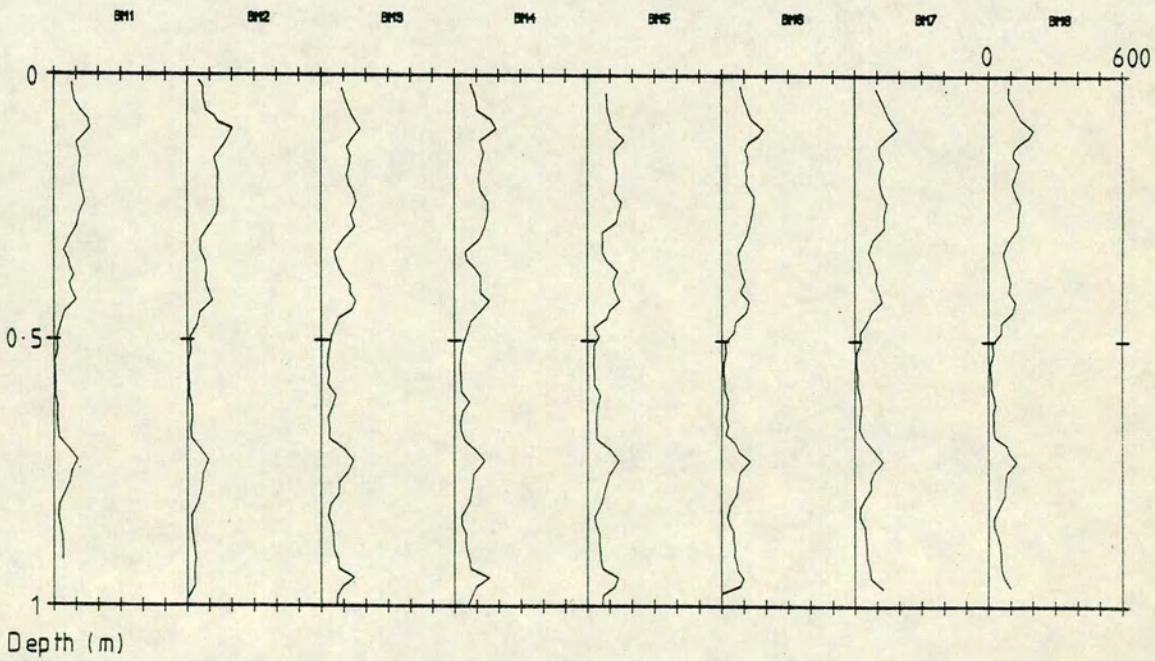

3.6 Conclusions

The cores obtained from Lac du Bouchet show a strong and stable remanence, especially in the sediments found below assemblage B. The initial comparison between cores using sedimentological boundaries and susceptibility reveal that the NRM of the different cores are coherent in time, despite the effects of varying rates of sedimentation. Matching the variations in intensity reveal that the directional data agree very well. These show a quasi-periodic variation on the depth scale independent of the sedimentological variations and it is highly probable therefore that they are geomagnetic in origin. The very wet sediment near the sediment/water interface are also easily correlated from core to core and reveal a similar pattern of oscillatory variations, with a smaller amplitude. The records from the minicores are much poorer quality than the long cores however. This is ascribed to the nature of the sediment and the rate of deposition, and shows how the changes in these rates can seriously affect the quality of the palaeomagnetic signal.

In order to interpret the meaning of these results it is necessary to establish a time scale to replace the depth scale (chapter 5). If the variations are definitely geomagnetic in origin (chapter 4) they can be analysed to find out the principle periods of variation and possible source geometries (chapter 6). In addition rather than use the rather crude method of normalisation by susceptibility, other methods may be able to reveal the variation in geomagnetic intensity recorded in the sediments (chapter 7). The results for the 12m cores, taken in April 1985, are summarised in chapter 8.

CHAPTER 4
IDENTIFICATION OF THE CARRIERS OF REMANENT MAGNETISATION

4.1 Introduction

The relaxation time of a magnetic grain depends not only upon temperature but also on its own size and the size of the magnetic domains within it. **Neel (1949,1955)** has shown that the relaxation time is proportional logarithmically to the volume of the grain and the reciprocal of absolute temperature. A sediment will consist of a variety of grains, some magnetic, which will have a spectra of relaxation times, ranging from a few seconds to millions of years. In order for it to be useful palaeomagnetically, it has not only to accurately record the direction of the field when it was laid down, but also to keep the acquired magnetisation for long enough to be measured. The relaxation time must obviously be greater than the age of the sediment in order for the NRM measurements made upon them to be valuable. To ascertain the stability of the remanent magnetisation carried by the sediment, it must be shown that the sediments have recorded a remanent magnetisation, and that this is the primary remanence obtained when the sediment was laid down by the mechanism of PDRM, or a secondary remanence that can be removed to obtain information about the primary. If this is the case, then the relaxation time of the bulk of the minerals carrying the remanence must be greater than the age of the sediment.

In addition a knowledge of the coercive spectrum of the grains carrying the NRM, and those of the grains acquiring an IRM and ARM can help identify the likely magnetic minerals that are carrying the remanence. Measurements of the growth of IRM and ARM can help identify the distribution of grain sizes of the carrier and possible domain states. From this can be defined normalising parameters, for relative intensity estimations (see chapter 7). High temperature, high field, susceptibility measurements are also described. These reveal the Curie points of the magnetic minerals that are present.

Note that the order in which the results are presented is not the order in which the experiments were carried out as some of the measurements are destructive. The sequence of measurements carried out upon the suite of subsamples taken from the set of cores from Lac du Bouchet was

(i) Measurement of NRM
(ii) Step demagnetisation of pilots taken from cores B47 and B49.
(iii) Bulk demagnetisation in a peak alternating field (af) (10mT) determined from an examination of the results of (ii) and remeasurement
(iv) Measurement of the initial, low field susceptibilities
(v) ARM growth in the pilots taken from B47 and B49
(vi) Step af demagnetisation of the pilot ARMs
(vii) IRM growth to saturation and back IRM measurements on the pilots from core B49
(viii) Step af demagnetisation of the pilots' SIRM
(ix) Bulk ARM measurements in a peak field determined by an inspection of the results from (vi)
(x) Bulk SIRM measurements

The results of the first four sets of measurements have been described in chapter 3. Those of the last two sets are described in chapter 7; the remainder are described in this chapter.

4.2 Demagnetisation of a Remanent Magnetisation

There are two standard techniques for step demagnetisation of samples having a remanent magnetisation. Thermal demagnetisation (**Thellier and Thellier (1959)**) is not suitable for wet sediments as the drying effect of water removal and chemical changes may mask the characteristics of the true NRM carriers (and would also ruin the plastic sample boxes). Alternating field demagnetisation provides an alternative method by randomising the magnetic moments due to different coercivity bands within the material. The theory of af demagnetisation has been described by **Stacey (1963)** and is reviewed by **Collinson (1983)**.

To demagnetise a sample completely using an alternating field requires that all the different components of magnetisation within the sample be exposed to the changing field. This is achieved either by tumbling the sample within the field or by positioning the sample in three different orientations. The method

employed in this work for the demagnetisation of a sample was to demagnetise to the peak field level in three mutually perpendicular orientations and then reverse the third orientation and halve the peak field level. This method (**Snape (1971)**) presents each component of the sample to the demagnetising field and reduces the effect of any instrumental ARM. Odd harmonics of the alternating field induce a small ARM in each of the orientations in which the sample is placed during the demagnetisation. For small values of the peak field the demagnetisation in the second and third orientations removes the small component of ARM induced during the first and second orientations respectively. This means that only the ARM induced during demagnetisation in the third orientation need be removed. **Snape (1971)** showed that the ARM induced in the sample during demagnetisation in a fourth orientation, the reverse of the third, in half the peak field, was sufficient (for practical purposes) to cancel that induced in the third.

The demagnetising coils lie within mumetal shields, thus there is, approximately, a zero field at the centre of the coils, where the sample is placed. All samples were transported and stored after demagnetisation and prior to measurement within mumetal shields. The volume affected by the coils of the demagnetiser allows the simultaneous demagnetisation of eight samples; tumbling would allow fewer samples. The same sequence of sample orientations was used for all demagnetisations, tests showed that this sequencing did not affect the demagnetisation results.

4.3 Demagnetisation results

The results for the step demagnetisation of the NRM, SIRM and ARMs are presented in the next sections.

4.3.1 Demagnetisation of NRM

A suite of samples from cores B47 and B49 were subjected to step af demagnetisation using the method described above. About ten per cent of the samples from a core (32 in total) were taken from each core. The pilots were chosen by accepting (at random) all subsample numbers ending in one. All the samples were found to have two remanent magnetisations. The first was found to be unstable to fields greater than 7 - 8 mT and has been identified as a secondary, viscous remanence associated with low coercivity grains. The

second component was stable up to a field of 60 mT and has been identified as a primary remanent magnetisation acquired when the water level within the sediment reduced sufficiently to allow the magnetisation to become fixed. Some samples acquired a high field ARM in 80 mT attributed to instrumental effects (each orientation would need to be reversed and halved to allow for the high peak field instrumental ARM induced by the odd harmonics (**Snape (1971)**)). Some examples of the demagnetisation of samples from different levels from pilots from core B49 are shown in **figure 4.1**.

The loss of remanent magnetisation intensity with increasing values of the peak af field is illustrated in **figure 4.1b**. This illustrates some typical demagnetisation results for six samples taken from the six different sediment assemblages defined for the top 8.5m of the Bouchet cores. These pilots are all taken from core B49, pilot S1 from assemblage A and pilots S31, S51, S151, S231 and S301 from assemblages B to F respectively. The NRM intensity changes with depth but the demagnetisation results remain essentially identical. Such behaviour emphasizes the differences in the quantities of magnetic minerals but indicates that their properties are very similar throughout the core. The field at which half the original remanent magnetisation is lost, the median destructive field (MDF), lies usually within the range 15 - 20 mT, with the exception of pilot S31. This shows a slightly 'harder' coercivity spectrum than the other pilots. Having been taken from the very organic assemblage B the quantity of magnetic minerals is slightly less than for other pilots but there must also be a difference in their nature. The extra 'hardness' could be ascribed to an increase in the number of single domain (SD) grains or a change in the type of mineral. The values of the MDFs for the pilots from B49 are given in **table 4.1**.

That the primary remanent directions are stable can be seen from an inspection of **figures 4.1a** and **4.1c**. **Figure 4.1a** shows the declinations and inclinations plotted on a stereographic projection. Tight clustering means that the angles remain constant as the peak af field increases. Most of the examples show this tight clustering, with α_{95} values ranging from 2° to 10°. **Table 4.1** also gives the α_{95} values for all the pilots. It can be seen that the pilots taken from the assemblages C, D E and F have particularly small α_{95} values indicating the excellent NRM recording abilities of these levels. The two uppermost levels produce slightly more scattered values but still remain quite well clustered (10-20°).

This angular stability can also be seen by the use of Zijderveldt diagrams (**As and Zijderveldt (1958)**), plotting the north component against east and down

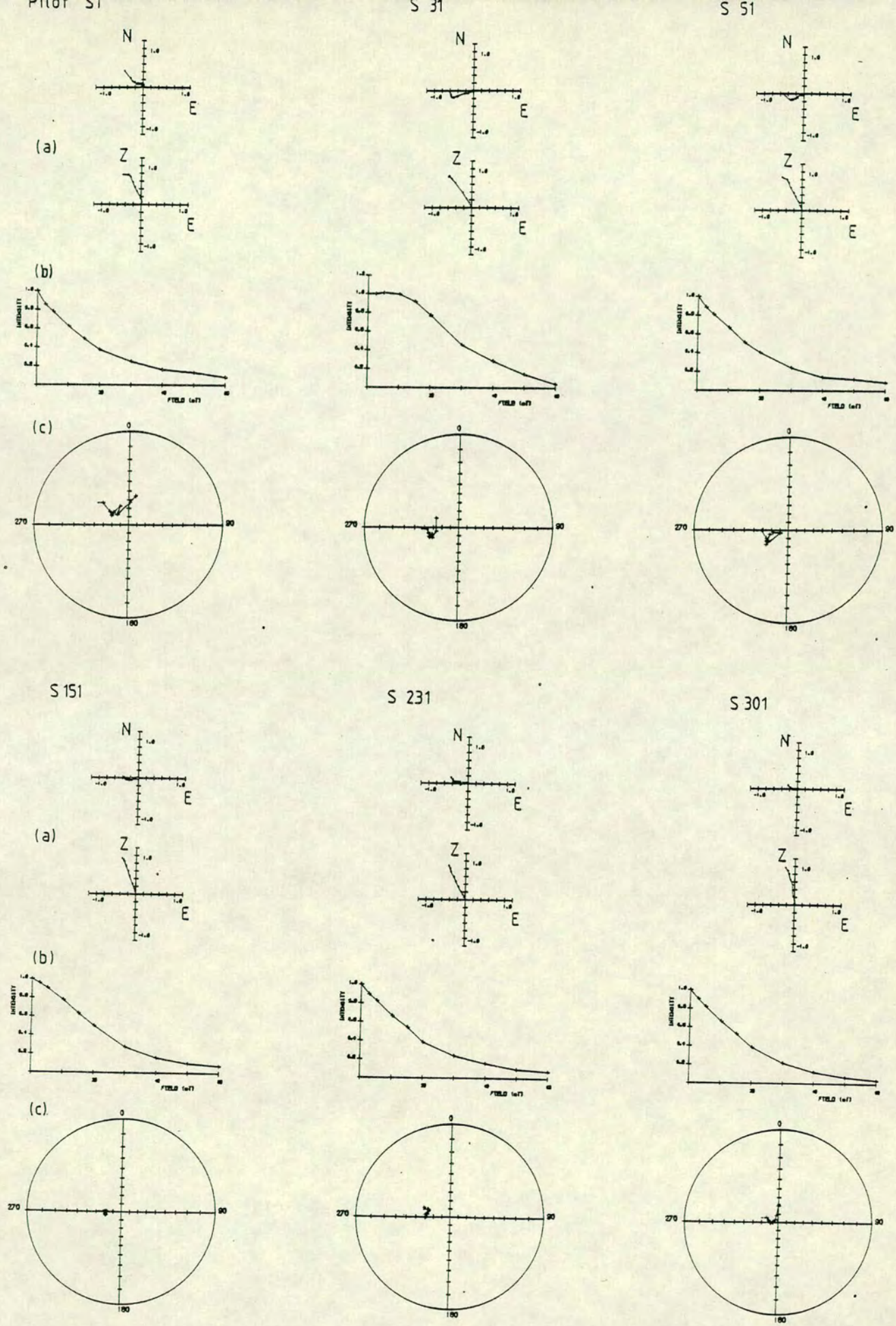

Figure 4.1 The step af demagnetisation of six typical pilots from core B49 showing (a) the normalised Zijderveldt plot, (b) the variation of normalised NRM intensity and (c) the stereographic projection for each of the pilots.

Table 4.1: Variation of the MDF of the NRM, ARM and SIRM with depth including the α_{95} values for the NRM for core B49.

		MDF (mT)							
No.	Z(cm)	NRM	ARM (30mT)	ARM (40mT)	ARM (50mT)	ARM (60mT)	ARM (80mT)	SIRM	α_{95}
1	45.0	14.6	14.0	16.3	19.2	18.9	21.1	15.0	13.76
11	69.5	21.2	15.0	16.0	19.7	21.2	23.1	17.1	10.20
21	94.0	17.1	15.5	18.0	20.8	21.3	23.3	15.2	17.35
31	135.0	28.5	16.9	20.0	23.0	25.2	26.4	17.5	7.60
41	159.0	16.7	15.4	17.7	20.7	20.4	22.2	15.5	23.78
51	183.0	15.4	15.3	17.7	20.2	20.5	22.6	16.8	8.15
61	205.3	18.4	14.5	16.7	19.4	19.1	21.2	15.1	4.78
71	228.6	18.7	14.5	16.8	19.2	19.0	20.9	14.9	3.17
81	251.9	18.2	14.3	16.9	19.5	19.1	21.2	15.4	4.70
91	275.2	18.5	14.5	16.8	18.7	19.1	20.0	14.8	3.87
101	298.5	20.6	14.0	16.2	18.5	18.9	20.9	14.3	3.24
111	321.8	18.2	14.3	16.6	18.7	19.1	20.9	15.1	3.59
121	345.0	17.1	14.6	16.7	19.2	19.6	21.5	15.0	3.77
131	370.0	21.6	14.9	17.2	19.5	19.8	21.6	15.6	4.94
141	395.5	19.3	14.5	16.7	19.1	19.5	21.4	14.4	4.47
151	418.9	20.0	14.7	16.9	19.3	19.6	21.2	15.2	2.29
161	442.5	17.2	14.4	17.2	19.3	19.4	21.1	15.4	4.32
171	466.2	15.8	14.5	17.1	18.9	18.8	20.1	15.1	5.33
181	489.8	17.6	14.5	17.1	19.1	19.4	21.4	15.0	2.94
191	513.5	16.7	14.6	17.2	19.1	19.2	21.1	14.6	5.44
201	537.1	15.6	14.4	17.2	19.1	19.0	20.6	15.1	8.53
211	560.7	17.0	15.0	16.0	19.7	21.2	23.1	17.1	2.44
221	584.4	16.6	14.6	17.2	19.2	19.3	21.5	14.7	4.00
231	608.0	16.2	14.7	17.3	19.3	19.4	21.5	14.6	3.83
241	631.3	16.5	14.6	17.2	19.3	19.6	21.4	15.8	7.71
251	654.9	15.5	14.8	17.4	19.2	19.5	21.2	15.6	11.68
261	678.5	17.3	14.5	16.9	19.1	19.5	21.9	15.7	17.98
271	702.2	15.3	14.2	16.8	18.9	18.8	20.8	14.6	7.02
281	725.8	16.7	14.7	17.3	19.4	19.7	20.8	15.6	6.40
291	749.5	9.5	14.2	16.5	18.3	18.5	19.5	15.1	21.99
301	773.1	15.9	14.9	17.5	19.4	19.9	21.2	15.2	8.33
311	796.7	10.0	14.5	17.0	18.8	19.1	20.3	15.3	12.18

respectively. These have been normalised and in general reveal two straight lines. The first line is the viscous remanence lost after a peak field of 7 - 8 mT is reached and the second field is the primary remanence, seen to be stable since the direction remains constant as the intensity reduces to zero (**figure 4.1c**).

4.3.2 Demagnetisation of SIRM

The growth of SIRM (both forward and back) is described in the next section. The results of the demagnetisation of the SIRM for the same pilots from core B49 are shown in **figure 4.2**. All the MDF values are also shown in **table 4.1**, these are found to be in a similar range (14 - 18 mT) as for the NRM demagnetisations. The MDF values do however show a consistent trend to be lower than those of the NRM. This indicates that the spectrum of coercivities affected by the SIRM is in general 'softer' than that of the NRM. All the samples gave a single remanent direction at all levels of the demagnetisation again indicating the stability of the magnetic carriers.

4.3.3 Demagnetisation of ARM

The step demagnetisation of the ARM acquired in different peak fields has been examined. Five different peak field levels were used, 30, 40, 50, 60 and 80 mT respectively, although the DC bias field was left constant at 0.1mT. The results are consistent, with the lower peak field ARMs tending to give lower MDF values. The MDF values for each pilot given in **table 4.1**, and the demagnetisation plots shown in **figure 4.3**, indicate that the high field ARMs affect the higher coercivity grains in the sample, as would be expected. In particular, note that the different ARMs give consistent MDF values down the core, remaining essentially constant within each ARM level. This can be seen more clearly in **figure 4.4**, which shows the variation of MDF with depth down core B49 and indicates how the coercivity spectra of the ARMs increases at different peak fields.

4.3.4 Comparison of the demagnetisation results

The actual shape of the demagnetisation plot obtained depends on the coercivity spectrum of the carriers of the remanent magnetisation. A direct

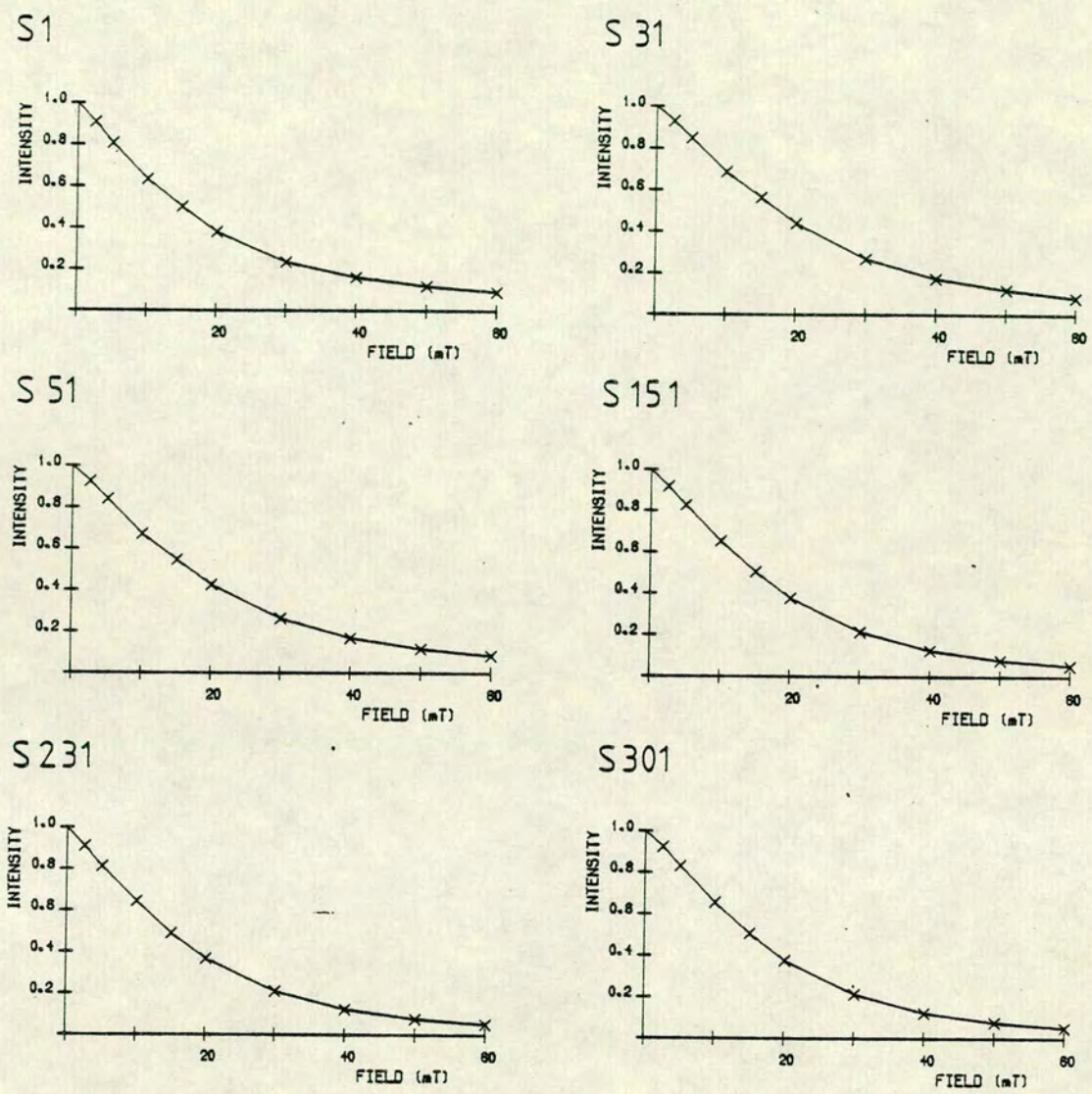

Figure 4.2 The step demagnetisation of the SIRM given to six typical pilots down core B49; the intensity has been normalised.

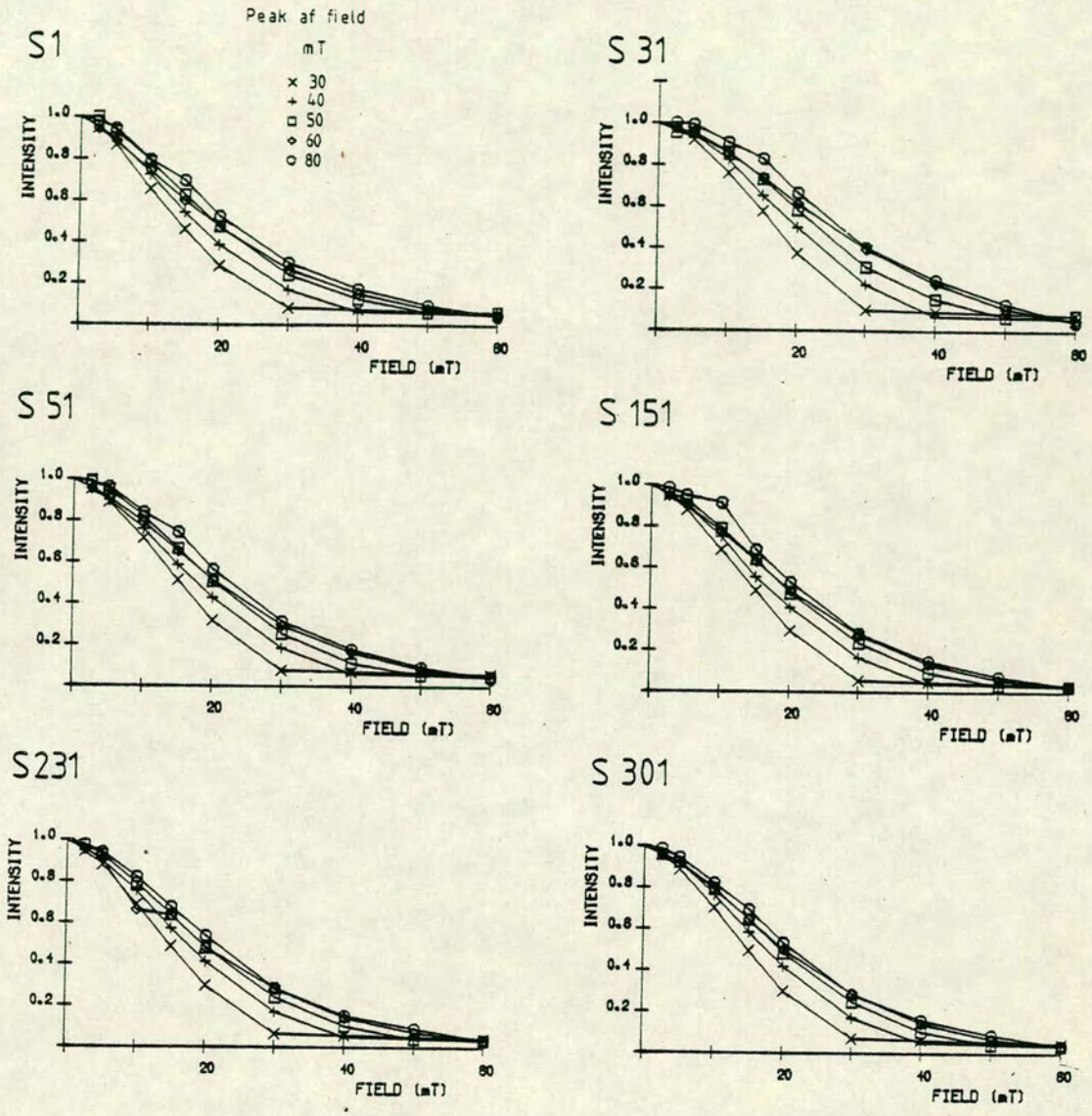

Figure 4.3 The step demagnetisation of the ARM acquired in five different peak fields for the six typical pilots from core B49.

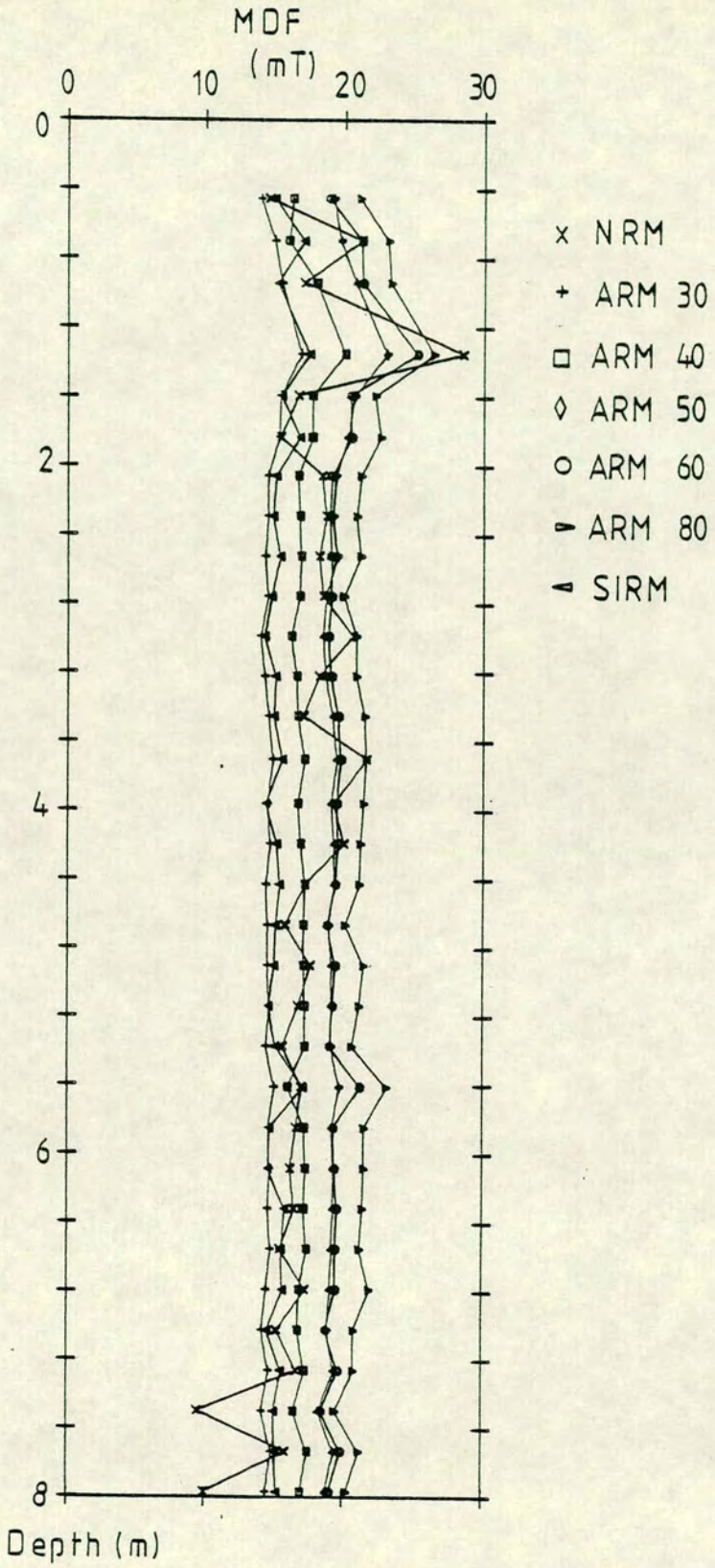

Figure 4.4 The variation of the MDF found during demagnetisation of the NRM, the SIRM and five different ARMs for the six typical pilots from core B49.

comparison of the demagnetisation results from the samples from core B49 shows that although the individual samples are very similar there are slight differences in the shape. For clarity the ARMs given in peak fields of 40 mT and 60 mT are not included in **figure 4.5** which shows the demagnetisation plots for the different types of remanent magnetisation.

Generally the demagnetisation plot of the SIRM lies below that of the NRM, i.e. the coercivity spectrum affected by the SIRM is slightly 'softer' than that of the NRM. The spectra are, however, very close, as can be seen from both **figures 4.4** and **4.6**. **Figure 4.4** shows the variation of the MDF with depth down core B49 for different types of remanent magnetisation. The variations are very similar and show that in general grains of a similar coercivity are being affected by the different types of remanent magnetisation. The average values of the MDF (about 17mT) show that the haematite content is very low (since this has a much higher coercivity of remanence, about 0.1–0.5T (**Collinson (1983)**)). As the MDF values are low, even for magnetite, it seems that there is a high percentage of multidomain (MD) grains. The average gradient obtained by plotting the normalised NRM against the normalised SIRM is found to be 0.99 (**figure 4.6, table 4.2**). This indicates a remarkable similarity between the coercive spectra affected by the NRM and the SIRM. This is despite the fact that the SIRM intensities are typically 2,000–5,000 times greater than those of the NRM.

All the ARMs give average gradients greater than 1, with that of the ARM at 60 mT being closest at 1.05. Note that the standard deviation of the ARM gradients are less than those of the SIRM, indicating a slightly greater consistency.

The results indicate that the likely carrier is magnetite. Certainly high coercivity haematite can be ruled out from the values of the MDF, although low coercivity haematite cannot be. There is a very small spectrum of coercivities however, as illustrated by the changes in the demagnetisation plot for ARMs at different levels of peak af field. This indicates that the magnetite content down the core is remarkably uniform in grain size, despite there being variations in the concentrations. This aspect is investigated more in chapter 7.

Using the conclusions of **Lowrie and Fuller (1971)** modified for use with ARM rather than TRM (**Johnson et al. (1974)** the best matching ARM coercivity spectrum lies above those of the NRM and SIRM indicating the likely carrier to be either pseudo-single domain (PSD) or MD magnetite.

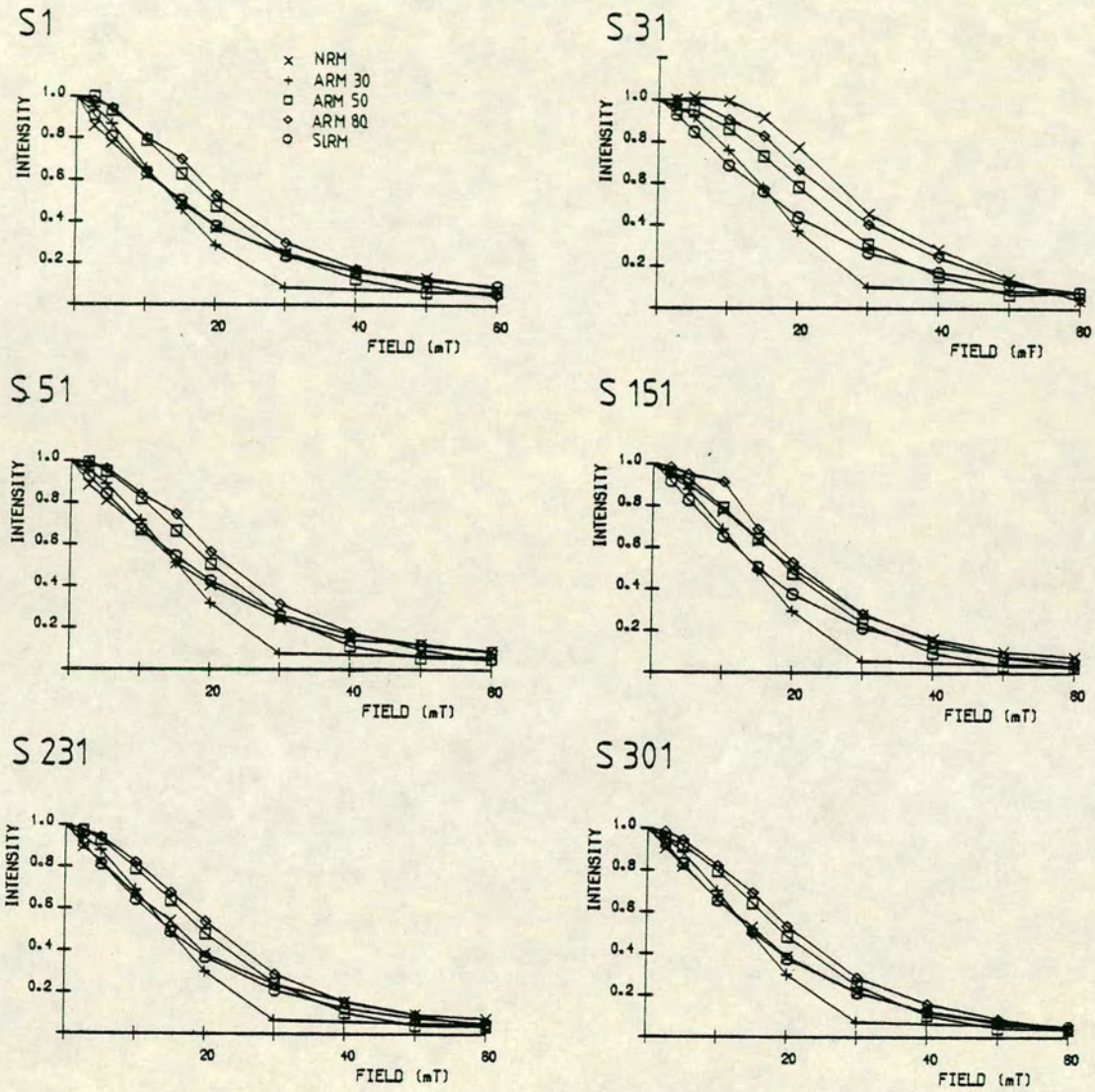

Figure 4.5 A direct comparison of the step demagnetisations of the NRM, the SIRM and three of the ARMs given to the six typical pilots from core B49.

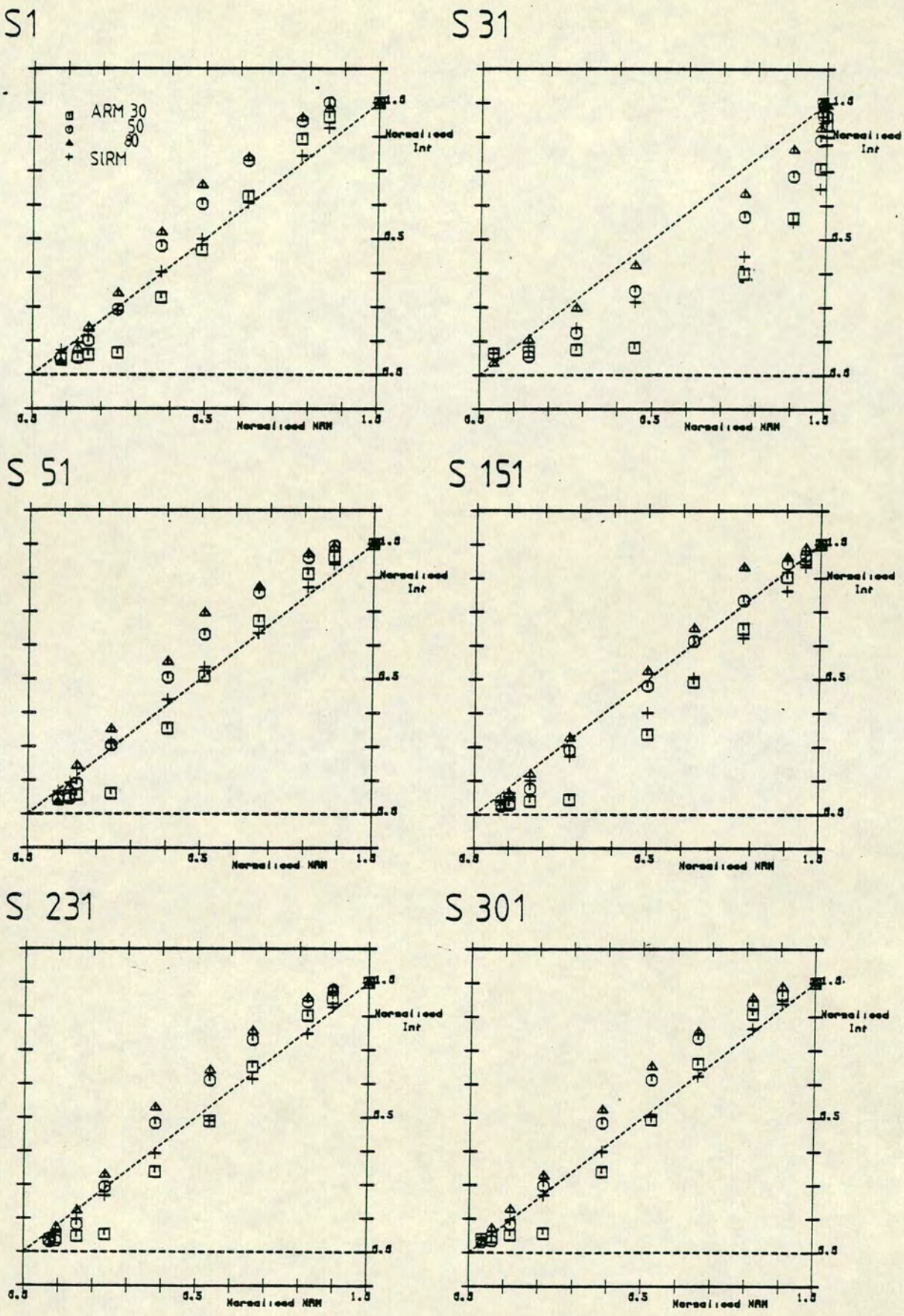

Figure 4.6 A least squares comparison of the step demagnetisations of the NRM, the SIRM and three of the ARMs given to the six typical pilots from core B49.

Table 4.2: Variation of the gradients of the least squares straight line between the normalised NRM demagnetisation results and the normalised results of ARM and SIRM.

		Least squares gradient					
No.	Z(cm)	ARM (30mT)	ARM (40mT)	ARM (50mT)	ARM (60mT)	ARM (80mT)	SIRM
1	45.0	1.179	1.186	1.169	1.109	1.128	1.035
11	69.5	1.094	1.110	1.020	1.028	1.078	0.924
21	94.0	1.095	1.112	1.096	1.050	1.076	0.959
31	135.0	0.939	0.991	0.973	0.942	0.983	0.834
41	159.0	1.162	1.162	1.152	1.105	1.127	1.011
51	183.0	1.158	1.149	1.156	1.084	1.106	1.019
61	205.3	1.052	1.059	1.049	1.005	1.045	0.940
71	228.6	1.079	1.081	1.074	1.024	1.060	0.964
81	251.9	1.066	1.079	1.068	1.027	1.075	0.959
91	275.2	1.072	1.075	1.069	1.024	1.076	0.966
101	298.5	1.076	1.081	1.074	1.036	1.082	0.972
111	321.8	1.112	1.113	1.099	1.066	1.164	1.002
121	345.0	1.083	1.081	1.079	1.034	1.072	0.961
131	370.0	1.079	1.089	1.076	1.037	1.085	0.968
141	395.5	1.062	1.077	1.057	1.026	1.066	0.969
151	418.9	1.089	1.093	1.086	1.040	1.086	0.976
161	442.5	1.095	1.164	1.088	1.042	1.064	0.996
171	466.2	1.115	1.114	1.093	1.056	1.075	0.993
181	489.8	1.091	1.095	1.080	1.041	1.057	0.991
191	513.5	1.120	1.125	1.103	1.083	1.081	1.009
201	537.1	1.079	1.079	1.042	1.009	1.018	0.948
211	560.7	1.092	1.101	1.090	1.045	1.059	0.996
221	584.4	1.088	1.087	1.068	1.029	1.041	0.982
231	608.0	1.140	1.141	1.127	1.059	1.091	1.029
241	631.3	1.129	1.117	1.096	1.064	1.075	1.007
251	654.9	1.124	1.134	1.110	1.051	1.084	1.028
261	678.5	1.133	1.133	1.122	1.068	1.083	1.017
271	702.2	1.150	1.196	1.127	1.088	1.103	1.047
281	725.8	1.096	1.097	1.079	1.039	1.052	0.976
291	749.5	1.366	1.268	1.224	1.187	1.194	1.165
301	773.1	1.097	1.104	1.074	1.041	1.054	1.002
311	796.7	1.200	1.178	1.145	1.101	1.109	1.071

The ability of the SIRM and ARMs to mimic the coercivity spectrum of the NRM has been used in an attempt to normalise the sedimentological effects of intensity in the hope of obtaining an estimate of the variation of the geomagnetic field intensity. This is discussed in detail in chapter 7.

4.4 IRM Measurements

The step demagnetisation of the SIRM has been discussed in the previous section. To establish the field required to saturate the sample remanent magnetisation, (H_{sat}), the growth of IRM was measured with field. A Molspin Ltd. pulse magnetiser was used to give pilots a magnetisation in increasing field values. Before starting the samples were completely demagnetised in an 80 mT peak af field. On reaching saturation the samples were given an IRM in increasing values of field in the reverse direction. The results are shown in **figure 4.7** and the values obtained for H_{sat}, the saturation remanent magnetisation (M_{sat}), the coercivity of remanence (H_{CR}) and the S_{100} values (**Stober and Thompson (1979)**) are given in **table 4.3.**

The field required to saturate the samples appears not to have been reached in any of the samples but the non saturated content is not great. A level of 95% saturation is reached in all samples before 200mT and it is this value that has been taken as M_{sat}. The values of H_{CR} are between 37 and 39 mT for almost all the samples. Again both results are indicative of MD magnetite. The ratio between saturation remanence and the sample susceptibility also gives an indication of the domain size within the sample. The SIRM will be larger for SD grains and smaller for multi domain grains; the inverse of the variation for the susceptibility. Thus the closer the ratio is to zero the more likely the carrier is MD. The ratios here show the samples' MD nature with ratios of about 50 - 500 A m^{-1} (compared with that of SD magnetite which is about 5 x 10^4 A m^{-1}).

That there is a slight haematite content within the samples is illustrated by the continued growth of IRM even in very large fields. The S_{100} value is the modulus of the ratio of the back IRM at 100mT to the back SIRM. The closer this is to 1, the closer the sample has become to saturation at 100mT and the greater the importance of pure magnetite as a carrier. The values of S_{100} cluster around 0.8 indicating the haematite content. That this is not fine grained has been illustrated by the demagnetisation diagrams (**figure 4.1b**). Any MD haematite would offer little effect to the NRM values measured, being swamped by the magnetisation of the magnetite.

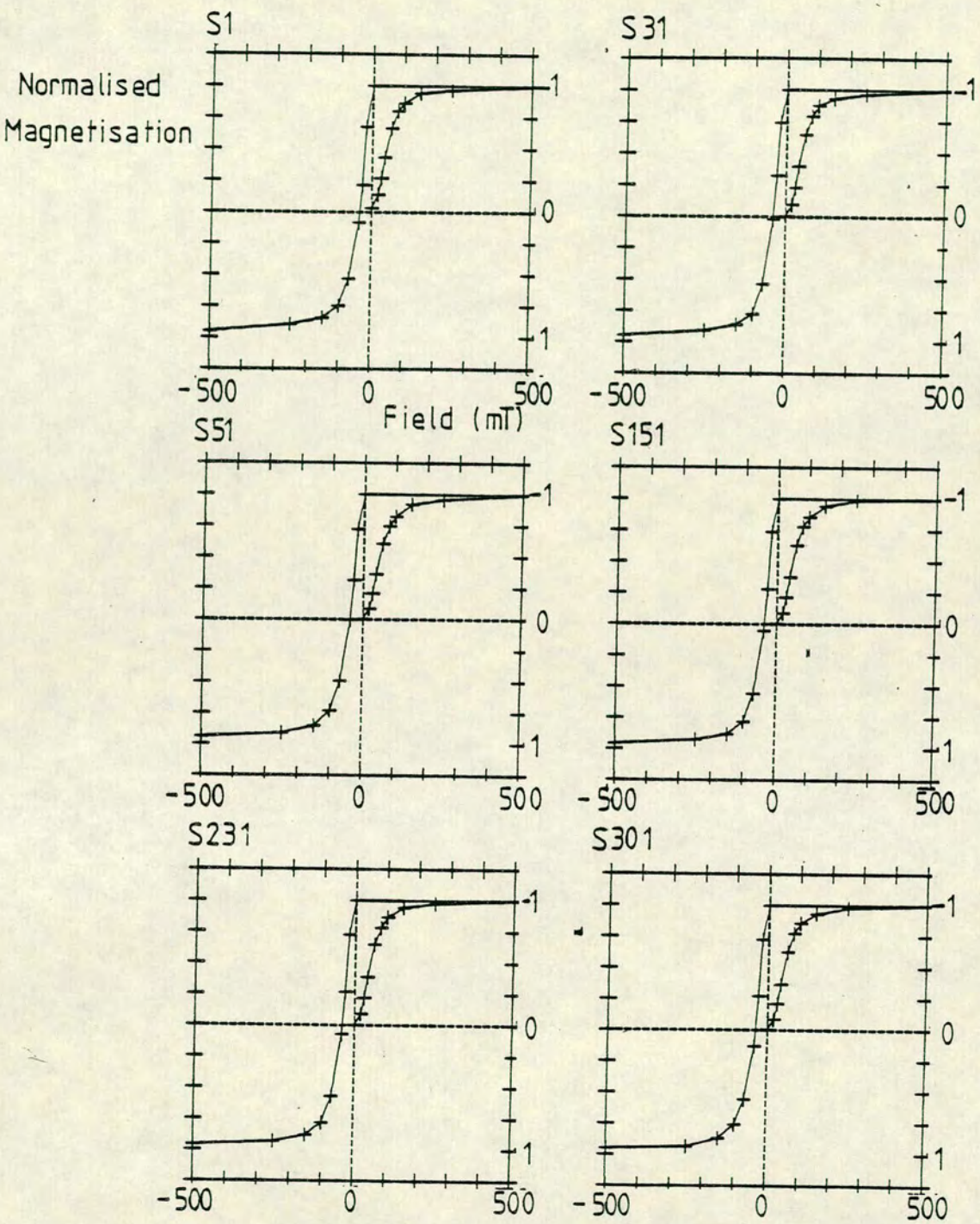

Figure 4.7 The growth of IRM and back IRM for the six typical pilots taken from core B49.

Table 4.3 Variation of IRM growth parameters with depth for the pilots taken from core B49.

No.	Z(cm)	M_{sat} (Am^{-1})	H_{sat} (mT)	H_{CR} (mT)	S_{100}
1	45.0	16.70	173.10	37.27	0.79
11	69.5	1.75	333.80	39.45	0.67
21	94.0	15.86	229.60	38.66	0.75
31	135.0	5.45	202.10	39.41	0.82
41	159.0	34.10	153.70	37.23	0.83
51	183.0	78.46	224.00	39.98	0.78
61	205.3	111.42	153.10	37.88	0.82
71	228.6	102.30	148.90	37.94	0.82
81	251.9	94.33	196.80	38.05	0.82
91	275.2	124.75	148.00	37.49	0.83
101	298.5	168.32	153.90	37.10	0.83
111	321.8	132.16	169.50	38.27	0.81
121	345.0	135.18	147.30	37.57	0.83
131	370.0	113.83	209.80	38.47	0.80
141	395.5	162.22	160.60	37.36	0.83
151	418.9	119.38	167.90	38.43	0.82
161	442.5	117.82	200.20	38.21	0.80
171	466.2	94.72	175.10	37.92	0.82
181	489.8	110.42	147.90	38.31	0.82
191	513.5	117.50	177.70	38.19	0.81
201	537.1	148.36	179.60	37.60	0.81
211	560.7	152.92	149.20	37.54	0.83
221	584.4	147.32	181.60	37.67	0.82
231	608.0	155.22	166.80	37.92	0.82
241	631.3	155.14	207.80	38.61	0.79
251	654.9	171.82	173.70	38.31	0.81
261	678.5	212.47	185.40	38.94	0.79
271	702.2	139.28	184.40	36.74	0.80
281	725.8	140.67	165.30	38.15	0.80
291	749.5	75.51	171.30	37.77	0.79
301	773.1	174.87	184.90	36.81	0.80
311	796.7	133.72	212.90	37.36	0.77

The incremental coercivity spectra for the six pilots discussed earlier, for the growth of IRM, are shown in **figure 4.8**. This shows the proportion of the SIRM grown in each increment of the applied field. The distributions show the most important range of coercivities to lie around 50mT, as would be expected for MD magnetite. Note also the great similarity of the coercive spectra for all the samples, showing the remarkable uniformity of the magnetite.

Some pilots were treated again with increased field values in the original direction thus completing a full remanent hysteresis loop cycle (**figure 4.9**). The forward H_{CR} values were in complete agreement with the back values as was H_{sat}. However an interesting feature of all the IRM growth results is that the original M_{sat} value obtained never seems to be reached a second time. Both the reverse saturation magnetisation and the second forward saturation magnetisation remain at about 95% of the original level. This is a very difficult phenomenon to explain and may be due either to viscous components only excited by the original forward IRM or to some effect caused by the experimental procedure or apparatus.

4.5 Growth of ARM

The growth of IRM can indicate the relative quantities of magnetic minerals and the likely type. The growth of ARM provides more information about the coercivity spectrum. **Figure 4.10** shows the incremental coercivity spectra for the growth of ARM with the same D.C. bias field but increasing values of peak field. The spectra again indicate the uniform nature of the magnetic mineral and the predominance of the low coercivity grains.

4.6 Thermomagnetic experiments

A series of experiments have been performed on the actual sediment and on magnetic extracts taken from the pilot core B49. These have been subjected to investigations into the variation of their high field susceptibility with temperature, using a translation balance. A description of the translation balance and its operation is given in **Collinson (1983)**. The Sirius microcomputer was also used to control the taking of measurements from the translation balance.

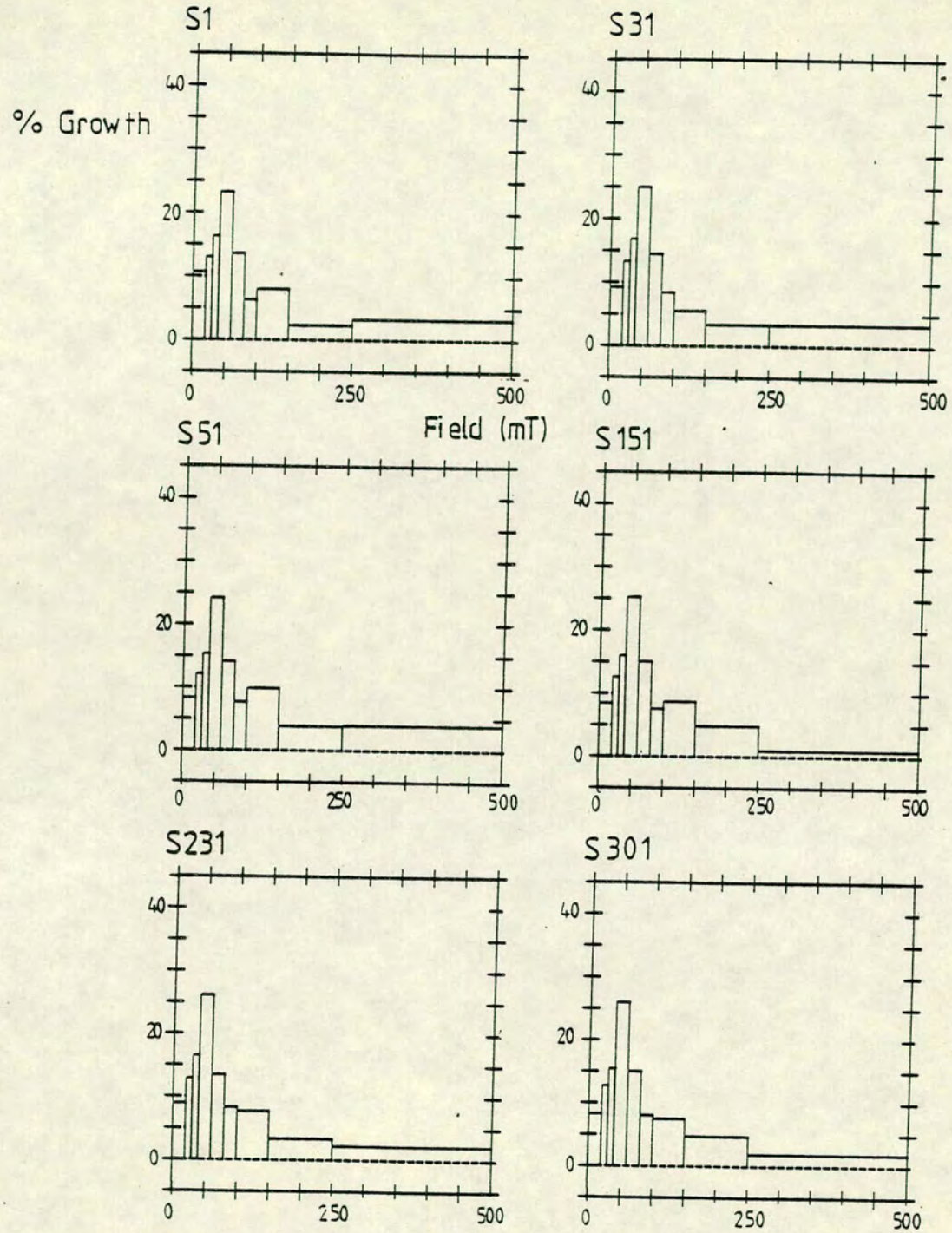

Figure 4.8 The incremental coercivity spectra for the six typical pilots taken from core B49 during the growth of IRM.

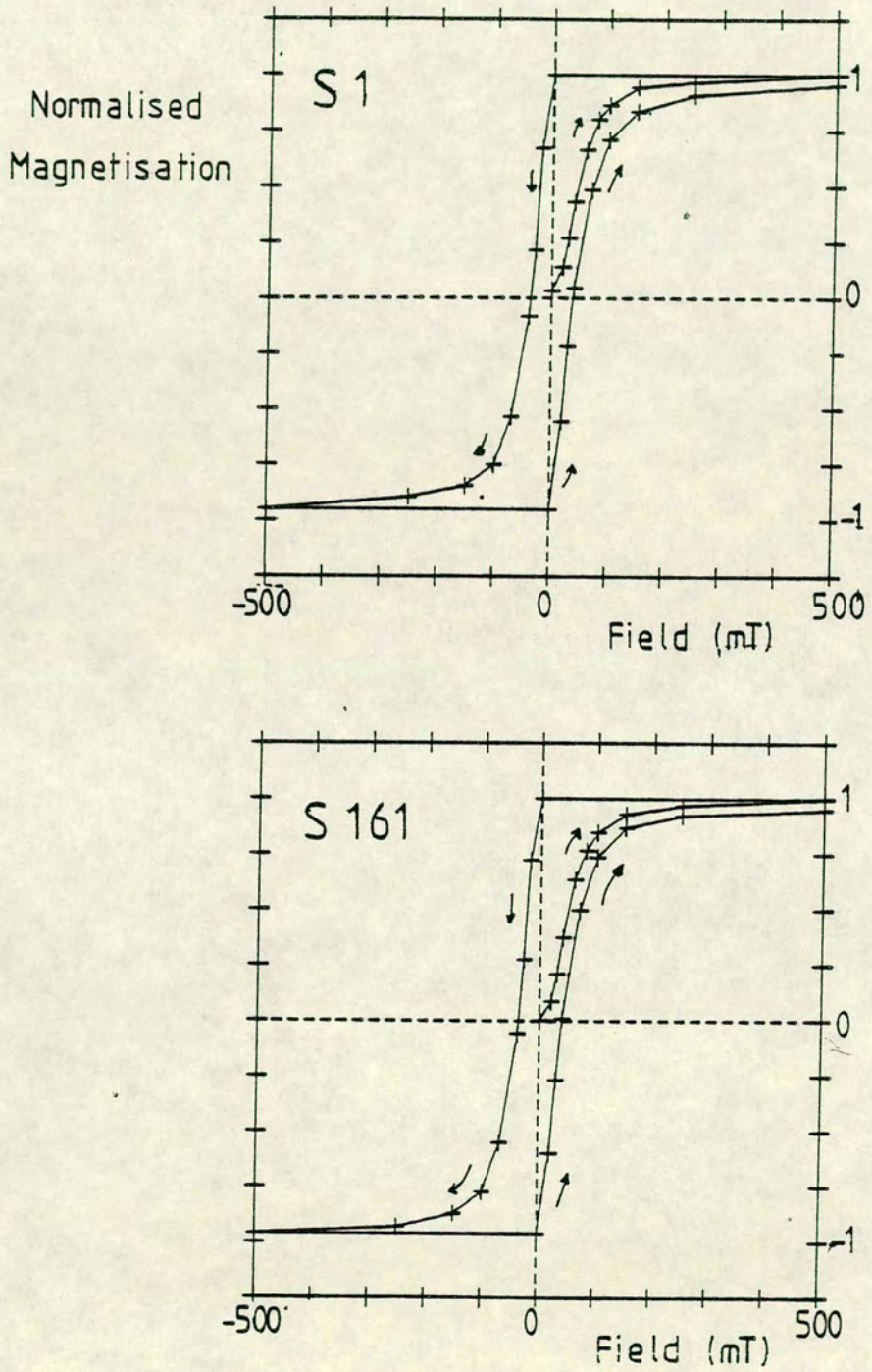

Figure 4.9 The remanent hysteresis loop found for two samples from core B49.

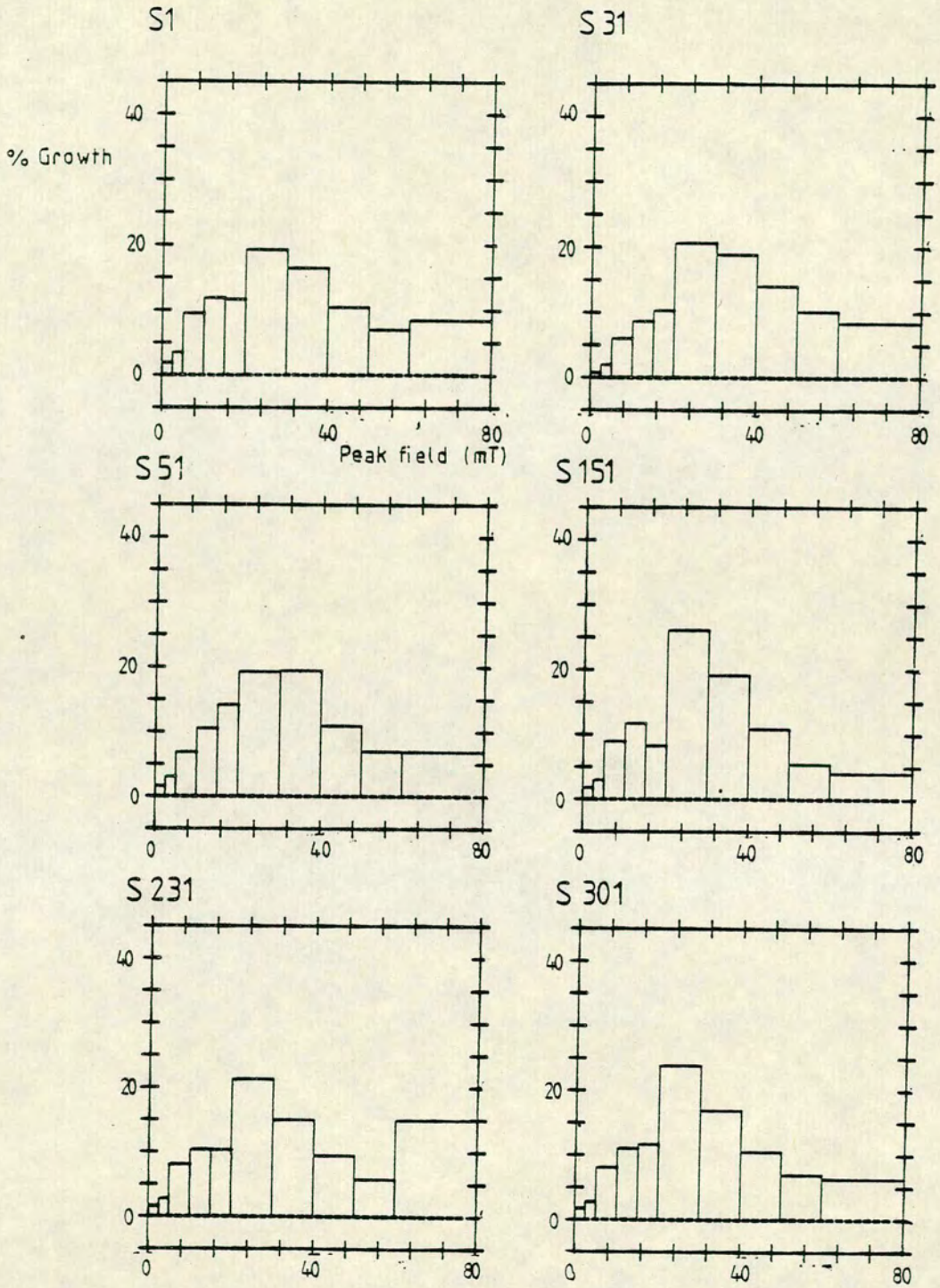

Figure 4.10 The incremental coercivity spectra for the six typical pilots taken from core B49 during the growth of ARM.

4.6.1 Obtaining the magnetic extract

Magnetic extracts were obtained from the raw sediment by constructing a continuous loop of sediment in excess water controlled by a peristaltic pump as used by **Papamarinopoulos (1978)**. The sediment passes through the poles of a horseshoe magnet where any magnetic minerals are held in the field gradient whilst the pump causes the non-magnetic fraction to be continuously moved. There is a large reservoir of sediment (in a beaker) from which the sediment is extracted and to which it is returned after passing through the poles of the magnet. The efficiency of the system is not as great as could be achieved by having a large magnetic gradient in direct contact with the solution but it is possible to obtain magnetic extracts.

4.6.2 Translation balance results

The extracts and the raw sediment were each subjected to the thermomagnetic experiments in an attempt to establish the Curie point of the sediments. The results are summarized in **table 4.4**. Typical results for the extract from pilot sample S161 from core B49 are shown in **figure 4.11a**. The results for the raw sediment from the same sample are shown in **figure 4.11b**. The Curie temperature for the extract is found to be about 550°C, about 30° more than for the raw sediment. An inspection of **table 4.4** confirms that this slight difference in Curie point affects all the samples and that the Curie points of the extract are slightly less than that of pure magnetite. (The figure given in **table 4.4** is the figure calculated for magnetite using the same equipment used in the Curie point determinations). The raw sediment also exhibits a strong growth of magnetisation in the initial stages of heating possibly due to reduction of the clay minerals to magnetite or haematite. However, since the 'alteration' is reversible and occurs at quite low temperatures (<120°C), it is more likely that the effect is purely instrumental. Such a pattern may arise if the sample arm was catching if it were moved too far by the field gradient. The rapid rise in magnetisation would be as the arm became free to swing again. However, inspection of the apparatus failed to reveal the cause. The results also indicate the very low quantity of haematite that must be present as neither analysis is capable of identifying its Curie temperature.

Table 4.4 Variation of the Curie points for raw and extracted sediment taken from pilots from core B49

No.	Z(cm)	Curie Points Raw (°C)	Extract (°C)
1	45.0	520 ± 40	520 ± 40
21	94.0	540 ± 40	550 ± 20
41	159.0	500 ± 40	540 ± 20
61	205.3	500 ± 40	540 ± 20
81	251.9	520 ± 40	520 ± 20
101	298.5	520 ± 40	550 ± 20
121	345.0	520 ± 40	550 ± 20
141	395.5	530 ± 40	550 ± 20
161	442.5	520 ± 40	550 ± 20
181	489.8	520 ± 40	550 ± 20
201	537.1	530 ± 40	560 ± 20
221	584.4	520 ± 40	540 ± 20
241	631.3	520 ± 40	550 ± 20
261	678.5	510 ± 40	550 ± 20
281	725.8	520 ± 40	550 ± 20
301	773.1	520 ± 40	540 ± 20
Magnetite		570 ± 10	

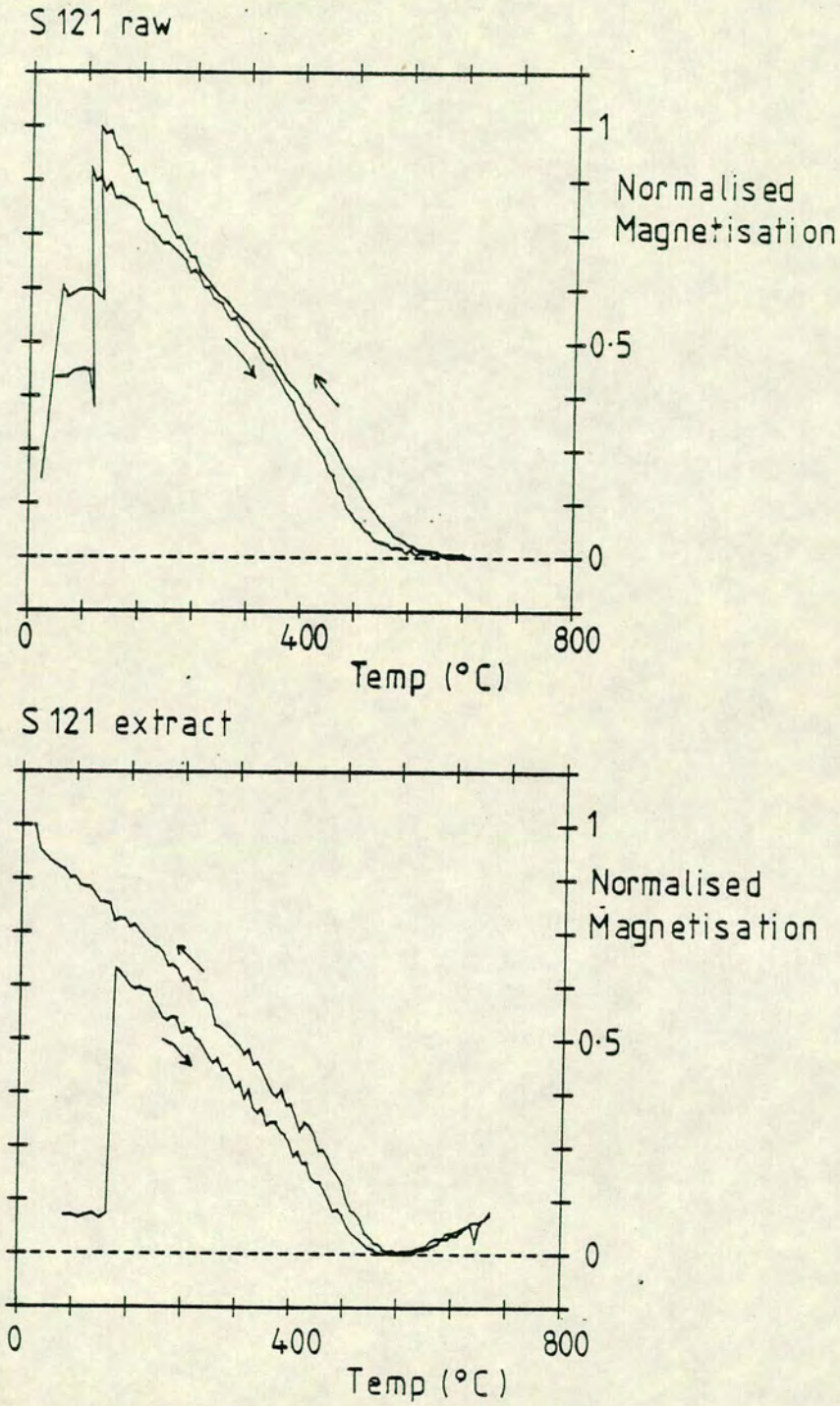

Figure 4.11 The variation of saturation magnetisation with temperature for a typical pilot sample taken from core B49 from the translation balance, showing the slightly different results for the raw sediment to the magnetic extract.

Since the Curie points determined for the extracts (and the raw sediments) consistently fall below the Curie point of magnetite (575° C) it seems likely that the carrier instead of being pure magnetite has a small titanium content. (Curie points reduce steadily from the value of 575° C for magnetite to less than zero for the titanium rich minerals in the solid solution series e.g. Ulvospinel).

4.6.3 Low temperature measurements

Attempts were made to produce a low temperature variation of SIRM. However, a problem arose in that the (very small) furnace aperture in which the sample was inserted very quickly froze, immobilising the balance arm and making accurate measurements impossible.

As an alternative, the pilots, which had been left with an SIRM and had been dried to determine the water content, were measured at three temperatures. The results are shown in **table 4.5** and demonstrate the change in magnetisation of the samples after cooling. The first column gives the room temperature value of the intensity, the second after cooling to -20° C (in a commercial deep freeze) and the third after cooling to -196° C in liquid nitrogen. There appears to be a small increase in magnetisation (of about 5%) for the first stage for all except the first 3 samples. This is attributed to the difference in the calibration of the Molspin, (on which they were measured). The loss of magnetisation shown by the first samples may be due to the effect of the Morin transition in haematite (as it becomes perfectly antiferromagnetic at about this temperature). All the remaining samples show a distinct decrease in magnetisation after the second cooling. This can be interpreted as direct evidence of the existence of MD magnetite (changing from its cubic to its orthorhombic structure occuring at -155° C (**Merrill, (1970)**)). The remaining magnetisation will be that associated with any SD or PSD grains which are not affected by this transition (**Ozima and Ozima (1964)**).

4.7 S.E.M. Analysis

In an attempt to directly observe the constituent magnetic minerals within the sediment, a scanning electron microscope (S.E.M.) analysis of the magnetic extract from sample S121 from core B49 has been performed. **Figure 4.12a** shows a micrograph of part of the extract magnified 640 times. The frame

Table 4.5 The variation of IRM with temperature for the pilot samples taken from core B49.

Sample No.	IRM ($A\ m^{-1}$) 18°C	-20°C	-196°C
1	9.849	9.284	8.626
11	0.411	0.332	0.099
21	10.064	10.462	9.608
31	2.834	2.974	2.649
41	18.430	20.334	11.329
51	48.157	53.130	47.651
61	62.726	69.204	57.629
71	57.214	63.268	50.230
81	44.300	49.858	40.741
91	69.034	78.388	64.887
101	102.424	111.830	91.036
111	80.939	87.611	75.208
121	78.287	85.966	68.854
131	66.587	71.322	57.684
141	96.479	104.416	86.870
151	71.876	79.746	65.710
161	68.943	74.521	60.984
171	56.900	61.412	49.951
181	66.776	72.179	58.220
191	70.866	76.580	62.518
201	94.883	98.879	84.895
211	94.074	101.126	86.153
221	84.282	89.946	74.943
231	96.237	104.988	88.321
241	88.067	94.130	81.133
251	106.589	114.333	94.275
261	132.439	141.396	117.899
271	78.639	87.936	72.976
281	83.307	90.782	77.797
291	49.083	52.687	45.892
301	107.988	116.550	91.403
311	87.389	95.513	81.016

width is about 150 microns and shows that there is a distribution of sizes within the extract from less than 1 micron to 50 microns. To further analyse the constituent elements of these grains, an X-ray analysis has been performed by means of an EDAX system (Energy dispersive analysis).

Elemental spectra for the five individual grains identified in **figure 4.12b** have been obtained, and are shown in **figure 4.13**. Grains 1, 2 and 5 are all silicates which have not been removed by the magnetic extraction. These show strong peaks for silicon and aluminium, much smaller amount of iron and titanium, and traces of other elements. Grains 3 and 4 are still predominantly silicates but have a larger iron content. Most interestingly, the assemblage of smaller grains give a strong iron contribution, a weaker titanium contribution and very little trace of the silicates. This indicates that the major magnetic minerals are these smaller grains found to lie in the 1-5 micron range.

A further magnification and EDAX analysis has allowed the inspection of individual grains within this assemblage. The results for a 5 micron grain, a 1.5 micron grain and a sub micron grain are shown in **figure 4.14**. The sub micron grain still reveals the strong silicate content. However, both the 1.5 and the 5 micron grains show distinct, strong, iron contents and weaker titanium contents, with almost no silicates. This confirms the existence of magnetic mineral grains lying in the MD range (**Dunlop (1981)**) with predominantly iron (oxide) as the main constituent but with a small amount of titanium as has been found in the magnetic experiments.

4.8 Conclusions

The most important conclusion that can be drawn from the magnetic mineral experiments that have been performed is that the DRM carried by the sediments is both stable and very likely to be accurately recording the geomagnetic field direction. The accuracy of the determination of the direction of the geomagnetic field when the DRM became fixed (post depositionally and, therefore, a finite time after the sediment was laid down - see chapter 7), can be readily improved by af demagnetisation in a peak field between 8 and 50mT. This removes a viscous component found to have arisen in some of the samples.

The carrier of the remanent magnetisation is likely to be MD magnetite usually with a small amount of titanium, which causes a slight reduction in the

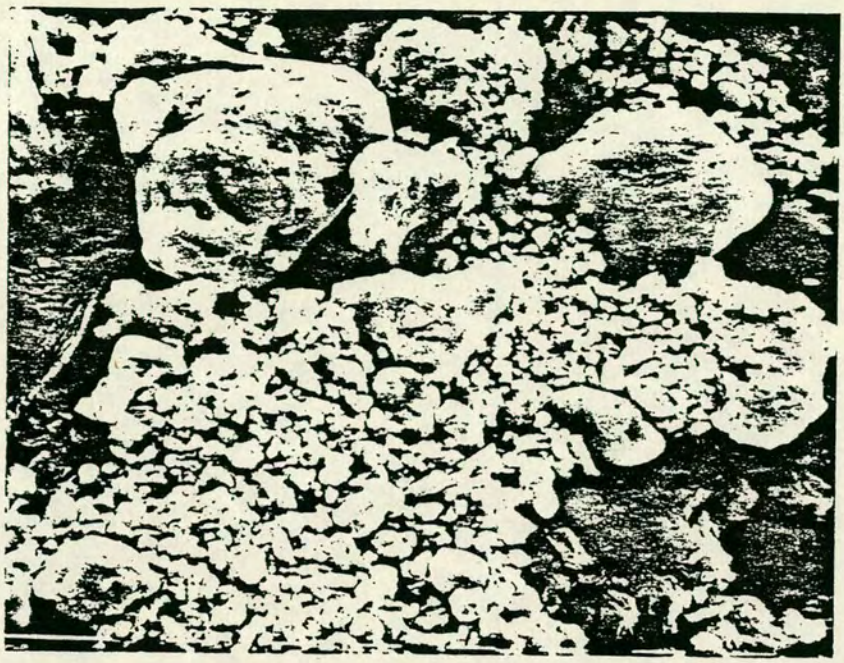

(a)

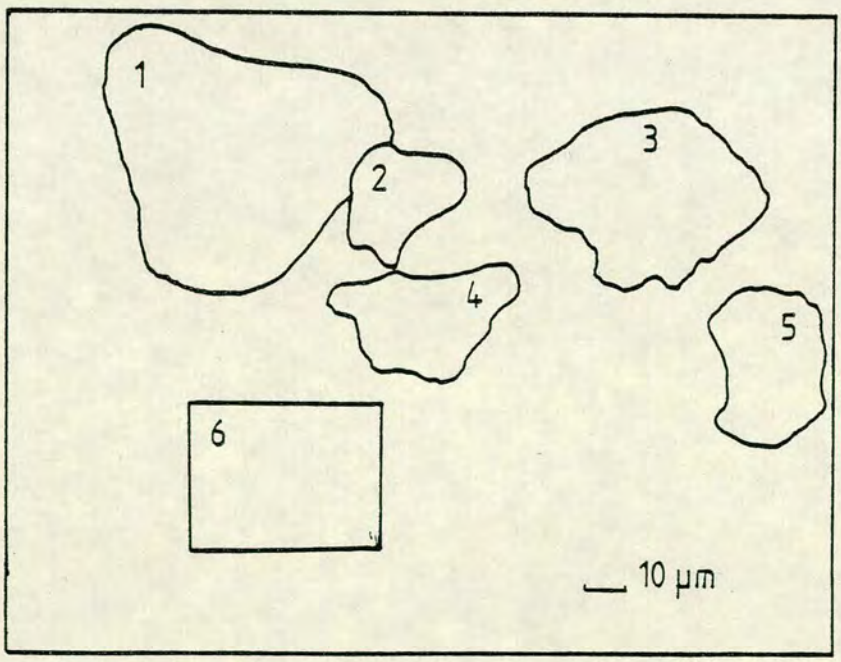

(b)

Figure 4.12 (a) A photograph of a part of the magnetic extract taken from pilot S121 showing the variation in the grain sizes and (b) the five grains and the assemblage that have been subjected to an EDAX analysis.

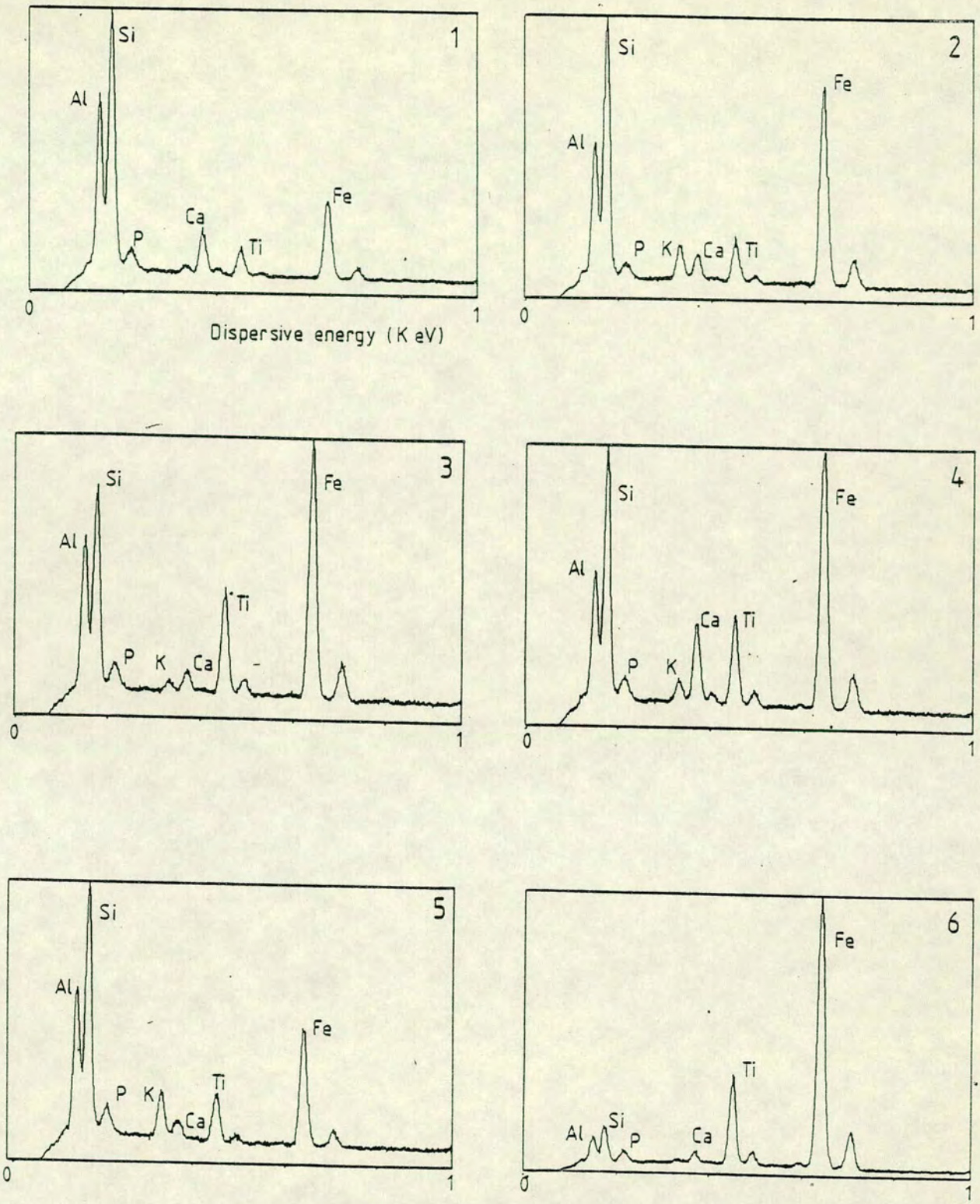

Figure 4.13 The EDAX spectra for the grains shown in figure 12b.

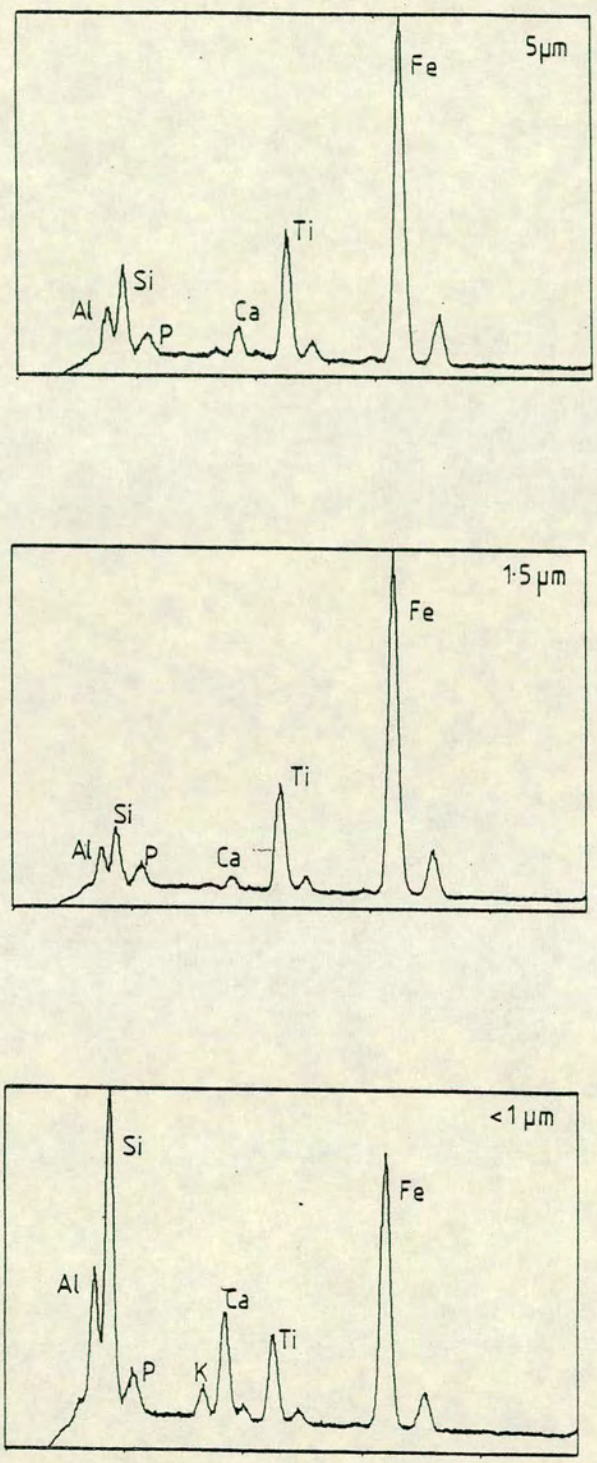

Figure 4.14 The EDAX spectra for three grains taken from assemblage 6 in figure 12b.

Curie point. In some sections of the core either the magnetite becomes more pure or the grain size decreases and the importance of SD grains increases. In general however, although the quantity of the magnetite does vary (governed by the quantity of water and the organic content of the sediment), its grain size and domain state appear to be very uniform. This is investigated further in chapter 7.

An interesting feature of the intensity record seen in **figure 3.1** for example are the "spikes" of high intensity. In addition, there is the region of very low intensity during the Holocene. These can now be explained in terms of the number of magnetic grains. **Figure 4.15** shows two typical grain size spectra from samples with low, medium and high intensity. The two low intensity samples (a and b) show a high percentage of large grains which have been shown to be principally non magnetic silicates. The medium intensity samples (c and d) have an even distribution of most sizes and the samples taken of the spikes (e and f) have predominantly grains in the range 2 - 8 microns. This shows that the more magnetic samples have more magnetic grains. (It is noted that some of these layers also have very large grains which could contain large amount of magnetic minerals but these are in the minority).

More work could be carried out in determining more closely the actual nature of all the remanence carrying minerals within the core. This information could be of great potential use to determine the erosion history of the crater and such factors as climatic variations. This type of work is beyond the framework of this project but should be investigated as part of the overall study of the history and development of the lake.

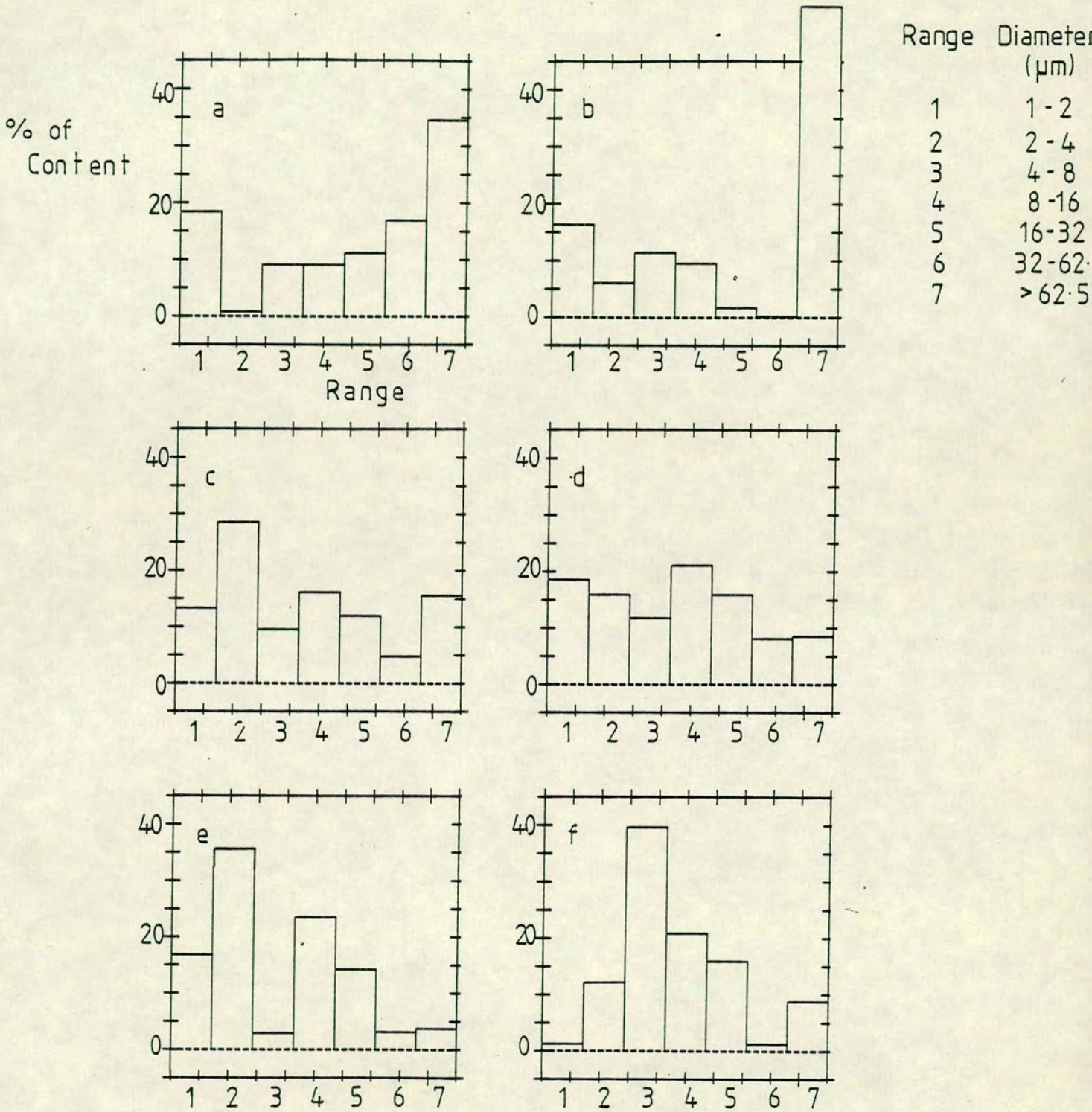

Figure 4.15 Grain size spectra for (a,b) low intensity samples, (c,d) average intensity samples and (e,f) high intensity samples.

CHAPTER 5
DATING THE SEDIMENTS:
CONVERSION OF THE DEPTH SCALE TO A TIME SCALE

5.1 Introduction

Similar sediments laid down in different places within Lac du Bouchet have been seen (in chapter 3), to appear at different depths within the core tube. However, the results from chapters 3 and 4 indicate that the sediments exhibit recognisable features that are both correlatable and contemporaneous. This chapter describes the conversion of the common depth scale, derived in chapter 3, to a time scale. This will reveal the variation of the geomagnetic field, with time, at Lac du Bouchet and allow further analyses to be made. (e.g. spectral analysis, VGP path analysis, intensity analysis etc.. See chapters 6 and 7).

5.2 Methods of dating sediments

Several methods of dating recent sediments are available. For those sediments rich in organic matter (e.g. assemblages A and B), palynological dating is useful. This involves examining the sediment for particles of pollen, identifying the pollen type and, provided that a local time scale is available, dating the sediment by associating the pollen type with the time that the parent plant was known to have lived. This method assumes that the local pollen record has been accurately determined beforehand.

A second method of dating recent sediments is conventional radiocarbon dating. Radiocarbon (C^{14}) is formed by the reaction $N^{14}(n,p)C^{14}$; that is, the C^{14} beta decays to N^{14} with a half life of 5730 years (**Lederer et al.. 1967**). Cosmic rays incident on the upper atmosphere produce neutrons by a spallogenic interaction with the abundant atmospheric nitrogen. (Spallation is the process, by which, bombardment of a nucleus by high energy particles, produces a

number of daughter particles). Subsequent photosynthesis of carbon, in the form of CO_2, causes it to enter the biosphere. The ratio C^{14}/C^{12} in the atmosphere varies with time, and the proportion is reflected in any living organisms whose ratio remains in dynamic equilibrium with the atmospheric supply until death. The difference between the proportion of C^{14} in a sample and that expected, reveals the amount that has decayed, and hence the age of the sample.

Conventional radiocarbon dating relies on counting the number of disintegrations of C^{14} nucleii, in a known mass of sample, in a given time. It is thus restricted (by a time factor alone), to measurements on samples less than about 50,000 years old, and is significantly less reliable for samples more than three halflives old (approximately 17,000 years). The radiocarbon method must also estimate the relative abundance of C^{14} in the atmosphere at the time of death. This is an obvious potential source of error. The methods and techniques of conventional radiocarbon dating are discussed in **Libby (1955)**. More recent developments include the use of an accelerator to produce a high energy mass spectrometer (HEMS). This allows the percentage of C^{14} atoms in a sample, to be accurately measured (by separating these atoms from the other carbon atoms). **Hedges (1981,1983)** reviews and previews the use of such an instrument.

There is, unfortunately, an additional problem with conventional radiocarbon dating in addition to those outlined by **Hedges (1983)** (e.g. 'hard water' effects, reworking of sediment etc.). For sediments which have a very low proportion of organic material (e.g. assemblage D), conventional radiocarbon dating requires a great deal of sediment. Up to 1g of carbon is needed to make an accurate determination of the age of the sample. This means that, in order to obtain sufficient carbon, such a large amount of sediment is needed, that the accuracy of the date is handicapped by the lack of information about the downcore depth (up to 50cm of sediment in a standard core tube would be needed). Alternatively, a sample could be made up by adding sediment from several cores which have been correlated beforehand. This requires great confidence in the correlation and does not allow for alterations at a later time. Also, the greater level of sample handling would increase the risk of contamination by recent carbon.

The HEMS method does not suffer from this drawback. The amount of carbon for such an instrument need only weigh 1mg. Thus, it is possible to use 1000 times less sediment to obtain the carbon, which greatly reduces the

uncertainty in depth. Eight samples have been prepared, and dated, using this method, which is the only one capable of accurately dating, the predominantly inorganic, lower sediments from Lac du Bouchet. The preparation of the samples for HEMS dating was performed during a trip to the Research Laboratory for Archaeology and the History of Art, Oxford, and is described in section 5.4.

Two other methods of dating have been used on samples from Lac du Bouchet; Thermoluminescence (TL) and potassium-argon (K-Ar). The latter method (based on the decay of potassium to argon) was used to date basaltic samples from the side of the crater (and hence the age of the crater). Two samples were dated (**Mitchell pers. comm.**), giving ages of 870,000 ± 60,000 years and 800,000 ± 40,000 years. TL dating is being carried out on samples from the 12m core B61; as yet these dates are not available.

5.3 Choice of samples to be dated

In order to produce an accurate depth/time transform function, it is much more useful to have all the samples taken from one core. Some dating had already been performed on core B5 but no further sediment was available from this core and it was only 6m in length. It was decided therefore, to use core B49, as this was the longest core available, and because all other pilot studies were performed upon this core.

The top 2m of sediment had been intensively dated in France, for core B5, by both palynological and conventional radiocarbon techniques. Thus, the samples were taken, predominantly, from below this level, with one sample (from between 175 and 180cm), as a check on the results from the different methods. The other samples from core B49 were taken at intervals down the core that were about a metre apart, in order to obtain a systematic sequence of dates.

5.4 Radiocarbon dating using a HEMS

The basic principles of using an accelerator as a high energy mass spectrometer, enabling the actual number of C^{14} atoms within a sample to be counted, are reviewed by **Hedges (1981)**. The accelerator used in this work is based at the Research Laboratory for Archaeology and the History of Art at Oxford, and is that previewed by **Hedges (1981)**.

The design of the instrument (**figure 5.1**), is such, that very small quantities of carbon are needed to provide a reliable date for the sample. In the case of the Bouchet sediments, this is important, as the percentage by weight of organic matter, estimated in France by burning a known weight of sediment, is less than 4% for some parts of the glacial muds. Although accurate measurements were not made, some of the samples dated contained less than 0.5%, by weight, of carbon.

In order to make a measurement of the C^{14} content of a sample of sediment, it is first necessary to remove any carbonate deposits, that may contain spurious carbon levels. After this, the organic carbon is converted to carbon dioxide, and thence graphite, by the process outlined below. This "wire" of graphite, is then used as the source of carbon atoms for the accelerator and hence, provides the raw material for the accelerator based date. The method used, outlined below, was developed for sediments by **Fowler (1984)**.

5.4.1 "Cleaning" the sediment

All the glassware used in the preparation of the sample was carefully cleaned. This was achieved by, first, washing in tap water, then in distilled water, rinsed in chloroform and dried in an oven at about 80° C. It was then filled with chromic acid, and left, at 80° C for 24 hours. Finally, it was rinsed again, in distilled water and then chloroform, and dried in the oven.

After this thorough cleaning of the glassware, the sediment sample was mixed with 2M hydrochloric acid, and kept warm for 24 hours at 80°C. This removes any carbonate precipitates within the sediment, leaving only organic carbon. The sediment was filtered from the acid using a Buchner funnel and carefully washed, until a neutral pH value was established. Finally, the sediment was dried in the oven overnight.

5.4.2 Preparation of graphite target wires

The conversion of the organic carbon from the sediment, to pure graphite, used as the target for the HEMS, involves 3 stages:

(i) combustion of the carbonaceous material within the sediment, to CO_2, by burning in excess oxygen,

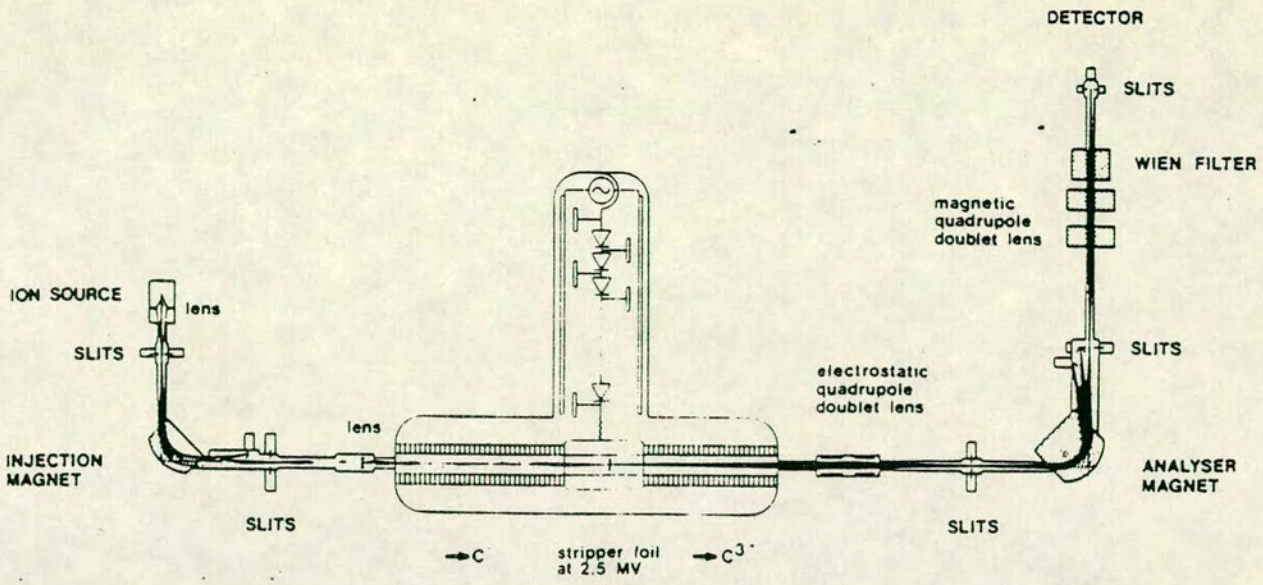

Figure 5.1 Schematic diagram of the beam handling arrangement for the Oxford High Energy Mass Spectrometer. (after **Hedges (1981)**).

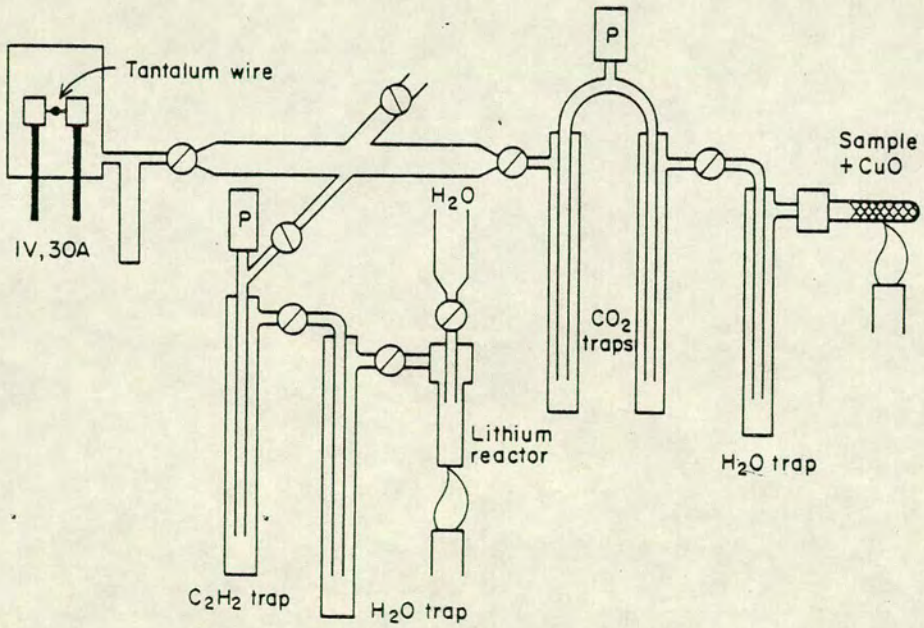

Figure 5.2 The graphite preparation rig for the Oxford high energy mass spectrometer. (after **Wand et al (1984)**).

(ii) conversion of the carbon dioxide to (lithium) carbide, and thence to acetylene (C_2H_2),

(iii) "cracking" the acetylene by pyrolysis onto a tantalum wire, in the form of graphite.

To ensure that all these stages produce an uncontaminated sample, the preparation of $CO_2(g)$, $C_2H_2(g)$ and thence C(s) is performed within a single closed rig. The whole apparatus can be evacuated using a vacuum pump, to ensure no airborne, modern, C^{14} is present.

The rig was connected up as in **figure 5.2**. The $N_2(l)$ trap for the vacuum pump was filled and the pumps turned on. All the sections of apparatus had been washed with cold tap water, and then 50% nitric acid, and placed in an ultra sonic bath for at least 3 minutes. After this, it was rinsed and 'ultra sonic'ed in methanol and when the excess methanol had been shaken off, placed in an oven at 80°C and left overnight to dry. Assembly was performed whilst the apparatus was hot, straight from the oven, to reduce the chance of leaks in the vacuum lines. The following method was then used to produce the wires.

5.4.2.1 Combustion

$$C + O_2 \rightarrow CO_2 \qquad (5.1)$$

The sediment was mixed with approximately the same amount of CuO (4g dry weight of sediment, containing ∿ 8% organic material, produced ample graphite), and placed in a large glass holder sealed with glass wool. The holder was placed in the burner position, with a water trap (at -65°C), made from mixing $N_2(l)$ and methanol(l), on the first trap, and a CO_2 trap of $N_2(l)$ on the second.

This part of the rig was then isolated and pumped to a good vacuum, ($< 10^{-3}$ torr), to remove any contaminant gases. Then the sample was gently warmed, to remove any trapped moisture, which was pumped away. After the gentle warming the pump line was closed.

The mixture was heated (∿ 800°C) for 20 to 30 minutes, with the valve between the two traps closed, then this valve was opened to allow the dry gases to pass into the CO_2 trap. At this stage, only gases with a low boiling

point (e.g. oxygen, hydrogen, sulphur dioxide etc.) remain. These gases can be pumped away, after which the CO_2 trap can be removed to allow the trapped gas to sublime. The amount of CO_2 so produced was measured on a pressure gauge (**table 5.1**).

5.4.2.2 Preparation of Acetylene

$$10\ Li(s) + 2CO_2(g) \rightarrow 4Li_2O(s) + Li_2C_2(s) \qquad (5.2)$$

$$Li_2C_2(s) + H_2O \rightarrow Li_2O(s) + C_2H_2(g) \qquad (5.3)$$

The preparation of acetylene is a two stage process. Initially one converts the carbon dioxide to lithium carbide, by heating with solid lithium. Then the addition of cold water to the carbide, causes the production of acetylene.

Approximately 50 mg of lithium was placed into the bottom of the reactor pot, which was then inserted onto the rig, with a water cooled collar to prevent heating other elements of the rig. The acetylene preparation path was then isolated and evacuated, whilst the lithium was outgassed by heating the pot. This outgassing produced 3 noticeable deflections on the pressure gauge. The pumping continued until the pot had cooled back to room temperature. 550 mbars of CO_2 were drawn across into the pot by cooling the Li pot with liquid nitrogen. Any non frozen gases were then pumped away, and the preparation path was then re-isolated and the mixture heated. The pressure on the gauge drops as the CO_2 is used. After heating, all non frozen gases were removed, and the two traps (to freeze the water and C_2H_2) were put in position.

The pot was allowed to cool completely to room temperature, whereupon about 1ml of cold water was carefully added (ensuring there were no contaminant air bubbles). A rise in the pressure on the gauge indicates the formation of acetylene. This is allowed to equilibrate then any non frozen gases are removed. More water is added until no more acetylene is produced. Finally the acetylene trap is removed and the pressure of gas measured.

5.4.2.3 Preparation of Graphite

The cracking unit was assembled with a known weight of tantalum wire. The wire was outgassed by heating slowly to $\sim 380^{o}C$ (by the application of a

Table 5.1 Summary of the sample preparation data for the samples dated by the HEMS at Oxford.

Sample Name	Depth (m)	CO_2 (mb)	C_2H_2 (mb)	Carbon wire 1 (mg)		wire 2
A1	1.75-1.80	750 (550)	86	0.93		0.60
B3	3.00-3.05	450	184	1.07		0.92
C1	4.20-4.25	490	200	0.14	0.33	0.64
C2	5.00-5.04	406	165	1.66		1.88
C3	6.00-6.06	460	180	0.95		1.23
D1	6.61-6.66	100 (550)	170	0.89		1.04
D2	7.10-7.15	960 (500)	198	1.85		1.94
D3	8.12-8.17	855 (500)	168	1.46		0.80

CO_2 figure in parentheses indicates amount taken for preparation of C_2H_2.

Table 5.2 Radiocarbon dates obtained from the HEMS

Sample Name	Depth (m)	Date (yrs bp)
A1	1.75-1.80	9,700 ± 200
B3	3.00-3.05	12,900 ± 180
C1	4.20-4.25	14,300 ± 250
C2	5.00-5.04	19,200 ± 300
C3	6.00-6.06	23,100 ± 600
D1	6.61-6.66	27,300 ± 900
D2	7.10-7.15	28,500 ± 900
D3	8.12-8.17	30,600 ± 1,300

current), then cooling back down (more slowly), to room temperature, whilst pumping away any gases produced. Then the acetylene was drawn into the trap on the cracking unit using $N_2(l)$. Approximately 70 - 80 mbars of acetylene was sufficient for a 1mg wire of graphite. The trap was then removed allowing the C_2H_2 to warm. After this it was cracked, by setting the wire temperature to ∿ 350°, ∿ 400°, ∿ 450° for 6 minutes each. After this the temperature was reduced slowly and any excess gases were pumped away. Argon was then allowed to enter to seal the graphite and then pumped away. The small, (1 cm long), wire now has approximately 1mg of pure graphite attached to it, which can be extracted and weighed.

Two wires were produced from each sample to provide a method of double checking any dates obtained. **Table 5.1** gives the amounts of carbon dioxide, acetylene and carbon produced for the eight samples, prepared using this method. Each sample contained approximately 5g, dry weight, of raw sediment before burning. As can be seen from **table 5.1**, this resulted in varying amounts of carbon dioxide, depending on the amount of organic material within the sample. The general trend of this variation agrees with the estimates of the organic matter content, made in France, for other cores. Note that sample C1 was subject to a small leak during the final cracking. This leak had to be sealed using silicon rubber sealant, which contains modern carbon, and could result in a date that appears too young. A further consequence of the leak is the very poor amount of carbon obtained. Due to the small size of the wires produced for this sample, only one could be dated, resulting in a very poorly constrained date (in addition to the possible contamination error).

The wires produced were then stored, and used as the target for the ion source, to produce a beam of carbon atoms, which enters the HEMS. This procedure is described by **Hedges (1981)**.

5.5 Results from the HEMS measurements

The measurement of the age of the samples prepared, as described above, was done by Dr. R. E. M. Hedges in Oxford. The age of each of the samples is given in **table 5.2**, with their respective downcore depths. As previously stated, sample C1 could only be dated on one wire. Sample A1 produced two results that were surprisingly divergent (hence the rather large error). **Figure 5.3** shows the transform function produced for core B49 using these samples. The

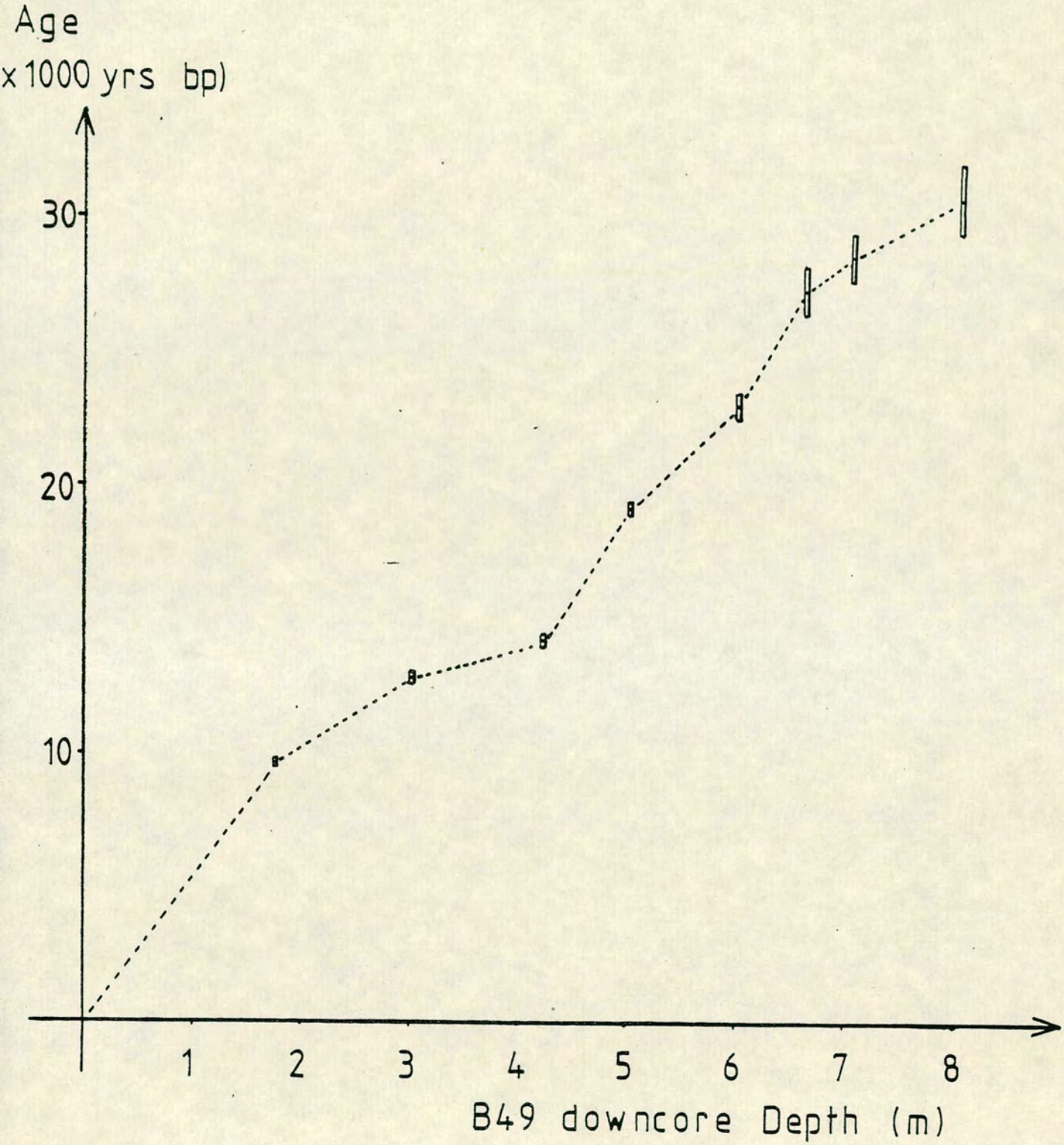

Figure 5.3 The depth time transform function defined by the ages obtained from the dating of core B49 using the Oxford high energy mass spectrometer.

function appears to be almost linear (in which case sample C1 would appear to be too young). A linear fit would be even more appropriate, if the last three samples (D1-D3), were offset by about 50cm. If this were so, it would mean a period of either no sedimentation or erosion. It is interesting to comment that the depth that this offset should occur (600-650cm), exactly corresponds to a layer in the lake that is impossible to core through, using the current design of corers, in some parts of the lake. This offset cannot be performed with the current amount of evidence, and the subsequent development of the depth/time transform function takes no account of this interesting feature. However, if subsequent dating of the longer cores reveals two periods of apparently similar sedimentation rates, with a break in slope about 600cm, then a break in sedimentation rate, at this point, should not be excluded. (The period of time that this break would last would be about 1500 years - less if any erosion took place).

5.6 Results from core B5

The results obtained from the samples taken from core B5 are shown in **table 5.3** and **figure 5.4**. The blocks show the 5 conventional radiocarbon dates, and the crosses the palynological dates. The downcore depths have been adjusted to the equivalent B49 depths based on the transform function shown in **figure 3.6**. There is a heavy concentration of results in the upper two metres, corresponding to the various pollen zones of the Holocene. Each pollen zone is named in **table 5.3** along with an indication of the prevalent conditions. The dates are given as the time for the local onset of the period and were determined by J. L. de Beaulieu, A. Pons and M. Reille. More detailed accounts of the pollen zonation appear in **Bonifay et al. (1985)** and **Creer et al. (1985)**.

The radiocarbon results appear to agree quite well with the pollen zonations, but are subject to noticeably large error estimates. Up to 20cm of sediment were used to obtain sufficient carbon to date. This is equivalent to a period of 1000 years at a sedimentation rate of 0.2mm per year. The error bars quoted for the error in the date represent purely the measurement error. No account is taken for the error induced in locating the depth of the sample.

The results seem to indicate two different rates of sedimentation, with the change in rate occuring at the boundary between the late glacial period and the Holocene. This is investigated more fully in the next section.

Table 5.3 Dates obtained from core B5.

PALYNOLOGICAL DATING FOR CORE B5

B5 Depth (m)	B49 Depth (m)	Pollen Zone	Climate	Date (yrs bp)
0.52	0.58	Sub Atlantic	Mild,wet	2,600
0.88	0.98	Sub Boreal	Cool,dry	4,700
1.30	1.32	Atlantic	Warm,wet	8,000
1.55	1.60	Boreal	Warm,dry	9,000
1.73	1.71	Pre Boreal	Cold,wet	10,300
1.82	1.79	Younger Dryas	Cold	10,700
2.00	1.96	Bolling/Allerod	Warm	13,000
3.00	2.85	Oldest Dryas	Cold	15,000

The date given corresponds to the start of the pollen zone in the Massif Central region of France.

CARBON 14 DATING FOR CORE B5

B5 Depth (m)	B49 Depth (m)	Date (yrs bp)
0.45-0.55	0.50-0.61	2,280 ± 90
0.90-0.92	1.00-1.03	5,500 ± 100
1.60-1.70	1.63-1.69	8,340 ± 150
2.80-2.90	2.67-2.86	15,800 ± 900
5.30-5.47	5.77-6.00	19,400 ± 1,300

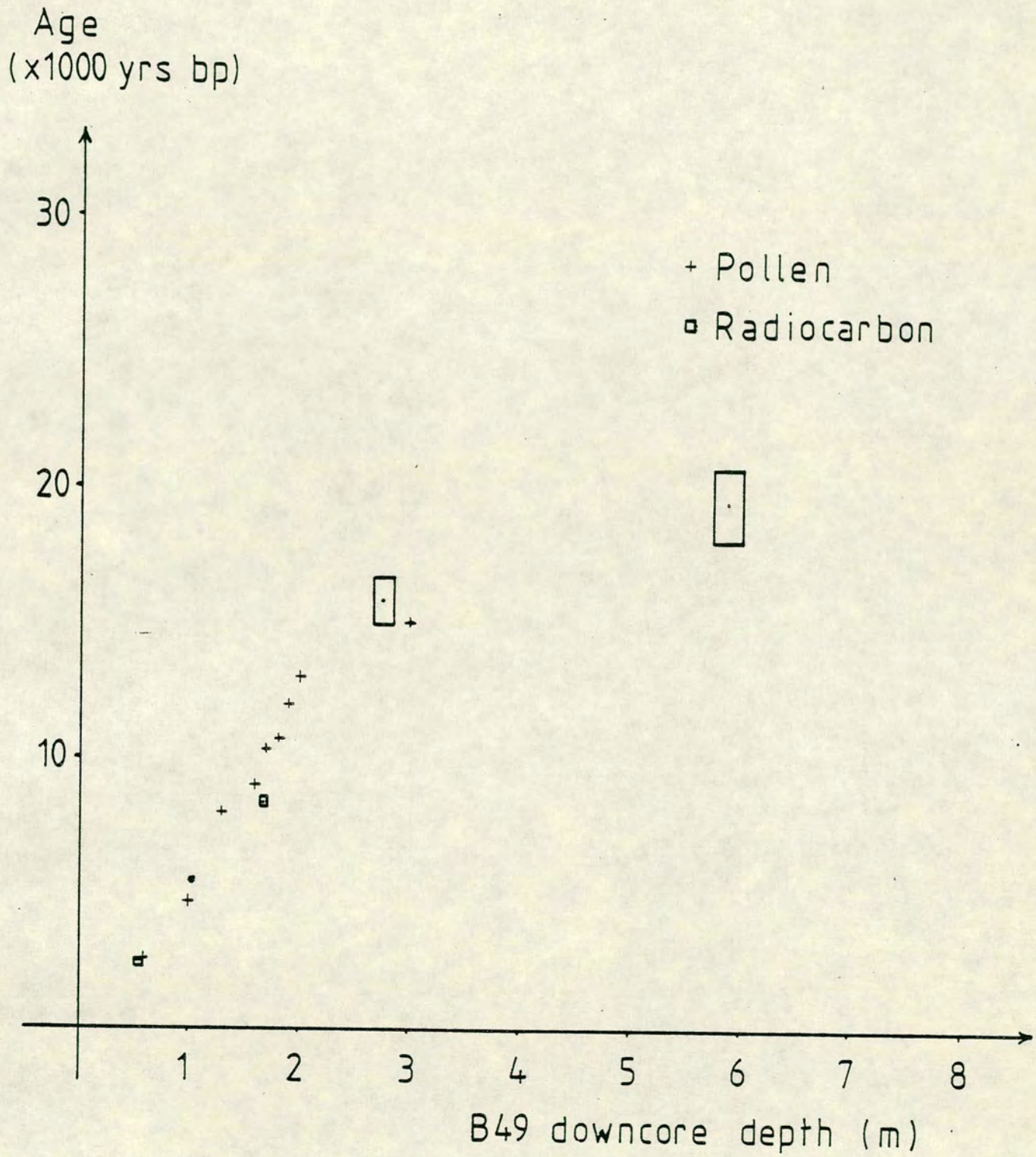

Figure 5.4 The palynological and radiocarbon dates obtained for samples taken from core B5 after adjustment to a B49 depth scale.

5.8 Transformation to the time scale

With the transform functions described in the previous section, it is now possible to transform the results obtained on the common (B49) depth scale, to a time scale. The result of this transformation is shown in **figure 5.6** for the cores shown in **figure 3.8**. The basic patterns and phase relations are preserved, but the results for the top two metres appear much more spread out. It is clear that the very slow rate of sedimentation, coupled with the high water content (and subsequent disturbance), has resulted in a highly smoothed record for the Holocene. However, the record for the late glacial remains remarkably detailed.

5.9 Comparison with other European records

With the records from Lac du Bouchet on a time scale it now becomes possible to compare these records with similar ones from elsewhere in Europe. The UK record is particularly well established for the Holocene (**Turner and Thompson, (1981)**), and therefore, this curve has been chosen for comparison in the period 0-10,000 years bp (as defined by **Creer and Tucholka (1982)**). For the late glacial, the only dated results available are for the Black Sea and Lac de Joux (**Creer et al.. (1974), Creer et al.. (1980)**). The Lac de Joux record for the late glacial is only about 3,000 years in length, and so the Lac du Bouchet records have been compared with the Black Sea records only.

5.9.1 The Holocene record 0-10,000 years bp

Figure 5.7 shows a comparison of the Bouchet records, from the minicore BM7, and the results from the UK for the period 0-6,000 years bp. The Bouchet record is clearly noisier and hence, less well defined than the UK record, which is explained as being due to a combination of the smoothing due to the low rate of sedimentation, and disturbance (during transport and sampling) due to the high water content.

As can be seen from **figure 5.7**, the inclination record for the Bouchet minicores clearly agrees with the smoothed UK type curve. This is all the more remarkable when one considers the natural smoothing that has occured in the former record. The declinations reveal the effects of this smoothing more with

a) Declination

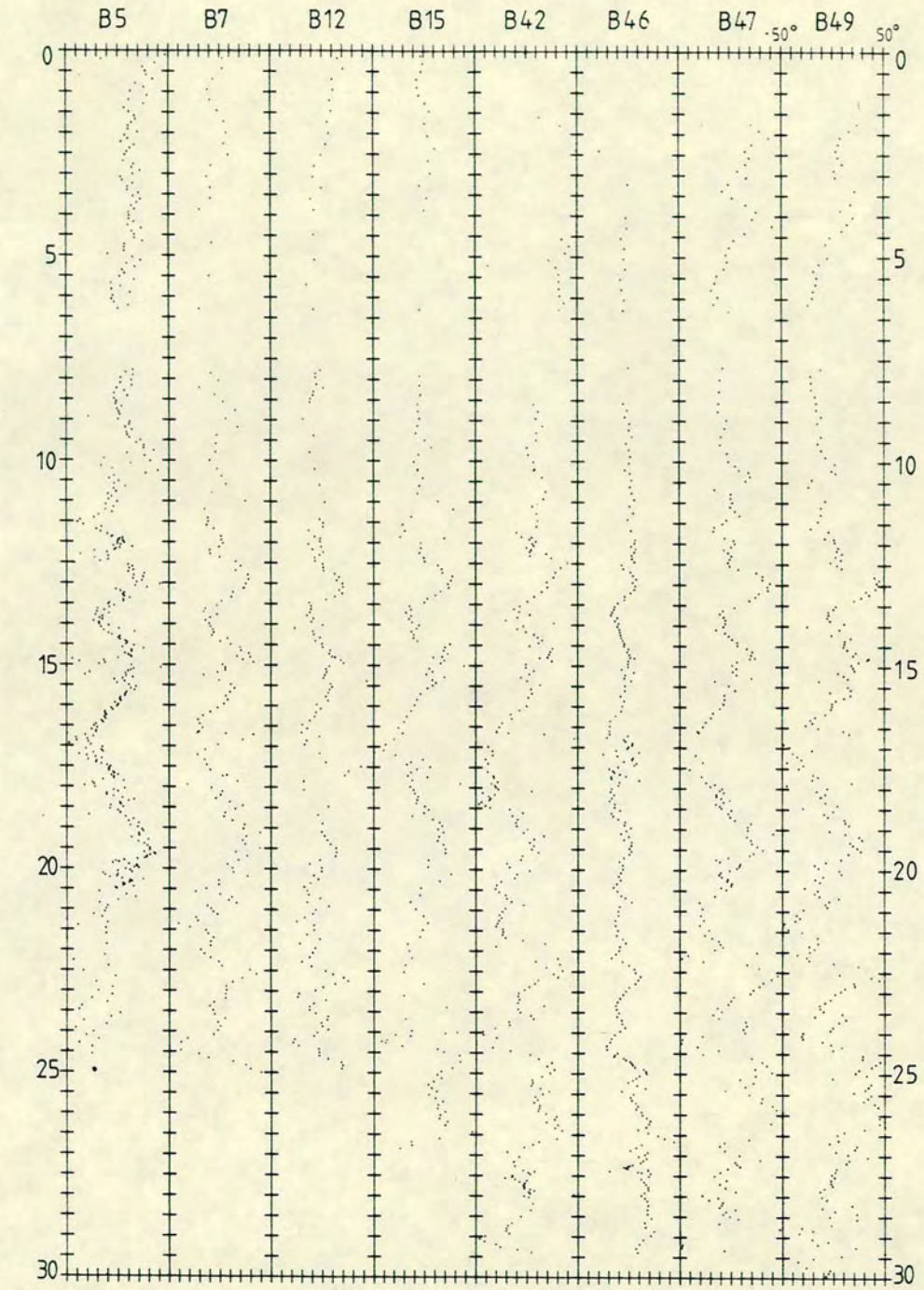

Figure 5.6a The declination records for eight cores taken from Lac du Bouchet after transformation to the time domain.

b) Inclination

Age (x 1000 years bp)

Figure 5.6b The inclination records for eight cores taken from Lac du Bouchet after transformation to the time domain.

c) Intensity

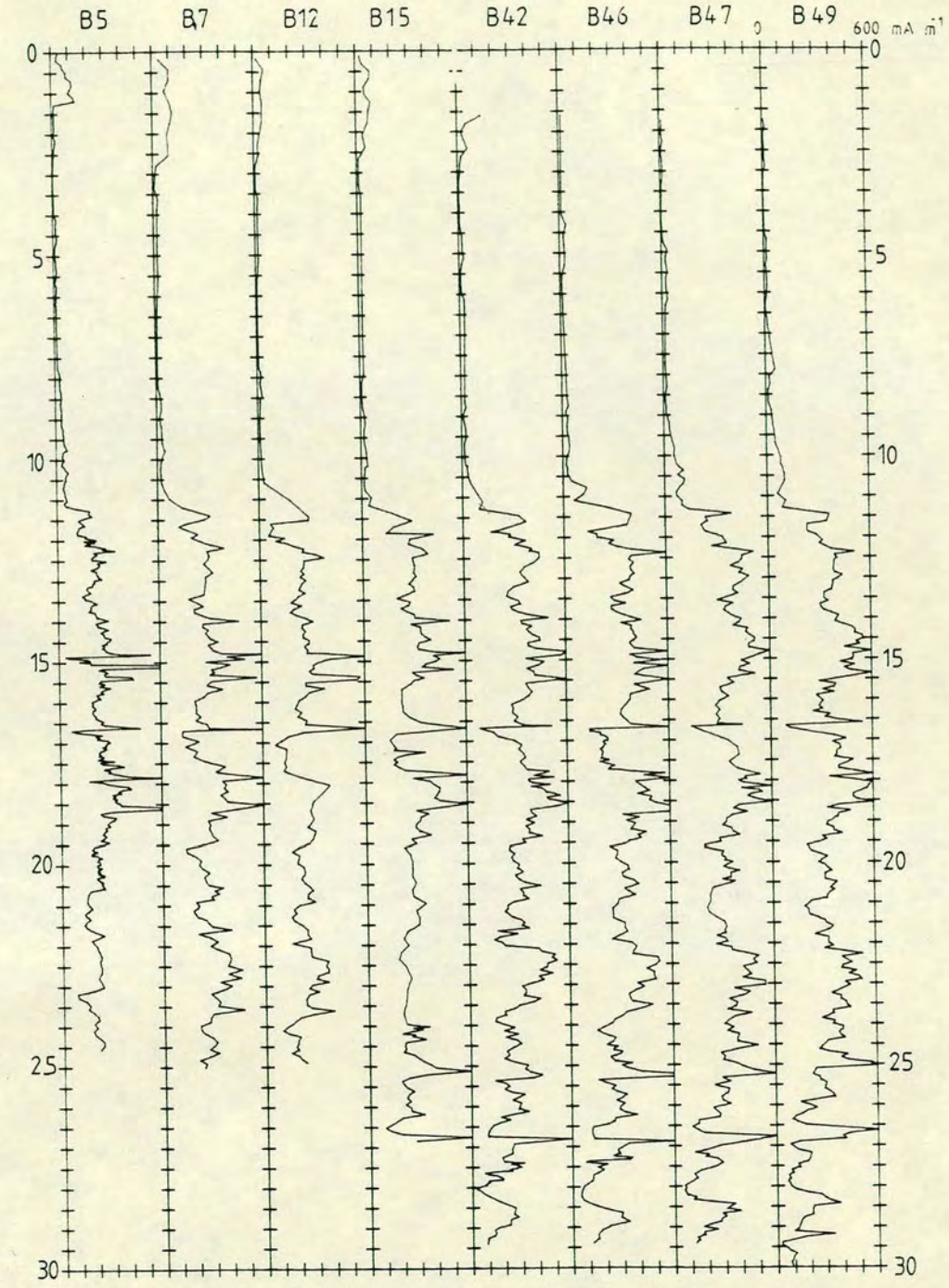

Figure 5.6c The intensity records for eight cores taken from Lac du Bouchet after transformation to the time domain.

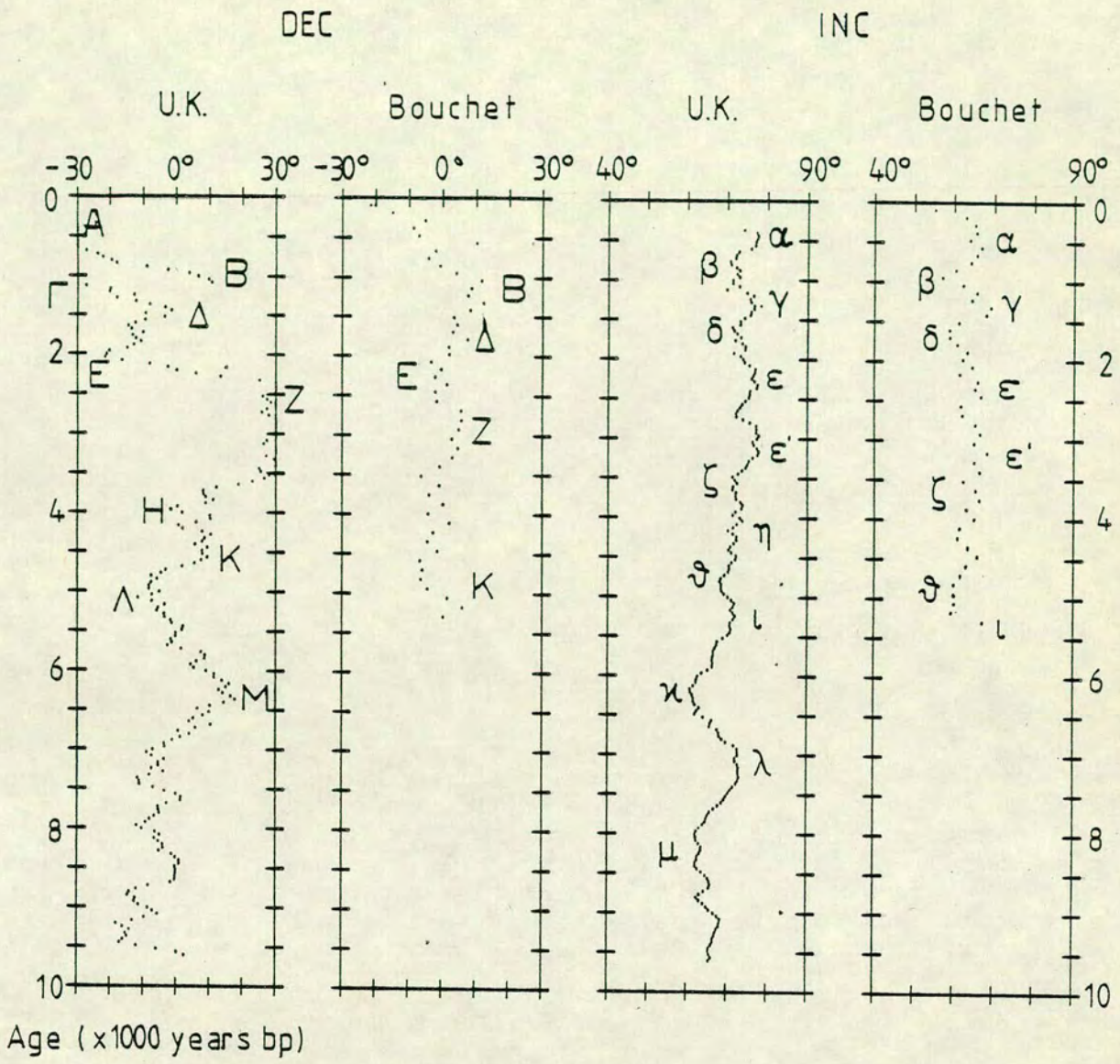

Figure 5.7 A comparison of the Lac du Bouchet records with the U.K. records defined by **Turner and Thompson (1981)**.

5.7 Comparison of the results from the three methods

The three methods reveal very consistent results for the top 2m of (organic rich) sediment. **Figure 5.5** reveals however, the differences that appear below this level. As previously discussed, the accelerator date C1 would appear to be too young, possibly as a result of the leak during preparation. A change in the gradient appears to occur at the Holocene/late Glacial boundary (2.00m).

Given the number of dates available it would not be sensible to pick some and not use others. With no other criteria with which to accept or discard a date, the most sensible approach would be to construct a depth/time transform function, that consists of two straight lines, meeting at the Holocene/Late glacial boundary (where one would expect a change in depositional environment). With the doubt expressed about the validity of the date for C1 however, this date has not been included. To fit the lines, minimisation of the mean square errors (least squares) has been used. The resulting transform functions are

$$T_1(d) = 6.62d - 1.38 \qquad (5.4)$$

and

$$T_2(d) = 2.92d + 6.03 \qquad (5.5)$$

where the depth (d) is in metres and the age (T) is in years (x 1,000) bp. The function $T_1(d)$ represents the rate of sedimentation for the top 2m and results in a rate of 0.15mm per year, which is less than half that described by $T_2(d)$ for the late glacial, of 0.34mm per year. This results in the age of 11,870 years bp for the change in the deposition rates, occuring at a depth of 2.00 metres.

This type of transform function inherently assumes constant rates of sedimentation. Clearly this is not true on a short time scale due to periods of slumping or severe climatic conditions, but is likely to be valid over longer periods of time. As discussed above, periods of zero deposition or erosion may have occured also but, at the present time, these cannot be identified confidently within the sediments of Lac du Bouchet.

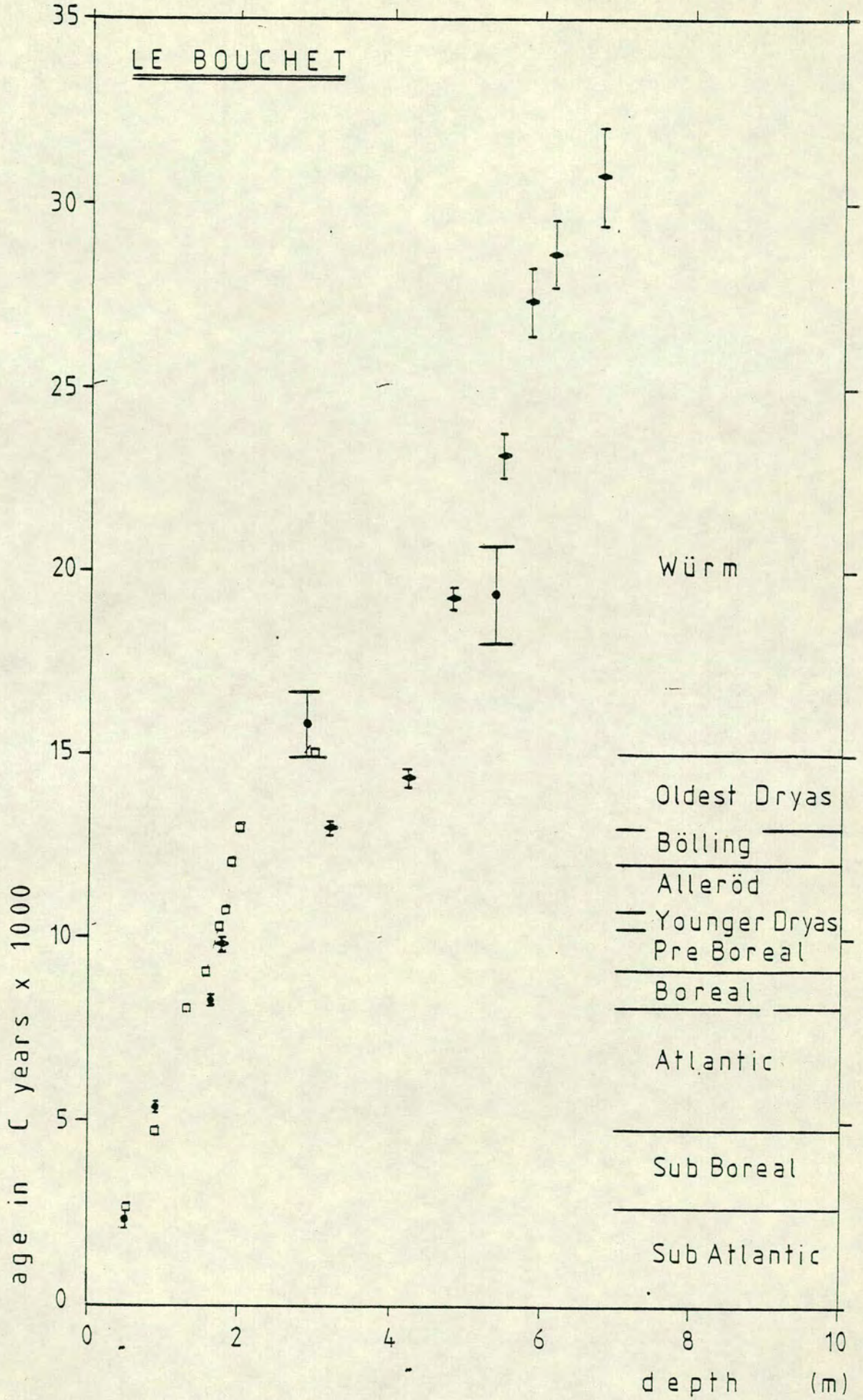

Figure 5.5 The dates available from the cores from Lac du Bouchet that have been used to define the depth time transform function.

a definite amplitude modulation.

The record between 5,000 and 10,000 bp is very poorly defined in the Bouchet sediments due to the extremely high organic matter level, which made subsampling (and hence measurement) extremely difficult.

5.9.2 The late Glacial record 10,000–30,000 bp

The late glacial record is very well defined in all the cores from Lac du Bouchet, and consequently, easier to compare with other records. There are however, no records from Europe that span the same period of time. Only the records from Lac de Joux and the Black Sea have periods of contemporaneous variations and neither of these are well dated. However, the Black Sea record has been used to compare the results from Lac du Bouchet and it can be seen (**figure 5.8**), that features are common to both the records. The differences in the ages of the variations could be attributed to the poor age control for the records, and emphasise the great importance of accurate dating. Alternatively, since it appears that the Black Sea features all appear approximately 1000 years before the Bouchet record, and lies (at a longitude of 36.7° E) 33 degrees east of Bouchet, the sources of the variations could be drifting westwards at a rate of about 0.03° per year. This rate is significantly different from present day rates of drift, of ∿ 0.2° per year (**Yukutake and Tachinaka (1968)**) and is therefore likely to be the result of dating errors.

Despite the discrepancy in the ages attributed to the features of the records confidence is held in the results from the Bouchet cores which have been more intensively dated by newer, more accurate techniques.

5.10 Conclusions

Dating is very important. No investigation of lake sediments is complete without accurate age control. Twenty three different age determinations have been made on the cores obtained from Lac du Bouchet and yet the depth/time transform function could still be improved. Two least squares lines have been fitted: the Holocene sedimentation rate is well defined and agrees well with the established curves for western Europe, (for the last 6,000 years). The late glacial rate of sedimentation is almost twice that of the Holocene, and again, gives results that agree with the (less well established), available curves. The

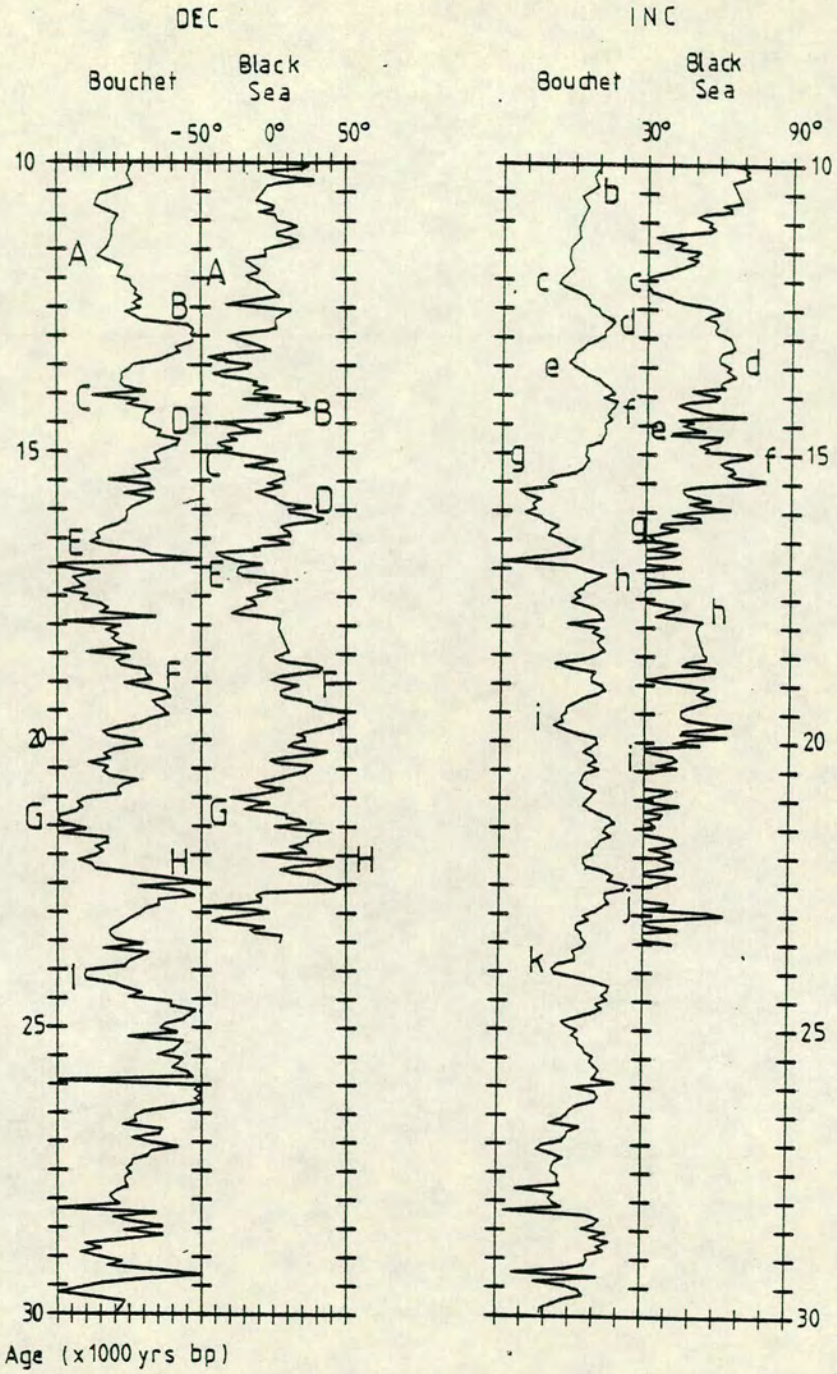

Figure 5.8 A comparison of the Lac du Bouchet records with the Black Sea records defined by **Creer et al (1974)**.

interception of these two lines is found to occur at the Holocene/late glacial boundary.

With the records now on a time scale, we can proceed to analyse the variations of the geomagnetic vector, in an attempt to recover any important periodicities and to discover whether or not the strong features, seen in the period 12,000 - 17,000 years bp are drifting westwards.

CHAPTER 6
SECULAR VARIATION OF THE GEOMAGNETIC FIELD IN FRANCE SINCE 30,000 YEARS BP

6.1 Introduction

Several authors have attempted to establish whether or not there is a periodic nature to the secular variations of the non dipole field, (**Mackereth (1971), Creer et al. (1972), Creer (1974), Verosub and Banerjee (1977), Tucholka (1980), Barton & McElhinny (1981), Lund and Banerjee (1985)**). A major problem of all such attempts is both the quality and the length of the records available. Most of the work noted above consists of analyses on records that are 12,000 years or less in length. It is immediately apparent that if any long period variations exist they will be very difficult to resolve given such a short length of record.

At Lac du Bouchet we have a strong stable record over the last 30,000 years - over ten full periods of between 2,000 and 3,000 years - which have been found in other records. Unfortunately however, the Holocene record in Bouchet is poor and this restricts our time window to 20,000 years between 30,000 and 10,000 bp. This window has been shown in chapter 3 to have very well defined declination and inclination records. In addition if we remove the spike-like features of the intensity record which can be correlated to high magnetic mineral contents , then this record too appears to have an oscillatory behaviour. Indeed, chapter 7 reveals how these oscillations are most likely to be geomagnetic in origin and so they are analysed as such in this chapter.

Other features of the record can also be analysed. The phase relations between the three components and the shape of their virtual geomagnetic pole (VGP) paths can reveal information about the direction of drift (if any) of the sources of the secular variation.

Rather than use just a single record, the analysis is performed on a stack of the eight cores presented in chapter 3. Two types of stack have been used, the production of which are discussed in the next section.

6.2 Production of a stack

There are many different ways in which the eight cores could have been stacked. These include stacking before or after transforming to the time scale, before or after smoothing by several different methods, and by adding and averaging or merging together. All these methods cause a smoothing of the data. Any random noise should be reduced by adding the results from several cores which is a great benefit. Unfortunately, in contrast, we could introduce false qualities to the data by linear interpolation and averaging.

Clark (1977) and **Clark and Thompson (1978,1979,1984)** have developed a method of smoothing a time series using cubic splines whilst optimising the information remaining. **Creer and Tucholka (1983b)** indicate that this method can be best used by merging several cores together and then using the Clark method to find the best curve. Another procedure is to equally space the data and then average the results from each level. These are the two methods that have been examined in most detail.

6.2.1 Stacking by merging

The cores were merged together using the program MERGE (appendix 3). This program creates a single monotonically increasing time scale from those of the original cores by mixing the results together and averaging any that occur at the same time. The criterion for accepting results as being contemporaneous can be adjusted at run time. In this work results had to occur within fifteen years of each other to be averaged and for which the errors were calculated. The merged results were then smoothed using a cubic spline smoothing method with the number of knots determined by use of Clark's CVMSE technique (BESTKNOTS). Ten per cent of the data points were used in the cross validation, smoothing being performed by cubic splines with the number of knots increasing from 1 to 75. The merged plots are shown in **figure 6.1a**; the results of the cross validation are shown in **figure 6.2** Note that the cross validation was performed for the whole time period 30kyrs to 0kyrs bp. The results indicate a broad minimum with little change in the CVMSE for smoothing using between 30

and 70 knots. Thus 50 knots have been chosen which minimises the degree of smoothing whilst remaining safely within the broad minimum. **Figure 6.1b** has the 50 knots cubic spline smoothed version superimposed upon it.

6.2.2 Stacking by averaging

The program STACK (see appendix 3) has been written to perform the averaging of cores after being equally spaced. The result is easily obtained as are estimates of the standard deviation of the mean and the expected value for the element at each level. The former error estimate is included in **figure 6.1c** which shows the result of stacking the (time transformed) 8 cores B5, B7, B12, B15, B42, B46, B47 and B49 using averages calculated using Gaussian statistics. (An alternative would be to use **Fisher (1953)** statistics for the declination and inclination. However, the errors calculated using this method are expressed in angles. Plotting such errors on a linear scale as in **figure 6.1a** and **figure 6.1c** results in apparently much larger errors than are real. This is due to the fact that the linear errors can tend to infinity if the angular error encompasses two pi radians - which will occur no matter how small the angular error at high inclination values). The data were interpolated prior to stacking at 100 year intervals.

The program can incorporate both smoothing and normalisations prior to stacking. Experiments have been performed using these different facilities but it was found that too much information was lost at too early a stage. Smoothing is very important and must be carefully monitored. More control could be achieved by smoothing after stacking and this is discussed later.

Since the stacking requires evenly spaced data the transform to the time domain was performed beforehand. Analyses based on correlation and Fourier transforms require equally spaced data; this approach ensures the minimum amount of interpolation.

6.3 Modelling Secular variations

The geomagnetic field can be harmonically analysed to reveal the main source components. The main field is essentially dipolar with the dipole axis close to the geographic axis. Any differences between the dipolar field and the real field are contained within the lower order terms of the harmonic expansion.

Merged Stack

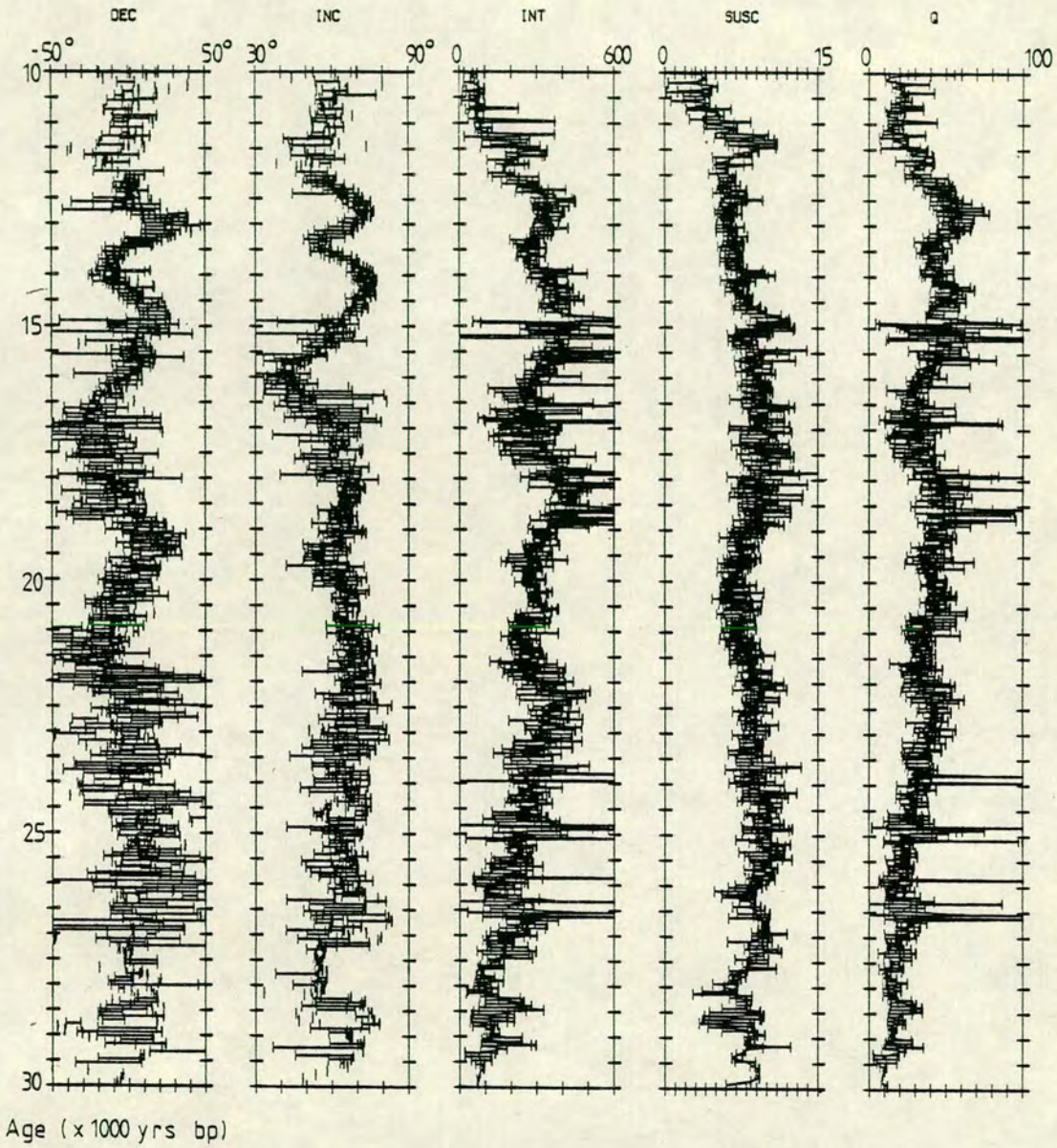

Figure 6.1a The merged records of eight of the cores taken from Lac du Bouchet with the errors calculated by averaging over a period of 15 years.

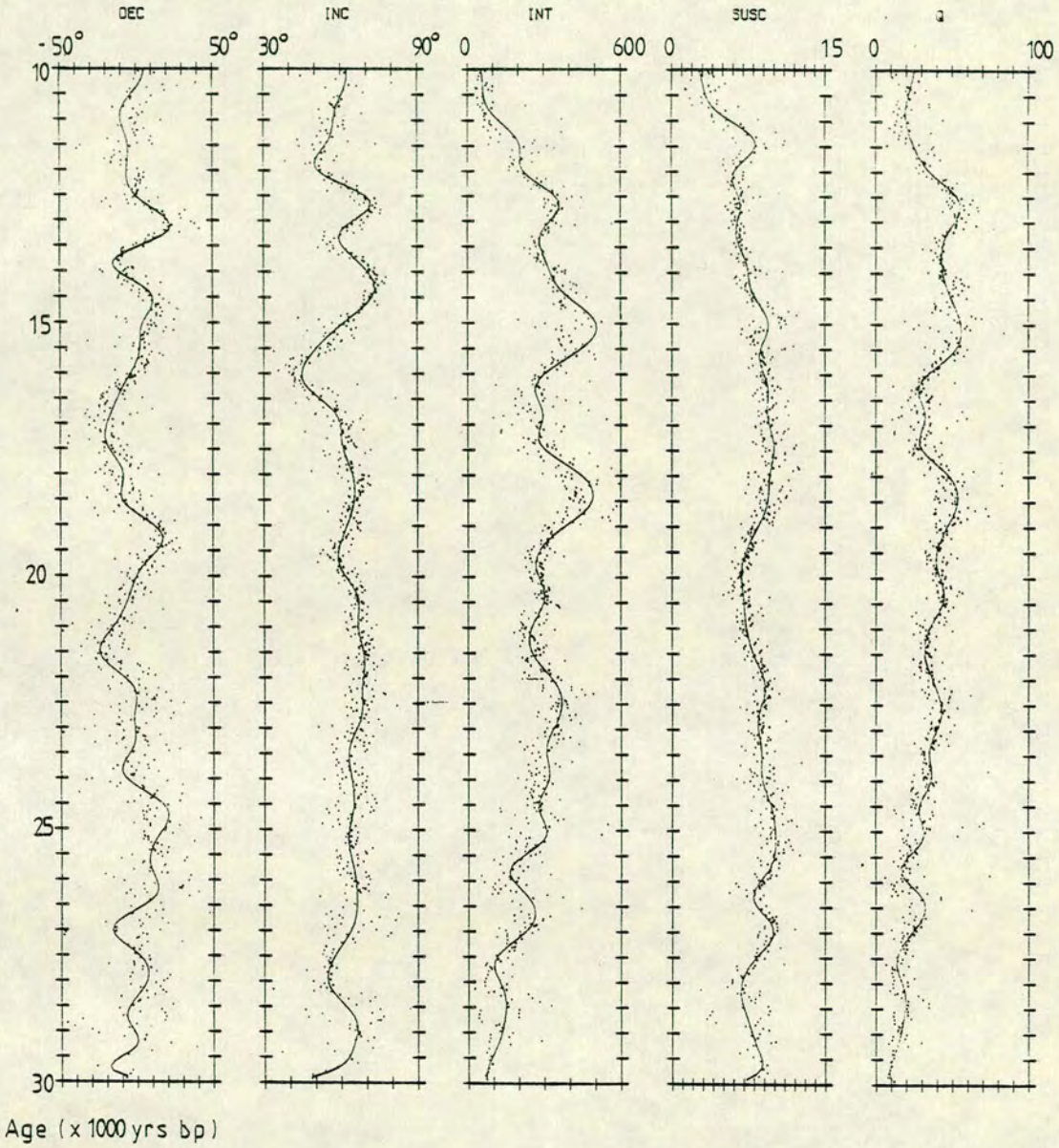

Figure 6.1b The merged records of eight of the cores taken from Lac du Bouchet after a 50 knot cubic spline smoothing.

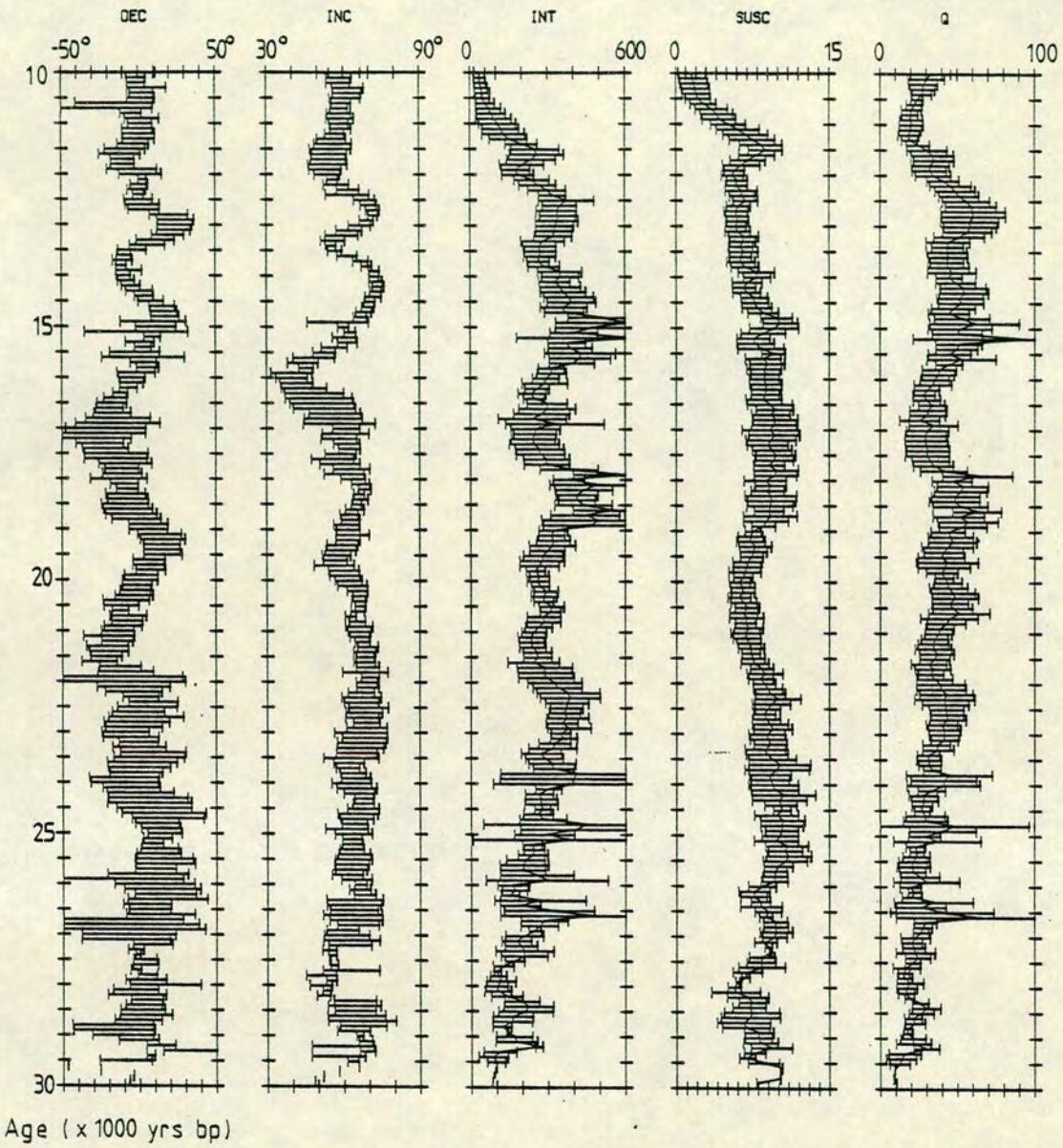

Figure 6.1c The stacked records of eight of the cores taken from Lac du Bouchet with the errors calculated by averaging all the cores at each level.

a) Merged Stack

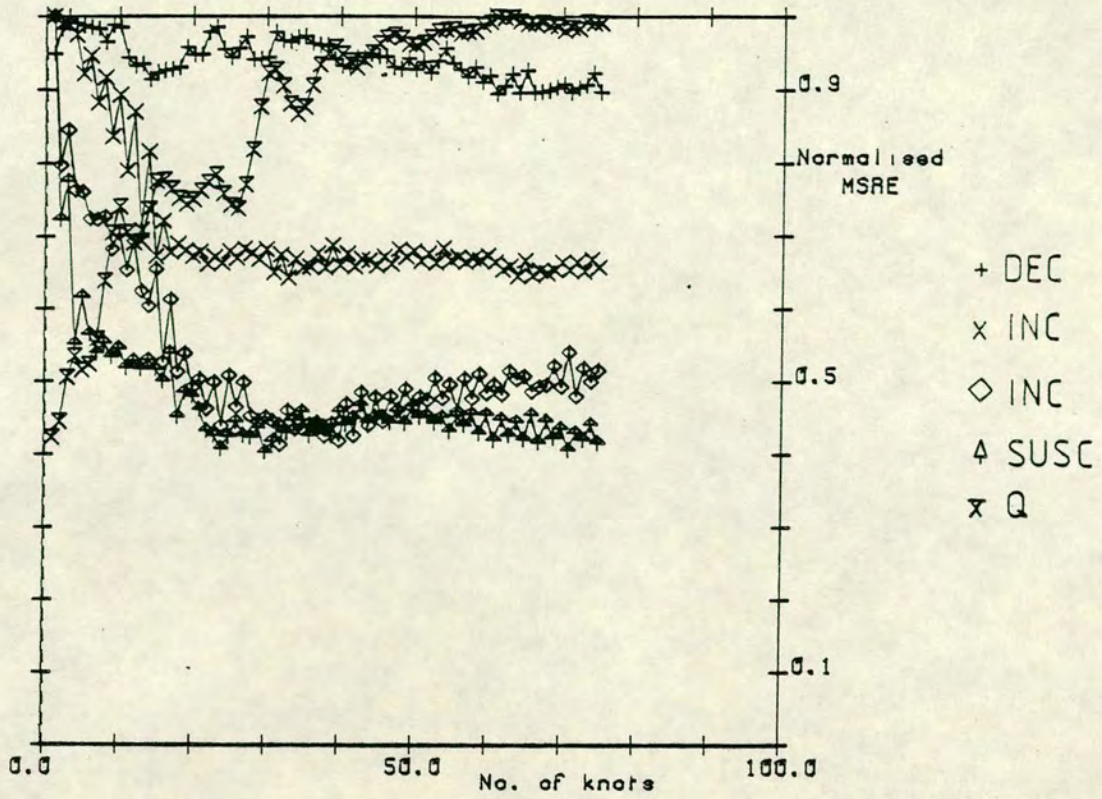

b) Gaussian Stack

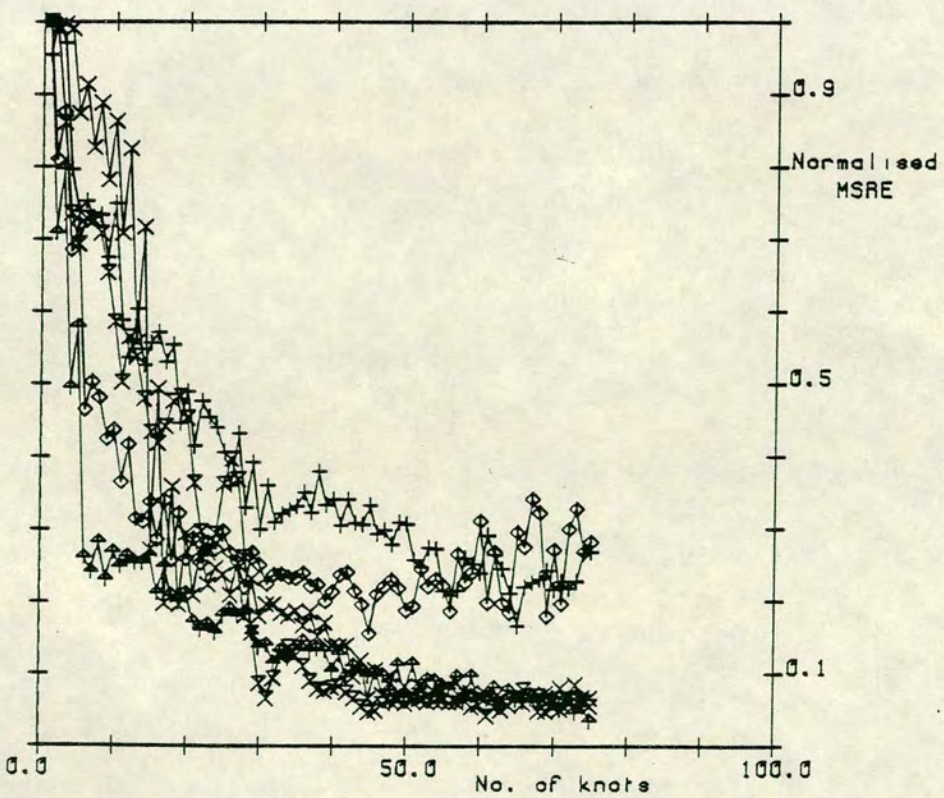

Figure 6.2 The results for the CVSME analysis for the two stacks.

The field can thus be regarded in two parts; dipolar and non-dipolar. The non-dipole field can be investigated by subtracting the dipole component from the total field values. **Yukutake and Tachinaka (1968)** have examined the present day non dipole field and compared it to that of earlier epochs. They have identified non-dipole foci that change in magnitude and either drift or remain stationary. Such a field can be modelled using current loops, or their first order approximation, radial dipoles. **Hurwitz (1960)** has shown what the general effect of a radial dipole (RD) of known strength situated within a sphere, is, on the surface of the sphere. With **Alldredge (1964)** he has modelled the earths magnetic field for epoch 1945. Using such models **Creer (1983)** has shown how the observed secular variation is dependent upon both the type of radial dipole source and the location of the observer with respect to the source. Such models are thus useful for analysing the geomagnetic field.

RDMODEL (appendix 3) allows the secular variation at a site due to drifting and or pulsing radial dipoles to be examined. More importantly noise can be added to the variations in an attempt to mask the actual signal. This allows the programs used to perform the analyses on the Bouchet records to be tested. For each of the analyses performed and described below the results obtained from 2 models are shown prior to the results from Bouchet. The 2 models consist of (i) a single radial dipole drifting westwards at a rate of one complete revolution every 5000 years. (0.07° year^{-1}). and (ii) a single radial dipole drifting westwards as in (i) and pulsing simultaneously with a period of 2000 years.

Figure 6.3 shows the secular variation records produced by the models for a time span of 10,000 years (the variation due to the pulsation alone are also shown). Note that the maximum magnitude of the drifting RD is 0.2 times the moment of the present day main field and that the RD dipoles are located at the core/mantle boundary. In addition, for the spectral analyses, the models have a 10% noise level added to simulate depositional and sampling errors.

6.4 Harmonic analysis of the geomagnetic field

There are two possible approaches to the determination of the harmonic content of the secular variation records of the geomagnetic field. These differ in that one set performs the analysis in the time domain and the other in the frequency domain. Emphasis in this work has been towards the latter approach in particular the use of the discrete Fourier transform method (DFT) using computationally efficient Fast Fourier transforms (FFT) and maximum entropy

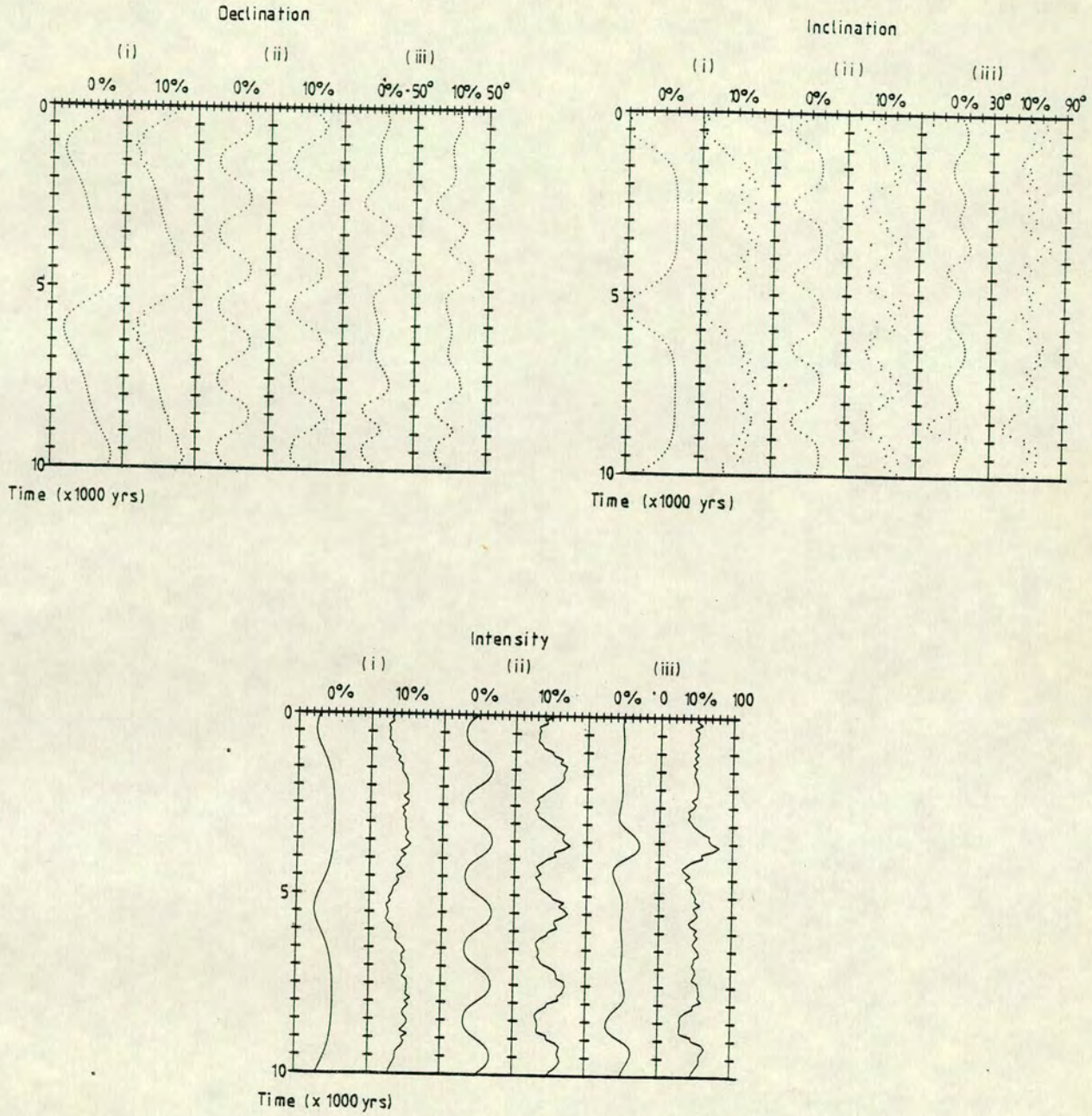

Figure 6.3 The secular variation records produced by (i) a radial dipole drifting westwards at a rate of one revolution every 5,000 years, (ii) a stationary radial dipole whose strength varies sinusoidally with a period of 2,000 years, and (iii) the combination of (i) and (ii). Each plot shows the effect of adding 10% random noise.

method (MEM) analyses.

6.4.1 Time domain analysis

Two methods have been used to determine the major periodicities of the declination, inclination and intensity records in the time domain; by inspection and by correlation.

6.4.1.1 Inspection

A preliminary inspection of a time series always provides valuable information about the spectral content, albeit approximate. A striking feature of the three records examined here, apart from their obvious similarity, is an apparent long period variation, especially within the declination and intensity records. The declination record appears to have a strong periodic content with a period of about 5,000 years (e.g. between 25,000 years and 15,000 years bp) and the intensity record one of about 3,500 years (e.g. four peaks occur at about 25,000, 22,000, 18,500 and 15,000 years bp respectively).

The inclination record has a much smoother pattern for the 10,000 year interval between 30,000 and 20,000 bp. Peak to peak amplitude variations here are between 10° and 15° whereas for the next 10,000 year interval the variation increases to as much as 40°. Note that the record for the UK for the last 10,000 years (**Turner and Thompson, (1979, 1981)**) would also appear "smooth" on this scale as the average peak to peak variation found in those sediments is also about 10° to 15°. Results from North America have peak peak values of between 15° and 25°. Thus although the variations of the inclination record between 18,000 and 12,000 years bp are more spectacular they would still appear to be typical of the variations of the geomagnetic field. The periodicity of the larger amplitude variations is between 1,500 and 2,500 years, shorter than those of the other records, and about 3,000 years for the smaller amplitude variations, similar to those of the intensity record.

The susceptibility record has not been subject to spectral analysis. It too would appear to have a long period variation that, not being reflected in the intensity record, would appear to be sedimentological in origin. The susceptibility may follow the variation in the concentration of magnetite within the sediment which in turn will vary with other external factors. The period of between 7,000

and 8,000 years would then reflect changes in the depositional environment affecting the sediment and is thus probably climatological in origin.

6.4.1.2 Autocorrelation

For all the analyses described below, the 20,000 year late glacial record was examined using a sampling interval of 100 years in four 'windows'.

(a) A 20,000 year record, 30,000–10,000 years bp (window A, N = 200).
(b) Three 10,000 year records as follows:
    (i) 30,000–20,000 years bp (B, 100).
    (ii) 25,000–15,000 years bp (C, 100)
    (iii) 20,000–10,000 years bp (D, 100).

where N is the number of data points.

The purpose of these different windows is to establish the stationarity of the variations. The figures show the results for the two stacks for window A only. Note that for comparison the results for the models have been calculated for a similar 20,000 year window (200 points).

Autocorrelation and cross correlation were performed on the records using the program CORRELATE. The results for the models are shown in **figure 6.4a**, the results for the four windows of the three records are given in **table 6.1** and the autocorrelation functions are shown in **figure 6.5a**. The main periods that are apparent from the autocorrelations are 4,500 years for the declinations, 4,000 years for the inclination and 1,800 years for the intensities. The periods correspond to successive peaks in the autocorrelation function as shown in **figure 6.4a** and **6.5a**.

6.4.1.3 Cross correlations

The cross correlation functions between the three combinations of pairs of records are also calculated by CORRELATE. The cross correlation functions obtained for the models and the stack are shown in **figures 6.4b** and **6.5b**. None of the pairs show clear cross correlations, only weak features indicate periods of 6,000 years for the declination – inclination pair. Similar periodicities occur for the other pairs, but these too are very weak.

(i)

a) Autocorrelation

b) Cross correlation

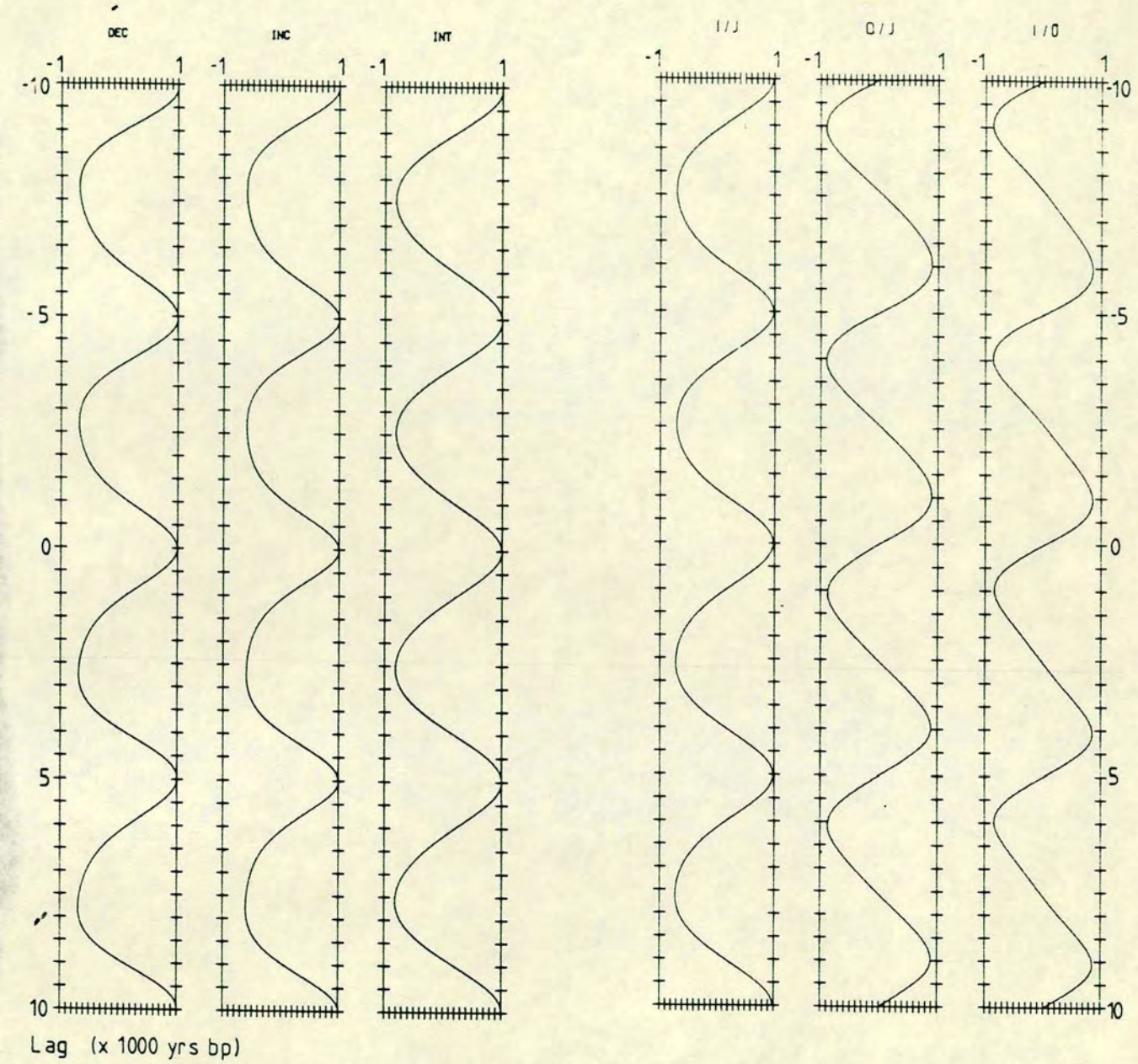

Figure 6.4 a) autocorrelation and b) cross correlation results for model (i) (see text).

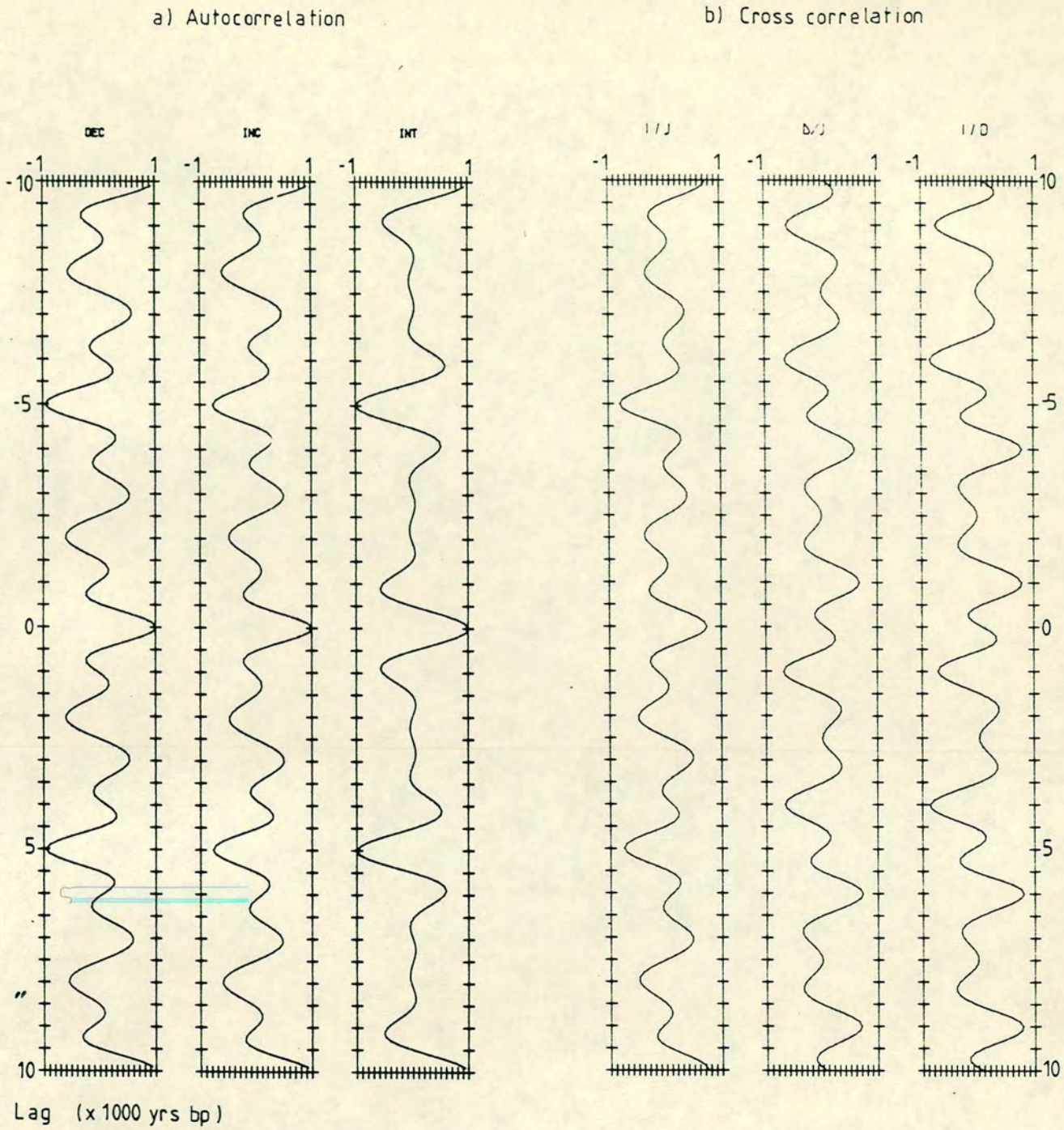

Figure 6.4 a) autocorrelation and b) cross correlation results for model (ii) (see text).

Table 6.1 The main periods obtained from an examination of the autocorrelation functions. The minus sign indicates that the correlation is negative; the order given is the order of relative strengths of the correlations.

Window	Main Periods (years)					
	Merged Stack			Gaussian Stack		
	Dec	Inc	Int	Dec	Inc	Int
A	2500- 6000	4000	4700-	2400- 2900	4000	4700-
B	4500	4000 2100	1800 3000	3400- 2700	2400	1800
C	2500-	3600	1800- 3800	2100-	3500 2400-	1800- 3500
D	4500	2200- 4200	3200	4000 2200-	2200- 4200	1800- 3000

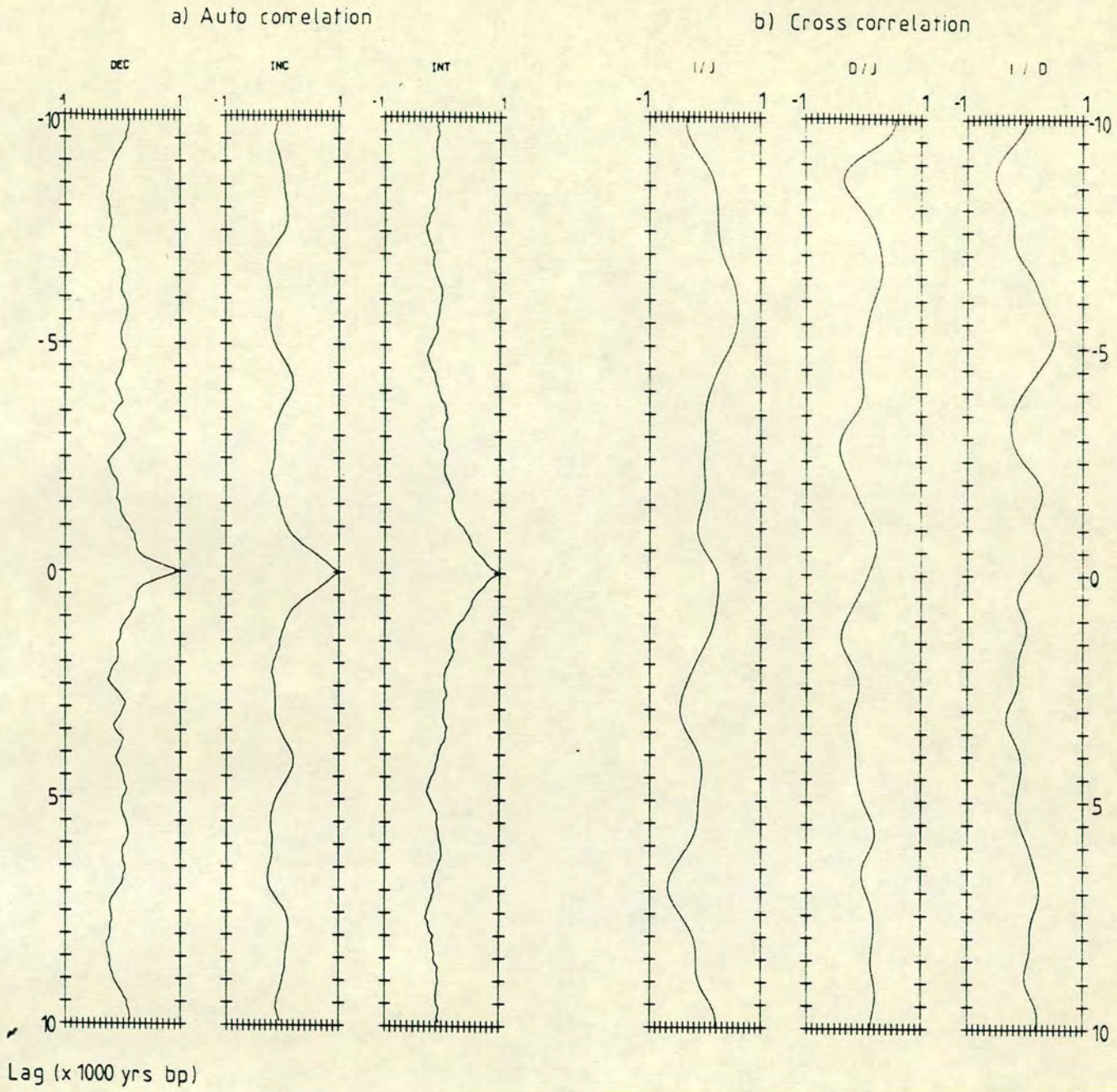

Figure 6.5 The result of a) autocorrelation and b) cross correlation for the merged stack of eight Lac du Bouchet cores.

6.4.2 Frequency domain analysis

Two different power spectral analysis techniques have been used to analyse the Bouchet records. A multivariate complex FFT (**Singleton, (1968)**) has been used to obtain the DFT spectra and algorithms based on **Burg (1967,1968)**, **Anderson (1974)**, **Smylie et al.. (1973)** and **Barton (1983a,1983b)** for the MEM analysis.

6.4.2.1 Fourier Analysis

For an evenly spaced, stationary, time series of infinite length the Fourier transform method (**Schuster (1898)**, **Jones (1965)**), is a powerful tool. In practice it requires strong assumptions about the nature of the series outside the window being analysed, namely that it be periodic and stationary.

With short time windows resolution can also be a problem since the Fourier components (and thus the power) can only be determined at harmonics of the fundamental frequency, which is the reciprocal of the length of the data window. The first FFT's developed were based on the fact that these harmonic coefficients are easily determined if the number of data points is a factor of 2 (**Cooley and Tukey (1965)**). The less restrictive method used here relies on the number of data points being factorisable by prime numbers (**Singleton (1968)**). This method can usually cope with the full input data set, if not the last point in the set is discarded and a new attempt made. It follows that this provides a more accurate spectral estimate for data sets that are not a factor of two, than by padding with zeros or reducing the number of data points to the next factor of two. The program developed for this work is called FOURIER.

Before the FFT is performed the data is detrended by removal of a first order polynomial. It can then optionally be tapered by multiplying the first and last 10% of the data by a half cosine bell. More sophisticated tapers are not used since the likely errors introduced by leakage will be less than the likely measurement and recording errors of the geomagnetic field from the sediment.

The program has been thoroughly tested using synthetic data generated by the programs WAVES and RDMODEL. **Figure 6.6** shows the results obtained for the models. A cosine taper was applied to the data and the power spectra generated only as far as a 1,000 year period. The diagrams show the normalised

(i)

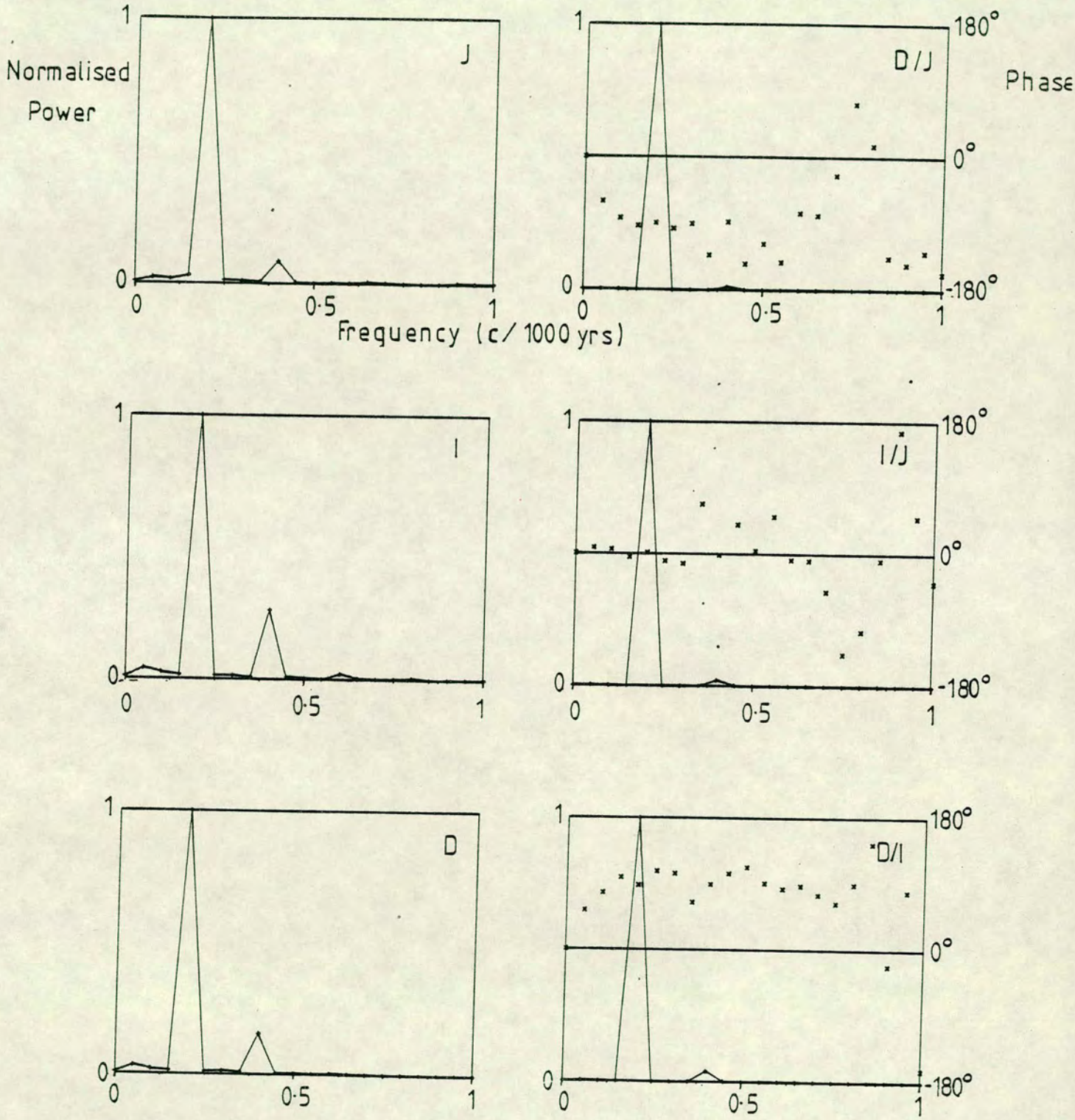

Figure 6.6 The Fourier transform spectra for model (i).

(ii)

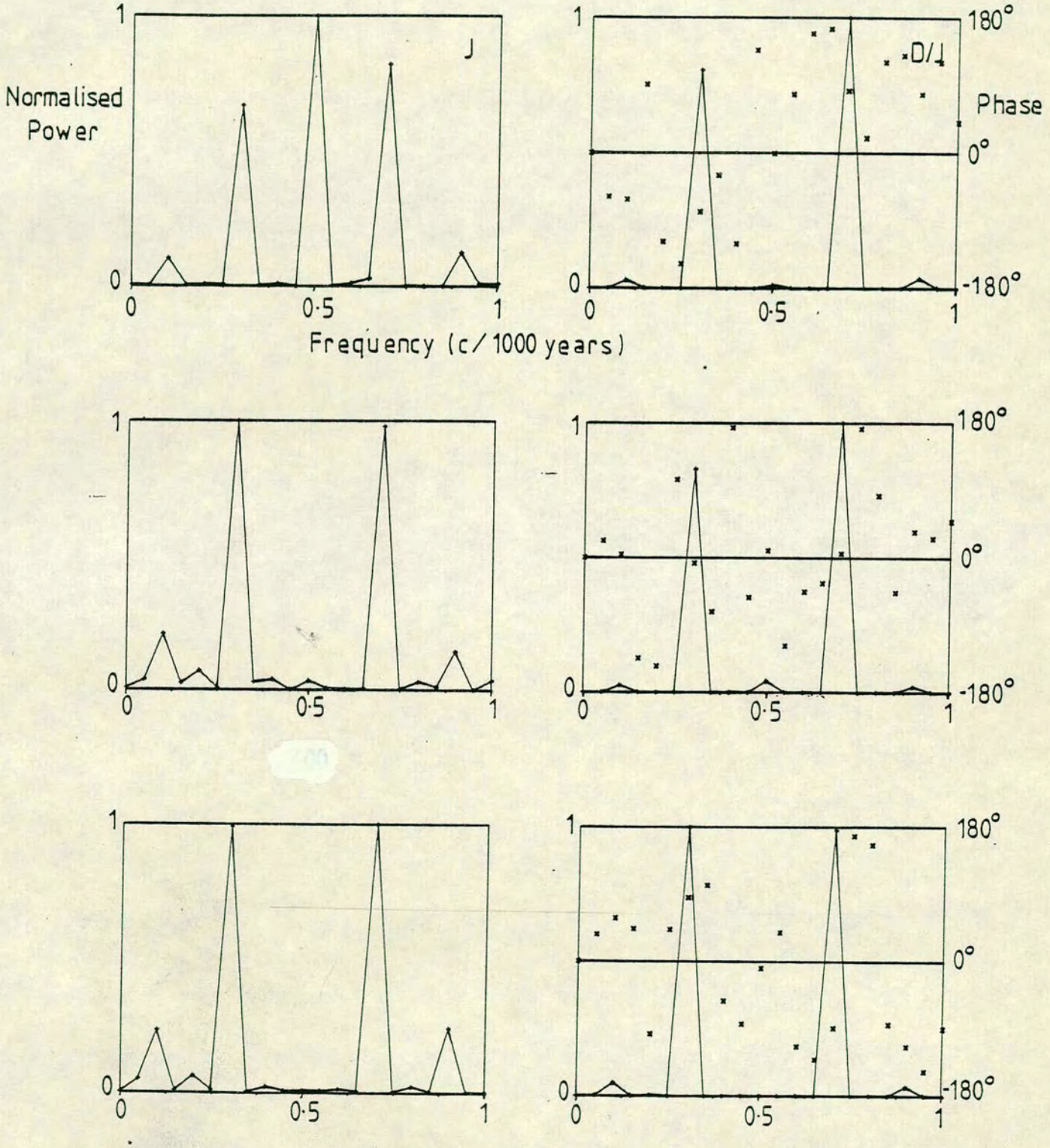

Figure 6.6 The Fourier transform spectra for model (ii).

power spectra for the declination, inclination and intensity. In addition there is the coherency spectrum and phase spectrum for the three pairs. The coherency is shown as a continuous line through the points and the phase as crosses superimposed upon the coherency spectra.

The analysis of the Bouchet records is shown in **figure 6.7** for the two stacks. The main periods are shown in **table 6.2.**

The most striking feature of the results of the Fourier analysis is the consistency of the appearance of the 2,000 year harmonic. Other major periods are 5,000 years and 3,300 years. Obviously the resolution of these periods is dependent on the window being analysed but the maximum errors for these periods are 100, 715 and 300 years respectively. Most of the power in the spectra is found at periods between 3,000 and 10,000 years and as would be expected if the source were noise, the power drops appreciably for periods less than 1,200 years.

The coherency spectra confirm these observations; most of the power being in the same period range. The phase spectra reveal that only the inclination and intensity are in phase at the 2,000 year harmonic. In particular the declination and inclination appear to be out of phase by about 60°; the positive value indicating that the declination is leading the inclination (indicative of westward drift), agreeing well with the direct inspection described in section 6.4.1.1.

6.4.2.2 MEM Analysis

Maximum entropy method analysis is a parametric modelling approach to the estimation of the power spectrum of a time series. The method is data adaptive being based upon an autoregressive (AR) modelling process. An AR process is predictive; any point (after the first) can be calculated by a linear combination of a previous number, m, of the values of the data points with the addition of some "innovation" factor (**Yule (1927)**). The order of the process, in this case m, is the number of immediately previous points that have been used in the calculation of the new point. The mean of both the process and the innovation are made to be zero. The power spectrum of such a process can then be easily calculated (e.g. **Ulrych and Bishop (1975)**).

Burg (1967,1968) introduced the idea of the MEM. This essentially involves fitting an AR model to the data with the constraint that the resultant estimate of

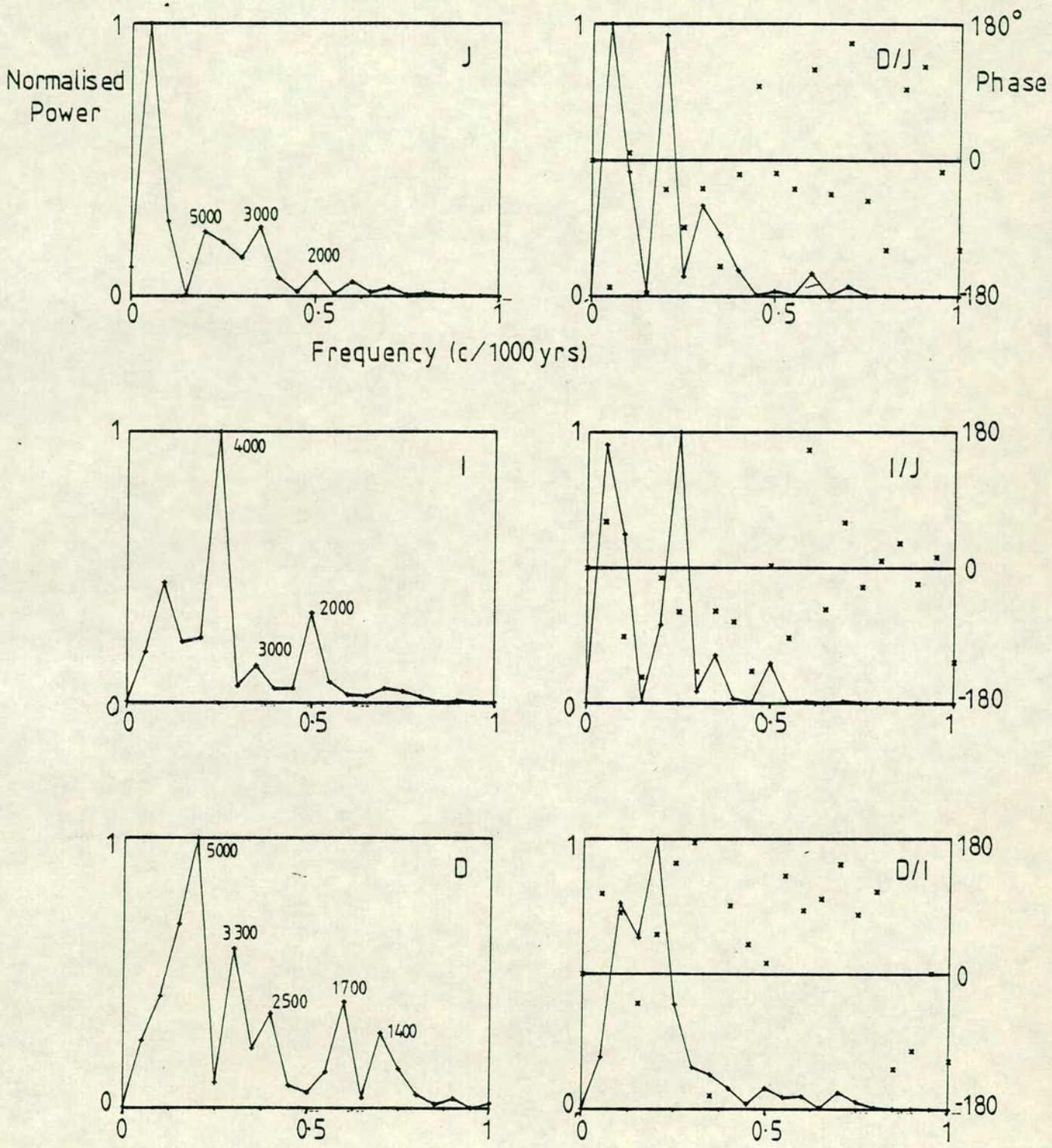

Figure 6.7a The Fourier transform spectra for the merged stack.

(b) Gaussian Stack

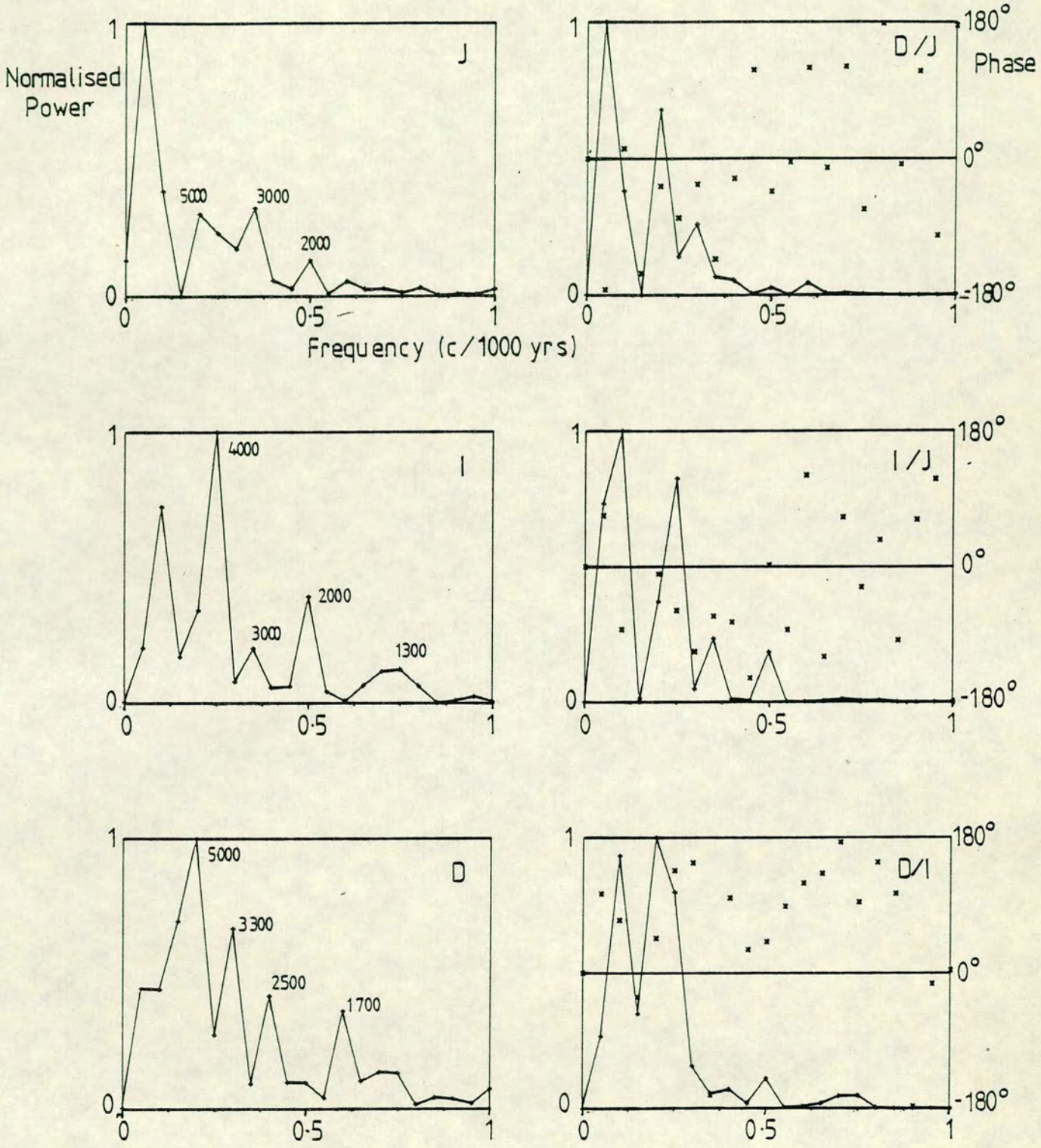

Figure 6.7b The Fourier transform spectra for Gaussian stack.

Table 6.2a The main periods obtained from an examination of the Fourier transform spectra for the merged stack. Note that periods found in the spectra of the same order as the length of the data set have been ignored.

a) Main periods

Window		>4000	3000-3500	2000-2500	1500-2000	1000-1400
A	D	5000	3300	2500	1700	
	I	4000	3000	2000		
	J	5000	3000	2000		
B	D			2250	1700	
	I		3300	2000		1400
	J			2000		
C	D	5000				
	I		3300	2000		
	J		3300			
D	D	5000		2000		1400
	I	5000		2000		1400
	J		3300		1700	

b) Coherency (Phase)

Window		>4000	3000-3500	2000-2500	1500-2000	1000-1400
A	DI	5000 (60)		2000 (45)		
	IJ	4000(-60)		2000 (0)		
	JD	5000(-60)	3300(-45)	2000(-45)		
B	DI			2000(-30)		
	IJ		3300 (0)	2000 (0)		
	JD			2000 (45)		
C	DI	5000(135)				
	IJ		3300(-60)			
	JD	5000(-60)				
D	DI	5000 (60)		2000 (60)		
	IJ	5000(-20)				
	JD	5000(-20)				

Table 6.2b The main periods obtained from an examination of the Fourier transform spectra for the Gaussian stack. Note that periods found in the spectra of the same order as the length of the data set have been ignored.

a) Main periods

Window		>4000	3000-3500	2000-2500	1500-2000	1000-1400
A	D	5000	3300	2500	1700	
	I	4000	3000	2000		1300
	J	5000	3000	2000		
B	D			2250		
	I		3300			1430
	J		3300	2000		
C	D	5000			1700	
	I		3300	2000		
	J	5000				
D	D	5000			1700	
	I	5000		2000		1430
	J		3300			

b) Coherency (Phase)

Window		>4000	3000-3500	2000-2500	1500-2000	1000-1400
A	DI	5000 (60)				
	IJ	4000(-60)				
	JD	4000(-45)				
B	DI			2500(180)		1430(120)
	IJ		3300(-60)			
	JD					
C	DI		3300(120)			
	IJ		3300(-60)			
	JD	5000(-60)				
D	DI	5000 (60)		2000 (60)		
	IJ	5000 (0)				
	JD		3300(-60)			

the spectra should be based upon information totally contained within the data and make no assumptions about the data outside the window analysed. This constraint is satisfied by an AR process of order m. The coefficients of this process are called the prediction error filter (pef) because the convolution of this filter with the data will result in the model error (the "innovation" above). The spectra for such a model can thus easily be estimated with a single additional condition; the mean of the prediction error powers (obtained by running the pef along the data (but not off) in a forward and reverse direction), should be a minimum. The power spectral estimate is then based purely upon the data available and makes no assumptions about data outside the window. For this reason this method is (and such data adaptive methods in general are) particularly suitable for short series.

There remains a problem: the selection of the length of the pef. If m is chosen to be too small, the model smooths the data excessively and the resulting estimate of the power spectra is poorly resolved. If m is chosen to be too large, frequency shifting and spontaneous splitting of peaks can occur resulting in a poorly defined estimate of the spectrum (**Fougere et al. (1976)**). Objective methods do exist, although the lack of agreement on which is best shows how the choice is very dependent on the data being analysed.

The program MEM uses the suggestions made by (a) **Ulrych and Bishop (1975)** and (b) **Berryman (1978)**. These are

(a) that m is between $^{N}/_{3}$ and $^{N}/_{2}$

(b) that m = $^{2N}/_{\ln 2N}$

where N is the number of data points. Modelling of the secular variation has shown that m = $^{N}/_{3}$ is too short and excessively smooths the data and that m = $^{N}/_{2}$ is too long, producing spurious peaks. For this work the optimum order for all the models is found to be close to that suggested by Berryman. **Figure 6.8** shows the MEM spectra produced for the declination for the models. The four plots for each record are the three orders given above with an additional order midway between the Berryman criterion and the larger Ulrych/Bishop suggestion. In this case, with low noise data the lowest order has adequately determined the spectral content (but note the spiky structure of the higher order). The best estimate is at the order suggested by Berryman. Interestingly this method works better with noisier data especially with short data sets. Even a pef length of $^{N}/_{3}$ is too long for the noise free data. **Figure 6.9** shows the results from

(i)

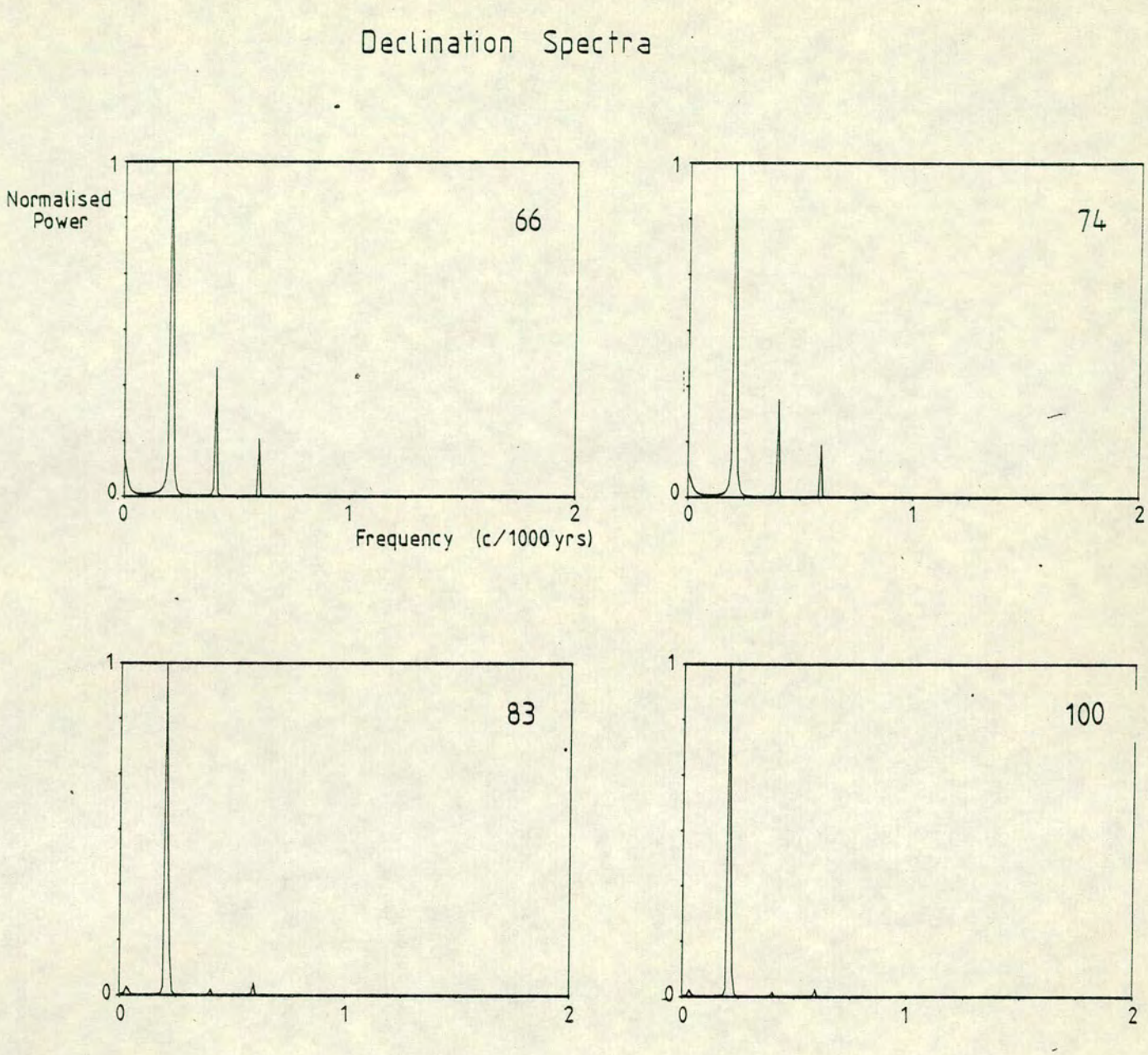

Figure 6.8 The MEM spectra for the model (i) declinations showing the effect of varying the pef length.

(ii)

Declination Spectra

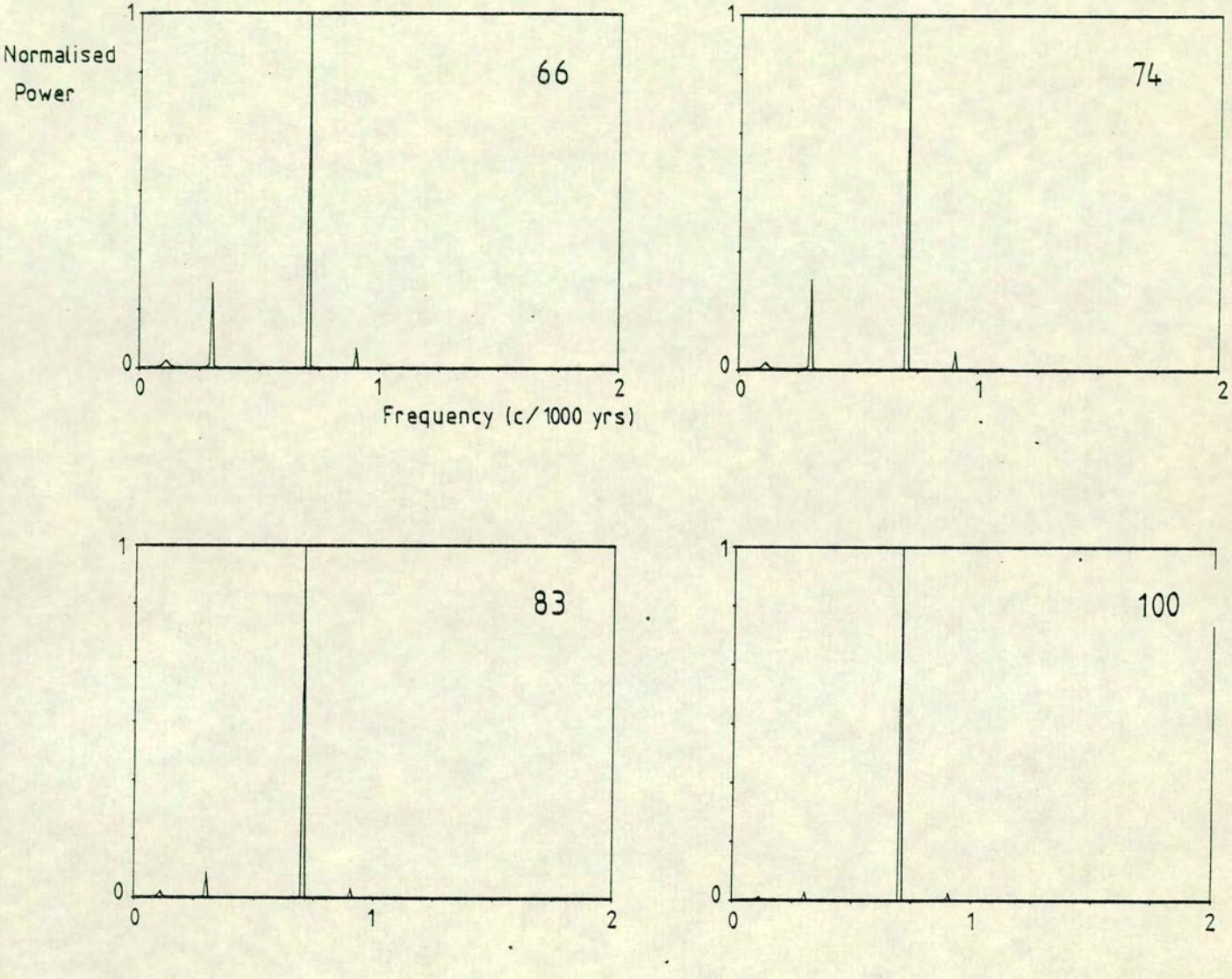

Figure 6.8 The MEM spectra for the model (ii) declinations showing the effect of varying the pef length.

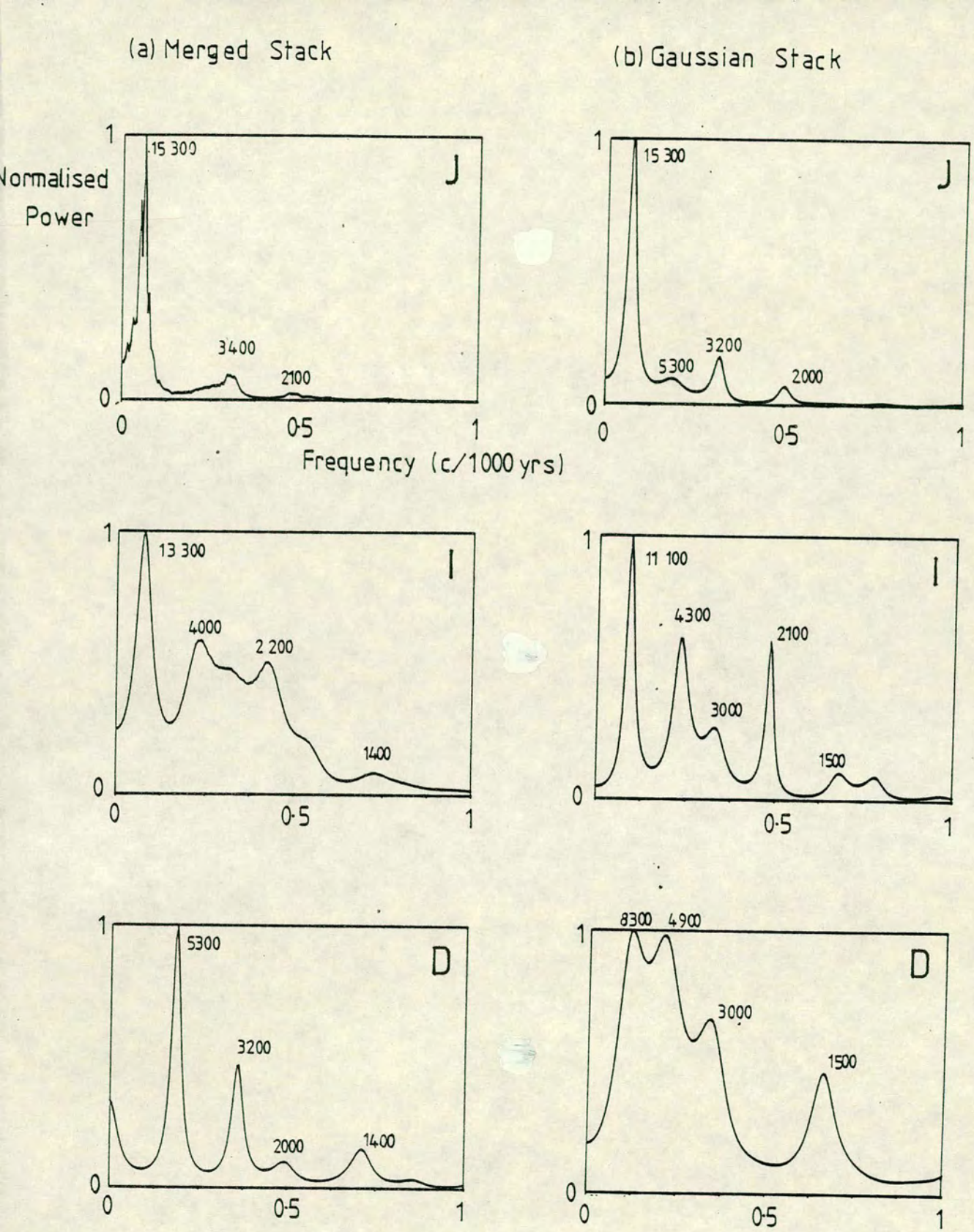

Figure 6.9 The MEM spectra for a pef length of 67 for a) the merged stack and b) the Gaussian stack.

Table 6.3 The main periods found from an examination of the MEM spectra for the two stacks.

a) Merged Stack

Window		>6000	4000-5500	3000-3500	2000-2500	1500-2000	1000-1400
	D		5300	3200	2000		1400
A	I	13300	4000		2200	1800	1400
	J	15300		3400	2100		
	D	8600			2300		1200
B	I		5200		2200		1400
	J	8000			2300		1350
	D		5200			1550	
C	I	8300		3400		1900	
	J			3300	2100		
	D		5000	3100	2100	1550	
D	I		4700			1900	1350
	J	8700		3300		1800	

b) Gaussian Stack

Window		>6000	4000-5500	3000-3500	2000-2500	1500-2000	1000-1400
	D	8300	4900	3000		1500	
A	I	11100	4300	3000	2100	1500	
	J	15300	5300	3200	2000		
	D	7700			2500		1400
B	I				2300		
	J	8000			2100		
	D		4900	3000			
C	I	8300		3800		1700	
	J			3800		1800	
	D		5700				
D	I		5000		2100		1300
	J	8700		3100			

stacks for the Berryman order (67) and **table 6.3** summarises the results of the analysis of the four windows.

The spectra produced in **figure 6.10** is the spectra of the model declination and inclination together forming a complex variable in **Denham's (1975)**, method of projection. This approach results in power being found in negative (positive) frequencies when the northern pole of the virtual geomagnetic pole (VGP) is moving in a clockwise (anticlockwise) sense. Such paths are discussed in more detail in the next section. The model with a single drifting radial dipole illustrates the type of spectrum produced. Westward drift would give clockwise precession of the northern pole of the VGP and hence the power appears at a negative frequency.

Both **Dodson (1979)** and **Creer (1983)** have brought attention to the non-uniqueness of the association of SV source drift direction and the motion of the magnetic vector in the VGP plot. (See next section).

The result of the application of the complex MEM analysis on the Bouchet stacks is illustrated in **figure 6.11** and the results are summarized in **table 6.4.**

The results of the MEM analysis agree exceptionally well with the results of the Fourier analysis. Power is found at the long period end of the spectrum in particular at periods of about 5,300, 3,300 and 2,000 years. In these records the intensity and inclination spectra also have power at longer periods, not resolved by the Fourier method and for which this method is better suited. Error estimates are more difficult to obtain for this method, but by averaging the results from the different stacks and windows, appear to be of the same order as those for the Fourier spectra or less. (The results appear to be in agreement with the general conclusions drawn by **Swingler (1980)** about the effectiveness of the two techniques as frequency estimators).

6.5 VGP Paths

Bauer (1899) suggested plotting the SV of the geomagnetic vector as the locus of the point on a unit sphere defined by the declination and inclination. **Runcorn (1959)** observed that a westward drifting non dipole field source would result in a clockwise looping VGP path, and vice versa. Despite the non-uniqueness of this property (**Dodson (1979), Creer (1983), Skiles (1970)**), the VGP paths described by the secular variation provide an insight into source

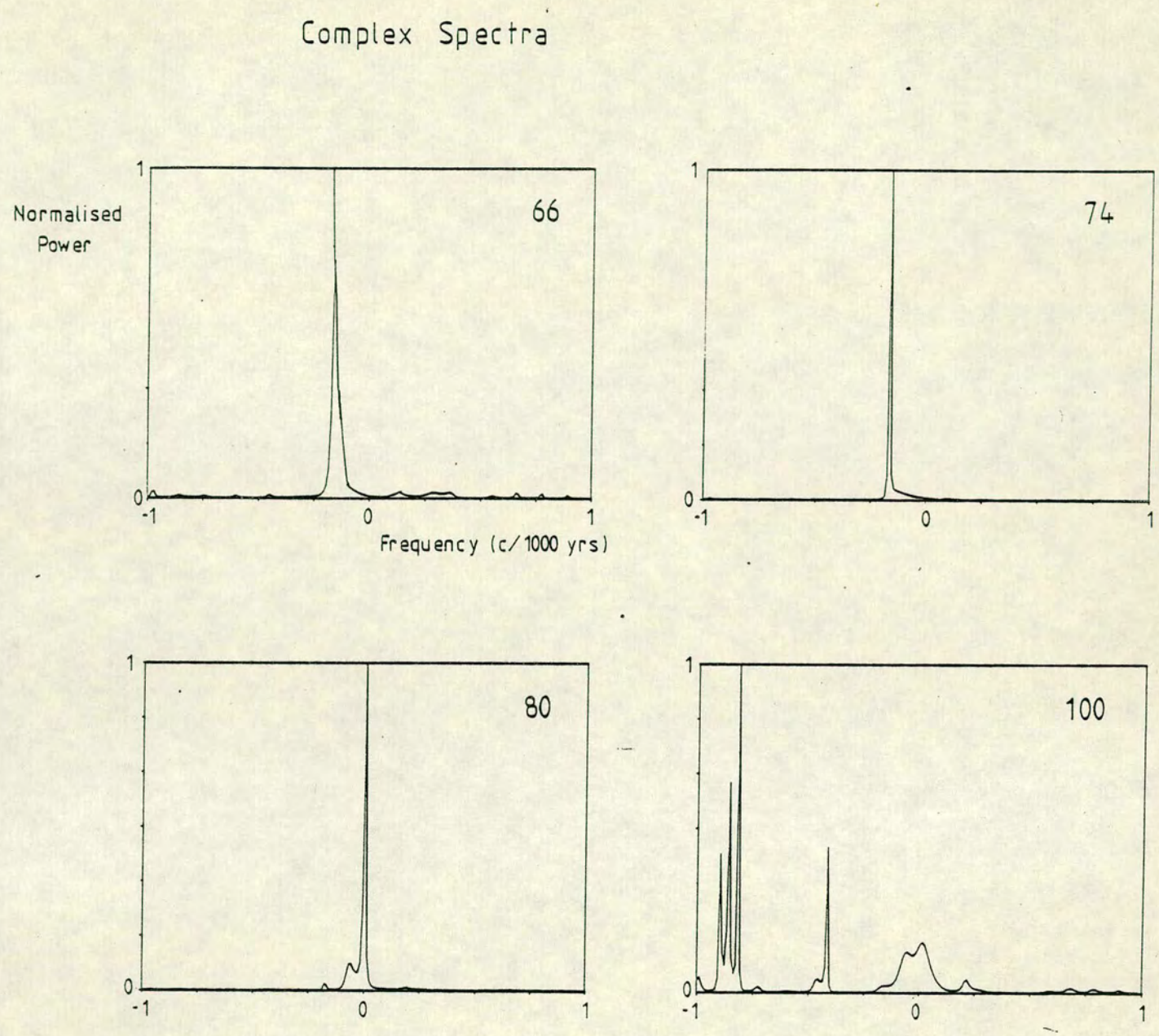

Figure 6.10 The complex MEM spectra for model (i).

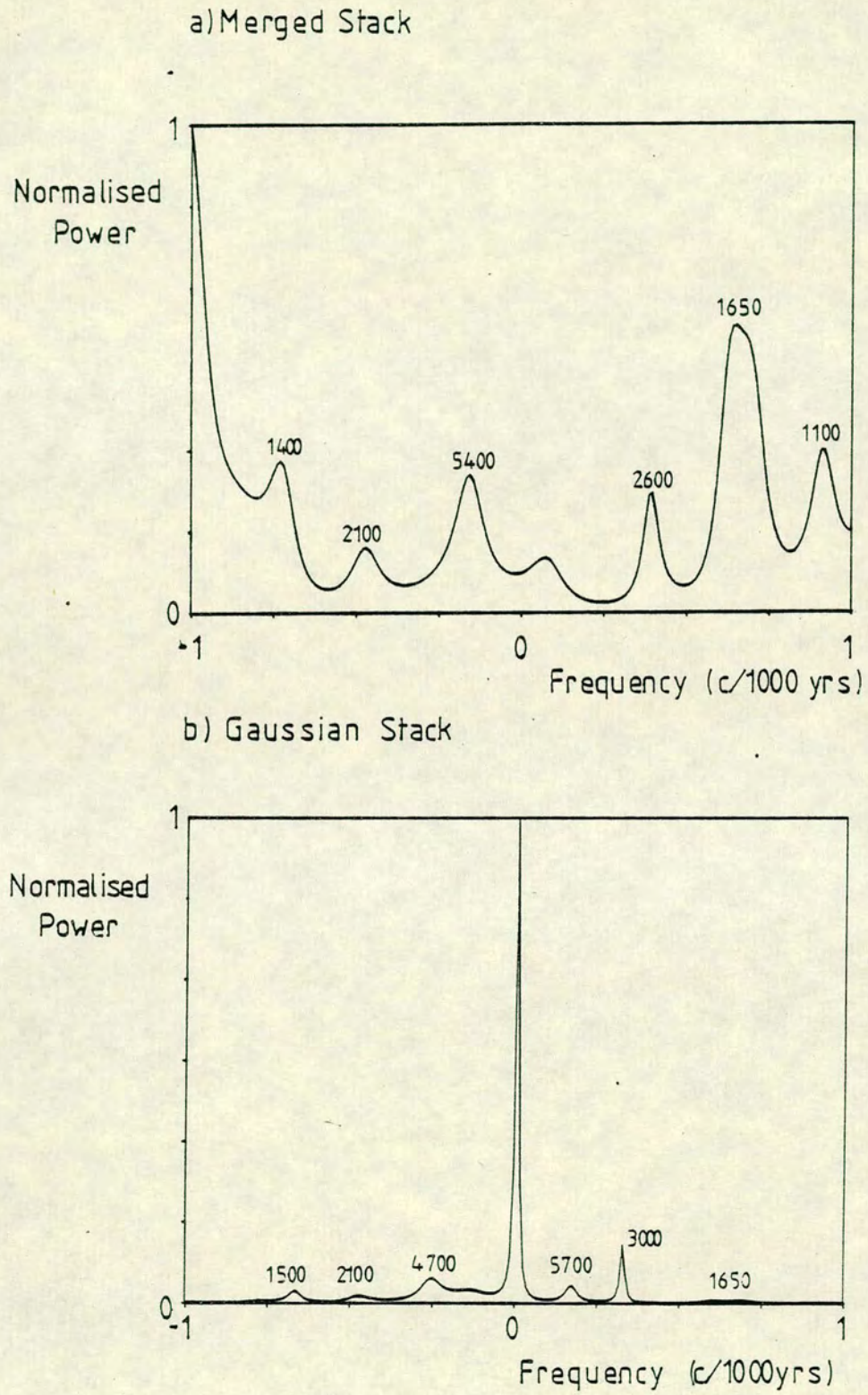

Figure 6.11 The complex MEM spectra for a) the merged stack and b) the Gaussian stack.

Tables 6.4 The main periods found from a complex MEM analysis of the two stacks.

a) Merged Stack

Window		>6000	4000 5500	3000 4000	2000 3000	1500 2000	1000 1500
A	+				2600	1650	1100
	-		5400		2100		1400
B	+		4900			1800	
	-			3900		1550	
C	+					1900	1200
	-					1800	
D	+					1900	
	-				2700		1200

b) Gaussian Stack

Window		>6000	4000 5500	3000 4000	2000 3000	1500 2000	1000 1500
A	+		5700	3000		1650	
	-		4700		2100		1500
B	+	7400			2700		1400
	-	8700			2500		1400
C	+	6900		3000			1500
	-			3900		1800	1200
D	+	6900				1600	
	-		5400		2800	1600	1300

motions and provide a means of comparing the results from different sites. Modelling of the VGP paths produced by RD sources drifting and pulsating at different frequencies can, by comparison with real records indicate the nature of the source motions. The VGP paths produced by the noise free models are shown in **figure 6.12**. Note the open clockwise looping of the drifting source and the linear path of the pulsing source. The combination of the two produces the petal pattern observed in **figure 6.12c**.

6.5.1 VGP Paths from Lac du Bouchet

Window A from the previous section has been further subdivided to allow the VGP path to be clearly observed. 2,500 year intervals are plotted in **figure 6.13**. The merged stack has been used after smoothing using 50 knots in the same range (as found by calculating the minimum CVMSE using BESTKNOTS). If we define three types of motion of the VGP path namely

(i) Open clockwise looping
(ii) Open anticlockwise looping
(iii) linear tracking

then we can summarise the motion of the VGP path. In the record from 30,000 to 10,000 years bp there is predominantly clockwise looping (65%). This would be expected if the sources were drifting predominantly westwards. If the data were white noise the variation would become 50% clockwise and 50% anticlockwise over any window. (This may occur over specific windows even without noise). The main period of clockwise looping occurs between 17,500 and 12,500 years bp, with other periods also occuring. There are periods of linear tracking (e.g. between 22,500 and 18,000 years bp) and anticlockwise looping (e.g. between 28,500 and 25,000 years bp).

One observation from the variation of the VGP paths that must be noted is that there are clear periods of open, clockwise looping whilst the periods of anticlockwise looping generally last for very short intervals of time and tend to link periods of either open clockwise looping or linear tracking. This would be the expected effect from westward drifting sources passing the site. The periods of anticlockwise looping and weak clockwise looping would be directly associated with the time between the main anomalies.

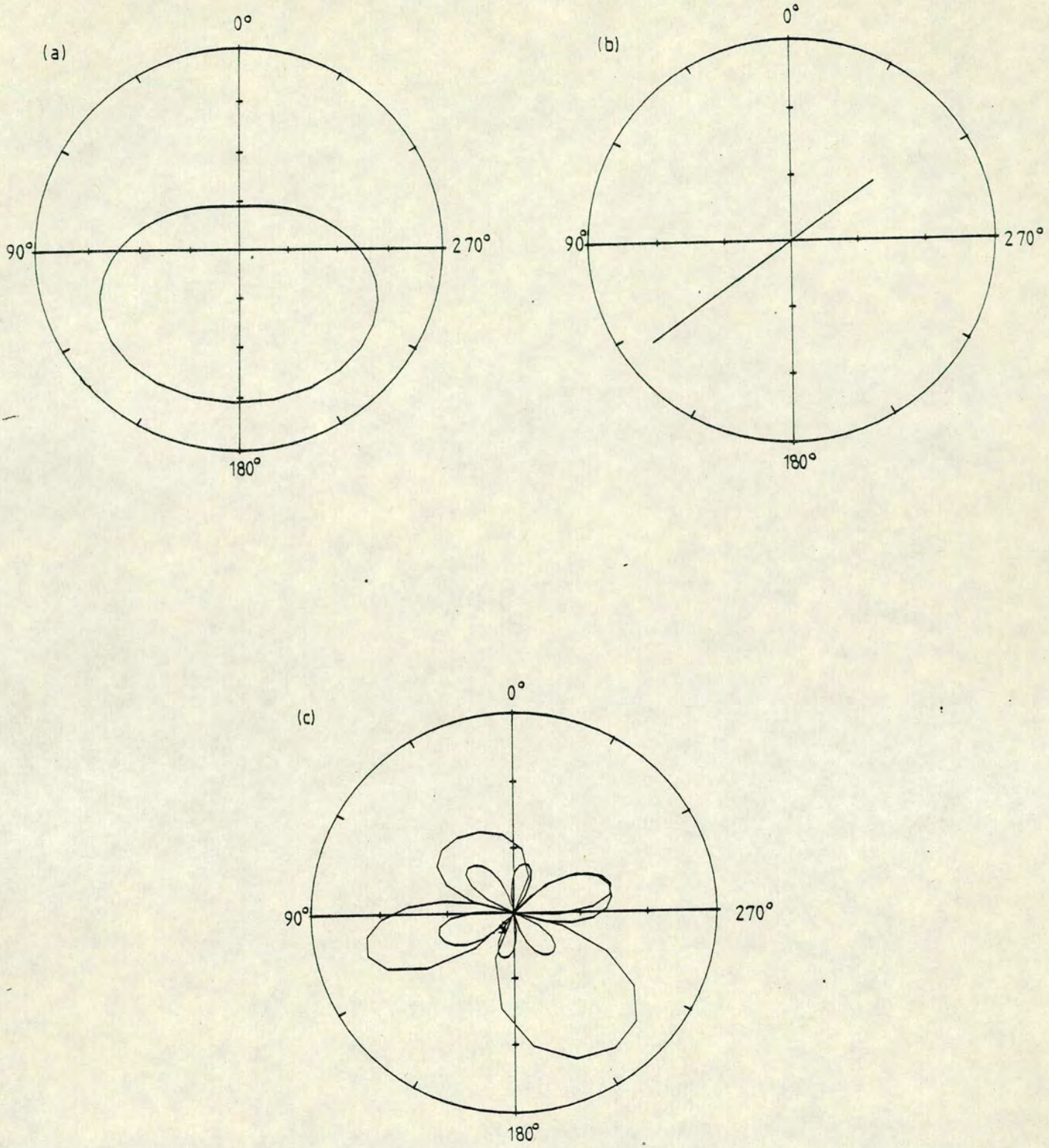

Figure 6.12 The VGP path of a) model (i) showing open clockwise looping, b) the stationary pulsing model showing a linear path and c) model (ii) which combines pulsing and drift and produces a 'petal' pattern. The latitude is 90° at the centre and marked in 10° increments.

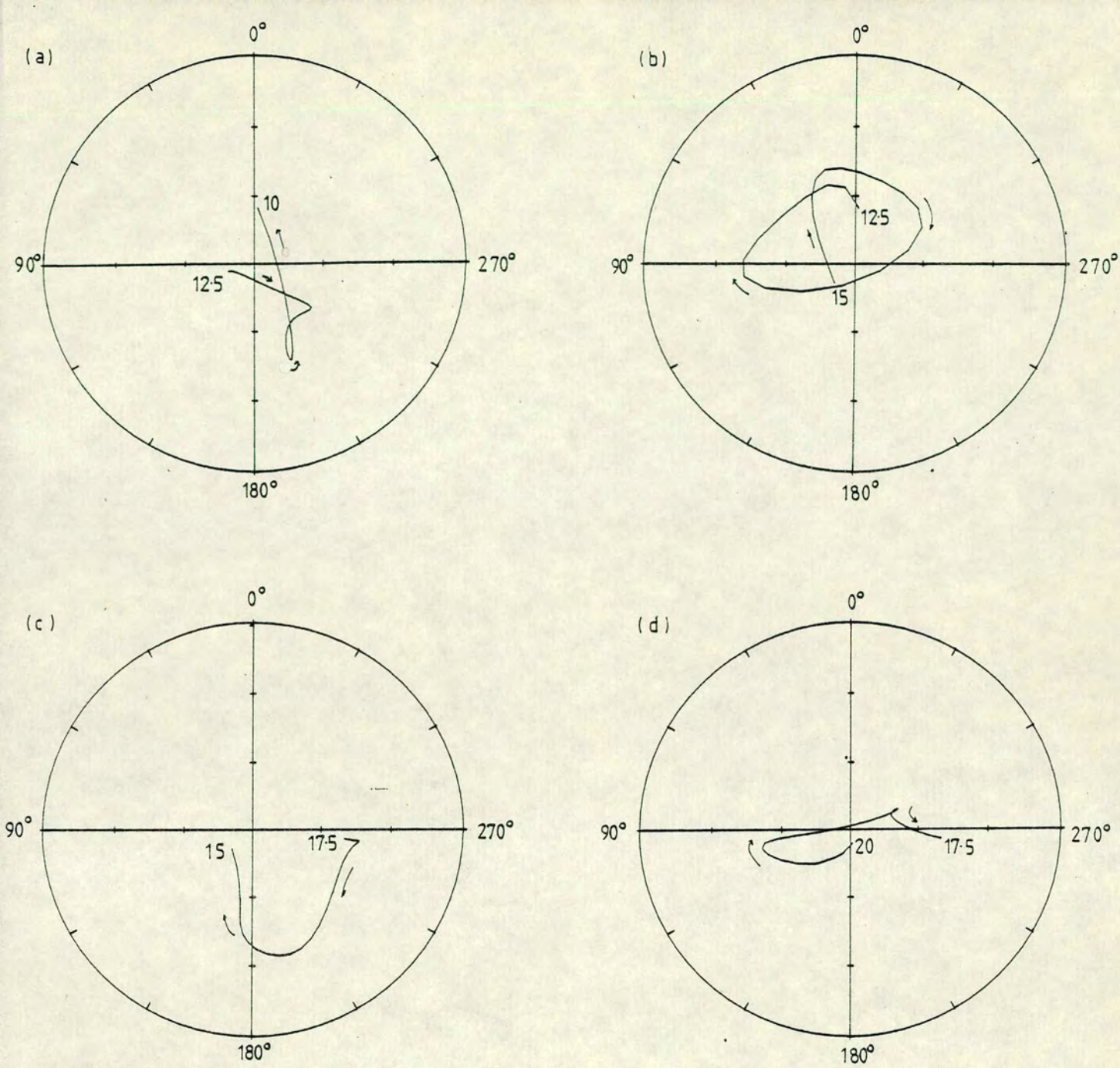

Figure 6.13 The VGP paths for the 50 knot smoothed merged stack in 2,500 year increments. a) 12,500 - 10,000 years bp b) 15,000 - 12,500 years bp c) 17,500 - 15,000 years bp d) 20,000 - 17,500 years bp

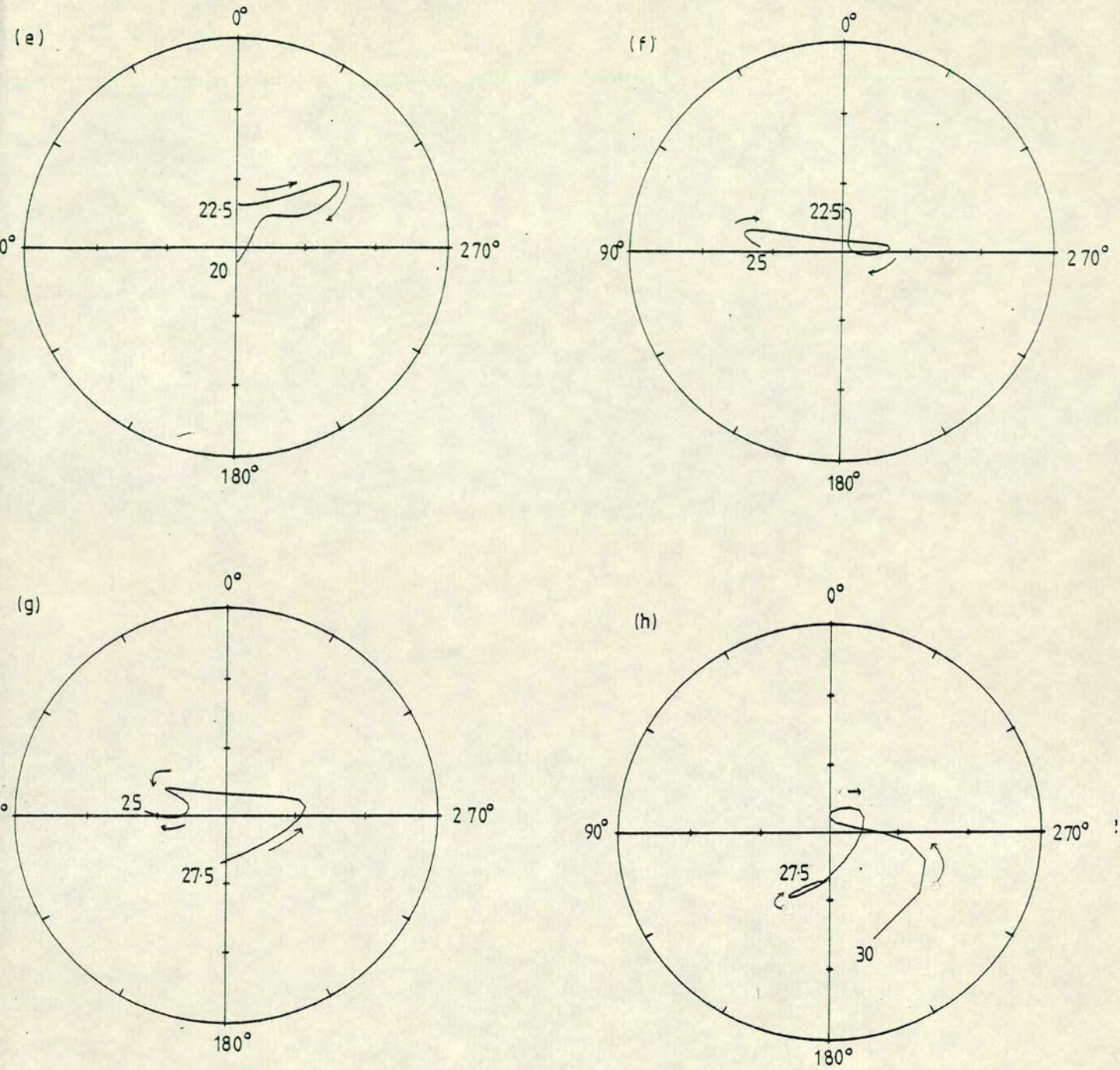

Figure 6.13 The VGP paths for the 50 knot smoothed merged stack in 2,500 year increments. e) 22,500 - 20,000 years bp f) 25,000 - 22,500 years bp g) 27,500 - 25,000 years bp h) 30,000 - 27,500 years bp

The two stacks analysed in the last section all give similar results. Note that since the curvature of the VGP plot changes with time, this might be an interesting parameter with which to compare the results from different sites.

6.5.2 Curvature of the VGP plots

If we define the curvature of the plot as the angle A made by three successive points of the VGP plot as shown in **figure 6.14**, positive if the curvature is clockwise (i.e. $0^\circ <= A <= 180^\circ$) and negative if the curvature is anticlockwise ($-180^\circ <= A <= 0^\circ$), then the variation of curvature with time can be examined on a linear scale. **Figure 6.15** shows such a curvature plot for the same data as **figure 6.13**. Note how the periods of looping described above become clearly visible on this type of plot, which makes it possible to examine the change in the curvature introduced by changing the degree of smoothing of the data. This may reveal how different periodic components of the geomagnetic field are behaving.

A comparison of five different degrees of smoothing is shown in **figure 6.16** using (a) low pass filtering and (b) cubic splines. The looping becomes more rounded as the level of smoothing increases and the relative amounts of clockwise and anticlockwise looping changes. One would expect a white noise spectrum to give 50% of both clockwise and anticlockwise looping (in short bursts). If the data was due to purely westward drifting sources this would change to essentially 100% clockwise rotation.

In these figures the amount of clockwise looping appears to increase with the degree of smoothing, leaving only sharp "peaks" of anticlockwise looping associated with the magnetically quiet periods.

To examine the "looping spectrum" of the curvature plot, the percentage of clockwise curvature was examined as a function of the degree of smoothing. To have a confident knowledge of the frequency band being analysed a bandpass filter was used rather than cubic splines (whose effect in the frequency domain will vary with the data being smoothed). The width of the bandpass filter was altered to examine the effect of smaller and larger frequency ranges. The results for 2 different bandwidths of 10^{-1} and 10^{-2} c/kyr are shown in **figure 6.17** (calculated using CVCLOCKB). There is a substantial decrease in the percentage of clockwise curvature for periods around 3,000 to 4,000 years. This would indicate that the components of the field at these frequencies drift eastwards

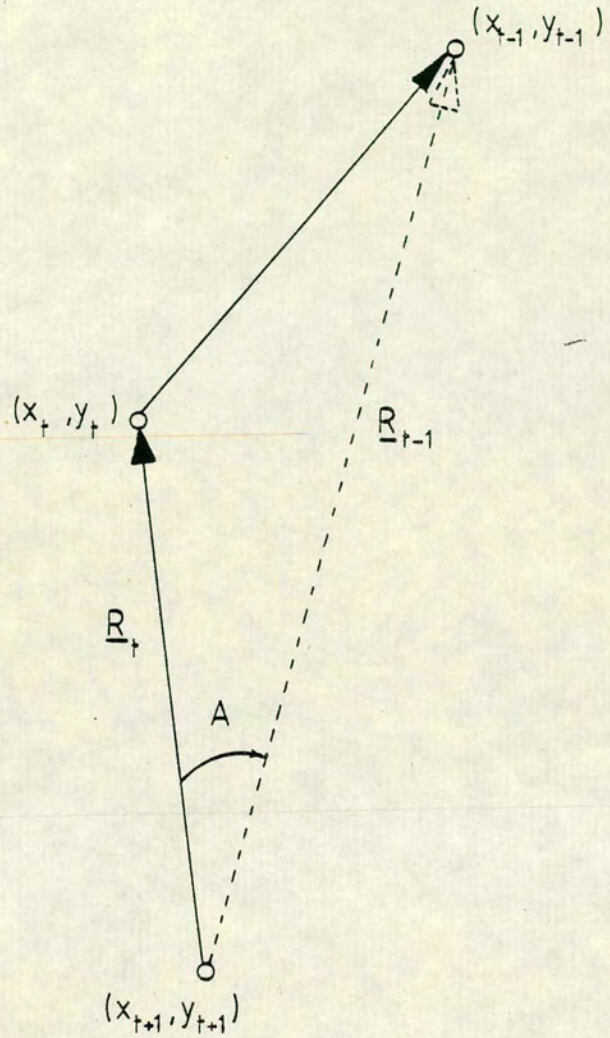

Figure 6.14 The definition of the curvature angle A for the two VGP path points (x_t, y_t), (x_{t-1}, Y_{t-1}) after (x_{t+1}, y_{t+1}).

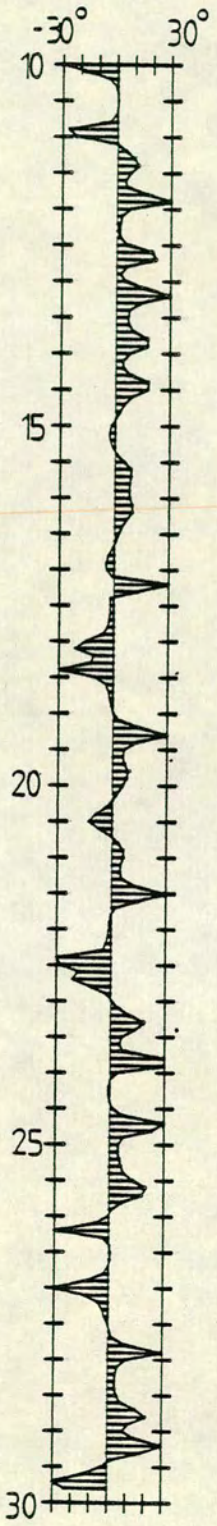

Figure 6.15 The curvature plot for the merged stack after smoothing using a 50 knot cubic spline.

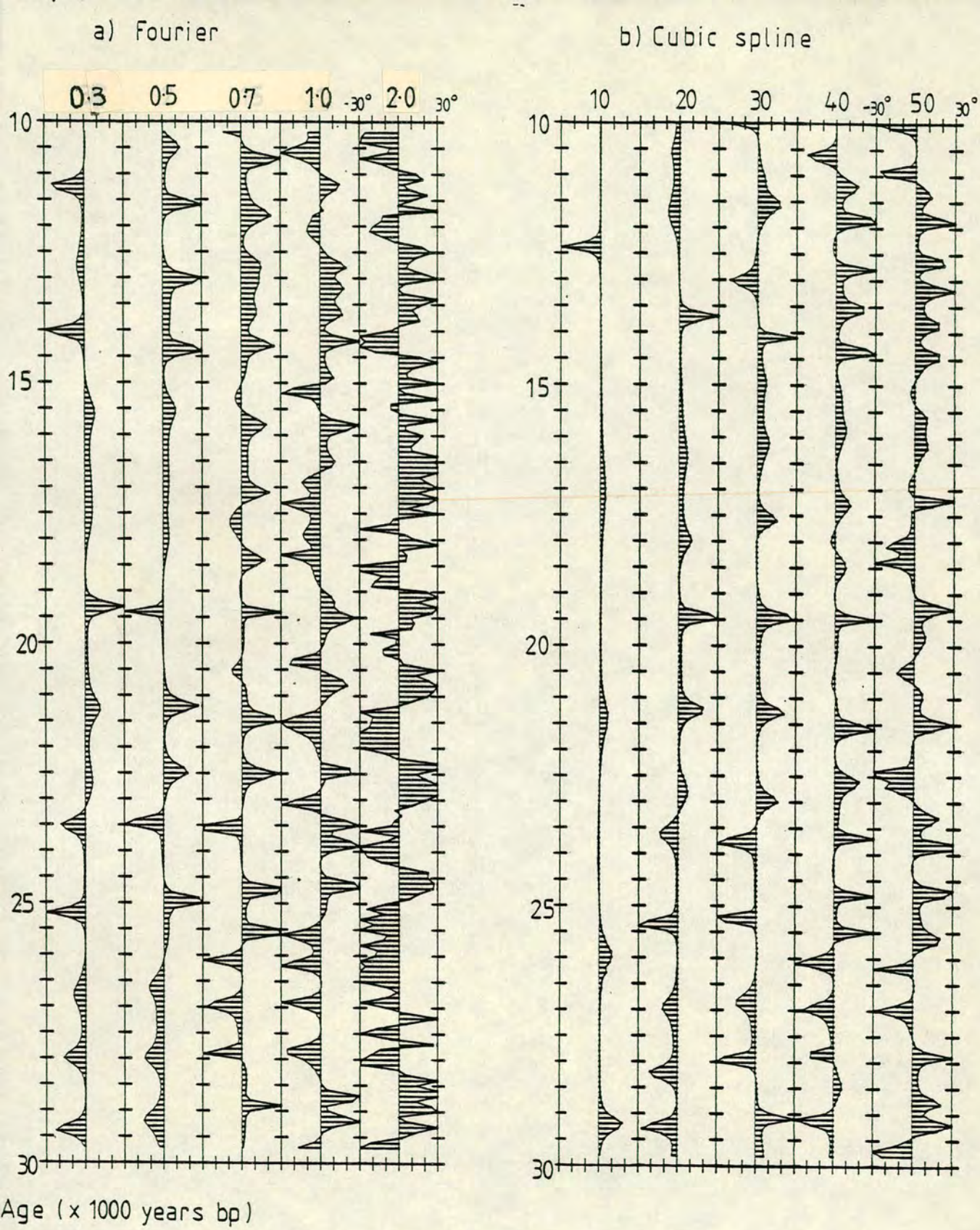

Figure 6.16 The effects of smoothing on the curvature plot. a) Smoothing using a low pass Fourier filter with the cut off frequency in cycles per 1000 years and b) smoothing using cubic splines with the number of knots as specified.

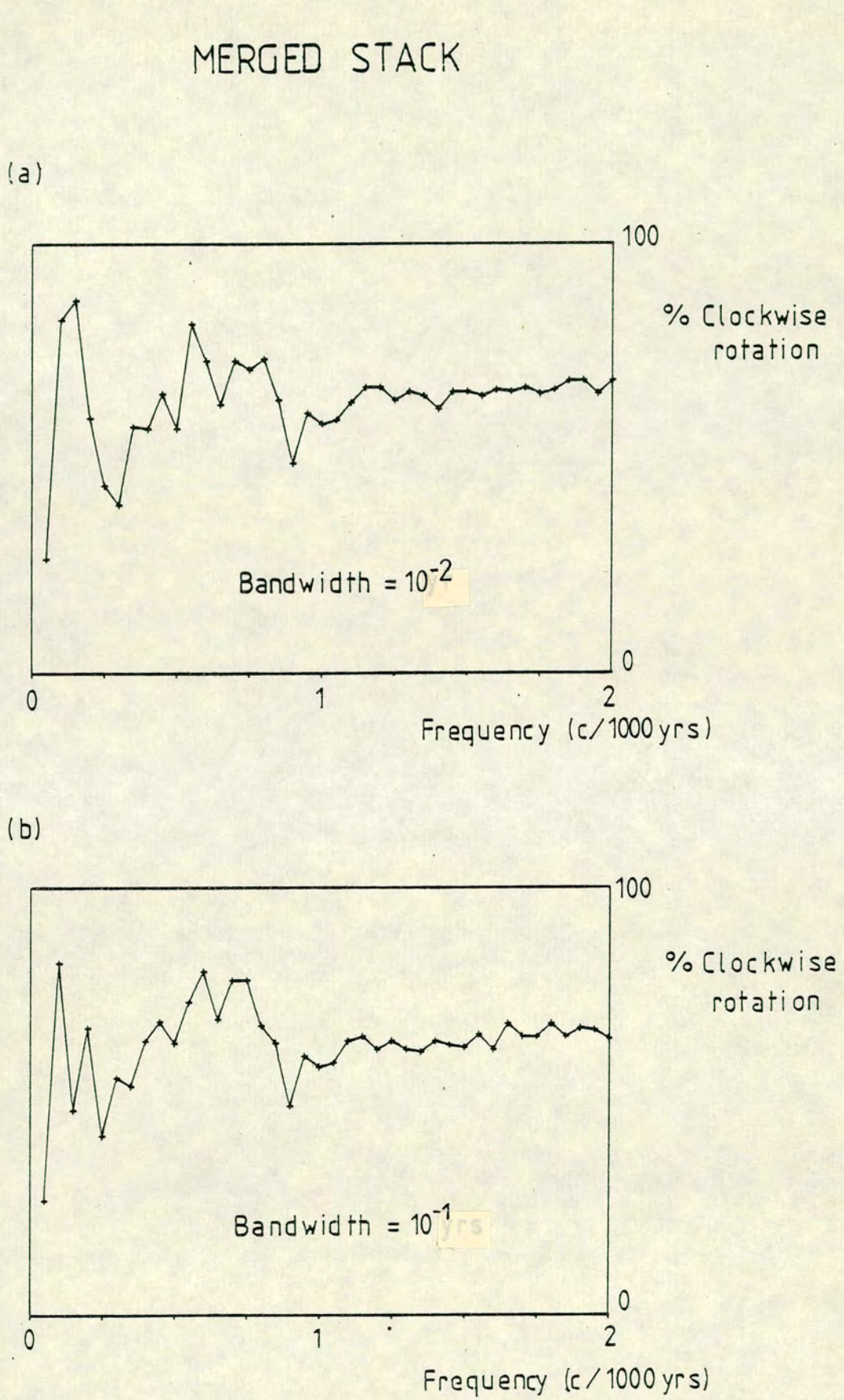

Figure 6.17 The curvature spectrum for the merged stack with a bandpass filter with a bandwidth of a) 10^{-2} and b) 10^{-1} c/kyr

more often than those of other frequencies. Interestingly the phase spectrum of the FFT indicates an approximately 60° lag at these periods and the MEM results in the complex notation has power in the positive band, again indicating eastward drift.

Whether or not this is an effect peculiar to the Bouchet record for this time window was investigated by performing a similar analysis on the "type" curves produced by **Creer and Tucholka (1982)** for western Europe and North America. The results from these analyses produce a less obvious increase in the amount of anticlockwise rotation (**figure 6.18**) and are inconclusive as to the generality of the result. The western European response is somewhat similar to that of Lac du Bouchet (despite the analysed records not being contemporaneous), but the North American record shows no reduction in the amount of clockwise rotation. There are several possible explanations of these results. Maybe there is no increase in the percentage of anticlockwise rotation and the results for Lac du Bouchet and western Europe are inaccurate. Alternatively, those of North America could be inaccurate and the results could be valid. In this case it would seem then that sources affecting Europe are more inclined to cause an eastern drift bias to long period secular variations. This indicates something 'special' about the source motions below Europe and would therefore seem to be an unlikely interpretation. More work is required to establish if this phenomenon is local or global.

6.6 Conclusions

The harmonic content of the geomagnetic field variations observed at Lac du Bouchet during the late Glacial have been found to give consistent results under different methods of analysis. However the interpretation of these results is still very difficult. It has still not been proved that the periodicities found in these records are a true reflection of a stationary geomagnetic spectrum or the result of random local effects. The agreement of the periodicities found within the Bouchet record with those found for North America, Western Europe (**Creer and Tucholka (1983a)**) and Australia (**Barton and McElhinny (1982)**) is excellent. **Creer and Tucholka (1983a)** have found periods of 3,200, 2,300, 1,700, 1,400 and 1,100 years from their analyses of shorter time windows. This agreement with the strongest Bouchet periods of 5,000, 3,300, 2,000, and 1,400 years is striking and may indicate that these are fundamental periods rather than random variations.

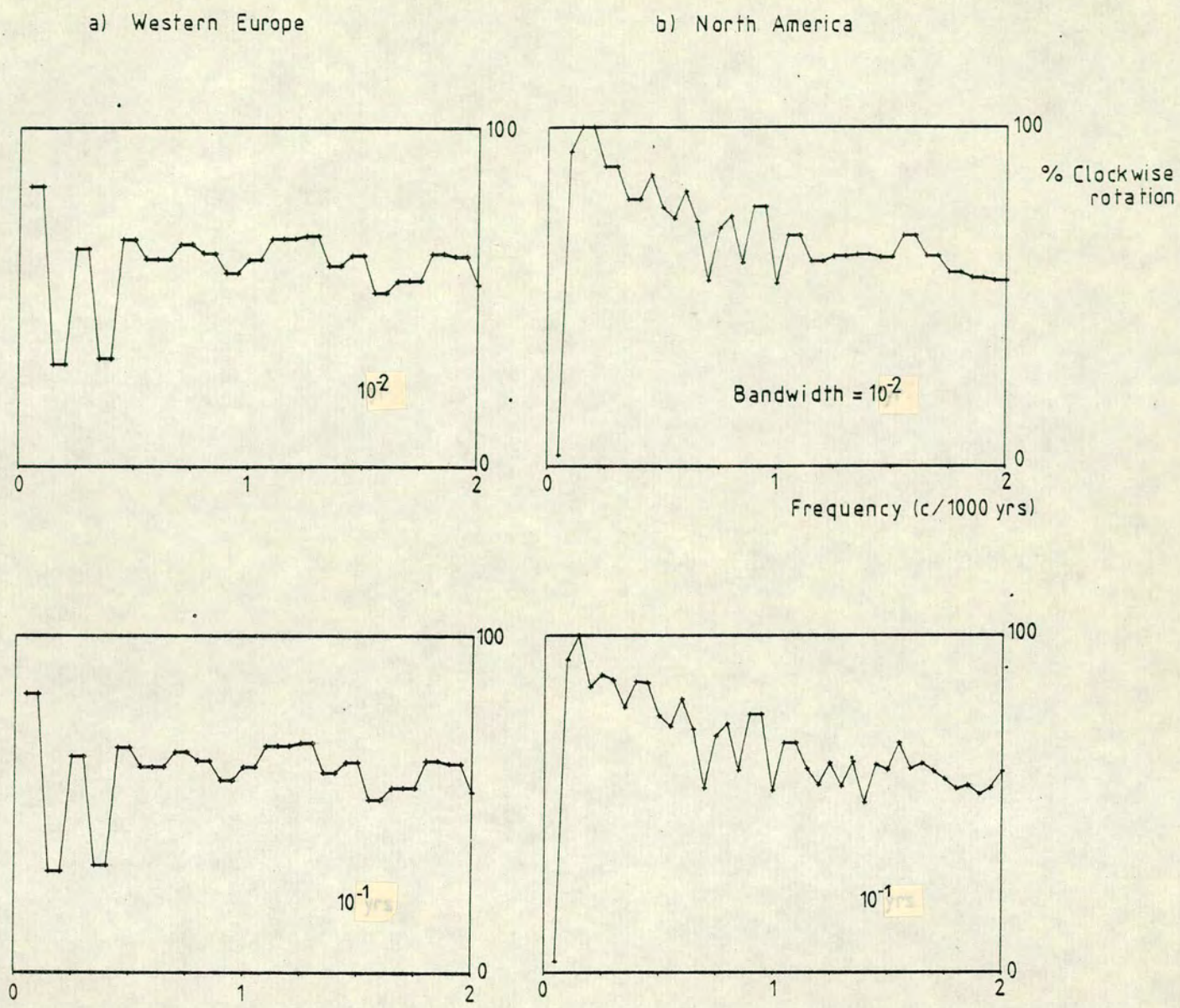

Figure 6.18 The curvature spectra for a) Western Europe and b) North America for two bandwidths (10^{-1} and 10^{-2} c/kyr)

Creer's (1983) discussion of the modelling of SV included the effects of drifting and oscillating RD sources. However, it is clear from an analysis of the modern field (**Yukutake and Tachinaka (1968), Thompson (1982)**), that the non dipole sources both drift and vary in intensity at the same time. If the drift rate is different from the pulse rate then the result of multiplying the two periods is two different periods. One will have a period equal to the product divided by the sum and the other to the product divided by the difference, (by the addition theorum for sinusoids sin A sin B = $\frac{1}{2}$ cos (A+B)-cos (A-B)). This implies that even if the drift rate is constant, any period can be obtained. This is illustrated in **figure 6.19** which shows the possible periods obtained as the growth rate (T_g) varies given a fixed drift rate (T_d). The two possible frequencies that the combination of T_d and T_g can produce are shown as T_a and T_b where

$$T_a = T_d \times T_g / |(T_d - T_g)| \qquad (6.1)$$

and

$$T_b = T_d \times T_g / (T_d + T_g) \qquad (6.2)$$

As T_g approaches T_d the difference tends to zero and T_a tends to infinity: as T_g increases both T_a and T_b tend to T_d which would cause T_d to become more noticeable within a harmonic analysis.

Three strong periods have been found within the spectra obtained. If the 2,000 year harmonic is associated with a fixed drift rate, (this figure is not noticeably different from the present day value of 1,800 years), then the other two periods could be the T_a values caused by a combination of the drift rate and two growth rates. These two growth rates would have to be 3,300 and 5,000 years for their combination with 2,000 years to produce the observed rates. coincidentally these are the same values as appear in the spectra. Thus if the average lifetime of a non dipole field source were 3,300 or 5,000 years and the drift rate were 2,000 years then the spectra would show these as three strong periods which is what is observed. The corresponding T_b periods would then have to be 1,250 and 1,400 years, both of which are observed in the spectra with lower power. Note that this set of periods (5,000, 3,300, 2,000, 1,400 and 1,250 years) have no other obvious relationship.

Obviously, results from other areas would have to be compared. The periodicities observed at Bouchet are local periodicities associated with the drift, growth and decay of sources close to the site. If other sources had different

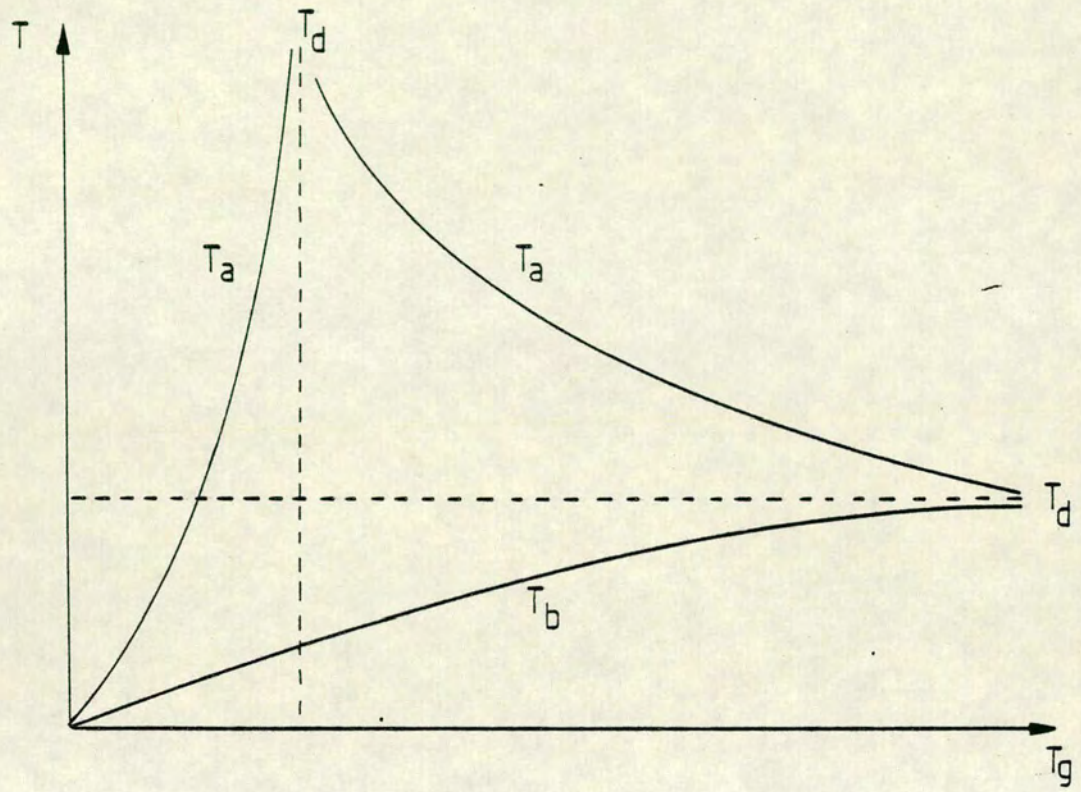

$$T_a = \frac{T_d \times T_g}{|T_d - T_g|} \qquad T_b = \frac{T_d \times T_g}{(T_d + T_g)}$$

Figure 6.19 The possible period combinations that can be derived from a source that is drifting whilst changing in magnitude (at fixed rates). The periods are as defined in the text.

lifetimes, the drift rate could remain constant and yet spectral analyses would yield different results because of the possible relations between T_d, T_g, T_a and T_b. Despite **Creer and Tucholka's (1983)** analysis revealing similar periodicities more analyses must still be made.

Note that despite the apparent long lifetime of a source (3,300 or 5,000 years) predicted by this analysis the spectral content would be apparent for longer than the source would be observed as an anomaly. Observation of the anomaly produced by the source would only occur for the much shorter time that the strength of the source was close to the maximum value. The length of this period of time would depend on the relative strengths of both the dipole field and the anomaly. It is apparent therefore how quickly even a simple model of such a variation can become complicated.

Another "apparent" effect of combining pulsing with westward drift is either zero drift or eastward drift. This can be caused by the growth of the focus adding to another to give an apparent eastward nature to the drift (or stationarity if the rate of growth is slightly less). It follows then that a comparatively simple source model could adequately describe the complicated SV records observed at the surface and yet still remain extremely difficult to identify without a great reduction in present noise levels. More detailed analysis of longer records is the only means that are available to solve these problems, but as has been demonstrated great care must be taken in the interpretation of such analyses.

CHAPTER 7
DRM NORMALISATION:
AN ATTEMPT TO RECOVER PALAEOINTENSITIES FOR THE LATE GLACIAL

7.1 Introduction

At present there is still no technique for quantitatively examining the variations of the geomagnetic intensity from the DRM of sediments. The Thellier method (**Thellier and Thellier (1959)**) for TRM based rocks is unsuitable due to the different magnetisation acquisition method for sediments. However, several methods have been proposed to normalise the DRM of sediments and so obtain relative estimates of the geomagnetic intensity. All these methods rely on the use of other magnetic properties of the sediments and, perhaps optimistically, assume that the combined effects of the environmental temperature and pressure, water content, organic matter content and other sediment parameters are minimal. The implicit assumption of the normalisation is that the intensity of remanence is linearly related to the field that has caused it.

Konigsberger (1938) used the magnetic susceptibility and **Johnson et al. (1948)** used the IRM in probably the first attempts at obtaining relative palaeointensity estimates from sediments. Other workers have used various other magnetic parameters to obtain estimates, e.g. susceptibility, SIRM, ARM, redeposition etc. In particular, **Levi and Banerjee (1976)**, argue that the parameter that has a coercivity spectrum most closely related to that of the DRM should be used. In the case of their work they argued that it should be the ARM and showed examples in which the intensity estimates agreed very convincingly with the archaeomagnetic estimates based on the Thellier method. However, they also discovered that not all sediments were suitable for this type of work.

In an attempt to develop a rapid indirect method of determining the average grain size of magnetite within a sample **Banerjee et al. (1981)** compared the

initial susceptibility to the anhysteretic susceptibility (ARM) in a sample in which the size of grains was known. Since, in general, the ARM would affect the smaller grains more and the susceptibility the larger grains, this approach would seem quite valid and appears to give consistent grain size estimates. However, they have not taken into account the possible effect of superparamagnetic grains which would seriously alter the susceptibility values. Despite this problem **King et al. (1981,1983)** have developed a set of criteria which, they argue, need to be satisfied by a core of sediment in order for that core to be used for palaeointensity estimations. In essence these are that the core should contain magnetite as the dominant magnetic mineral, that the particle size range should be of the order 1 to 15 microns and that the maximum magnetite concentration is less than 20–30 times greater than the minimum. The results of their work again agreed very well with the archaeomagnetic estimates.

The combination of the criteria suggested by **Levi and Banerjee (1976)** and **King et al. (1983)** appear to give consistent results and so for this work the parameters that best mimic the coercivity spectrum of the DRM have been used after checking that the magnetic mineral is magnetite (chapter 4) and that the grain size distribution lies within the range suggested. Unfortunately, the equipment available does not make it possible to accurately determine the concentration of magnetite.

There is a problem with the Bouchet cores not encountered in the work described by earlier researchers. The reliability of their results could be estimated by a direct comparison of contemporaneous sequences of established archaeomagnetic records.For the Bouchet sediment the record for the last 6,000 years has been shown to agree quite well with **Kovacheva (1980)**, **Thomas (1981)** and **Walton (1979)**. The normalisations were performed on three of the minicores by **Bray (1985)**. The most useful, (and reliable), section of the Bouchet cores spans the late glacial period from 30,000 to 10,000 years bp for which there are, of course, no archaeomagnetic results. It is necessary therefore to attempt to check the reliability of the estimates by some other means.

A test of the normalised curves can be constructed using a model of the acquisition of remanent magnetisation. By experiment, **Hamano (1980)** has shown how the magnetisation of a sediment is fixed in over a period of time. **Hyodo (1984)** has modelled this using a linear system theory by considering the magnetisation of a sediment to be the result of a convolution between the Hamano fixing function (which he models as an exponential) and the geomagnetic field variations. At some time after deposition this model requires

that half the magnetisation is fixed. The depth at which this occurs is an indicator of the suitability of the sediment as a recorder of the geomagnetic field. The deeper the depth the less suitable the core is for palaeomagnetic investigation. This will of course not produce absolute reliability in the confidence held in the estimates but can indicate whether or not the results are more or less likely to be valid.

7.2 Estimation of the optimum normalisation parameter

The coercivity spectra of the DRM, SIRM and a range of ARMs have been investigated in chapter 4. From the linearity of the NRM/induced RM ratios it would appear that the optimum normalisation parameter was the SIRM. However, since the SIRM is up to 5,000 times greater than the DRM and the ARM only 2-3 times greater it was felt that both these parameters should be tested. In addition although the ARM gave a less linear comparison to the NRM, the MDF values of the demagnetisations are closer to that of the NRM. Therefore, the two normalisation parameters used are the SIRM and the ARM imparted in the sample by a peak field of 60mT (see chapter 4).

7.3 Bulk measurements of ARM and SIRM

Bulk ARM measurements and bulk SIRM measurements were performed on five of the cores used in the stacks described in chapter 6. These were B7, B12, B15, B47 and B49. The results for the 12m cores are given in chapter 8. The measurements were made on the Molspin mini spinner magnetometer controlled by an Epson microcomputer. The Epson control program was adapted to allow the results to be printed on magnetic tape which were subsequently transferred to the mainframe computer via the Sirius microcomputer.

The ARMs were imparted in a peak field of 60mT as described in chapter 4. The SIRM was given to each sample by inserting the sample in a field of 1.5T between the poles of an electromagnet. The sample was held in the field for about 5 seconds then the field was reduced to zero and the sample removed. Removal in this way prevents any spurious magnetisations being induced in the sample by stray fields at the edges of the poles of the electromagnet. The results are shown in **figure 7.1** for the ARMs and **figure 7.2** for the SIRMs. The values are plotted against the downcore depth transformed to the B49 depth scale using the transform functions defined in chapter 3. There is clearly a

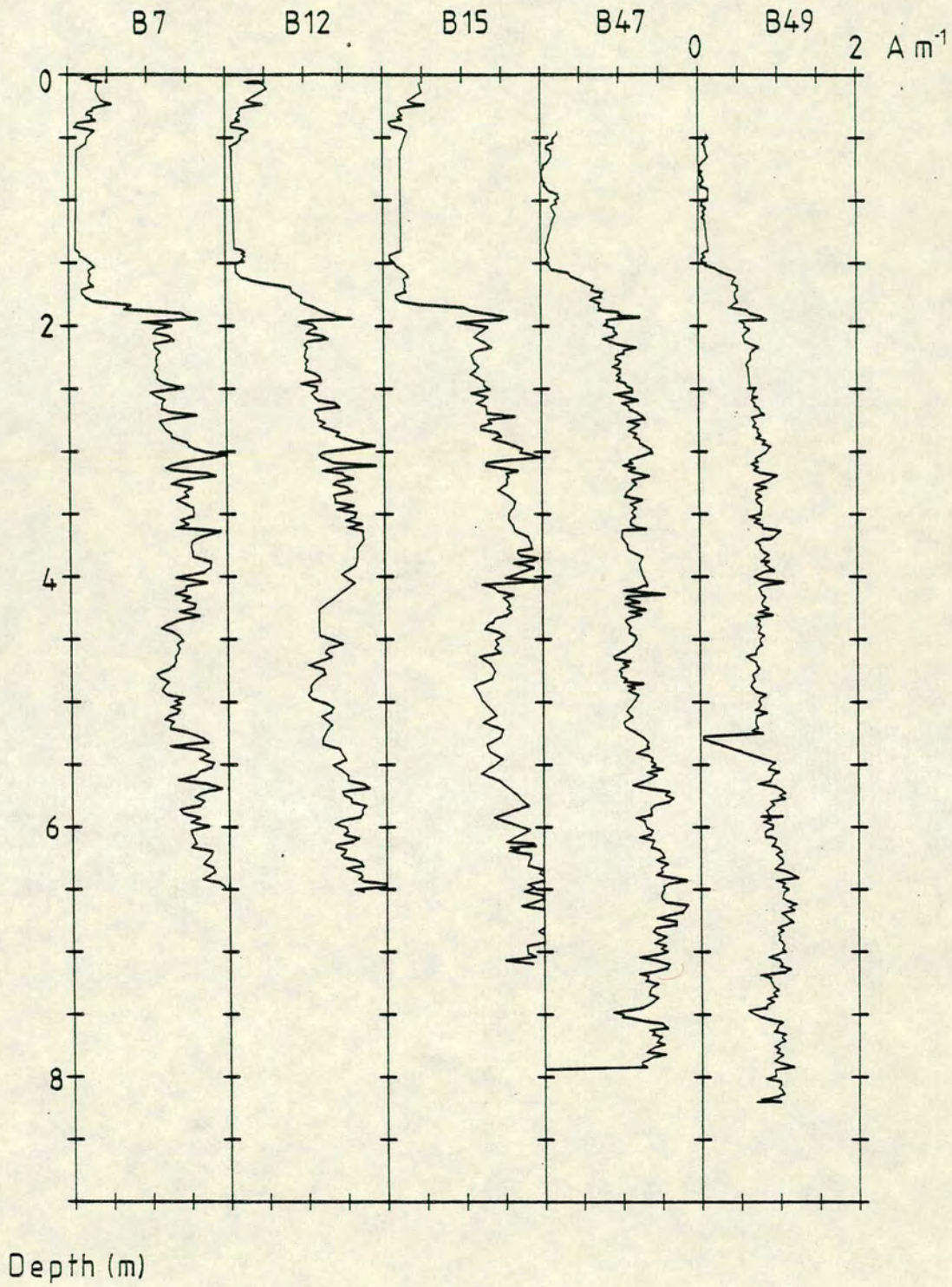

Figure 7.1 Variation of ARM with depth for five of the Lac du Bouchet cores.

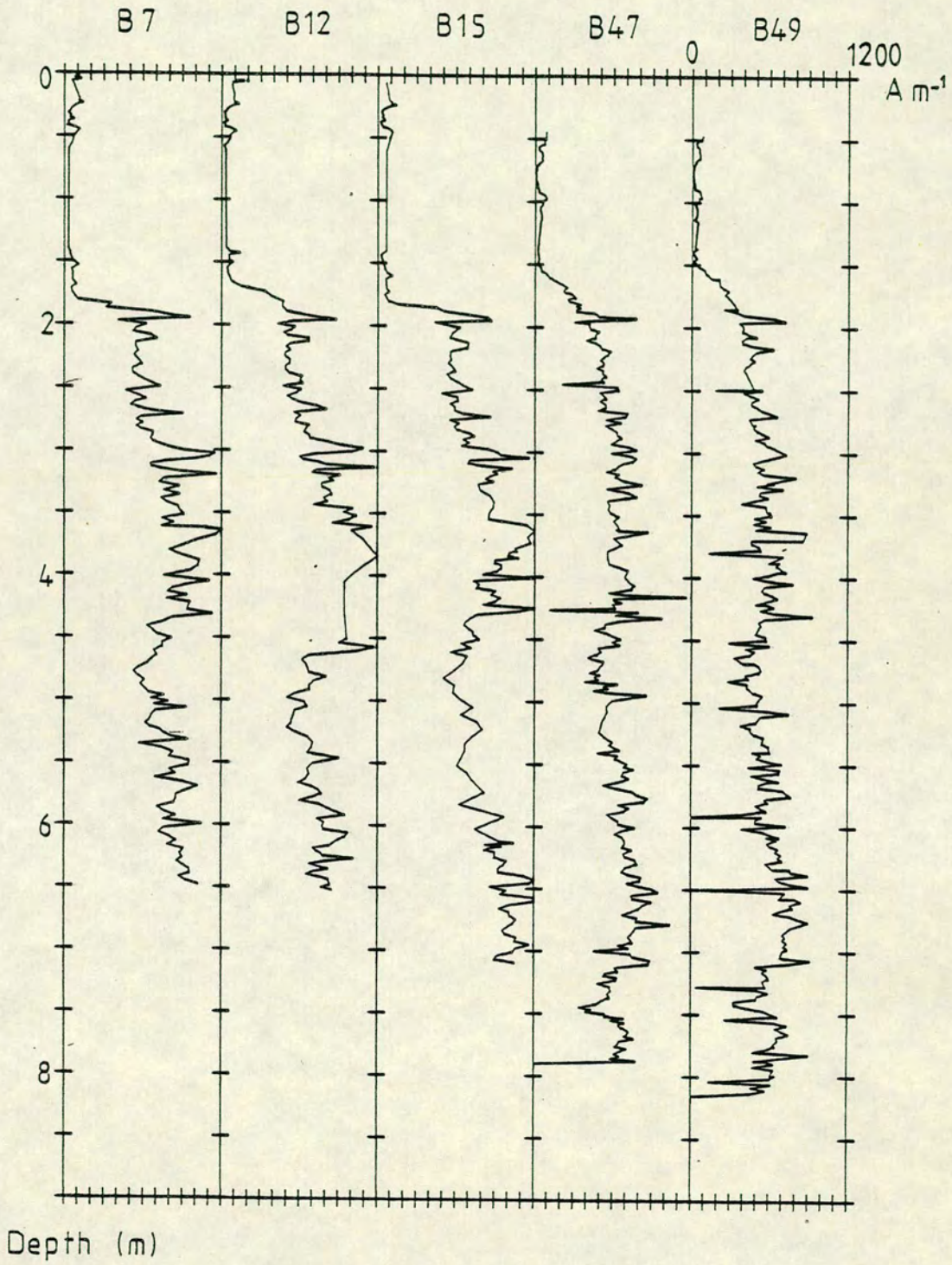

Figure 7.2 Variation of SIRM with depth for five of the Lac du Bouchet cores.

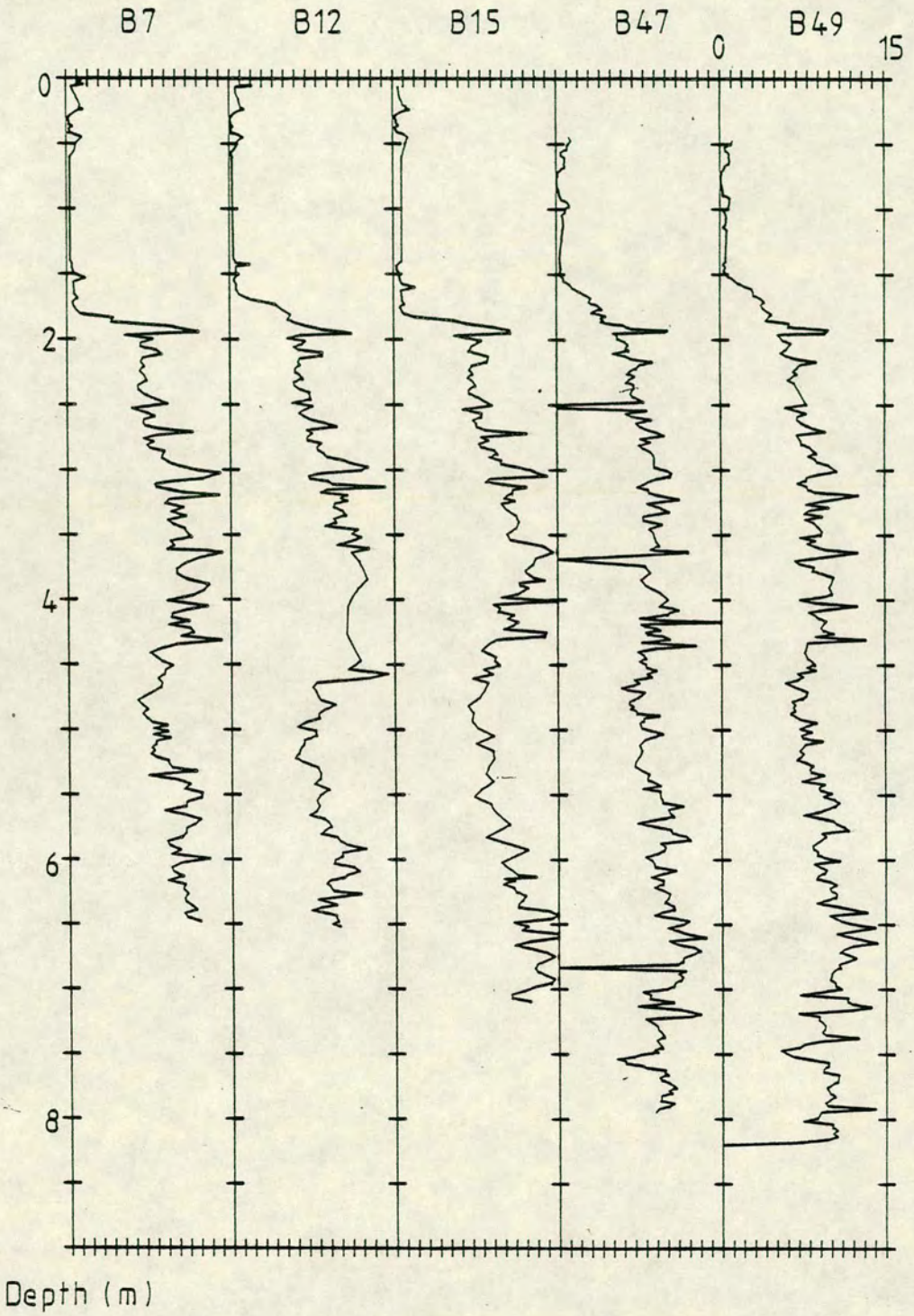

Figure 7.3 Variation of susceptibility with depth for five of the Lac du Bouchet cores.

great similarity in the patterns of the variations both with each other and with the variations in susceptibility (**figure** 7.3). The long period trend in the susceptibility record is likely to be associated with the variation in the magnetite content down the core. It appears that the other two magnetisations are following these trends also.

7.4 The variation in the grain size of magnetite

Assuming that there is no substantial contribution from superparamagnetic grains it is possible to determine the variation of the grain size of magnetite using the method suggested by **Banerjee et al. (1981)**. The model developed by **King et al. (1982)** to explain the Banerjee method indicates that if the ARM to susceptibility ratio is between 2.5 and 0.5 then the grain size lies between 1 and 20 microns. (Note that in general they found that the ratio increases with decreasing grain size and used a bias field of 0.1mT. Since the bias field used in this work (0.1mT) is the same, the ratio would be expected to be the same).

In an attempt to get the relative grain size distribution and to test whether or not the Bouchet sediments are magnetically uniform the ARM to susceptibility ratio has been calculated and is shown in **figure** 7.4 for the five cores. Note that the grain size appears to stay relatively constant throughout the length of the core indicating a uniform distribution of grain sizes. Since the grain size of the NRM carrier has been found to be 1 - 5 microns (chapter 4) and this ratio is constant it follows that the grain size of most of the NRM carriers are in this range. An alternative approach would be to normalise using the SIRM which will also indicate the relative distribution of sizes. In particular, this will emphasise any very fine grain constituents which will give extremely low values for the ratio.

The ARM to SIRM ratio is probably a better parameter to use for the estimation of relative grain size as they are both measurements of magnetic remanence whereas in the case of the susceptibility the value is an in field measurement, affected especially by any superparamagnetic grains. This ratio is plotted in **figure** 7.5 and bears a striking resemblance to the ARM to susceptibility ratio indicating that there are few very fine grains and in particular there are few superparamagnetic grains. This agrees well with the deductions made in chapter 4, that the main magnetic mineral is a multi domain magnetite.

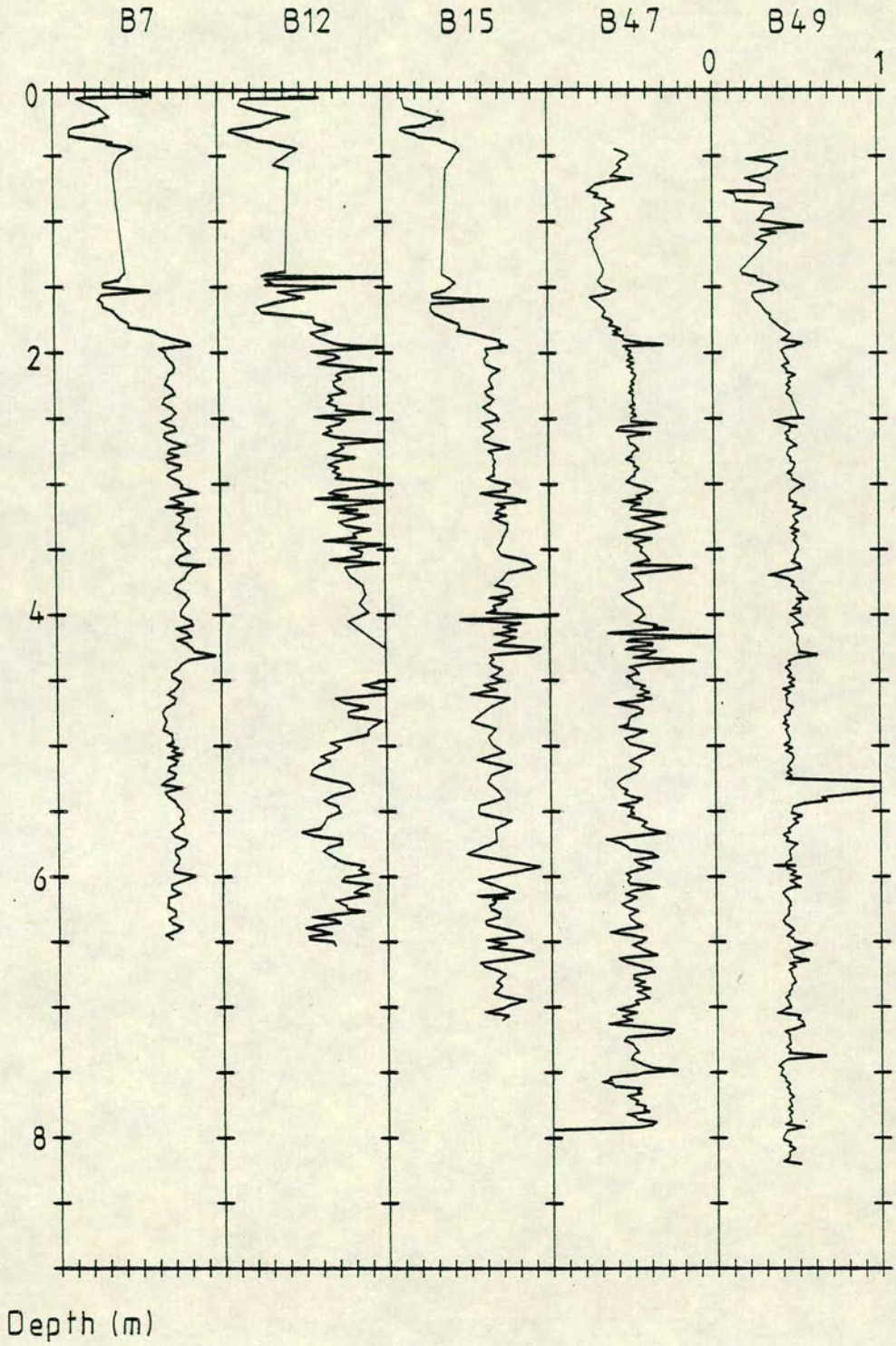

Figure 7.4 The ARM/susceptibility ratio for five cores taken from Lac du Bouchet.

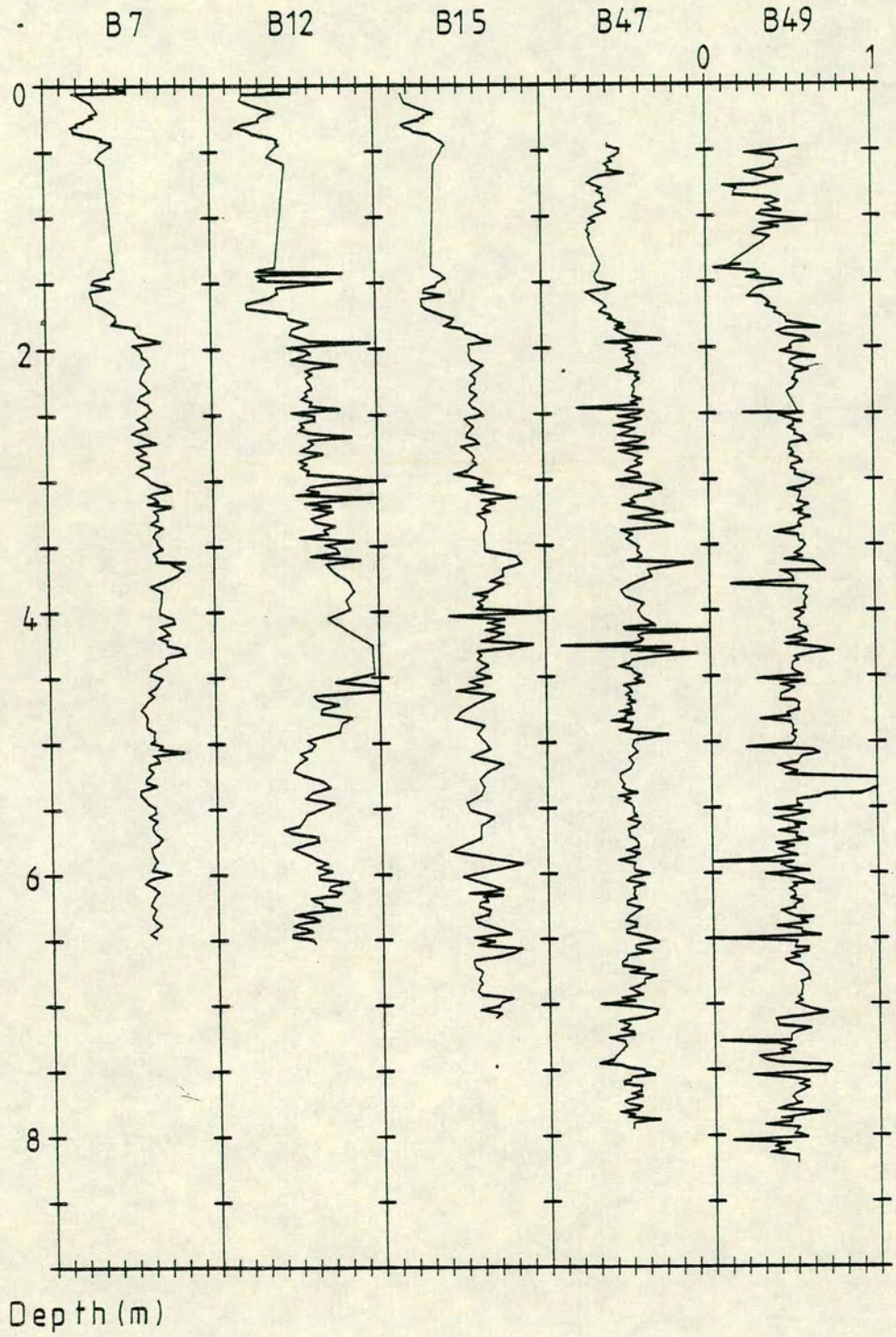

Figure 7.5 The ARM/SIRM ratio for five cores taken from Lac du Bouchet.

7.5 Normalisation of the DRM

Having established that the cores seem to contain predominantly magnetite of a uniform size, the normalisations can be applied. The resulting estimate of the relative geomagnetic field intensity variations are shown in **figure 7.6**. The mean intensity has been constrained to be 0.5. There are two things to note; that the Holocene sediments clearly contain a smaller amount of magnetite than the late glacial sediments (as was expected from the results of chapter 4). These sediments are unlikely to be accurately recording the variations of the geomagnetic intensity because the sedimentological effects are not uniform (due in part to the very large organic content). The second point is that the variations in intensity have been amplitude modulated by the normalisation. This is an interesting feature and is in contrast to the expected behaviour, predicted from the model discussed later. No frequency modulation is apparent from the normalisation. A spectral analysis performed upon the normalised variations showed that the main periodicities found in the DRM record examined in chapter 6 are still found. The analysis was performed upon a cubic spline smoothed, merged stack of the five records. (Stacked after transform to the time domain). The two merged estimates of the variation of the geomagnetic field through the late glacial are shown in **figure 7.7**. Note in particular the apparent periodicity of the signal and the steady increase in the field intensity between around 30,000 and 18,000 years bp.

There are two noticeable peaks in the intensity at about 18,000 and 15,000 years bp separated by a pronounced trough at about 16,500 years bp. The change in the actual character of the sediment masks the geomagnetic effects at the Holocene/late glacial boundary. These features are common to both normalisations and yet there are some differences. The ARM normalisation produces a much better definition of the stack (average standard deviation is 0.3 for the merged stack and 0.2 for the Gaussian compared with 0.34 and 0.3 for the SIRM) and the amplitudes of the variations are slightly larger. Examination of the agreement between the records shows that the SIRM is being affected by the concentration of magnetic minerals in the same way as the susceptibility. (Their correlation coefficient is 0.98). The ARM and SIRM are different (0.8) indicating that the ARM is likely to be the better normalisation parameter and that the normalised intensity variation shown in **figure 7.7**, for the ARM is a reflection of the variation of the geomagnetic intensity during the late glacial.

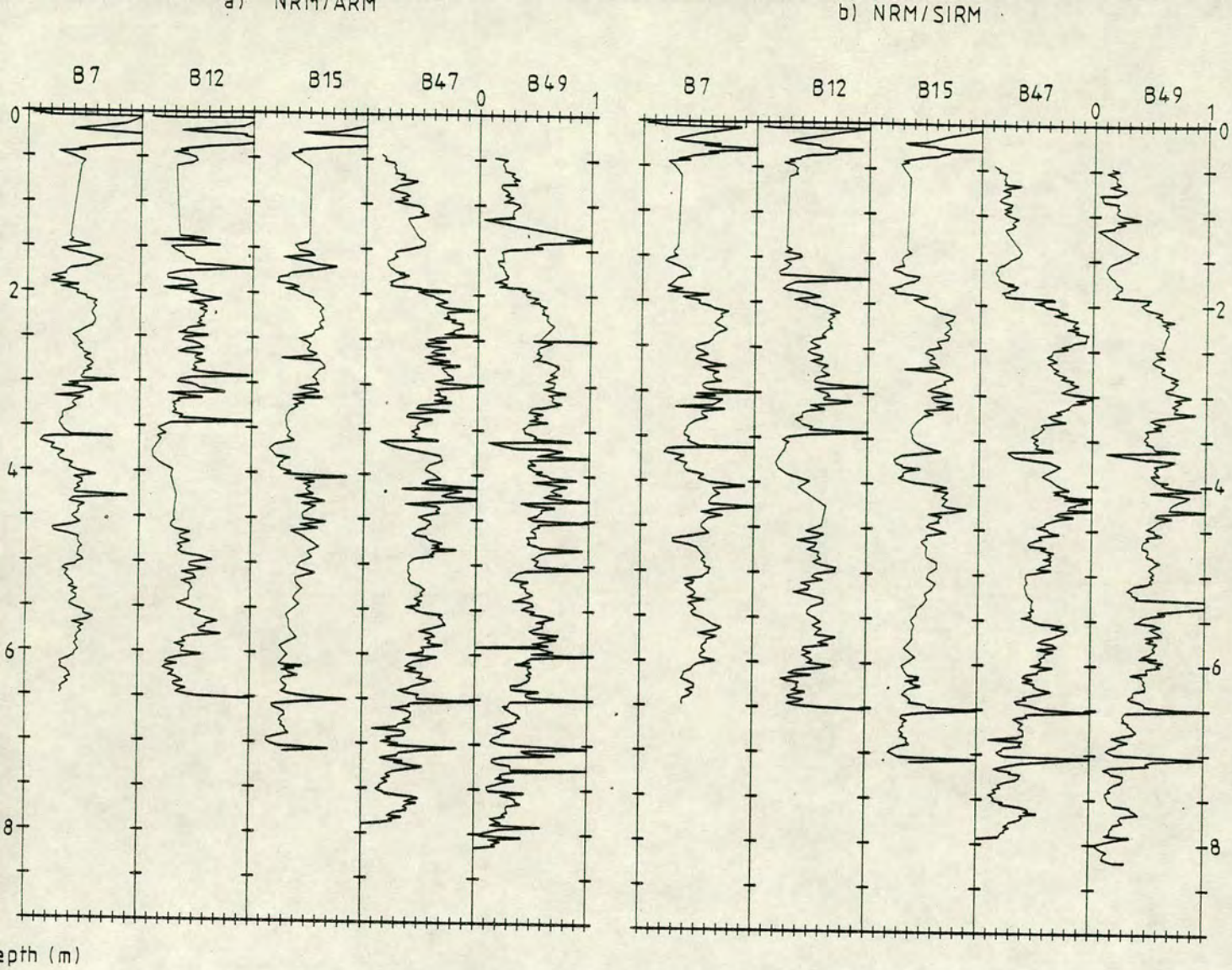

Figure 7.6 The NRM after normalisation using a) ARM and b) SIRM.

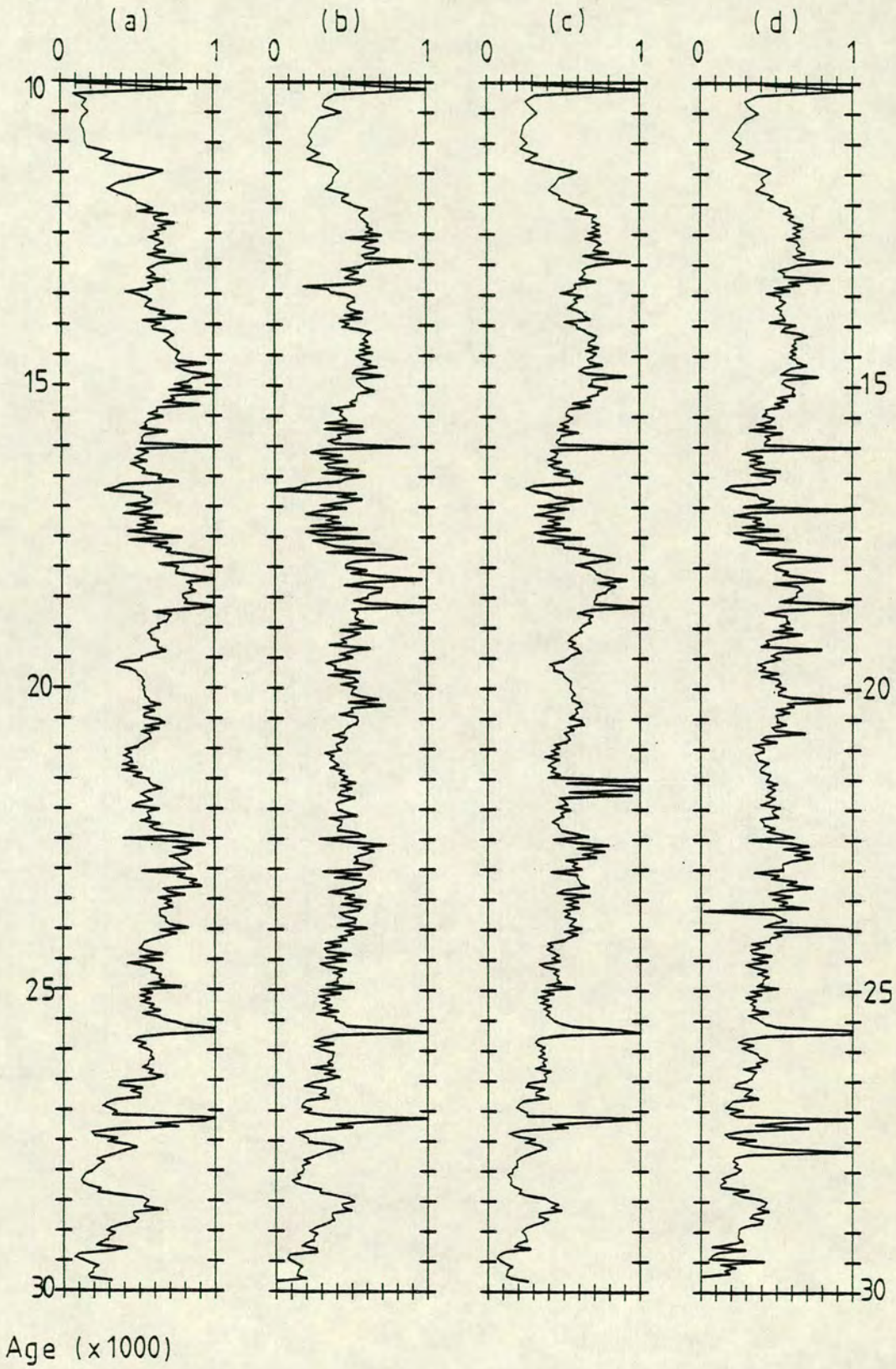

Figure 7.7 The variation of intensity during the late glacial showing a) the NRM b) NRM/susceptibility, c) NRM/ARM and d) NRM/SIRM. All the variations have been produced using a merged stack.

However, in order to further test the reliability of the sediment as recorders of the geomagnetic signal a magnetic acquisition model of the sediments will be compared with the results to examine whether or not the sediments appear to be truly likely to be recording the signal.

7.6 Modelling the acquisition of magnetisation

The acquisition of magnetisation by a sediment is not instantaneous. Experimental work has shown three very important features of the way in which the applied field fixes the magnetisation within the sediment. Perhaps the most important observation is that the remanent magnetisation is due primarily to post depositional realignment (**Lovlie (1974), Kent (1973), Barton and McElhinny (1979)**). The second observation is that the total magnetisation of a section is the sum of the individual magnetisations of its component thin sheets (**Otofuji and Sasajima (1981)**). The third is that the magnetisation acquired by a sediment in a uniform field takes a finite time to become fixed.

It has been shown by **Hamano (1980)** that the acquisition of magnetisation is particularly high near the sediment/water interface and that the rate decreases as the depth increases. **Hyodo (1984)** has modelled this using an exponential function and considered the acquisition of magnetisation to be the result of a convolution between the ambient field and this fixing function.

The fixing function can be arbitrarily defined by a general exponential function r(t) such as

$$r(t) = Ce^{-At} \qquad (7.1)$$

where A and C are constants. Before the sediment is laid down there is no remanent magnetisation so if the time that the sediment starts to acquire a remanence is denoted t_0 then

$$r(t) = 0 \text{ if } t < t_0 \qquad (7.2)$$

If we define two further times t_1 and t_2 when half the moment is fixed (t_1) and the acquisition is complete (t_2) then we also have

$$\int_0^\infty r(t)\, dt = 1 \qquad (7.3)$$

$$_{t1}\int^{\infty} r(t)\, dt = 0.5 \qquad (7.4)$$

$$_{t2}\int^{\infty} r(t)\, dt \simeq 0 \quad (t_o < t_1 < t_2) \qquad (7.5)$$

The magnetisation of a unit sediment sheet of age τ will then be given by the convolution integral

$$\underline{m}(\tau) = {}_{o}\int^{\tau} m_o/f_o\ \underline{f}(t) r(\tau - t)\, dt \qquad (7.6)$$

where m_o is the moment fixed in a uniform field of f_o and $\underline{f}(t)$ is the variation of the geomagnetic field intensity between τ and t (**Hyodo (1984)**).

Since convolution in the time domain is the same as multiplication in the frequency domain it is possible to transform the magnetisation observed in the sediment to the frequency domain and divide by the transformed fixing function. The inverse transform of the magnetisation filtered in this way should be the original field variation.

Appendix 4 shows the derivation of the required filter $R(\omega)$. Note that the filter is not that obtained by **Hyodo (1984)** which seems to contain a set of misprints. In fact, as shown in appendix 4, the filter is

$$R(\omega) = 1 / (1 + i\omega/A) \qquad (7.7)$$

where the constant is given by

$$A = \ln 2 / T_{0.5} \qquad (7.8)$$

so that the amplitude spectrum is

$$|R| = 1 / \sqrt{(1 + (\alpha T_{0.5}/T)^2)} \qquad (7.9)$$

and the phase spectrum

$$\Phi = -\tan^{-1}(\alpha T_{0.5}/T) \qquad (7.10)$$

where $\alpha = 2\pi/\ln 2$ and $T = 2\pi/\omega$.

It follows that large values of $T_{0.5}$ will substantially attenuate the field intensity and cause a phase lag in the observed declination and inclination

records. Appendix 4 discusses these effects in more detail but it should be noted that the larger the half fixing time ($T_{0.5}$) the less suitable the sediment would be for palaeomagnetic analysis.

7.6.1 Determination of the $T_{0.5}$ value for Lac du Bouchet

The effect of varying the half fixing time has been examined in the 'depth' domain; before transform to the time domain. This results in the determination of a half fixing depth which will indicate the efficiency with which the Bouchet sediments have recorded the geomagnetic field. The program INTMODEL has been used to calculate the effect upon the observed magnetisation values of a fixing function r(z) with various half fixing times. **Figure 7.8** illustrates the effect upon the intensity record of applying 5 different filters equivalent to half fixing times of 50, 100, 200, 500 and 1,000 years. As would be expected from the effect of multiplying the inverse of the transform of the fixing function the short period (high frequency) components are being amplified. In fact there is little alteration of the long period variations upon which the superimposed short period variations are found. The filters with half fixing periods of less than 500 years have very little effect upon the intensity.

The main features of the intensity record are still clearly visible despite the amplification of the short period features. The latter will cause a particular emphasis upon sedimentological effects contributing to the record since these will be of the order of 1 to 10 years. (This is equivalent to the thickness of an average non-uniform layer within the cores). The geomagnetic field however is clearly visible as a longer period variation. The half fixing depth whose amplitude best fits the normalised curve is most likely to be the half fixing depth for the Bouchet sediments. However, as has been seen from the normalisation there is a reduction in the amplitude of the variations recorded. This will only occur for negative half fixing depths!

The reason for this paradox is that the geomagnetic field variations are of a long enough period compared to the half fixing depth to make the reduction in their amplitude negligible (i.e. $T_{0.5}/T \simeq 0$). This means that the sediments for Lac du Bouchet are particularly suited to palaeomagnetic investigation since the signal recorded is almost exactly that of the geomagnetic field with virtually no amplitude or frequency modulation. Note that the normalisation by the ARM is still valid. The model assumes that the effect of the sediment is linear. Variations in the sediment properties will change the response of the sediment

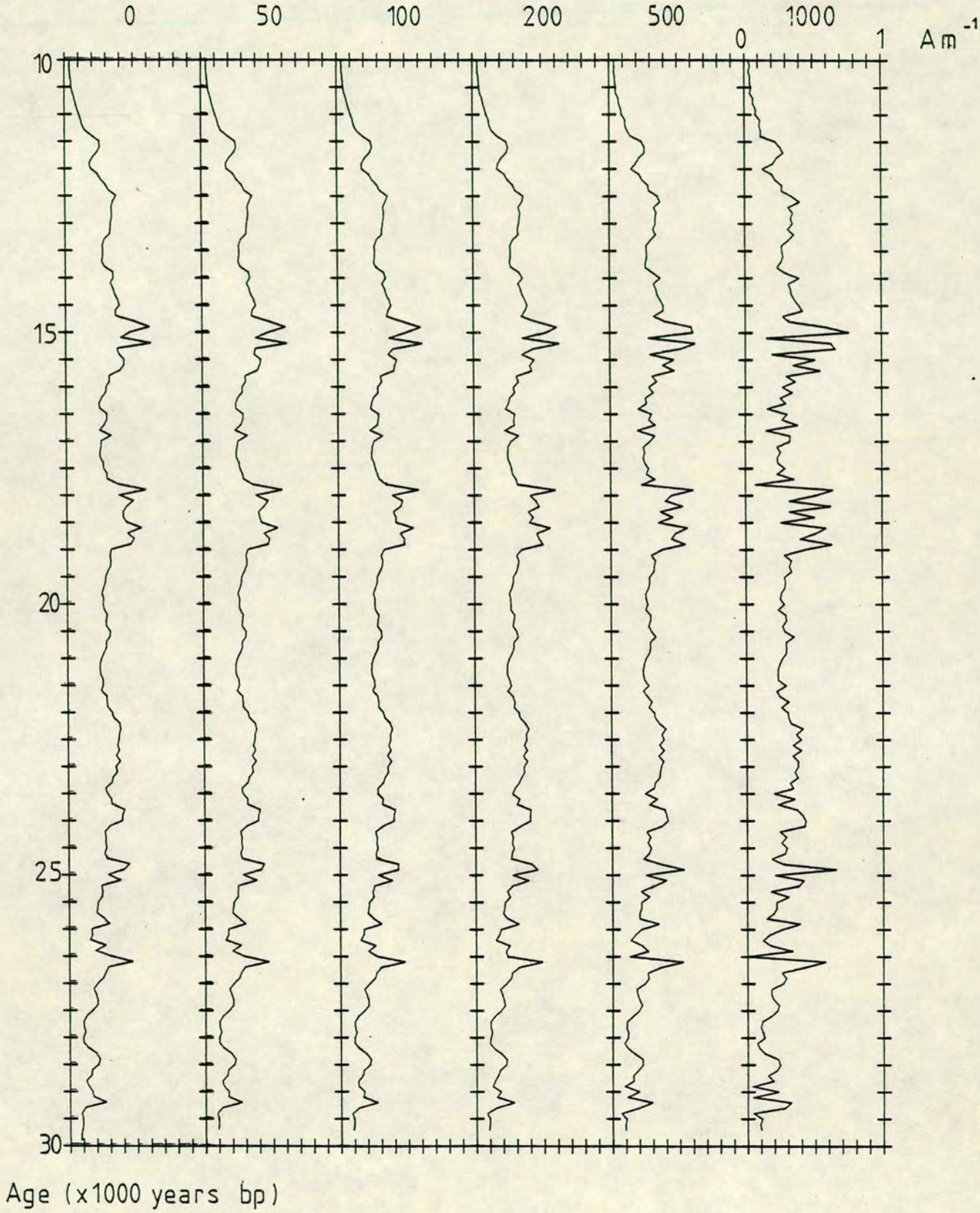

Figure 7.8 The stacked intensity record after deconvolution of the exponential fixing function with half fixing times of 50, 100, 200, 500 and 1000 years.

so that the normalisation by the ARM is required to remove the sedimentological effects. The model shows that the result is a valid estimation of the variation of the geomagnetic field.

7.7 Conclusions

The Bouchet sediments record the variation of the geomagnetic field faithfully. The amplitude of the intensity variations are affected by the characteristics of the sediment which have been shown to be uniform and able to be accounted for during the late glacial period. The directional variations are generally those of the geomagnetic field.

The parameter that best reduces sedimentological effects is the ARM induced in a peak field of 60mT. This factor eliminates the effects due both to the variation in concentration of magnetic minerals and the domain sizes.

The magnetisation appears to be acquired in a very short time within the Bouchet sediments. This again indicates that the important carrier of the NRM signal is coarse grained (MD) magnetite since smaller grains would take longer to fix and be more susceptible to PDRM.

The geomagnetic field appears to have had a large moment during the last 10,000 years of the late glacial period. For the immediately preceding period of 10,000 years the moment seems to be growing from a much smaller moment. This long period intensity record still has the shorter period variations superimposed upon it. Strong non dipole features could clearly cause a local reversal if the geomagnetic moment were substantially reduced. This is discussed again in chapter 8.

CHAPTER 8
EXTENDING THE RECORD:
RESULTS FROM THE SINGLE PIECE 12M CORER

8.1 Introduction

The single piece 9m corer had been used successfully to obtain cores from Lac du Bouchet in 1983. In order to extend the record still further it was decided that a single piece 12m corer of the same design should be built. This chapter describes the results from the cores taken in April 1985 with this corer, which have a maximum length of 11.2m. All the techniques described and developed in the preceding chapters have been used on these cores to produce an extended record of the geomagnetic variations in France.

8.2 Coring and sampling

Six cores were taken during the field campaign of which 3 were brought back to Edinburgh for subsampling and analysis. Subsampling was performed as described in appendix 2. For cores B61 and B63 sampling commenced below assemblage B as the wet sediment found above this layer was found to have been disturbed during coring or transport. **Tables 3.1** and **3.2** include information about the length of the three cores and the number of subsamples.

8.3 NRM, demagnetisation and susceptibility results

All the NRM, pilot demagnetisation and bulk demagnetisation measurements were made on the cryogenic magnetometer and the susceptibilities were measured on the Bartington bridge. The NRM records are shown in **figure 8.1** for B64, the longest of the three cores. As can be seen from an inspection of **figure 8.1** the records are essentially identical to those of the other cores for the overlapping sections and continue to show clear variations below the 9m level.

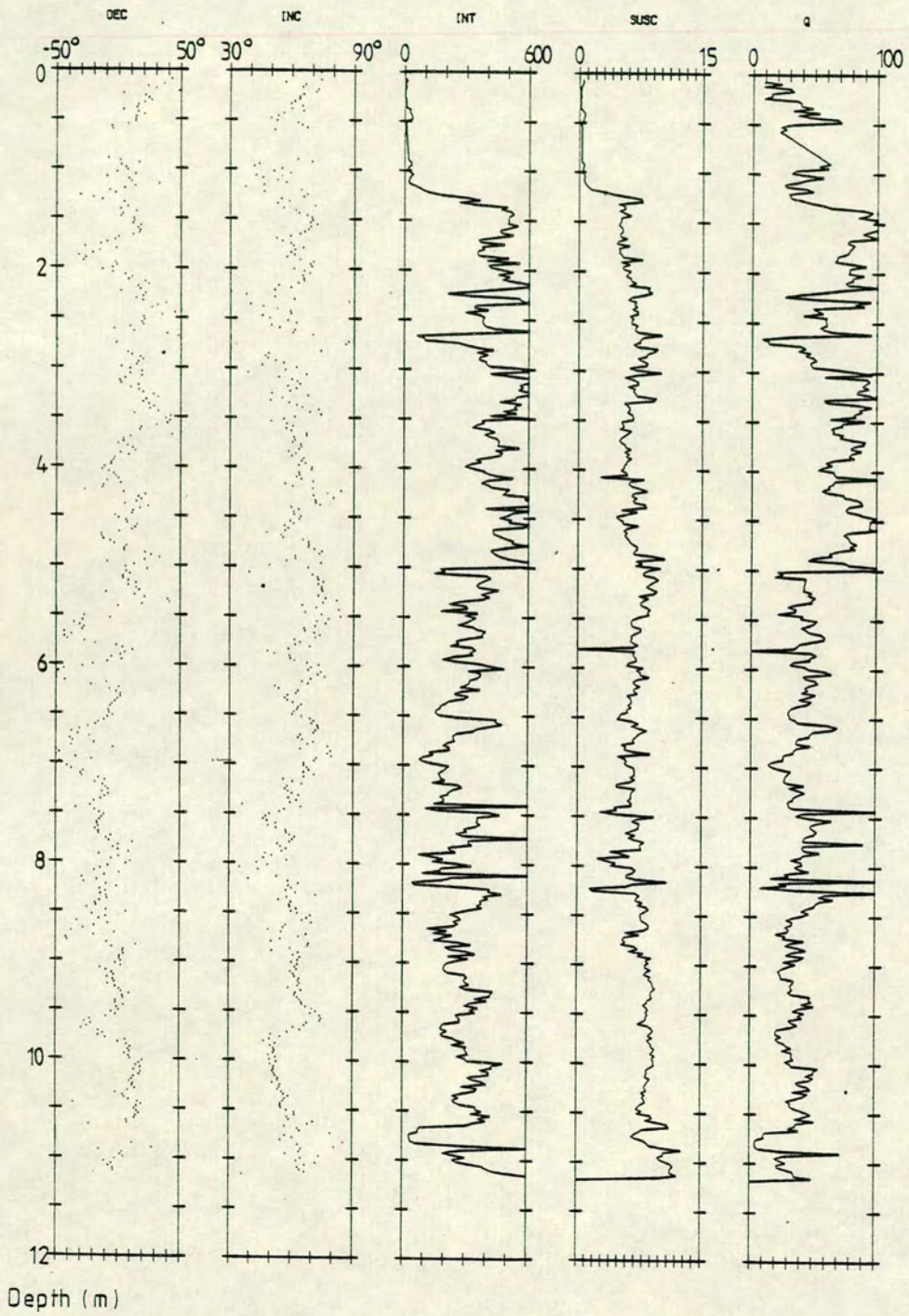

Figure 8.1 The NRM records for core B64 showing the variations in declination, inclination and intensity (mA m^{-1}).

Similar features to the upper part of the record are apparent with the declination and inclination being approximately 90° out of phase. The amplitude of the variations remains similar to the preceding record and there are no negative inclination values. In the declination record there is a section between 10.6 and 10.9 metres where the angle varies through 360° however. This feature is less apparent in core B63 and not reached in any other core. It is associated with a large decrease in intensity (a factor of ten) but no apparent change in the sediment and only a slight reduction in susceptibility. At this stage, since it is not correlatable with any other core, it cannot be regarded as geomagnetic in origin.

The step demagnetisation results of the pilots gave similar results to those of the pilots from the earlier cores. **Table 8.1** shows the variation of the MDFs with depth and **figure 8.2** gives two examples of the demagnetisation behaviour of the pilots taken from below 9m. Note that they still reveal the two components of remanent magnetisation observed before. An inspection of **table 8.1** reveals that there are some pilots that have very low MDF values. These are interpreted as being due to the NRM being carried by very large MD grains. Since they occur at depths that overlap the shorter cores which have been found to have a uniform grain size distribution these are likely to be associated with this particular area of the lake and not a general feature. (It is also possible that the later results have been affected by the demagnetiser. This was not always working properly during these measurements).

The bulk demagnetisations were performed as before in a peak field of 10mT. The common depth transform functions were established using the variations in intensity and the resulting transformed records of the three cores on a B49 depth scale are shown in **figure 8.3**. The B49 depth scale is retained as the only available dated scale. Some samples were taken from the 12m cores for TL dating but as yet these dates are unavailable. The transform to the time scale is thus via the same transform function as is given in chapter 5. For depths below the maximum length of B49 (8.2m) the equivalent B49 depth has been calculated as being that of the longest core (B64) adjusted by the same amount as the last available transform depth.

The equivalent B49 maximum depth reached after the transform was found to be nearly 12m equivalent to an age of about 42,000 years bp. Thus we have effectively extrapolated the record for 12,000 years. It follows that any analyses based on this extrapolation can only be a first approximation and further analyses should be performed when more dates become available.

Table 8.1 The variation of the MDF and α_{95} down core B63 from an analysis of pilots taken at different depths.

Sample No.	Depth (cm)	MDF (mT)	α_{95} ($^{\circ}$)
10	118.6	14.2	6.5
20	141.6	15.8	13.9
30	167.3	14.6	2.7
40	190.9	15.6	2.9
50	214.5	16.6	2.2
60	238.1	16.4	2.1
70	261.7	14.3	8.4
80	285.3	12.9	10.3
90	309.0	17.5	2.5
100	332.1	16.1	2.4
110	355.6	15.5	4.9
120	379.1	14.1	5.7
130	402.6	15.6	3.7
140	426.1	15.4	3.4
150	449.6	15.3	6.8
160	473.8	17.1	3.1
170	497.6	12.9	4.2
180	521.3	14.1	3.0
190	545.1	13.5	4.3
200	568.8	9.3	8.2
210	592.6	17.4	12.3
220	626.4	10.9	3.2
230	650.1	22.3	4.8
240	673.8	10.8	11.7
250	697.4	10.5	22.9
260	721.1	9.7	3.6
270	744.8	13.1	4.9
280	767.9	7.8	8.8
290	791.2	10.9	25.7
300	814.5	11.4	2.3
310	837.8	14.2	8.8
320	861.1	10.8	13.4
330	884.3	8.5	12.8
340	907.6	9.3	10.9
350	930.4	9.0	19.7
360	953.4	11.4	8.4
370	976.4	14.9	2.3
380	999.4	12.4	7.2
390	1020.3	14.0	5.0
400	1044.7	22.0	23.5

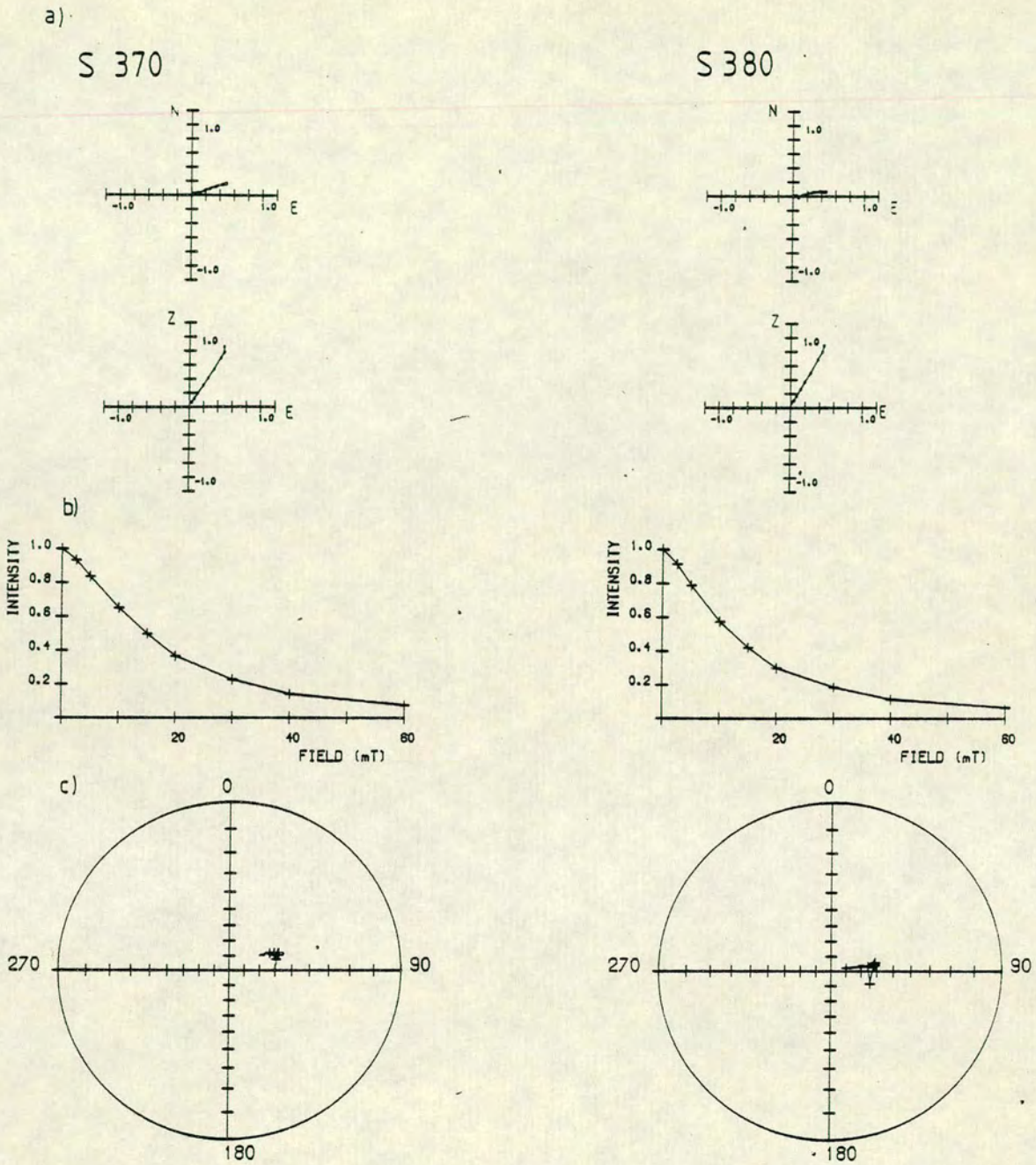

Figure 8.2 The step af demagnetisation of two samples from core B64 showing a) the Zijderveldt diagram, b) the step demagnetisation plot and c) the stereographic projection.

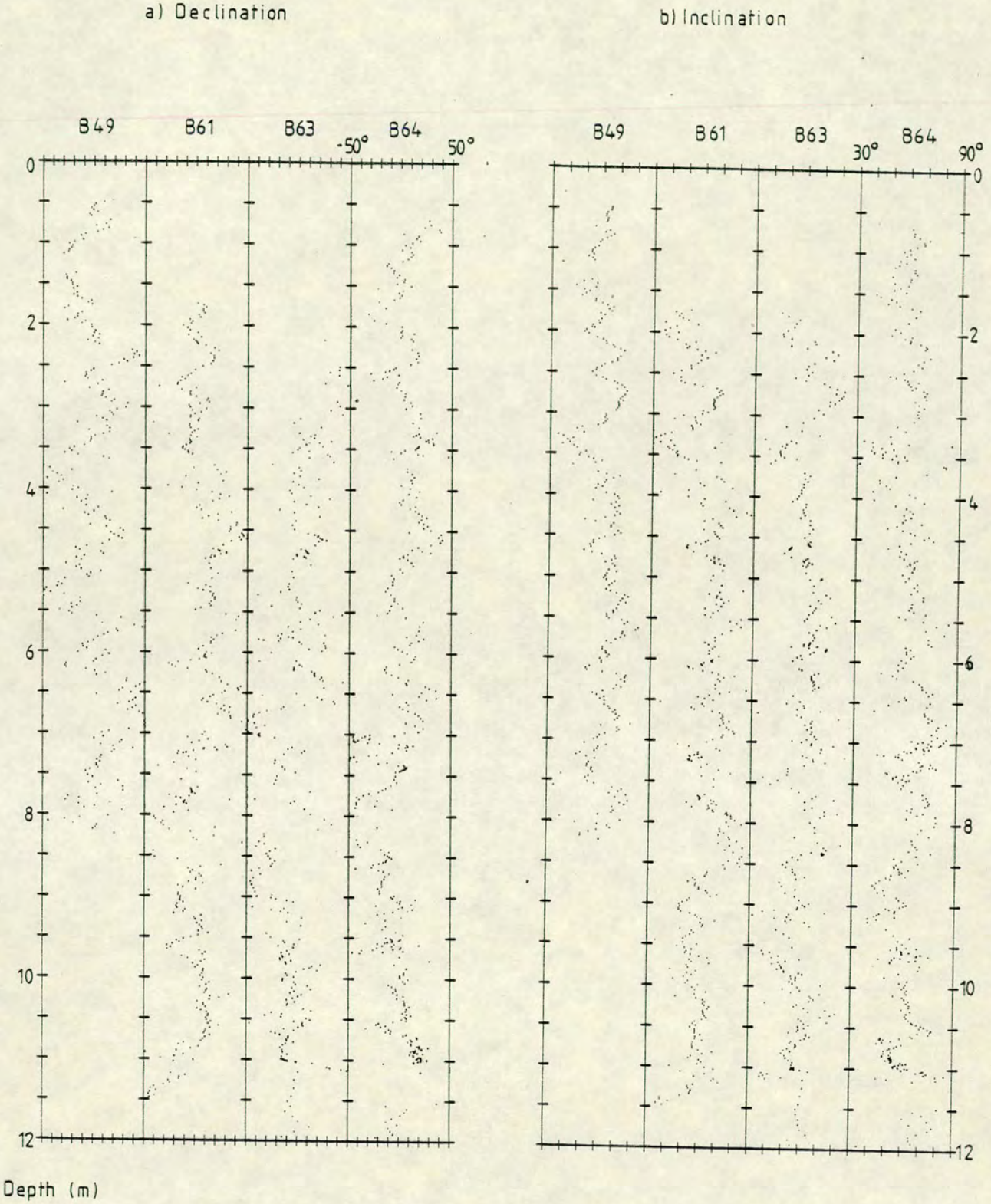

Figure 8.3 A comparison of the long core records in a) declination and b) inclination.

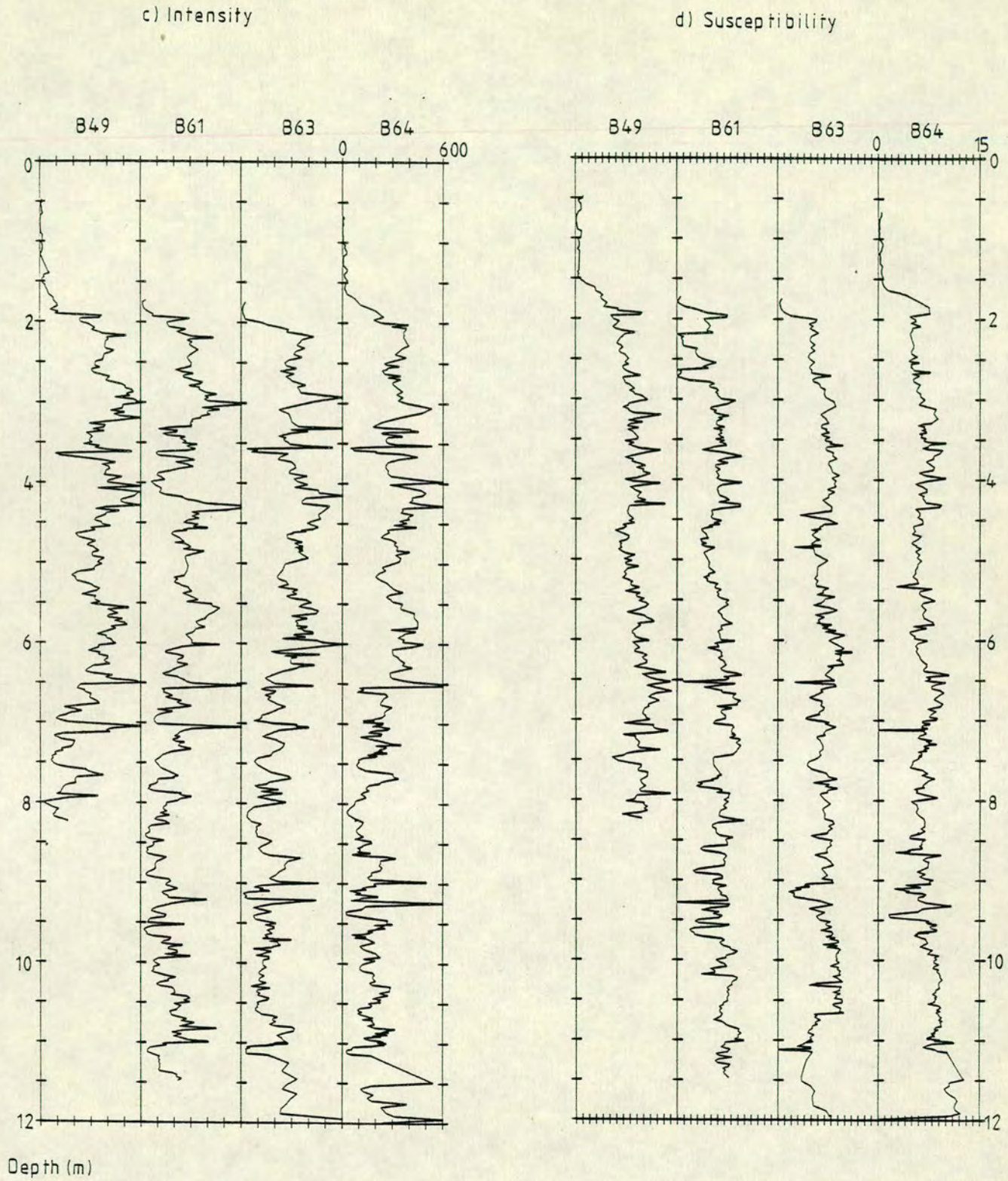

Figure 8.3 A comparison of the long core records in c) intensity and d) susceptibility.

8.4 Spectral analysis

The three cores have been merged and stacked after transformation to the time scale, as described in chapter 6. The resulting merged stack was subjected to a cross validation analysis to determine the optimum degree of smoothing for the period 42,000 - 10,000 years bp (called window A') and for the window (B') 42,000 - 30,000 years bp. Again the CVMSE function has a broad minimum and so the midpoint of the minimum, corresponding to 50 knots has been chosen as the optimum smoothing level for window A'. Using this smoothed, merged stack, auto and cross correlation, Fourier and MEM analyses have been performed. The results are summarised in **tables 8.2 and 8.3** and the spectra produced for window A' for the merged stack are shown in **figures 8.4** and **8.5**. The results of the averaged stack were found to be almost identical once again. The auto and cross correlations give poor records for such long time windows but a period of about 5,000 years and one of about 2,000 years is noticeable. The spectral analyses reveal similar periods to the shorter window although more power is found about 7,000 years. Periods about 5,000, 3,000, and 2,000 years are still apparent with the latter being particularly strong in the intensity results. The latter period appears to have split with the improved resolution into a period about 2,200 years and one about 1,800 years. Note that these different frequencies do not invalidate the arguments in chapter 6; the actual periods obtained will still suffer from the same interpretational difficulties. These analyses are much less well defined than for the shorter record however, due to the errors that are likely to have been introduced by the extrapolation of the depth time transform.

8.5 VGP paths

The VGP paths produced by the declination and inclination pair for the earliest 12,000 year window available are shown in **figure 8.6**. The merged stack smoothed using a 50 knot cubic spline has been used and the window has been split into four equal time increments of 3,000 years.

For some of the period shown here the VGP vector is looping in an anticlockwise sense (42%). In this case the periods of clockwise drift are not as well pronounced as for the shorter record. This indicates either that there could have been a true eastward drifting source affecting this area over this period of time or that the errors introduced in the extrapolation have affected the data. More dating is required to resolve these features accurately as it is felt that the

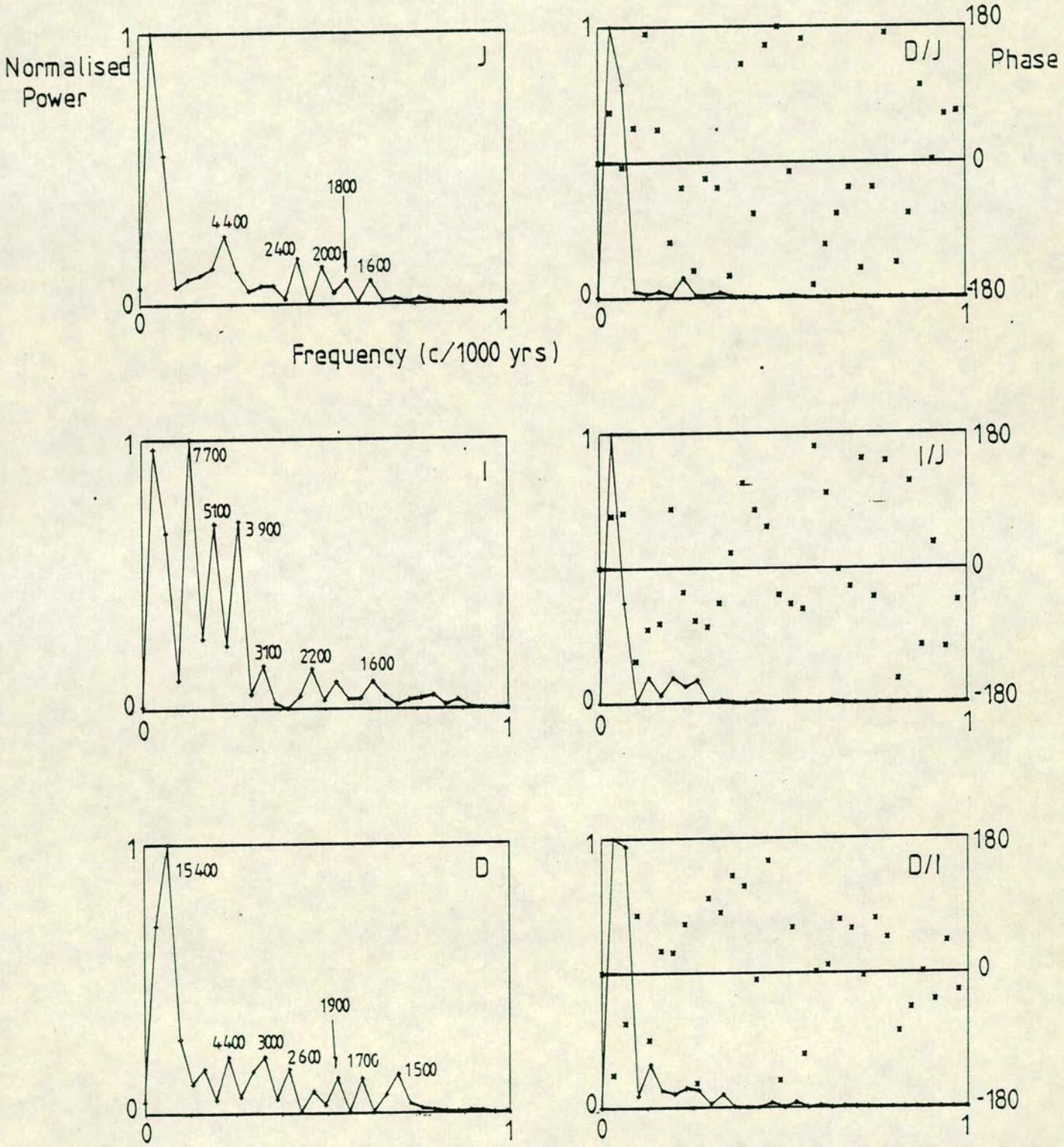

Figure 8.4 The Fourier transform spectra for the merged stack.

Table 8.2 The main periods obtained from a Fourier spectral analysis of the merged stack.

a) Merged Stack

Window		6000	4000-5500	3500-4000	3000-3500	2000-3000	1500-2000	1000-1500
A'	J		4400			2400	1800	
	I	7700	5100	3900	3100	2200	1600	
	D	15400	4400		3000	2600	1900	1500
	D/I	7700(-90)	4400(60)		3100(90)			
	I/J	7700(-90)	5100(60)	3900(-90)				
	J/D	6200(-30)						
B'	J	5800					1600	1300
	I	5800				2300		1400
	D			3900			1600	
	D/I	5800(-30)					1400(90)	
	I/J	5800(-90)					1600(120)	
	J/D			3900(120)				

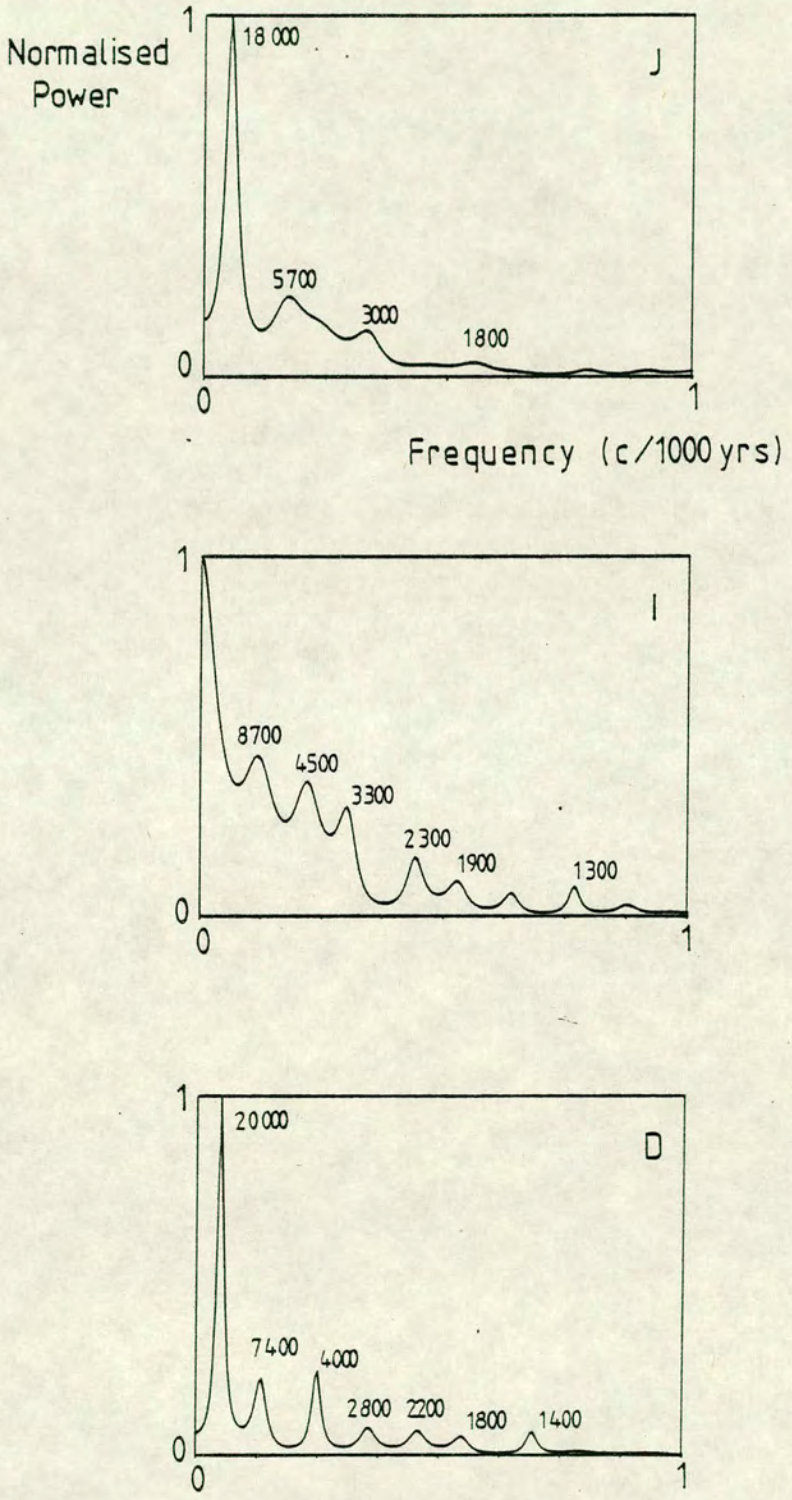

Figure 8.5 The MEM spectra for a pef length of 90 for the merged stack.

Table 8.3 The main periods obtained from a MEM spectral analysis of the merged stack.

Window		6000	4000-5500	3500-4000	3000-3500	2000-3000	1500-2000	1000-1500
	J	18000	5700		3000		1800	
A'	I	8700	4500		3300	2300	1900	1300
	D	7400	4000			2200	1800	1400
	-	7400	4100			2700	2000	1400
	+			3500		2500	1900	1500
	J			3800		2600	1700	
B'	I	6900				2000		1200
	D	9000		3600		2400	1500	
	-				3200		1600	
	+						1500	

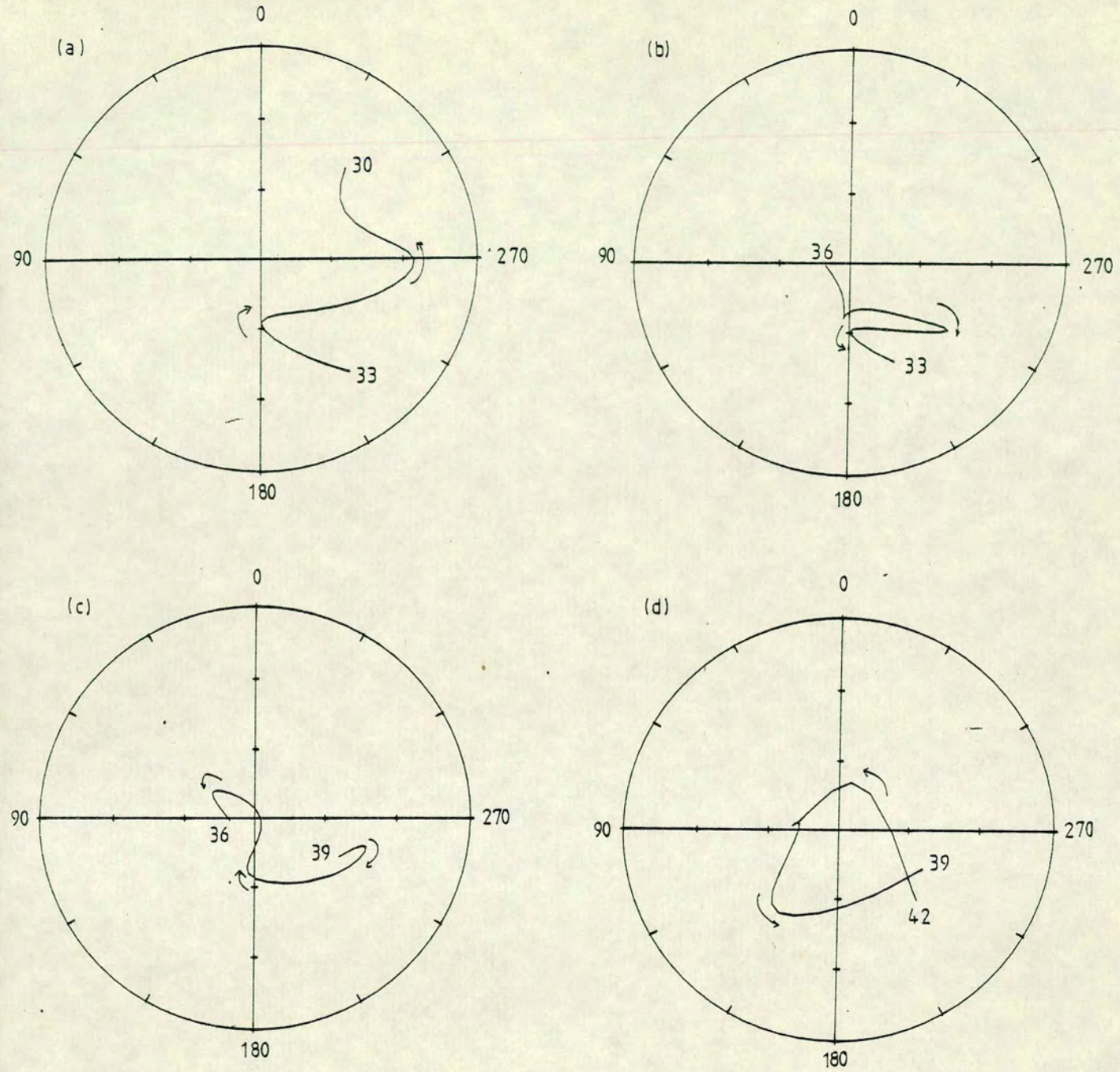

Figure 8.6 The VGP paths for the 50 knot smoothed merged stack in 3,000 year increments. a) 33,000 - 30,000 years bp b) 36,000 - 33,000 years bp c) 39,000 - 36,000 years bp d) 42,000 - 39,000 years bp.

errors introduced at the bottom of the record could cause this small increase.

8.6 Intensity normalisation

The same normalisation parameters as were used for the 9m cores were used on the 12m cores to extend the normalised intensity variations. The susceptibilities show the long period variations as do the SIRM and ARM_{60} values as can be seen in **figure 8.7**. The resulting normalised intensity variations are shown in **figure 8.8**. The reduced intensity feature observed to have started around 30,000 years bp (chapter 7), is still noteworthy. A further period of reduced moment could also have occured around 39,000 years bp. This latter date in particular is significant, as the estimated age of the Laschamp event, discussed in the next section.

8.7 Events and Excursions

There have been several reported reversals of the direction of the geomagnetic field found to occur within the last 50,000 years. **Table 8.4** gives a summary of the reversals and excursions that have been reported. **Jacobs (1984)** and **Creer (1985)** have discussed these recent "events".

The thorough investigation of the lake sediments from Lac du Bouchet has resulted in none being found. There are samples for which the magnetisation has a negative inclination value, seven in total from the 19 cores (more than 5,700 subsamples) measured, five of which were found to contain large pebbles and the remaining two were gritty. This indicates that these particular directions are unreliable palaeomagnetically since they imply a "noisy" depositional environment incapable of genuinely recording the palaeofield direction. Even so, the very wet and very peaty sediments of the top two assemblages were found to give positive inclinations. The lack of an inclination reversal means that either the Bouchet sediments have failed to record the reversals that have been found elsewhere or that the reversals did not happen (either locally or globally).

Lac du Bouchet is located in an almost ideal site for palaeomagnetic investigations. Its mid latitude means that the average inclination will be around 60° and the location in a relatively earthquake free area and lack of inflow and exflow (emphasised by the low deposition rate) means that the sediments have been deposited in a very quiet environment. The analyses performed upon the

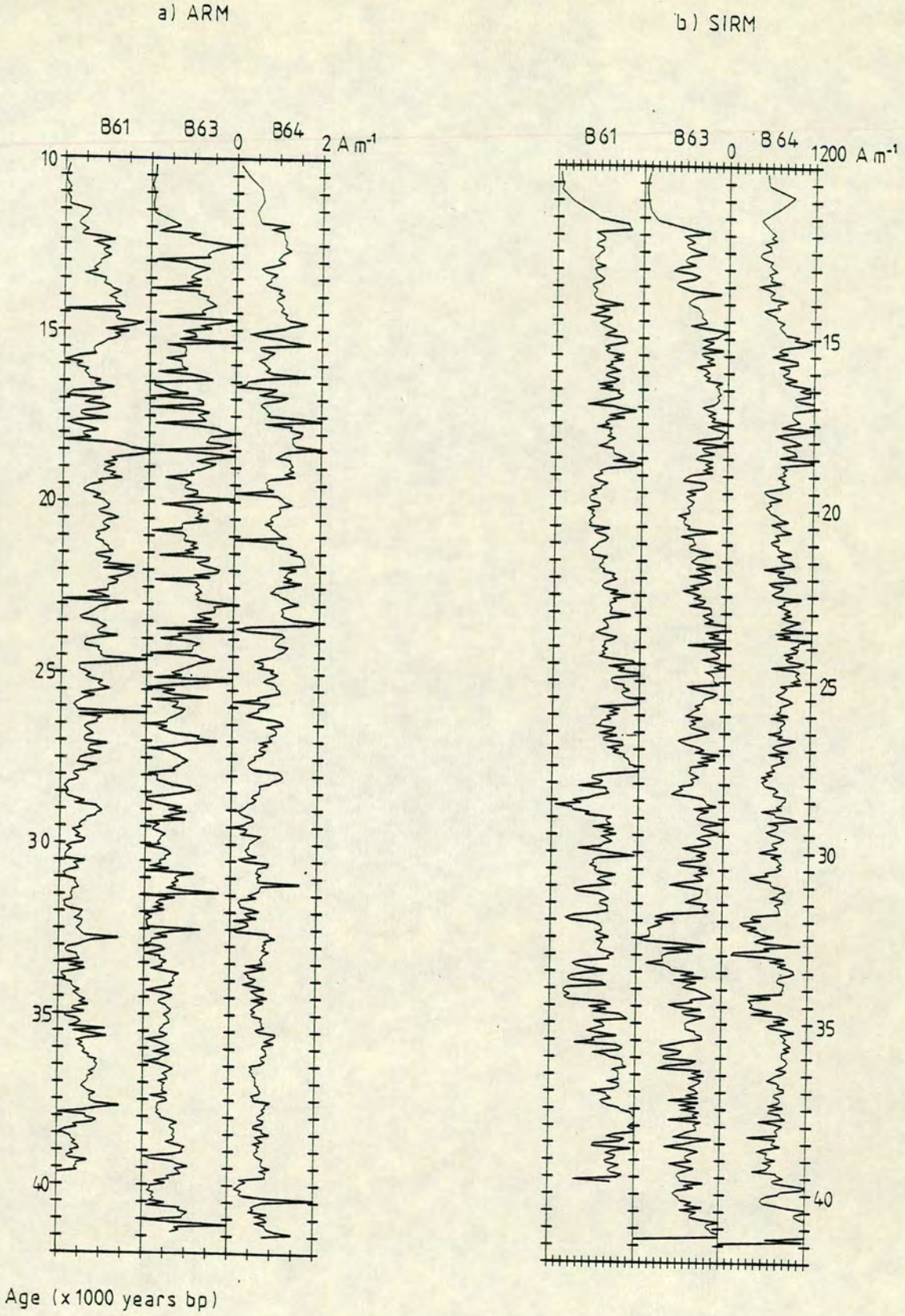

Figure 8.7 The variation of a) ARM and b) SIRM for the three long cores.

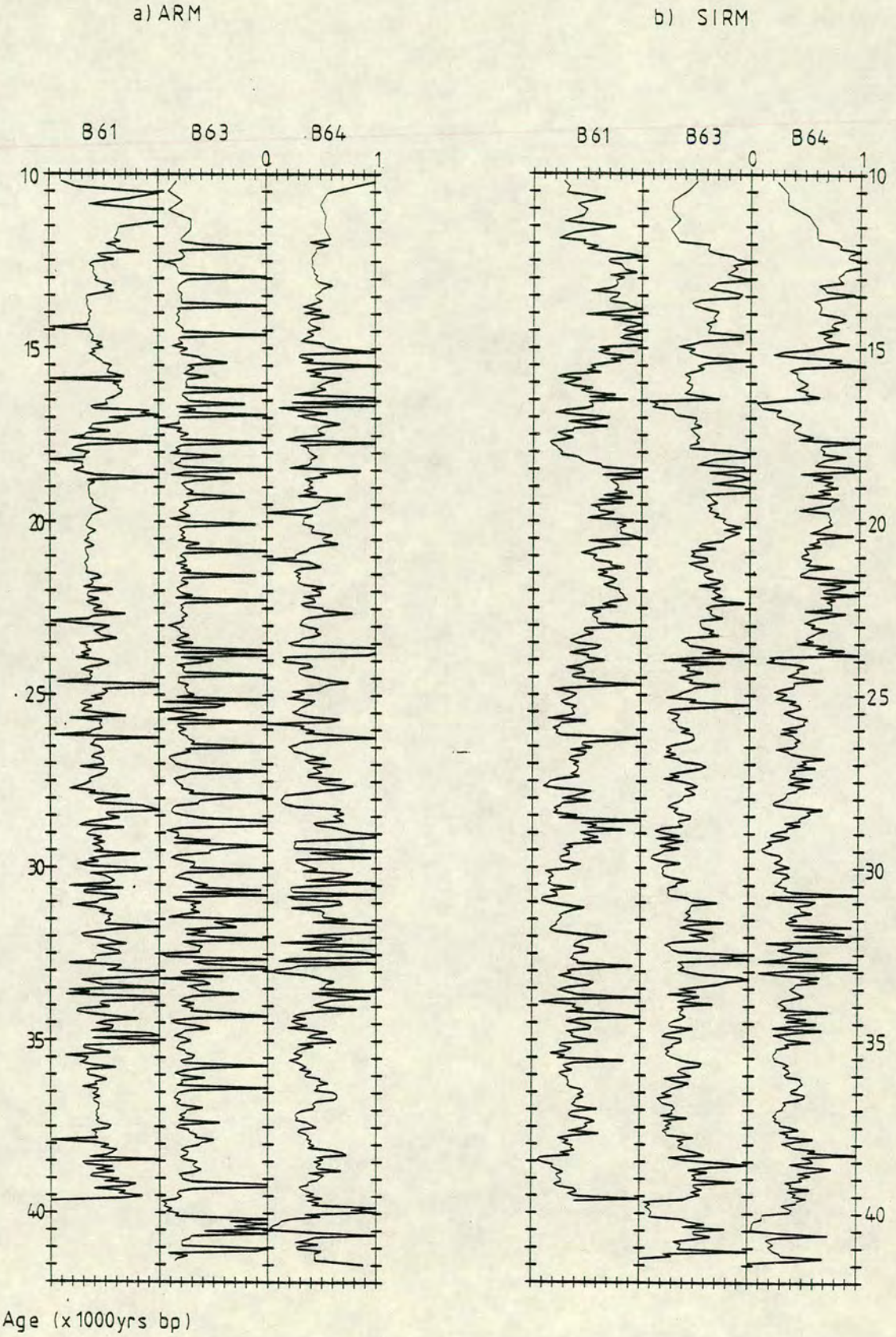

Figure 8.8 The NRM for the long cores after normalisation using a) ARM and b) SIRM.

sediments have indicated that the records do indeed show the variations of the palaeofield direction.

A well documented reversal that should certainly be found in the sediments from Lac du Bouchet is the Laschamp/Olby reversal (**Bonhommet & Babkine (1967)**). This is found in volcanic basalts in the Chaine des Puy region less than 150 km from Lac du Bouchet and has been dated using many different techniques at ages between 10,000 years bp and 45,000 years bp (**table 8.5**). The average of these dates clearly indicates that the Olby flow occurred earlier than the Laschamp (by about 5,000 years) and the period seems to be 38,900 ± 4,000 years (**table 8.6**). Almost all the estimates of the date of the Laschamp flow lie within the range of the Bouchet sediments; the Olby flow, although occuring earlier is still within the range.

Three explanations could explain not finding this event within the sediment taken from Lac du Bouchet. The first is that most of the dates are wrong and that the Laschamp event occured before 42,000 years bp. The second is the effect of smoothing.

The size of a subsample box is 2.5cm. The calculated depositional rate has been found (chapter 5) to be, on average about 0.34mm per year. Thus a single sample spans a period of about 75 years and the resulting magnetisation vector is an average of the field directions over this period directly and slightly longer from the rate of fixing of the magnetisation (a maximum of 200 years). It follows that one explanation could be that the Laschamp and Olby events could have occured and had a duration of less than this time period which would be the maximum limiting period. This would require the production of a short intense (local?) source opposed to the main field direction and would <u>not</u> constitute a true reversal. In addition, an examination of the averaged results for the ages of these reversals indicates that where samples from both locations have been dated by the same method the Olby event is consistently about 4,000 years older. If these rocks are recording the same event then it must have lasted for at least this length of time.

The final explanation would be that the event did not occur at all and that the rocks examined at Laschamp and Olby have obtained a secondary magnetisation that is reversed. This could be due either to self-reversal or lightning strikes (**Heller (1980), Heller and Petersen (1982)**).

Table 8.4 Palaeomagnetic excursions that have been reported for the last 50,000 years.

Name	Approx. Age (years bp)	Location	Reference
Laschamp/Olby	38,000	France	See table 8.5
Lake Mungo	30,000	Australia	Barbetti & McElhinney (1972,1976)
Mono Lake	24,000	North America	Denham & Cox (1971) Liddicoat & Coe (1979)
Gothenburg	12,500	Sweden	Morner et al (1971) Morner & Lanser (1974)
Gulf of Mexico	15,000 32,000	Mexico	Clark & Kennett (1973) Freed & Healy (1974)
Lake Biwa	18,000	Japan	Yaskawa et al (1973)
Erieau	8-14,000	North America	Creer et al (1976a)

Table 8.5 The different ages that have been obtained for the Laschamp and Olby reversals.

Age (yrs bp)	Method	Reference
8,000	^{14}C of baked trees found in unit overlying flow (L)	Bonhommet & Zahringer (1969)
25,000	Whole rock K-Ar (L & O)	
-	TL (failed due to anomalous fading) (L & O)	Wintle (1973)
33,000 ± 4,000	TL (Quartz from granite inclusion) (L & O)	Valladas et al (1977)
45,400 ± 2,500	Whole rock K-Ar (L & O)	Hall & York (1978)
47,400 ± 1,900	K - Ar with step heating (L & O)	
39,000 ± 6,000	$^{230}Th/^{238}U$ Disequilibrium (O)	Condomines (1978)
25,800 ± 1,700	TL (Baked clay) (L & O)	Huxtable et al (1978)
43,000 ± 5,000	K - Ar (L)	Gillot et al (1979)
50,000 ± 7,500	K - Ar (O)	
35,000 ± 3,000	TL (Quartz from granite inclusions) (L)	
38,000 ± 6,000	TL (Quartz from baked palaeosols) (O)	
33,500 ± 5,000	TL (Plagioclase, ground rock) (L)	
44,000 ± 6,500	TL (Plagioclase, ground rock) (O)	
>36,000	C^{14} (O)	

Age (yrs bp)	Method		Reference
32,500 ± 3,100	TL (Plagioclase)	(L)	Guerin & Valladas (1980)
37,300 ± 3,500	TL (Plagioclase)	(O)	
32,500 ± 3,100	High temp TL	(L)	Guerin et al (1984)
37,300 ± 3,500	High temp TL	(O)	
38,000 ± 8,000	K - Ar	(L)	
42,000 ± 9,000	K - Ar	(O)	

N.B. (L), (O) indicate sample from Laschamp or Olby flow respectively.

Table 8.6 The averages of the ages obtained for the Laschamp and Olby flows by different methods indicating that they are not contemporaneous and that the 'event' must therefore last at least 4,000 years.

	TL	K/Ar	Other	All
Laschamp	33,700	40,500	-	36,400
Olby	39,800	46,000	39,000	41,750
Both*	29,400	46,400	-	37,900
All	34,900	44,300	39,000	38,900

* These ages are for combined samples and do not include samples from a single site.

Note that these explanations imply that a true geomagnetic reversal has not occured during the last 40,000 years and thus emphasises the difference between global and local reversals. Global reversals ("events") should be found in all records and should therefore constitute a dateable horizon. Local reversals ("excursions") would be found only over a restricted area and be associated with particularly intense non dipole field foci (and could thus effect either the declination or inclination independently). These need to be extremely carefully examined in order to establish conclusively that they are a geomagnetic effect and not an effect of the acquisition mechanism. If they do occur the actual size of the area that such an anomaly would affect is probably quite small, but should be of the order of at least 200–500 km. It is possible therefore that such excursions may not be observed at different sites on the earths surface but if one site is found that has such an excursion at least one other site should have to be found, in the same area, before it can be accepted.

8.8 Conclusions

The thorough examination of so many cores from Lac du Bouchet indicates how valuable it is to be able to compare the results from several cores from the same site. Although the cores exhibit the same general features of the magnetic record, localised depositional variations have obviously caused slight discrepancies. Stacking has minimised the effects of such discrepancies which without the safety of several cores may not have been possible. A criterion for accepting the results of lake sediment work should therefore be the clear repeatability of the magnetic variations in at least three cores. (Clearly, 6–8 are much better).

The most important aspect of this work, especially in the early stages of lake sediment investigations, as now, is the dating. The type curve developed for the late glacial in western Europe can be used to date other contemporaneous sequences from the same area by comparison of the magnetic records. In addition, all the spectral analysis results are dependent on the accuracy of the depth/time transform function. Although the dating of sediments is very expensive and time consuming it cannot be stressed enough how important it is. It is apparent how the spectral analyses of this chapter are much less convincing due to the possibilities of error in the time scale. In addition, since we do not know the age of the bottom of these long cores we cannot, with certainty, dismiss the Laschamp event. The rate of sedimentation could increase near the bottom of our cores and the Laschamp event could be beyond our

present maximum depth.

CHAPTER 9
CONCLUSIONS

9.1 The palaeomagnetic record of secular variation

Lac du Bouchet has been found to contain sediment that has been deposited in a very stable environment. The sediment contains a strong NRM signal which is stable both in direction and intensity. Although the character of the sediment changes between the late glacial and the Holocene, becoming more organic, the NRM still records the geomagnetic field vector. This has been shown to be comparable with the UK record for the last 6,000 years despite the low rate of sedimentation causing substantial smoothing of the signal.

The late glacial record is also comparable to established records. The Black Sea record shows the same variations in inclination and declination but the timings are not identical. This mismatch is attributed entirely to the dating, predominantly of the earlier record; more dates (especially accelerater based dates), will make it possible to more accurately define the depth time transform. The technique used in this work, (a least squares straight line), is a good first approximation from the few dates available. More dates, especially in the late glacial period should remove the doubts cast by the slight disagreements in the different dating methods.

The magnetic results show a very clear pattern of variations. These could be used as a method of dating other sedimentary sequences and should be used as a relatively cheap and non destructive method. Certainly the variations since 30,000 years bp can be used quite confidently. Those found earlier are open to more doubt but must still be a reasonable first approximation. Therefore, it follows that the existence of the Laschamp event must be seriously questioned since no reversals of the NRM have been found.

9.2 The spectral content of the geomagnetic field

Despite the small question marks over the effectiveness of the depth time transform the results of the spectral analyses are remarkable. They show that the periods found in other records (predominantly covering the Holocene), are found in the late glacial record also. However, the interpretation of the periodic nature of the sources is not as clear. If the sources grow and decay at the same time as they drift, as seems likely from an analysis of the present day field, then the spectral periods obtained will not be those of the drift and change. The observed periodicities within the spectra will be the periods obtained through a multiplication of these two frequencies and hence, from the addition theorum for sinusoids, will be proportional to the sum and difference of the two source frequencies. The relationship between these frequencies has been discussed and will tend to show the drift period in all records, estimated to be similar to the present day rate of approximately 2,000 years.

The direction of the drift of the sources causing the variations in declination and inclination has also been investigated. In general they are found to be westward drifting. Apparent stationary sources or eastward drifting sources are much less common. Some will arise from the combination of the growth of sources whilst they drift; others may drift eastwards but these are much rarer. Periods of open anticlockwise looping of the VGP vector, indicative of such drift are not common. However, such anticlockwise looping does appear to occur more frequently at spectral periods between 4,000 and 5,000 years. This result has not been conclusively demonstrated for the Holocene and is more apparent in the European records than in the North American.

9.3 The magnetic minerals and palaeointensities

The carrier of NRM has been convincingly shown to be a multi domain magnetite with a slight titanium impurity and likely to be found in grains between 1 and 5 microns. The variations in the proportions of such grains have been seen to cause changes in the NRM intensity. These effects have been minimised in an attempt to obtain an estimate of the relative palaeointensity during the late glacial by using an ARM and the SIRM. At present there are no records with which to compare the normalisation for the late glacial although a theoretical model does indicate that the variations are likely to be following

those of the geomagnetic field.

9.4 Further work

It is clear that much further work is needed to clarify some points raised in the course of this project. The question of dating has already been discussed but is quite obviously of extreme importance. Once a consistent time scale has been attached the questions about the spectral content of the records and the existence of the Laschamp/Olby event can be resolved. This also entails the extraction of longer cores from the lake. The Mackereth corer design is close to its maximum realistically operational length with 12m, (since the corer requires twice its own length of depth of water to operate effectively). Thus the method of extraction must be adapted.

The spectral content of cores covering a period of greater than 15,000 years can be analysed. Longer periodicities should then become apparent. The sources of such variations may then be evaluated. The 5,000 year period for example, if proved to be generally featured in such records, could be due to the variations of the earth's orbit, (precession of the equinoxes). Such proposals however, depend upon the quality of the data available. This must be at least maintained and, if possible, improved.

If palaeointenisties are to be obtained from sediment studies then more study must be undertaken of both the theoretical relationships between the NRM acquisition of the sediment and the intensity of the local geomagnetic field and the relation between the natural remanent magnetisation and induced magnetisations. This is difficult not least because of the long time scales involved.

The investigation has also revealed the long period variations of susceptibility and induced magnetisations. These are clearly related to the magnetic mineral content which must, in turn, be related to the climate. It may be possible that an investigation of the variations of these parameters (in conjunction with sedimentological analyses), may reveal more information about climatic changes.

Many different, but related topics can benefit from a study of lake sediments. I have investigated some magnetic aspects from a single lake in France. Many lakes will not have such good magnetic recording ability but a thorough

investigation of the properties of the sediment from these lakes will provide more insight into the processes which occur within and upon the Earth.

Appendix 1. The Mackereth Corer

A1.1 Introduction

The Mackereth corer is a pneumatically controlled sediment corer. Developed in 1958 (**Mackereth (1958)**) the force to drive the core tube into the sediment is derived from compressed air. Several modifications have been made to the original corer to ease core tube loading and operation by increasing the coring pressure.

A1.2 Operation of the Mackereth corer

Figure A1.1 shows a schematic diagram of the 9m and 12m corers used for a portion of this work. The aluminium anchor drum is pushed into the sediment by pumping air into the drum which rises to the only exit; the 1" tube. At the top of the 1" tube is a one way valve that is open when the corer is lowered. The air passes through the open valve carrying with it a "head" of water. This water has been taken from the anchor drum which is sealed at its lower end by the sediment. Thus a pressure difference develops between the inside and outside of the drum. The pressure on the sides is equal and opposite, the pressure on top of the drum, being opposed only by the sediment, drives the drum down.

After a period of time, monitored by observing the position of a buoy attached to a rope in turn attached to the top of the corer the air to the drum is shut off. The drum is now securely anchored in the lake bottom sediment.

Air is now introduced at about 150 lbs/in^2 (10 bar) on the top of the main piston. This initial burst closes the one way valve at the top of the 1" tube and effectively seals the anchor drum. The pressure on the main piston drives the core tube down the core barrel into the sediment, which should be undisturbed towards the centre of the drum. Orientation is maintained using a screw inset into a groove parallel to the long axis of the core tube.

Under ideal circumstances, coring proceeds until the main piston passes the hole in the core barrel attached to the anchor drum. Air thus bypasses the

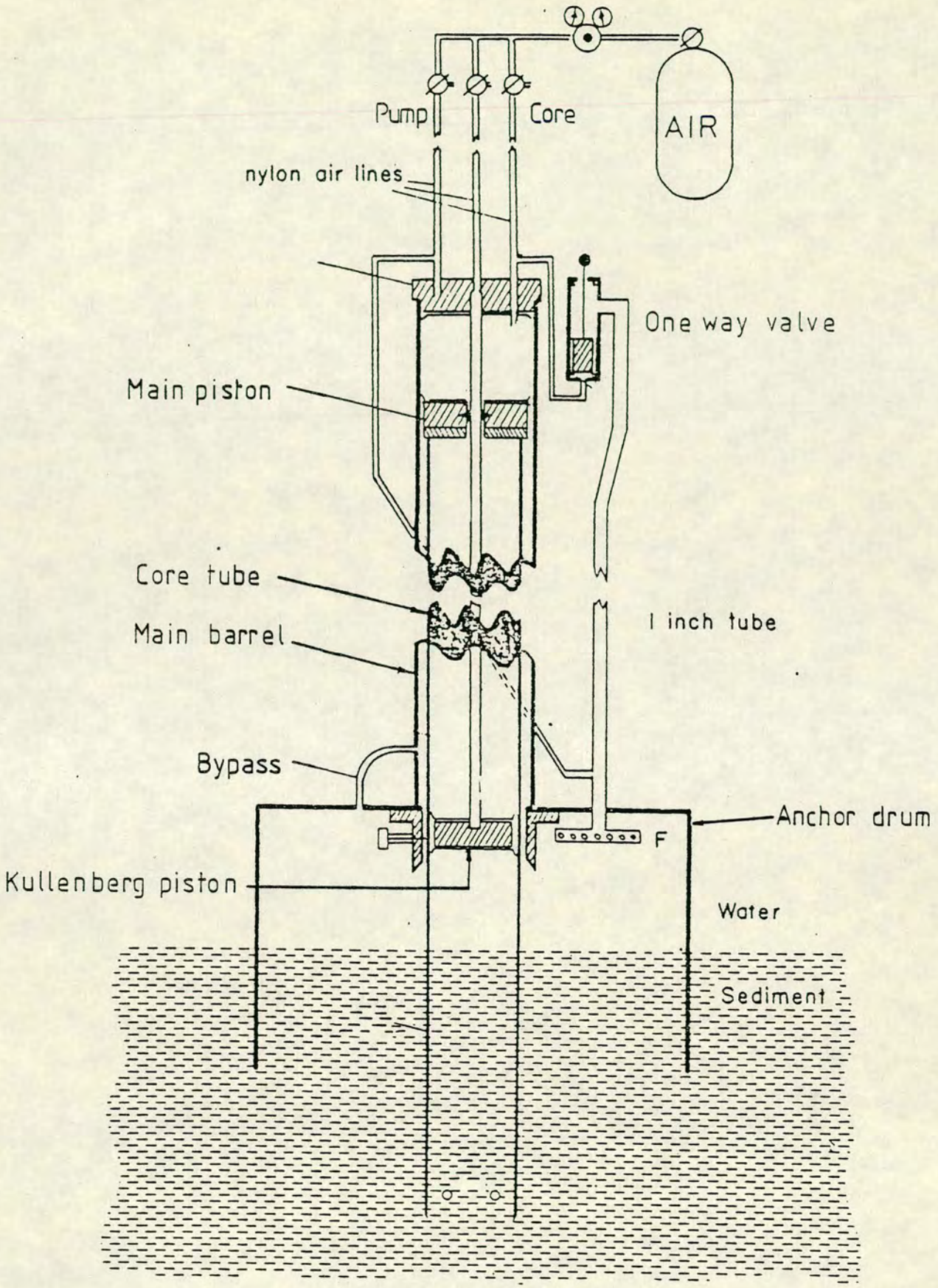

Figure A1.1 A schematic diagram of the Mackereth pneumatic corer.

piston, coring stops, and the drum rises due to the buoyancy of the air in the drum. The Kullenberg piston stays in place and produces a vacuum that holds the sediment in the core tube.

Due to friction along the sides of the core tube, air is also introduced into a buoyancy bag to provide extra lifting force

A1.3 Modifications to the corer

There have been two major modifications to the design of the corer. The first is to increase the diameter of the main core barrel; the second is a new design for the main piston.

A1.3.1 Increased main barrel diameter

P.V.C. core tubes of internal diameter (i.d.) 54mm have been used for some time. The earlier 6m corers had a main barrel i.d. of 80mm. This has been increased to 100mm, increasing the coring force by 50% whilst still maintaining the same coring pressures.

A1.3.2 Modifications to the main piston

Figure A1.2 shows the new design of main piston. It now has a central tapered cylindrical wedge which fits snugly into the flange on the core tube. (This flange used to be removed before a thread was cut on the core tube itself. In the case of the 12m corer the flange has to be stuck on to the tube using glue.) The piston itself now has a screw thread to which a brass collar is attached which has been passed up the core tube on the outside. The tube is thus held fixed in position below the seals of the main piston and between the piston wedge and collar.

This new system has two great advantages. In the fieldwork preparation stage the time consuming task of cutting threads on the core tubes is abolished. During assembly of the corer the loading operation takes less than half the time taken previously due to the simplicity of the new system. (During the last two field seasons it was possible to take 2 12m or 3 9m cores in one day).

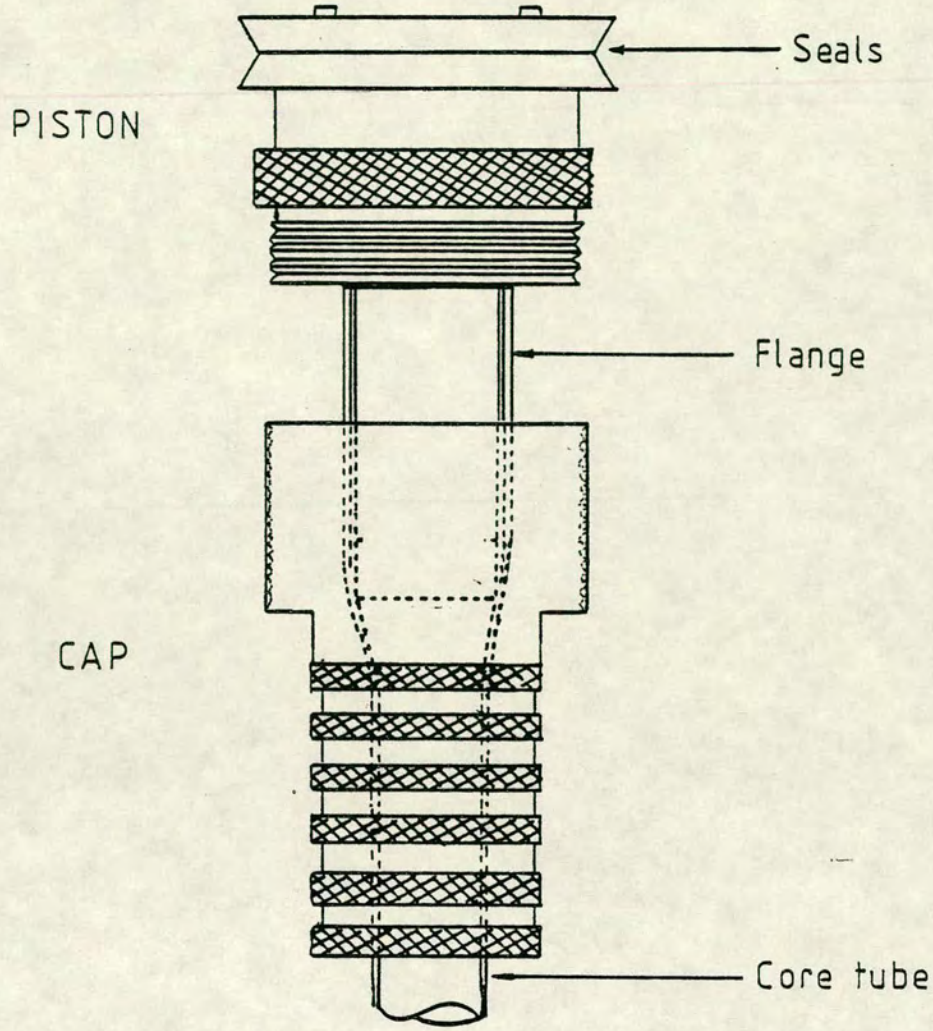

Figure A1.2 A schematic diagram of the new main piston for the Mackereth corer which incorporates both the piston and the fixing of the core tube.

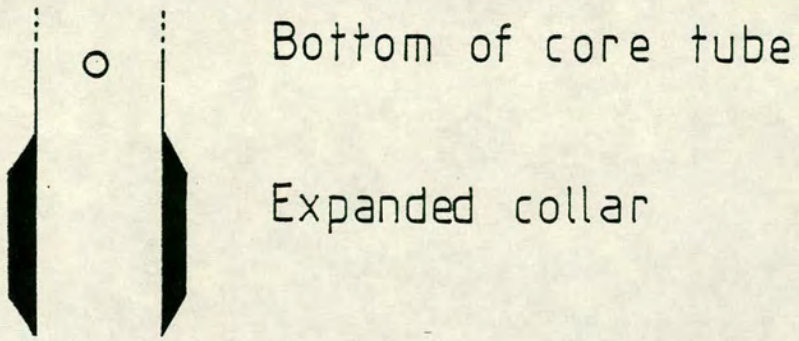

Figure A1.3 The collar for the lower end of the core tube which forces the sediment slightly away from the walls of the tube, improving recovery.

A1.3.3 Other modifications

Other less significant modifications include

(i) The use of a rubber "dunnage" (lifting) bag attached to the top of the corer to increase the lifting power available.

(ii) The use of a wedge (**figure A1.3**) at the bottom end of the core tube to increase the diameter of the hole forced into the sediment without causing an increase in disturbance internally. This decreases the friction on the walls of the core tube during recovery.

(iii) Holes drilled into the core tube above the Kullenberg piston allows water into the core tube whilst the corer is being sunk. This decreases the time taken for the corer to submerge initially.

Appendix 2. Subsampling

A2.1 Introduction

This is performed ideally in a clean dust-free environment so that no contamination occurs although this is difficult to achieve in practice. Cores are stored prior to opening in a cold room to reduce water loss. Some will occur so it is most useful to subsample quickly after obtaining the cores.

A2.2 Subsampling 6m, 9m or 12m cores

Note that the core tubes can be opened in different ways depending on the use to which the subsamples are to be put. Since we require minimally disturbed sediment we split the cores down the centre and then proceed as follows:

(i) open the cure tubes by removing the caps or bungs.

(ii) mark the two halves to be used along the whole core. Note that for 6m the orientation groove makes this operation relatively straightforward but for 12m cores with no groove the whole core must be marked so that samples are taken from a consistent orientation along the core.

(iii) Mark the cutting points on either side of core

(iv) Open the core tube (using a circular saw) being careful to note that the saw does not disturb the sediment (by cutting to leave a small thickness of tubing). Finish opening with a knife.

(v) Carefully clean the core tube of cuttings and place in V-blocks then draw a wire along the core to split the two halves.

(vi) Using a piece of wood covered in polythene and dampened to reduce sticking, separate the two halves. Enclose the half to be saved in an airtight polythene container.

(vii) Clean the half to be sampled and record its length and the positions of major stratigraphical boundaries.

(viii) Subsample, by pushing the plastic, cubic, boxes in the same orientation into the core sediment trying to ensure that the sample does not encroach on the side of core tubes as this section of sediment will be disturbed.

(ix) Each subsample box has a hole in its top face to allow air to escape without disturbing the sediment as the box is inserted. Seal these holes using "Lasso" tape or glue.

(x) Number subsample boxes consecutively along core. The position of each subsample box can now be noted or the position of the first and last box in a continuous section, the others can then be calculated by interpolation.

(xi) Carefully remove boxes without disturbing neighbours, cap and clean.

(xii) Store in a cool damp environment in zero field.

A2.3 Minicores

(i) Connect pump as in figure A2.1. This allows the hydraulic pressure of the water to push the sediment out of the open top of the core tube.

(ii) Pump until about 2 cm of sediment is visible above the core tube.

(iii) Slide the thin plastic sheet through the sediment cutting the top 2cm from the rest of the core and allowing this piece to be subsampled without further disturbance of the sediment below.

(iv) Insert sample box (same orientation for all boxes!)

(v) Remove samples, seal, number, clean and store as above.

Note that the orientation for the minicores is different from that of the longer cores. The "arrow up core" convention leaves the arrow on a side face rather than the top face of the subsample box. This should be noted carefully at the measurement stage.

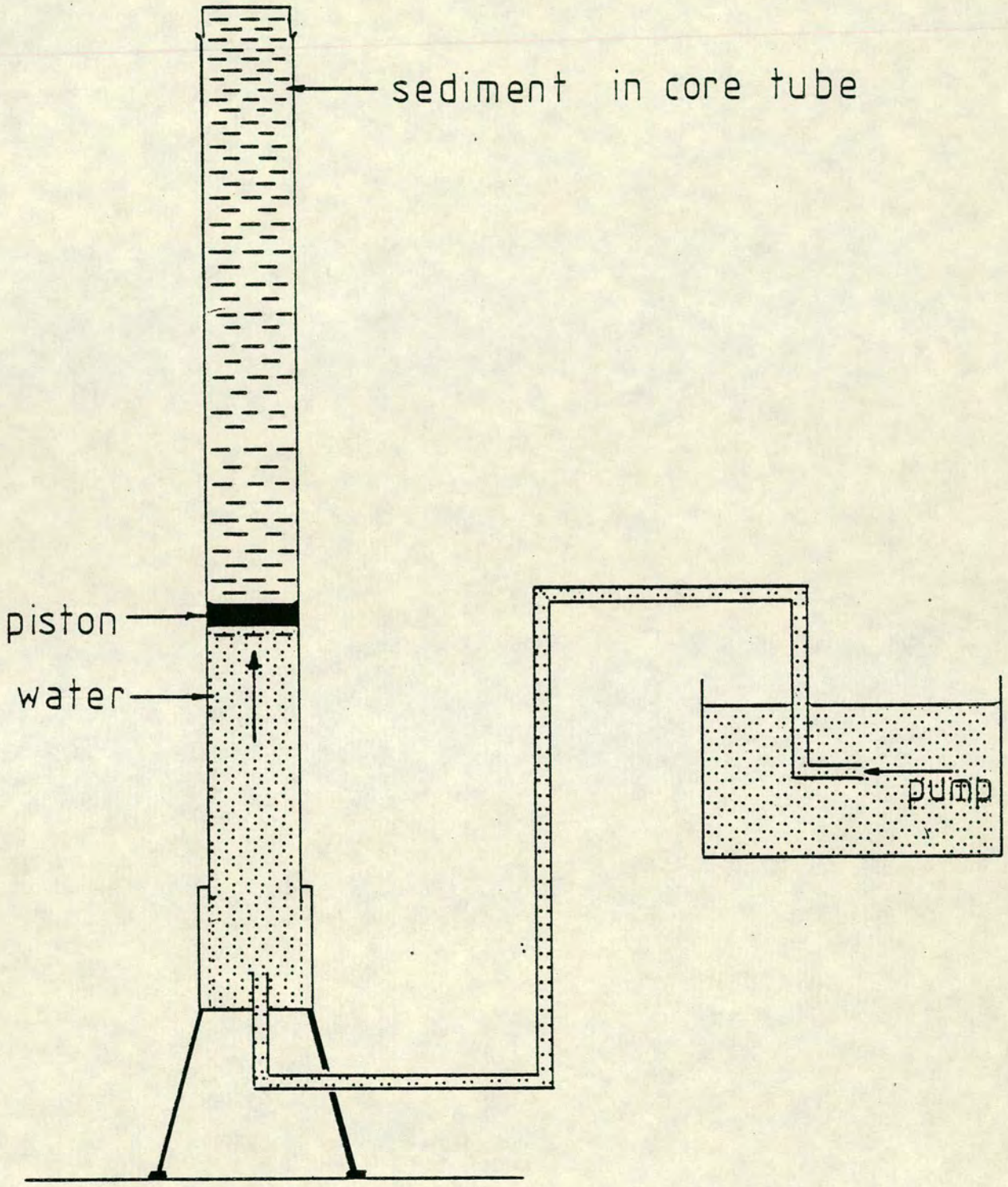

Figure A2.1 The hydraulic pump system for subsampling the minicores.

Appendix 3. PALAEOMAG - A lake sediment oriented palaeomagnetic program package

A3.1 Types of program available

There are several categories of programs available which range from elementary conversion and manipulation programs to more complicated data analysis and plotting programs. Each program is individually described in section A3.4 under the following categories.

(1) Conversion and manipulation
(2) Smoothing
(3) Magnetic mineral analysis
(4) Palaeomagnetic time series analysis
(5) Modelling
(6) Plotting
(7) Miscellaneous

For each program a brief description of its purpose is followed by descriptions of the general input and subsequent output. For detailed information of the operation of the program the listings must be read.

Note that all the programs are written in the Edinburgh Regional Computing Centre (ERCC) implementation of FORTRAN 77 that allows certain extentions to the standard (especially regarding character representation). Section A3.3 lists some of the commercailly available subroutines that have also been used.

A3.2 "Standard" input/output formats

The programs all use a standardised form of input data files (and produce output files capable of being used directly as input files for other programs). The form of the input file has evolved from earlier versions that required card input and may seem a little awkward at first. Each data file can be summarised as having

(a) A title line to allow the user to know what the data is

(b) A format line that gives the format of the subsequent data in the file. Note that this includes the brackets and should be a standard FORTRAN 77 format statement.

(c) The number of data points. This need not be accurate! It is included for user information rather than a requirement for the programs.

(d) The data. Most programs can cope with a least 1000 lines of data, some as many as 2000. Each line of data should be formatted according to the statement given in line two of the data file.

The only important exception to this input file format are the scaling files used in the plotting programs these are used to provide the scaling limits for the plots for each column and consist of a line of delivery information followed by

(a) The length (in cm) of a unit of the depth/time scale of the plots and the width (in cm) of the plots.

(b) Five lines of limits (one line for each column of the data file) in order lower limit then upper limit.

(c) There should be five lines of limits for EACH input data file.

All other input is prompted for at the screen using the ERCC intrinsic FPROMPT and is in free format. Any errors in the input of program control information should result in a re-prompt for the data.

A3.3 External directories of subroutines

Not all the subroutines used have been written personally. Some are commercially available routines or ERCC equivalents. The following commercial libraries have been used

(a) NAG FORTRAN library - Cubic spline fitting routines and random number generator

(b) CALCOMPICS graphics library - some plotting subroutines

(c) ERCC graphics library - other plotting subroutines

Whilst it proved impossible in some programs, the majority have been written so that the graphics section is independent of the analysis section. It should thus be straightforward to adapt the programs to use any graphics package. Obviously the cubic spline routines and random number generator can

be replaced by any equivalent subroutines.

A3.4 Program descriptions

A3.4.1 Conversion and manipulation

PROGRAM 1.1: ARRANGE

PURPOSE: Program to match columns of data from different files to produce a composite file. e.g. to pick out the intensity data from a set of demag type files to produce a file suitable for armplot.

INPUT:
(a) Files
Any type of data file

(b) User
(i) No. of columns in the data file
(ii) File name
(iii) Column to be taken (if positive will match column 1 of the input file with column one of the output file and interpolate if values are missing). Choose as many columns as required input 0 to stop.
(iv) Get a new file or stop
(v) Title

OUTPUT:

(b) Files
OUT2 created : Standard data file with new column arrangement

PROGRAM 1.2: CONVKIS

PURPOSE: Converts the values of suseptibility obtained on the Bartington bridge metre to true volume susceptibilities.

INPUT:
(a) Files
2 column data file (sample number,susc)

(b) User
(i) File name
(ii) Sample volume
(iii) Mass of the standard sample
(iv) Value the meter gave for the standard sample
(v) Susceptibility of the standard sample

OUTPUT:

(b) Files
OUT2 created : Converted suseptibility (suitable for input into CRYTOALL.

PROGRAM 1.3: CRYTOALL

PURPOSE: Program to convert "CRY" type data file to "ALL" type by converting sample numbers to depths and rearranging data columns. Decs centred on zero, Incs on geocentric axial dipole field value and moments converted to magnetisation per unit volume. Optional detrending and input of "ALL" type files for this.

INPUT:
(a) Files
(i) Either "ALL" type data file (depth,dec,inc,int,susc,q) or "CRY" type data file (sample no.,int,dec,inc)
(ii) (Optionally) two column susceptibility data (sample number then susceptibility)

(b) User The prompts depend on whether "ALL" type or "CRY" type

(A) Cry type
(i) File name
(ii) Volume
(iii) Type of sample no. to depth conversion
(0) Fixed size - Input subsample size
(1) Interpolation - Input sequence of sample numbers and depths e.g. 1,40 followed by 0,150 means sample 1 at 0cm, sample 40 at 150cm If (0) or (1) will attempt to read susceptibilities
(2) Known - Input name of ALL type file that already has the sample no. depth relations. Change format so that sample numbers can be read in i.e. (6F9.3).
(B) All type
(i) File name
(ii) New format. [(6F9.3)]
(C) For both there follows
(iv) Detrend 1=None, 0 gives
(0) Linear detrend
(1) Cubic spline - Input no. of knots
(v) Lake latitude
(vi) Title

OUTPUT:
(a) Screen
(i) Depends on route taken through program

(b) Files
(i) OUT3 created : Standard "ALL" files as prescribed
(ii) OUT4 created : Information about raw CRY file and OUT3

PROGRAM 1.4: DEPTHS

PURPOSE: Program to perform transform (see TRANSFORM) and output the equivalent depths of the new scale

INPUT:
(a) Files
2 column data file (new scale,old scale)

(b) User
(i) File name
(ii) Maximum depth for output file

OUTPUT:

(b) Files
OUT2 created : Equivalent depths of new scale

PROGRAM 1.5: NORMALISE

PURPOSE: Normalises the NRM intensity log using volume suceptibility ARM and SIRM data.

INPUT:
(a) Files
Adapted data files
Col 1: Sample number
Col 2: Depth (cm)
Col 3: NRM intensity
Col 4: Volume susceptibility
Col 5: ARM intensity
Col 6: SIRM intensity

(b) User
(i) File name

OUTPUT:

(b) Files
(ii) OUT2 created : Normalised version of input file suitable for plotting.

PROGRAM 1.6: TRANSFORM

PURPOSE: Performs the transform for the column 1 scale from the present scale to a new one.

INPUT:
(a) Files
(i) "ALL" type data file (depth,dec,inc,int,susc,q)
(ii) Transform file - 2 columns
Column 1 - New scale values
Column 2 - Present equivalents

(b) User
(i) All type file name
(ii) Transform file name

OUTPUT:

(b) Files
OUT2 created : All type file on new scale

A3.4.2 Smoothing

PROGRAM 2.1: BANDPASS

PURPOSE: Smooths the data using a prescribed window of years each side of a central frequency.

INPUT:
(a) Files
"ALL" type data file (time,dec,inc,int,susc,q)

(b) User
(i) File name
(ii) The central period around which smoothing to take place
(iii) The bandwidth in years
(iv) Title
(v) New bandwidth or stop

OUTPUT:

(b) Files
OUT2+ created : Standard "ALL" files smoothed as required

PROGRAM 2.2: BESTKNOTS

PURPOSE: Smooths the data using an increasing number of cubic splines. Before each smoothing it removes a percentage of the data points and then calculates what the residual is between the smoothed curve and the actual point. The root mean square residual error of all the removed points (called the Cross Validation Mean Square Error) is calculated for each data column and then plotted against the number of knots. This reveals the optimum number of knots required for smoothing.

INPUT:
(a) Files
"ALL" type data file (depth,dec,inc,int,susc,q)

(b) User
(i) File name
(ii) Lower and upper limits of data window to be smoothed
(iii) Percentage of points to be removed in cross validation
(iv) Maximum number of knots for which to calculate the CVMSE.
(v) Title

OUTPUT:

(b) Files
OUT80 created : Plot of CVMSE against number of knots for each input column

PROGRAM 2.3: CVCLOCKB (CVCLOCK)

PURPOSE: Smooths the data using a prescribed bandwidth then calculates the percentage clockwise rotation of the VGP plot. The bandwidth is left constant but the central period decreases resulting in a plot of curvature against degree of smoothing. Note that CVCLOCK uses a low pass FFT filter and increasing numbers of cubic spline knots instead of different bandwidths.

INPUT:

(a) Files
"ALL" type data file (depth,dec,inc,int,susc,q)

(b) User
(i) File name
(ii) Lower and upper limits of data window to be smoothed
(iii) Spacing of output depths if not evenly spaced
(iv) Cutoff period for calculations
(v) Two bandwidths
(vi) Site latitude and longitude
(vii) Title
(viii) New data range or stop

OUTPUT:

(b) Files
OUT2 created : The percentage curvatures for each bandwidth
OUT60 created : Plot of the two bandwidths versus frequency

PROGRAM 2.4: CSSMOOTH

PURPOSE: Smooths the data using a prescribed number of equally spaced cubic splines

INPUT:
(a) Files
"ALL" type data file (depth,dec,inc,int,susc,q)

(b) User
(i) File name
(ii) Lower and upper limits of data window to be smoothed
(iii) No. of knots
(iv) Spacing of output depths (0 = as input n = output equally spaced at n years
(v) New data range or stop

OUTPUT:

(b) Files
OUT2+ created : Standard "ALL" files smoothed as required

PROGRAM 2.5: EVENSPACE

PURPOSE: Linear interpolation of data to produce evenly spaced output

INPUT:
(a) Files
"ALL" type data file (depth,dec,inc,int,susc,q)

(b) User
(i) File name
(ii) Spacing interval

OUTPUT:
(a) Screen
New spacing interval

(b) Files
OUT2 created : Standard "ALL" file with even spacing

PROGRAM 2.6: FSMOOTH

PURPOSE: Low pass FFT based filter leaving periods greater than a user given cut off period.

INPUT:
(a) Files
"ALL" type data file (depth,dec,inc,int,susc,q)

(b) User
(i) File name
(ii) Limits of data window to be smoothed
(iii) Cutoff period (shorter periods rejected)
(iv) Spacing if not evenly spaced data

(v) Title
(vi) New range or stop

OUTPUT:

(b) Files
OUT2+ created : Smoothed data as user required

PROGRAM 2.7: MERGE

PURPOSE: Program to merge together up to 10 input files (on increasing depth/time) and average if required.

INPUT:
(a) Files
Standard "ALL" type data files

(b) User
(i) Number of input files
(ii) Limits of window over which merge will occur
(iii) File names
(iv) Range over which to consider equal (and average)

OUTPUT:

(b) Files
OUT2 created : Merged all type file (with errors in cols 7-11)

PROGRAM 2.8: STACK

PURPOSE: Stacks a number of input files after equally spacing on a common scale. Uses either gaussian or fisher statistics and can smooth or normalise over windows of the data set

INPUT:
(a) Files
All type data files (depth,dec,inc,int,susc,q)

(b) User
(i) No. of input files
(ii) Smooth option (uses a fourier low pass filter)
(iii) Stacking type (Fisher or Gaussian or with normalisation)
(iv) File names
(v) Title

OUTPUT:
(a) Screen
Mean error for each of the columns

(b) Files
OUT2 created : Extended all type file. First 6 columns as all, last five are the errors for 2-6.

A3.4.3 Magnetic mineral analysis

PROGRAM 3.1: ARMPLOT

PURPOSE: Plots diagrams of magnetisation growth or of step demagnetisation.

INPUT:
(a) Files
Up to 10 columns.
1: Field (mT or Oe)
2-10: Intensities (any units - these are normalised).

(b) User
(i) No. of samples (= No. of graphs)
(ii) No. of plots(on each graph)
(iii) Length of axes (in cm)
(iv) File names and titles

OUTPUT:
(a) Screen
Median destructive fields in mT.

(b) Files
OUT80 created : Graph(s) as directed by user

PROGRAM 3.2: COERSPECT

PURPOSE: Plots the incremental coercivity spectra for growth of ARM or IRM against increasing field.

INPUT:
(a) Files
Up to 10 data columns with growth values and the field (in mT) in col 1.
(b) User
(i) The number of samples within input file
(ii) The input file name
(iii) Axis length (in)
(iv) Titles for each column
OUTPUT:
(b) Files
OUT80 : created of incremental coercivity spectra for each column.

PROGRAM 3.3: DEMAG

PURPOSE: Plots A.F. step demagnetisation diagrams

INPUT:
(a) Files
4 columns. (Output from cryogenic CONTROL program)
1: Field (mT or Oe)
2: Intensity (any units - these are normalised).
3: Declination (^{o})
4: Inclination (^{o})

(b) User
(i) No. of graphs
(ii) Separate or same axes
(iii) Radius of primitive circle = length of axes (in inches)
(iv) Options - in any combination
Stereographic projection
Zijderveldt diagram
Step demagnetisation plot
(v) Type of line i.e. Mark points or not
(vi) File names and titles

OUTPUT:
(a) Screen
Median destructive fields in mT

(b) Files
OUT80 created : Graph(s) as directed by user

PROGRAM 3.4: IRMPLOT

PURPOSE: Plots diagrams of IRM growth and back magnetisation and includes the calculation of the coercive force (H_{cr}), the S_{100} value and an estimation of H_{sat} (defined to be the field level at which the magnetiation reaches 95% of its maximum value).

INPUT:
(a) Files
2 columns.
1: Field (mT or Oe - output converts Oe to mT)
2: SIRM Intensity (any units - these are normalised).

(b) User
(i) No. of graphs
(ii) Separate or same axes
(iii) Length of axes (in inches)
(iv) File names and titles

OUTPUT:
(a) Screen
Coercivity of remanence in mT. (if measured)

(b) Files
OUT80 created : Graph(s) as directed by user

PROGRAM 3.5: LEASTSQR

PURPOSE: Compares the linearity of demagnetisation plots with a base set of step demagnetisation results by comparing them to a straight line of gradient one.

INPUT:
(a) Files
Up to 10 columns.
1: Field (mT or Oe)
2: Base Intensity (any units - these are normalised).
3-10: Other intensities

(b) User
(i) No. of graphs
(ii) No. of plots (= no. of columns after base column)
(iii) Length of axes (in inches)
(iv) File names and titles

OUTPUT:

(b) Files
OUT80 created : Graph(s) as directed by user

PROGRAM 3.6: TBPLOT

PURPOSE: Plots diagrams of translation balance results

INPUT:
(a) Files
2 columns. (Output from Sirius program RD_TRANBAL)
1: Temperature (^{o}C)
2: Magnetisation (mV - these are normalised).

(b) User
(i) No. of graphs
(ii) Separate or same axes
(iii) Length of axes (in inches)
(iv) File names and titles

OUTPUT:

(b) Files
OUT80 created : Graph(s) as directed by user

A3.4.4 Palaeomagnetic time series analysis

PROGRAM 4.1: CORRELATE

PURPOSE: Calculates the auto and cross correlation for D,I and J

INPUT:
(a) Files
"ALL" type data file (time,dec,inc,int,susc,q)

(b) User
(i) File name (will evenly space if not so)
(ii) Limits for the data window
(iii) Title

OUTPUT:

(b) Files
OUT2 created : Lag, Autocorrelations for D,I,J
OUT3 created : Lag, Cross correlations for (I,D),(J,D),(I,J)

PROGRAM 4.2: FOURIER

PURPOSE: Calculates the fourier power spectrum for dec,inc and int and the coherence and phase spectra for the three pairs.

INPUT:
(a) Files
All type data files (depth,dec,inc,int,susc,q)

(b) User
(i) File name
(ii) Limits of window of data to be plotted
(iii) Apply a cosine taper or not
(iv) Cutoff period for plotting graph and calculating peaks
(v) Plot graphs (need type of scale and title)
(vi) New range or stop

OUTPUT:
(a) Screen
Peak periods of spectra

(b) Files
(i) OUT60 created : Spectra as described above
(ii) OUT2+ created : Spectral peaks

PROGRAM 4.3: MEM,MEMALL

PURPOSE: Calculates the MEM power spectrum for dec,inc and int and complex pair

INPUT:
(a) Files
All type data files (depth,dec,inc,int,susc,q)

(b) User
(i) File name
(ii) Limits of window of data to be plotted
(iii) MEM - Choice of which data set to perform analysis on the pef lengths are calculated automatically in the range N/2 to N/3. MEMALL - PEF length
(iv) Cutoff period for plotting and peak calculation
(v) Plot graphs (need type of scale and title)
(vi) New range or stop

OUTPUT:
(a) Screen
Updated variances

(b) Files
(i) OUT60 created : Spectra as described above
(ii) OUT2 created : Spectral peaks

A3.4.5 Modelling

PROGRAM 5.1: INTMODEL

PURPOSE: Calculates the deconvolution of an exponential fixing function from the RM data.

INPUT:
(a) Files
Standard all type data file
(b) User
(i) The input file name
(ii) The half fixing depth (or time) for the deconvolution.

OUTPUT:
(b) File OUT2 created containing the deconvolved data

PROGRAM 5.2: RDMODEL

PURPOSE: Uses drifting and/or pulsing radial dipoles in addition to a geocentric axial dipole to model secular variation. Noise can be added.

INPUT:
(a) Files
Special input file (standard format)
1: First three lines title, format and number of radial dipoles
2: For each RD model there should be one line of 7 columns
Column 1: The initial RD moment (units of earth dipole moment)
Column 2: The distance from the centre of the earth (in earth radii).
Column 3,4: The initial latitude and longitude of the RD.
Column 5: The drift rate as a time taken (in years) for one revolution
Column 6: The maximum pulse moment magnitude (in earth dipole moments)
Column 7: The pulse period in years.

(b) User
(i) File name
(ii) Observer latitude and longitude
(iii) Period of time between observations
(iv) Whether or not to add noise

OUTPUT:

(b) Files
(i) OUT2 created : "All" type output file (dec,inc,int)

PROGRAM 5.3: WAVES

PURPOSE: Sums a set of input sine waves to produce a model wave function to test spectral analysis programs.

INPUT:

(b) User
(i) For each wave. Dec and Inc period and phase
(ii) Add noise option - %age if required
(iii) Title

OUTPUT:

(b) Files
OUT1 created : Standard "all" type file (time,D,I,J,0,0)

A3.4.6 Plotting

PROGRAM 6.1: COMPLOT

PURPOSE: Program to plot the five columns from several input files next to each other in separate output files. (N.B. If the susceptibilities are predominantly zero then these and the Q ratios are not plotted).

INPUT:
(a) Files
(i) Standard "ALL" type data files
(ii) Standard scaling values file (limits for each input column)

(b) User
(i) Number of input files
(ii) Limits of window of data to be plotted
(iii) File names
(iv) Scaling file name
(v) Titles

OUTPUT:

(b) Files
OUT71+ created : Plots of columns 2+

PROGRAM 6.2: COREPLOT,COREPLOTER

PURPOSE: Plots the five columns of data in a standard "ALL" file. (with errors in COREPLOTER). (N.B. Only three columns are plotted if the suceptibilities are predominantly zero).

INPUT:

(a) Files
(i) Standard "ALL" type file (depth/time,dec,inc,int,susc,q)
(ii) Standard scaling values file (limits for each input column)

(b) User
(i) File name
(ii) Limits of data window to be plotted
(iii) File name of scaling values (iv) Type of line to be plotted, dots, line or a mixture.
(v) Title

OUTPUT:

(b) Files
OUT70 created : Plot of columns 2-6 versus column 1

PROGRAM 6.3: CURVEPLOT

PURPOSE: Plots the curvature data output from VGP and EASYVGP for up to 11 input files.

INPUT:
(a) Files
(i) All type data files (depth,dec,inc,int,susc,q)
(ii) Standard scaling values file

(b) User
(i) Number of input files
(ii) Limits of window of data to be plotted
(iii) File names
(iv) Scaling file name
(v) Titles

OUTPUT:

(b) Files
OUT70 created : Plots of the curvature for each input core

PROGRAM 6.4: EASYPLOT,PLOTTER

PURPOSE: User controlled plot of columns of data in a standard "ALL" file

INPUT:
(a) Files
(i) Standard "ALL" type file (depth/time,dec,inc,int,susc,q)
(ii) Standard scaling values file (limits for each input column)

(b) User
(i) File name
(ii) Limits of data window to be plotted
(iii) Scaling values or File name of scaling values
(iv) Size of the symbols and the plot separations
(v) Title
(vi) For each plot
    (a) Input file its from
    (b) The column to be plotted
    (c) Whether or not to plot scales
    (d) Symbol type
    (e) Colour
    (f) New frame or not
(vii) Option to plot more graphs

OUTPUT:

(b) Files
OUT70+ created : Plots as required by user

PROGRAM 6.5: EASYVGP,VGP

PURPOSE: Program to plot the VGP paths formed by time varying dec and inc values.

INPUT:
(a) Files
Standard "ALL" type data files

(b) User
(i) Site latitude and longitude
(ii) File name
(iii) Data window to be plotted
(iv) Scaling file name
(v) Title

OUTPUT:

(b) Files
(i) OUT71+ created : Plots of VGP paths
(ii) OUT2 created : summary of windows and curvature percentages
(iii) OUT3 created : curvatures **NOTE** VGP is the same except the user has more control over sizes etc.

A3.4.7 Miscellaneous

PROGRAM 7.1: ANALYSIS

PURPOSE: Program to calculate the average and standard deviation of the columns of the input file (windows the first column).

INPUT:
(a) Files
Any standard input file

(b) User
(i) File name
(ii) Number of columns to analyse (not to include first column)
(iii) Lower and upper limits of data to be analysed
(iv) Repeat or stop

OUTPUT:
(a) Screen
(i) Average, standard deviation, %age error, maximum value and minimum value of the range chosen.

PROGRAM 7.2: CHECKDATA

PURPOSE: Program to check that a "CRY" type file just received from the cryogenic has no repeats or missing values.

INPUT:
(a) Files
"Cry" type data file

(b) User
File name

OUTPUT:
(a) Screen
Sample number where any samples are missing or have errors

PROGRAM 7.3: CORENUMBER

PURPOSE: Program to sequentially number columns of data

INPUT:
(a) Files
Any standard input file

(b) User
(i) File name
(ii) Number of columns in input file
(iii) Title

OUTPUT:
(b) Files
OUT2 created - original columns of data with number beforehand

PROGRAM 7.4: WATERCNT

PURPOSE: Program to find the percentage water content in a sequence of samples.

INPUT:
(a) Files
4 column standard data file
1: Sample number
2: Depth
3: Wet weight
4: Dry weight

(b) User
(i) File name
(ii) Mass of the sample holder
(iii) Title

OUTPUT:
(b) Files
(i) OUT2 created - as input file except percentage water content in extra column and made suitable for plotting

PROGRAM 7.5: LINEFIT

PURPOSE: Program to fit a least squares straight line to a set of data

INPUT:
(a) Files
2 column data file

(b) User
File name

OUTPUT:
(a) Screen
(i) Gradient and intercept of best fitting l.s. line
(ii) Gradient and intercept for line constrained to pass through the origin.

PROGRAM 7.6: TRFIX

PURPOSE: Creates a standardised transform data file from a free format column of numbers (taken to be the present values)

INPUT:
(a) Files
Free format column of numbers

(b) User
(i) File name
(ii) New transform value corresponding to each value in input file

OUTPUT:
(a) Screen
Each present depth value in input file

(b) Files
OUT2 created : Transform data file column 1 is new scale column 2 is old

PROGRAM 7.7: XCORR

PURPOSE: Calculates the cross correlation coefficient for each column of two input files

INPUT:
(a) Files
2 "ALL" type data file (time,dec,inc,int,susc,q)

(b) User
File names

OUTPUT:
(a) Screen
Correlation coefficients for each column

Appendix 4. Calculation of the fixing function filter

If we assume that the geomagnetic field $\underline{f}(t)$ is recorded by the sediments under the influence of the fixing function defined by equations (7.1) to (7.5) to give the growth of magnetisation defined by equation (7.6) then to calculate the actual values of $\underline{f}(t)$ it is necessary to transform the convolution to the frequency domain. i.e. since

$$\underline{m}(t) = \underline{f}(t) * r(t) \qquad \text{(A4.1)}$$

where * indicates the convolution, it follows that

$$\underline{F}(\omega) = \underline{M}(\omega)/R(\omega) \qquad \text{(A4.2)}$$

if $\underline{F}(\omega)$, $\underline{M}(\omega)$ and $R(\omega)$ represent the field, the magnetisation and the fixing function in the frequency domain.

It is necessary to calculate the magnetisation frequency spectrum and divide by the frequency response of the fixing function. This is a simple filtering process in the frequency domain. To perform the calculation the Fourier transform has been used to the frequency domain, so the transform of the filter is required.

From equations (7.1)-(7.3) we have that

$$\int_0^\infty Ce^{-At}\,dt = [-C/Ae^{-At}]_0^\infty = 1 \qquad \text{(A4.3)}$$

so that C = A.

If we redefine t_1, the time after which half the magnetisation is fixed, to be $T_{0.5}$ then performing the integration of equation (7.4) gives

$$0.5 = [-A/Ae^{-At}]^\infty_{T0.5} = \exp(-AT_{0.5}) \qquad \text{(A4.4)}$$

so that $A = -\ln(0.5)/T_{0.5} = \ln 2 / T_{0.5}$.

We have thus calculated the moment fixing function to be

$$r(t) = \ln 2 \,/\, T_{0.5} \exp\,[-(\ln 2/T_{0.5})t] \qquad \text{(A4.5)}$$

The next stage is to calculate the Fourier transform. In general the Fourier transform $\underline{F}(\omega)$ of a time series $\underline{f}(t)$ is given by

$$\underline{F}(\omega) = {}_{-\infty}\int^{\infty} \underline{f}(t) \exp(-i\omega t)\, dt \qquad \text{(A4.6)}$$

so that the transform of the fixing function is

$$\underline{R}(\omega) = {}_{0}\int^{\infty} A \exp[-(A + i\omega)t]\, dt$$

$$= [-(A/(A + i\omega)) \exp-(A + i\omega)t]_0^{\infty}$$

$$= A \,/\, (A + i\omega) \qquad \text{(A4.7)}$$

This has to be separted into real and imaginary parts for the purposes of computation which gives

$$\underline{R}(\omega) = (A^2 - iA\omega)/(A^2 + \omega^2) \qquad \text{(A4.8)}$$

This means that the amplitude spectrum is given by the modulus of R

$$|R| = \surd[(A^2)^2 + (A\omega)^2](A^2 + \omega^2)$$

$$= A \,/\, \surd(A^2 + \omega^2) \qquad \text{(A4.9)}$$

and the phase spectrum by

$$\Phi(\omega) = -\tan^{-1}(\omega/A) \qquad \text{(A4.8)}$$

which by substituting for ω and A are the expressions given by equations (7.9) and (7.10).

Figure A4.1 shows the amplification and phase spectra for varying values of $T_{0.5}/T$. Note that the amplitude is rapidly reduced as the period decreases. This indicates that the short period features of the field are going to be severely modulated whilst the long period features will remain almost unchanged. The difference between 'short period' and 'long period' variations will also depend on

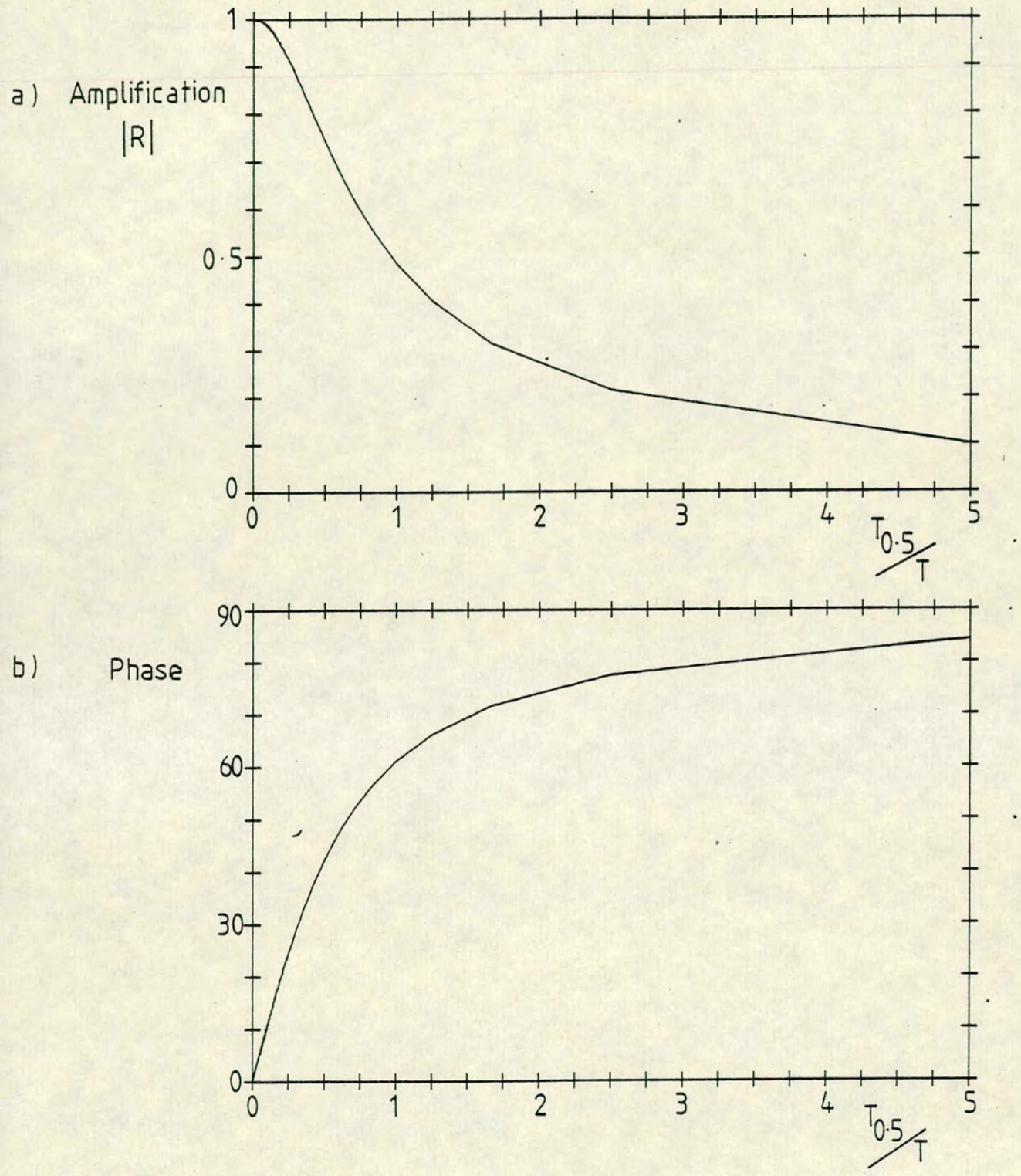

Figure A4.1 The response of the exponential fixing function in the frequency domain. As T decreases the amplification decreases and the phase increases.

the half fixing time $T_{0.5}$ since, as can be seen from **figure A4.1a**, it is the ratio between the spectral period and the half fixing period that is important. **Figure A4.1b** shows how the declination and inclination will be modulated. The signals will have a phase lag introduced that increases rapidly as the $T_{0.5}/T$ ratio increases.

APPENDIX 5. The cryogenic control program.

The control program is listed in part in the following pages. Due to the restriction of space not all the parts are listed. The routines not included are the system routines from "SS_CONSOLE" and "SCREENOPS" which control aspects of the keyboard and screen and the procedure from the "XTALK" unit. The latter controls the conversion of the Sirius to a terminal and has been adapted for use from the ERCC program called "TTY" and explained in their "XTALK" literature. For use within the framework of this program the ERCC version has been segmented and the number of facilities have been reduced.

The program is in six sections. The first section is the control file which is compiled. It contains calls for the compiler to include the four files of subroutines, which it also compiles, and to link pre-compiled units found in the system library and a user library called "GENERAL". This user library is also listed and has been created for frequently used routines. The units reside in library files; the system units in SYSTEM.LIBRARY and my units in GRAEMELIB.CODE (which also includes the assembler code routines). After compilation the program must be 'L'inked to these libraries.

Note that the UCSD system uses "segment" procedures which are stored on disc until required. This means that the whole program can be larger than the available memory as long as the procedures are not stacked in such a way that several are loaded at once. Those procedures prefixed by "SEGMENT" are of this type and are only loaded when called.

The main control routine is the GET COMMAND procedure that reads the user input and calls the appropriate routine. Each routine is named in such a way that it's function is obvious (hopefully).

After the program has been compiled the code file has been renamed SYSTEM.MENU. This filename is the system name for a file that is executed immediately after the operating system has been loaded. This means that the disc ("CRYOGEN") can be inserted into the Sirius and the program will run automatically without further user intervention. This, along with the fact that no files can be written to this disc, prevents any unintentional wiping of important files upon the disc. File security is the most important problem of these type of multi-user microcomputer programs.

```
{------------------------------------------------------------------------------}
{                                                                              }
                              PROGRAM CONTROL;
{                                                                              }
{                      (**** CRYOGENIC CONTROL PROGRAM ****)                   }
{                                                                              }
{                              (**** OCT 1984 ****)                            }
{                                                                              }
{------------------------------------------------------------------------------}
{                                                                              }
{                                                                              }
{     Program to control the 2-axis cryogenic magnetometer performing          }
{     both the sample movement and measurement. Note that the output           }
{     file is a user defined disc resident file which can be Transfered        }
{     to the main frame computer if required. All commands are called by       }
{     single keystrokes from the general purpose routine GET_COMMAND. All      }
{     SEGMENT routines are disc resident until called and are held in 3        }
{     "include" files CONTROL_S1, CONTROL_S2 and CONTROL_S3. The other         }
{     routines are held in CONTROL_R1.                                         }
{                                                 Graeme Smith Oct 1984.       }
{                                                                              }
{------------------------------------------------------------------------------}

                              (**** UNITS ****)

   USES  SCREENOPS,SS_CONSOLE,
         (*$U GRAEMELIB.CODE *) XTALK,GENERAL;
                                              {Independently compiled units}

{------------------------------------------------------------------------------}

{ These contain the following routines

            Screenops          a) SC_CLR_SCREEN

            SS_Console         b) SS_FNLABEL
                               c) SS_FNKEYGEN

            XTalk              d) TTY

            General            e) GET_IPFILENAME
                               f) GET_OPFILENAME
                               g) PROMPT
                               h) PAUSE
                               i) HELP
                               j) SAFE_OPEN                                    }
{------------------------------------------------------------------------------}

                           (**** CONSTANTS ****)

   CONST   GAIN_1     = 0;
           GAIN_10    = 32;
           GAIN_100   = 64;                { ADC Gain Binary equivalents }
           GAIN_1000  = 128;

           HI_TO_LO   = 100;          { Transition value for stopping carriage }

{------------------------------------------------------------------------------}

                              (**** TYPES ****)
```

```
TYPE    SMALL_ARRAY = PACKED ARRAY [1..3] OF REAL;
        LARGE_ARRAY = PACKED ARRAY [1..6] OF INTEGER;
        SIX_SMALLS  = PACKED ARRAY [1..6] OF SMALL_ARRAY;

        NAME_REC    =  RECORD
                        PREFIX,SUFFIX : STRING;
                        NUMBER,INC    : INTEGER;
                       END;

        RESULT_REC  = RECORD
                       SAMPLE         : STRING;
                       INTENSITY,
                       DECLINATION,
                       INCLINATION,
                       ERROR,
                       NORTH,
                       EAST,
                       DOWN           : REAL;
                      END;

        RESULT_ARR  = PACKED ARRAY [1..50] OF RESULT_REC;

        SUBSET      = SET OF CHAR;

{-------------------------------------------------------------------------------}

                        (**** VARIABLES ****)

  VAR   (* Arrays and Records *)

      CALS                              : SMALL_ARRAY; {Squid calibrations}
      VOLTS                             : SMALL_ARRAY; {Voltage readings}
      HOLDER                            : SMALL_ARRAY; {Holder magnetisation}
      THE_RESULTS                       : RESULT_ARR;  {The results}
      MEANS                             : SIX_SMALLS;  {Means for 4 positions}
      ALL_VOLTS                         : SIX_SMALLS;  {6 Measures of Volts}
      POSITION                          : LARGE_ARRAY; {Sample position}
      NAME                              : NAME_REC;    {Name for auto name}

        (* Integer Variables *)

      I,J,K                             : INTEGER;     {Increment counters}
      MESSES                            : INTEGER;     {Measurement no.}
      POSN                              : INTEGER;     {Sample position counter}
      INSERT                            : INTEGER;     {Special position}
      ADC_READS                         : INTEGER;     {No. of ADC conversions}
      AXIAL_A,AXIAL_B                   : INTEGER;     {ADC integers (for sum)}
      HORIZ_A,HORIZ_B                   : INTEGER;     {ADC sum}
      GAIN,GAIN_ADC,CHANNEL             : INTEGER;     {Gain,channel of ADC}
      GAIN_AMP                          : INTEGER;     {Gain of amplifier box}
      NO_OF_RESULTS                     : INTEGER;     {No. of results on disc}
      TOTAL_RES                         : INTEGER;     {No. of results to date}

        (* Character, String and Text Variables *)

      IP_TEXT,OP_TEXT,P_TEXT            : TEXT;        {I/P,O/P files}
      CH                                : CHAR;        {Prompt test char}
      C1,C2,C3,C4,C5,C6,C7              : CHAR;        {Used for function keys}
      S1,S2,S3,S4,S5,S6,S7              : STRING[10];  {Ditto}
```

```
        STG                                 : STRING;       {Temp variable}
        HELPS,KEYS                          : STRING;       {Info file names}
        IPFILE,OPFILE                       : STRING;       {File names}
        SAMP_NAME,OSAMP_NAME                : STRING;       {(Old) Sample name}

          (* Real Variables *)

        FACTOR,ZERO                         : REAL;         {Conversion ADC->Volts}
        INT,DEC,INC,ERROR                   : REAL;         {Results for pres read}
        OLD_INT,OLD_DEC,OLD_INC,OLD_ERR     : REAL;         {Results of prev read}
        VOLUME                              : REAL;         {Sample volume}
        OV1,OV2,OV3                         : REAL;         {Previous volts res}
        SUMSQ                               : REAL;         {Temp error variables}

          (* Boolean Variables *)

        AUTO_NAME,PRINT                     : BOOLEAN;      {Auto & hard copy tests}
        GAIN_UP,GAIN_DOWN,BELL              : BOOLEAN;      {Change gain tests}
        ADC_SATURATED,CALCULATED            : BOOLEAN;      {Satn/calcs checks}
        VOLTS_OUT                           : BOOLEAN;      {Output of volts check}
        QUANTUM_JUMP,REMOVE_HOLDER          : BOOLEAN;      {Background check}
        NO_GAIN_CHANGES                     : BOOLEAN;      {Gain stick option}
        HORIZ_OUT,AXIAL_OUT                 : BOOLEAN;      {Single squid check}

{-------------------------------------------------------------------------------}

                    (**** FORWARD DECLARATIONS ****)

 (* EXTERNAL *)

 PROCEDURE WARNPORT (VAR GAINCH:INTEGER); FORWARD;
 PROCEDURE READ_ADC (VAR DATA,GAINCH:INTEGER); FORWARD;
 PROCEDURE MOVE (VAR J:INTEGER); FORWARD;
 PROCEDURE GET_READING (VAR GAIN,R1,R2,R3,R4,NO_READS:INTEGER);FORWARD;

 (* ROUTINES 1 *)

 PROCEDURE MOVE_MEASURE; FORWARD;
 PROCEDURE RESULTS (VAR RSTG,RNAME:STRING;RINT,RDEC,RINC,RERR,
                                          RV1,RV2,RV3:REAL);FORWARD;
 PROCEDURE PRINT_RESULTS; FORWARD;
 PROCEDURE GET_NAME; FORWARD;
 PROCEDURE MAKE_MEASUREMENT; FORWARD;

 (* SEGMENTS *)

 SEGMENT PROCEDURE CALC_MAGNETIC_VECTOR; FORWARD;
 SEGMENT PROCEDURE CALC_NEW_VECTOR; FORWARD;
 SEGMENT PROCEDURE CHANGE_ADC_GAIN; FORWARD;


{-------------------------------------------------------------------------------}

       {$I CONTROL_S1.TEXT}      {Segment procedures in separate file}

{-------------------------------------------------------------------------------}


                    (**** SEGMENT ROUTINES 1 ****)
```

```
   (* Contains the following procedures

            a) GET_NEW_ADC_READS
            b) SET_YES_NO
            c) PROMPT_KEYS_FOR_SQUIDS
            d) NEW_VOLUME
            e) SQUID_FAILURE
            f) OUTPUT_DATA
            g) REPEAT_MEASUREMENTS
            h) SQUID_CALIBRATION
            i) SAVE_RESULTS
            j) CHANGE_FILES
                                                              *)

{-------------------------------------------------------------------------------}

      {$I CONTROL_S2.TEXT}     {Segment procedures in separate file}

{-------------------------------------------------------------------------------}

                    (**** SEGMENT ROUTINES 2 ****)

   (* Contains the following procedures

            a) SET_AUTONAME
            b) SETUP_CALS
            c) CHANGE_AMPLIFIER_GAIN
            d) CHANGE_ADC_GAIN
            e) CHECK_ADC_GAIN
            f) NEW_GAINS
            g) LAST_RESULTS
            h) CALC_HOLDER_MAGNETISATION
                                                              *)

{-------------------------------------------------------------------------------}

      {$I CONTROL_S3.TEXT}     {Segment procedures in separate file}

{-------------------------------------------------------------------------------}

                    (**** SEGMENT ROUTINES 3 ****)

   (* Contains the following procedures

            a) CALC_MAGNETIC_VECTOR
            b) CALC_NEW_VECTOR
            c) INITIALISE
                                                              *)

{-------------------------------------------------------------------------------}

              (**** ASSEMBLER LANGUAGE PROCEDURES ****)

PROCEDURE MOVE ;EXTERNAL;
```

```
 PROCEDURE WARNPORT ;EXTERNAL;
 PROCEDURE READ_ADC ; EXTERNAL;
 PROCEDURE GET_READING ;EXTERNAL;

{-------------------------------------------------------------------------------}

       {$I CONTROL_R1.TEXT}     {Procedures in separate file}

{-------------------------------------------------------------------------------}


                     (**** GENERAL ROUTINES 1 ****)


   (* Contains the following procedures

              a) RESULTS
              b) PRINT_RESULTS
              c) WAIT_FOR_STOP
              d) GET_NAME
              e) CALC_MEAN
              f) CHECK_BACKGROUND
              g) MOVE_MEASURE
              h) CALC_MAGNETIC_VECTOR
              i) DEF_COMMAND_KEYS
              j) MAKE_MEASUREMENT
              k) GET_COMMAND

                                              August 1984 *)


{-------------------------------------------------------------------------------}

                          (*** CONTROL ***)

{-------------------------------------------------------------------------------}

BEGIN
  INITIALISE;
  GET_COMMAND;
END.
```

```
{-------------------------------------------------------------------------------}

                    (**** SEGMENT ROUTINES 1 ****)


   (* Contains the following procedures

            a) SET_YES_NO
            b) PROMPT_KEYS_FOR_SQUIDS
            c) GET_NEW_ADC_READS
            d) NEW_VOLUME
            e) SQUID_FAILURE
            f) OUTPUT_DATA
            g) REPEAT_MEASUREMENT
            h) SETUP_CALS
            i) SQUID_CALIBRATION
            j) SAVE_RESULTS
            k) CHANGE_FILES
                                                 August 1984 *)

{-------------------------------------------------------------------------------}

 SEGMENT PROCEDURE SET_YES_NO;  {Generate function keys for yes & no}

    BEGIN
      C1:='Y';   C2:='N';
      S3:='';
      S1:='   Y(es  ';
      S2:='    N(o  ';
      SS_FNLABEL (S1,S2,S3,S3,S3,S3,S3);
      SS_FNKEYGEN (FALSE,c1,c2,c3,c3,c3,c3,c3);
    END; {of Set_Yes_No}

{-------------------------------------------------------------------------------}

 SEGMENT PROCEDURE PROMPT_KEYS_FOR_SQUIDS;

  BEGIN
    C1:='E';   C2:='A';   C3:='H';   C6:='I';  C7:='?';
    S5:='';
    S1:='  E(xit  ';
    S2:='  A(xial ';
    S3:='  H(oriz ';
    S4:='';
    S6:='  I(nfo  ';
    S7:='   HELP  ';
    SS_FNLABEL (S1,S2,S3,S4,S4,S6,S7);
    SS_FNKEYGEN (FALSE,c1,c2,c3,c1,c1,c6,c7);
  END; {of Prompt_keys_for_Squids}

{-------------------------------------------------------------------------------}

  SEGMENT PROCEDURE GET_NEW_ADC_READS;

    BEGIN
      SET_YES_NO;
      WRITE ('Performing ');
      WRITELN (ADC_READS,' conversions per channel per measurement.');
      REPEAT
```

```
        WRITE ('New number of conversions:');
        READ_INTEGER (ADC_READS);
        WRITELN ('Will now perform ',ADC_READS,' conversions.');
        CH := PROMPT ('O.K.?',['Y','N']);
      UNTIL CH = 'Y';
    END; {of Get_New_ADC_Reads}

{-------------------------------------------------------------------------}

 SEGMENT PROCEDURE NEW_VOLUME;

  BEGIN
   SET_YES_NO;
   WRITELN ('Volume = ',VOLUME:6:3,' ccs');
   REPEAT
    WRITE ('Give new volume (ccs):');
    READ_REAL (VOLUME);
    WRITELN ('Volume = ',VOLUME:6:3,' ccs');
    CH := PROMPT ('O.K.?',['Y','N']);
   UNTIL CH = 'Y';
  END; {of New_Volume}

{-------------------------------------------------------------------------}

 SEGMENT PROCEDURE SQUID_FAILURE;

  BEGIN
   PROMPT_KEYS_FOR_SQUIDS;
   CH := PROMPT ('Axial or Horiz squid failure ?',['E','A','H']);

   CASE CH OF

   'A' : BEGIN
          AXIAL_OUT := NOT AXIAL_OUT;
          IF AXIAL_OUT THEN WRITE ('Axial squid off. At least 3');
         END;

   'H' : BEGIN
          HORIZ_OUT := NOT HORIZ_OUT;
          IF HORIZ_OUT THEN WRITE ('Horizontal squid off. 3 or 6');
         END;

  END;
  IF AXIAL_OUT OR HORIZ_OUT THEN
       WRITELN (' measurements per reading now needed.')
  ELSE WRITELN ('Both squids working.');

 END; {of Squid_Failure}

{-------------------------------------------------------------------------}

 SEGMENT PROCEDURE OUTPUT_DATA;  {Outputs program variable info}

  VAR TEMP : STRING;

  BEGIN
    SC_CLR_SCREEN;

    {Last measurement}
```

```
WRITELN; WRITE ('SQUID   BGD1(mV)   270(V)     0(V)    90(V)');
WRITELN ('   180(V)  BGD2(mV)'); WRITELN;

WRITE   ('HORIZ  ');
FOR POSN := 1 TO 6 DO
 BEGIN
  IF (POSN<>1) AND (POSN<>6) THEN WRITE (MEANS[POSN,1]:8:3,' ')
                             ELSE WRITE (1000.0*MEANS[POSN,1]:8:3,' ');
 END;
WRITELN;

WRITE   ('AXIAL  ');
FOR POSN := 1 TO 6 DO
 BEGIN
  IF (POSN<>1) AND (POSN<>6) THEN WRITE (MEANS[POSN,2]:8:3,' ')
                             ELSE WRITE (1000.0*MEANS[POSN,2]:8:3,' ');
 END;
WRITELN;

WRITELN;
WRITELN('N = ',VOLTS[1]:9:3,' E = ',VOLTS[2]:9:3,' Z = ',VOLTS[3]:9:3);

{Squid calibrations and Holder Magnetisation}

WRITELN;
FOR I:= 1 TO 3 DO WRITELN (CHR(87+I),' CALIB = ',CALS[I]:8:3,
                           '         HOLDER = ',HOLDER[I]:10:6);
WRITELN;

{File and sample}

WRITELN ('Output file is ',OPFILE,'. ',
                           TOTAL_RES,' measurements are in it');
WRITE ('The present sample is ',SAMP_NAME,' measurement number ',MESSES);
IF AUTO_NAME THEN TEMP := 'on' ELSE TEMP := 'off';
WRITELN ('. Auto naming is ',TEMP,'.');
IF NO_OF_RESULTS >= 1 THEN
WRITELN ('The earliest alterable result is for ',THE_RESULTS[1].SAMPLE);
WRITELN;

{Booleans}

IF BELL THEN TEMP := 'on' ELSE TEMP := 'off';
WRITE ('The bell is ',TEMP);
IF PRINT THEN TEMP := 'on' ELSE TEMP := 'off';
WRITE (', the printer is ',TEMP);
IF VOLTS_OUT THEN TEMP := 'are' ELSE TEMP := 'are not';
WRITELN (' and the components ',TEMP,' being printed.');
IF REMOVE_HOLDER THEN TEMP := 'is' ELSE TEMP := 'is not';
WRITELN ('The holder magnetisation ',TEMP,' being removed.');
IF AXIAL_OUT THEN TEMP := 'The axial squid is not working.'
ELSE IF HORIZ_OUT THEN TEMP := 'The horizontal squid is not working.'
ELSE TEMP := 'Both the squids are working.';
WRITELN (TEMP);

{Gains}

WRITELN;
WRITE ('ADC gain is ',GAIN_ADC,' with ',ADC_READS,' conversions.');
IF NO_GAIN_CHANGES THEN TEMP := 'off' ELSE TEMP := 'on';
```

```
    WRITELN (' Auto ranging is ',TEMP,'.');
    WRITELN ('Amplifier gain should be set at ',GAIN_AMP);
    WRITELN ('The sample volume is ',VOLUME:6:3,'ccs.');
    WRITELN;

    PAUSE;

  END; {of Output_Data}

{-------------------------------------------------------------------------------}


 SEGMENT PROCEDURE REPEAT_MEASUREMENT;

  VAR J,K : INTEGER;
      T_NAME : STRING;

  BEGIN
   SET_YES_NO;
   WRITELN ('Repeat Measurement - Same sample, same orientation [1]');
   WRITELN ('                     Same sample, new orientation  [2]');
   WRITELN ('                     Previously measured sample    [3]');
   CH := PROMPT ('Which? [1,2 or 3]:',['1','2','3']);
   IF (CH <> '3') AND (MESSES = 0) THEN
     BEGIN
      WRITELN (CHR(7),'No measurements have been made!');
      EXIT (REPEAT_MEASUREMENT);
     END;
   CASE CH OF
    '1': BEGIN
          MAKE_MEASUREMENT;
          EXIT (REPEAT_MEASUREMENT);
         END;

    '2': BEGIN
          WRITE ('Present orientation = ',MESSES,' give new orientation:');
          K := MESSES;
          READ_INTEGER (MESSES);
          MAKE_MEASUREMENT;
          CH := PROMPT ('Continue from this orientation?',['Y','N']);
          IF CH = 'N' THEN MESSES := K;
          EXIT (REPEAT_MEASUREMENT);
         END;

    '3': BEGIN
          T_NAME := SAMP_NAME;
          SC_CLR_SCREEN;
          WRITELN;
          I := 0;
          REPEAT
            I := I + 1;
            WRITE ('        ',I:2,'  ',THE_RESULTS[I].SAMPLE,'    ');
            I := I + 1;
            IF (I<> NO_OF_RESULTS+1) THEN WRITELN ('          ',I:2,'  ',
                                                   THE_RESULTS[I].SAMPLE)
                                     ELSE WRITELN;
          UNTIL I >= NO_OF_RESULTS;
          WRITE ('Give sample number to be repeated [0=None]:');
          READ_INTEGER (K);
```

```
        IF (K <= 0) OR (K > NO_OF_RESULTS) THEN EXIT (REPEAT_MEASUREMENT);

        WRITE ('Sample name :');
        READLN (SAMP_NAME);

        J := NO_OF_RESULTS;
        NO_OF_RESULTS := K;

        MESSES := 0;
        REPEAT
         MESSES := MESSES + 1;
         MAKE_MEASUREMENT;
         IF MESSES<>6 THEN CH := PROMPT ('Continue ?',['Y','N']);
        UNTIL (CH = 'N') OR (MESSES = 6);

        IF (MESSES<>1) AND (MESSES<>5) THEN CALC_NEW_VECTOR;

        CH := PROMPT ('Save this result instead of former?',['Y','N']);
        IF CH = 'Y' THEN
         BEGIN
          TOTAL_RES := TOTAL_RES - 1;
          PRINT_RESULTS;
         END;
        NO_OF_RESULTS := J;
        EXIT (REPEAT_MEASUREMENT);
       END;

    END;
 END; {of Repeat_measurement}

{-------------------------------------------------------------------------}

 SEGMENT PROCEDURE SETUP_CALS ;  {Write in change to squid calibrations}

  VAR CH1:CHAR;
      DATE,TIME:STRING;

  BEGIN
    PROMPT_KEYS_FOR_SQUIDS;
    REPEAT
      SC_CLR_SCREEN;
      FOR I:= 1 TO 5 DO WRITELN;
      WRITELN ('   Present calibrations');WRITELN;
      WRITELN (' Horiz = ',CALS[1]:9:4);
      WRITELN (' Axial = ',CALS[3]:9:4);
      WRITELN;
      CH1:=PROMPT('Change Horiz or Axial -- Which ("E" TO EXIT) ? '
                                              ,['E','A','H','?']);
      IF (CH1<>'E') AND (CH1<>'?') THEN WRITE ('New value :');
      CASE CH1 OF
       'H':READ_REAL (CALS[1]);
       'A':READ_REAL (CALS[3]);
       '?':HELP (HELPS);
       'E':WRITELN ('Calibrations complete');
      END;
      CALS[2] := CALS[1];
    UNTIL CH1 = 'E';
    SET_YES_NO;

    CH1 := PROMPT('Save calibration values ?',['Y','N']);
```

```
    IF (CH1 = 'N') THEN EXIT (SETUP_CALS)
    ELSE
     BEGIN
      REPEAT
        WRITE ('Give time : ');
        READLN (TIME);
        WRITE ('Give Date : ');
        READLN (DATE);
        WRITELN ('It is ',TIME,' on ',DATE);
        CH:= PROMPT ('Is this correct? ',['Y','N']);
      UNTIL CH = 'Y';

      FOR I:= 1 TO 5 DO WRITELN(P_TEXT);
      WRITELN (P_TEXT,'Calibrations at ',TIME,' on ',DATE);WRITELN (P_TEXT);
      WRITELN (P_TEXT);
      WRITELN (P_TEXT,' Horiz = ',CALS[1]:9:4);
      WRITELN (P_TEXT,' Axial = ',CALS[3]:9:4);
      FOR I:= 1 TO 5 DO WRITELN(P_TEXT);

    END;

  END; {of Setup_Cals}

{-------------------------------------------------------------------------}

SEGMENT PROCEDURE SQUID_CALIBRATION; {Calibrates squids using a
                                      coil or standard sample}
 VAR SCAL : ARRAY [1..3] OF REAL;
     CALIBS : ARRAY [1..2] OF REAL;
     NUMBER_TO_AV : ARRAY [1..2] OF INTEGER;

 PROCEDURE GET_SQUID_CALIB;

 CONST PI = 3.1415926;

 VAR RADIUS, MOMENT, SAVED_MOMENT : REAL;
     AV_CALIB, CURRENT, CALIB : REAL;
     TURNS, CHAN    :INTEGER;
     COIL,STD : BOOLEAN;

 BEGIN
  SET_YES_NO;
  SC_CLR_SCREEN;
  STD := FALSE;
  COIL := FALSE;
  FOR I:= 1 TO 5 DO WRITELN;
  FOR I:= 1 TO 3 DO SCAL[I] := CALS[I];
  FOR I:= 1 TO 3 DO CALS[I] := 1;
  CH := PROMPT ('Are you using a coil ?',['Y','N']);
  IF CH = 'N' THEN STD := TRUE ELSE
    BEGIN
     COIL := TRUE;
     WRITE ('No. of turns :');
     READ_INTEGER (TURNS);
     WRITE ('Radius (cm) :');
     READ_REAL (RADIUS);
     MOMENT := 0.1 * PI * TURNS  * SQR(RADIUS);
     SAVED_MOMENT := MOMENT;
    END;
```

```
FOR I:= 1 TO 2 DO
 BEGIN
  NUMBER_TO_AV[I] := 0;
  CALIBS[I] := 0;
 END;

REPEAT
  PROMPT_KEYS_FOR_SQUIDS;
  MOMENT := SAVED_MOMENT;
  SCAL[2] := SCAL[1];
  SC_CLR_SCREEN;
  FOR I:= 1 TO 5 DO WRITELN;
  CH := PROMPT ('Which axis is being calibrated [Axial or Horiz] ? ',
                                                  ['A','H','E','I','?']);
  CASE CH OF
   '?' : HELP (HELPS);
   'H' : CHAN:= 1;
   'A' : CHAN:= 3;
   'I' : OUTPUT_DATA;
   'E' : EXIT (GET_SQUID_CALIB);
  END;
  IF (CH<>'?') AND (CH<>'I') THEN
   BEGIN
    WRITELN ('Prepare calibration standard');
    PAUSE;
    ADC_SATURATED := FALSE;
    CALCULATED := FALSE;
    MOVE_MEASURE;
    IF BELL THEN WRITE (CHR(7));
    WRITE ('*** CAL *** ');
    WRITELN(' INT = ',INT:9:3,' DEC = ',DEC:9:3,
                              ' INC = ',INC:9:3,' ERR =',ERROR:4:1);

    IF ADC_SATURATED THEN
       WRITELN (CHR(7),'**--WARNING - ADC saturated. Recalibrate--**');
    IF (GAIN_UP) OR (GAIN_DOWN) THEN CHANGE_ADC_GAIN;

    IF NOT ADC_SATURATED THEN

     BEGIN
      IF COIL THEN
       BEGIN
        WRITE ('Give the value of the current (mA):');
        READ_REAL (CURRENT);
        MOMENT := MOMENT * CURRENT;
        WRITE (TURNS,' turn coil on a former of radius ',RADIUS:6:3);
        WRITELN (' cm with a ',CURRENT:7:5,' mA current.');
       END
      ELSE
       BEGIN
        WRITE ('Give the moment of sample ( mA.turns.m@):');
        READ_REAL (MOMENT);
       END;

       {Assumes calibration coil of TURNS turns wound on a non conducting
       former of radius RADIUS. The calibration factor will convert the
       output voltage to an intensity of magnetisation given in A/m if the
       volume is given in ccs. Note the write in calibration option
       allows the actual output to be scaled up or down by the user.}
```

```
        CALIB := MOMENT/VOLTS[CHAN];   {Calibration factor = 1/Sensitivity}

        WRITELN('The magnetic moment is ',MOMENT:9:3,' mA.turns.m@');
        WRITELN('therefore the calibration is ',CALIB:9:3,' mA.turns.m@/V.');

        SET_YES_NO;
        CH := PROMPT ('Use this value in the average calibration ? ',
                                                        ['Y','N']);
        IF CH = 'Y' THEN
         BEGIN
          IF CHAN = 3 THEN CHAN := 2;
          NUMBER_TO_AV[CHAN] := NUMBER_TO_AV[CHAN] + 1;
          CALIBS[CHAN] := CALIBS[CHAN] + CALIB;
          AV_CALIB := CALIBS[CHAN]/NUMBER_TO_AV[CHAN];
          IF NUMBER_TO_AV[CHAN] <> 1 THEN
          BEGIN
           WRITE ('New average calibration is ',AV_CALIB:9:3,' mA.turns.m@/V.');
           WRITELN (' using ',NUMBER_TO_AV[CHAN], ' measurements.');
          END;
         END;

        IF CHAN = 2 THEN CHAN := 3;
        SCAL[CHAN] := AV_CALIB;
       END;
      PAUSE;

     END;

  UNTIL FALSE;

 END; {of Get_Squid_Calib}

 BEGIN
  GET_SQUID_CALIB;
  FOR I:= 1 TO 3 DO CALS[I] := SCAL[I];
  SETUP_CALS;
 END; {of Squid_Calibration}

{-------------------------------------------------------------------------------}

 SEGMENT PROCEDURE SAVE_RESULTS (NO_SAVED:INTEGER);

  BEGIN
   WRITELN ('Writing results to ',OPFILE);
   FOR I:= 1 TO NO_SAVED DO
    BEGIN
     WITH THE_RESULTS[I] DO
      BEGIN
       WRITE ('.');
       IF I = 25 THEN WRITELN;
       WRITELN (OP_TEXT,'  ',SAMPLE,'  INT = ',INTENSITY:9:3,
                                  '  DEC = ',DECLINATION:9:3,
                                  '  INC = ',INCLINATION:9:3,
                                  '  ERR = ',ERROR:4:1);
       IF VOLTS_OUT THEN
        BEGIN
         FOR J := 1 TO LENGTH(SAMPLE)+2 DO WRITE (OP_TEXT,' ');
         WRITELN (OP_TEXT,'    N  = ',NORTH:9:3,
                          '    E  = ',EAST:9:3,
```

```
                              '   Z  = ',DOWN:9:3);
        END;
      END;
    END;
   WRITELN;
   WRITELN (NO_SAVED,' results written, so ',TOTAL_RES, ' are saved on disc.');
   NO_OF_RESULTS := 0;
  END;


{-------------------------------------------------------------------------}

 SEGMENT PROCEDURE CHANGE_FILES;  {Closes output file then gets new one}

   VAR ST : STRING;

   BEGIN
    SET_YES_NO;
    IF OPFILE <> '' THEN
      BEGIN
       SAVE_RESULTS (NO_OF_RESULTS);
       WRITELN (OP_TEXT);
       CLOSE (OP_TEXT,LOCK);
       FOR I:= 1 TO 10 DO WRITELN (P_TEXT);
       WRITELN (OPFILE, ' closed and saved.');WRITELN;
       CH := PROMPT ('Transfer results to mainframe?',['Y','N']);
       IF CH = 'Y' THEN
        BEGIN
         TTY;
         SET_YES_NO;
        END;
       TOTAL_RES := 0;
      END;

    SC_CLR_SCREEN;
    FOR I:= 1 TO 5 DO WRITELN;

    SAFE_OPEN (OP_TEXT,OP_FILE,FALSE);
    CH := PROMPT ('Do you want to insert a heading ?',['Y','N']);
    IF CH = 'Y' THEN
     BEGIN
      STG := '';
      WRITELN ('Input ":" after prompt to stop');
      REPEAT
       WRITELN (OP_TEXT,STG);
       WRITELN (P_TEXT,STG);
       WRITE ('Text:');
       READLN (STG);
      UNTIL POS (':',STG)=1;
     END;
    IPFILE := CONCAT ('Do you want ',opfile,' to include old files ?');
    CH := PROMPT (IPFILE,['Y','N']);
    IF CH = 'N' THEN EXIT (CHANGE_FILES);
    WRITE ('How many ? ');
    READ_INTEGER (J);
    FOR K:= 1 TO J DO
      BEGIN
        SAFE_OPEN(IP_TEXT,IP_FILE,TRUE);
        WRITELN ('Reading ',IPFILE);
        WHILE NOT EOF (IP_TEXT) DO
```

```
        BEGIN
          READLN (IP_TEXT,ST);
          WRITELN (OP_TEXT,ST);
        END;
      CLOSE (IP_TEXT,LOCK);
    END;
END; {of Change_Files}
```

```
{-------------------------------------------------------------------------}

                    (**** SEGMENT ROUTINES 2 ****)


  (* Contains the following procedures

           a) SET_AUTONAME
           b) CHANGE_AMPLIFIER_GAIN
           c) CHANGE_ADC_GAIN
           d) CHECK_ADC_GAIN
           e) NEW_GAINS
           f) LAST_RESULTS
           g) CALC_HOLDER_MAGNETISATION
                                        October 1984 *)

{-------------------------------------------------------------------------}


SEGMENT PROCEDURE SET_AUTONAME;  {Automatic sample name generator}

  VAR TEMP:STRING[4];
      ST  :STRING;

  BEGIN
    C1 := 'S';  C2 := 'P';  C3 := 'N';  C4 := 'I';  C5 := 'E';  C6 := 'H';
    S1 := ' S(uffix ';                  S2 := ' P(refix ';
    S3 := ' N(umber ';                  S4 := 'I(ncrement';
    S5 := '  E(xit  ';                  S6 := '  H(elp  ';
    S7 := '';
    SS_FNLABEL (S5,S2,S3,S4,S1,S7,S6);
    SS_FNKEYGEN (FALSE,C5,C2,C3,C4,C1,C5,C6);
    WITH NAME DO
      BEGIN
        REPEAT
          SC_CLR_SCREEN;
          FOR I:= 1 TO 5 DO WRITELN;
          WRITE ('Present name is ',PREFIX,NUMBER,SUFFIX);
          WRITELN (' with an increment of ',INC);
          FOR I:= 1 TO 2 DO WRITELN;
          CH := PROMPT ('CHANGE: S(uffix,P(refix,N(umber,I(ncrement,E(xit :',
                                                 [C1,C2,C3,C4,C5,C6]);
          IF CH = 'E' THEN EXIT (SET_AUTONAME);
          IF (CH<>'H') THEN WRITE ('Change to :');
          CASE CH OF
            'S' : READLN (SUFFIX);
            'P' : READLN (PREFIX);
            'N' : READ_INTEGER (NUMBER);
            'I' : READ_INTEGER (INC);
            'H' : HELP (HELPS);
          END;
        UNTIL FALSE;
      END;
  END; {of Set_Autoname}

{-------------------------------------------------------------------------}

SEGMENT PROCEDURE CHANGE_AMPLIFIER_GAIN;  {Amplifier gain adjustment}
```

```
 VAR TEMP :INTEGER;

 BEGIN
  SET_YES_NO;
  WRITELN('This should only be used if you have changed the amplifier gains');
  CH := PROMPT ('Continue?:',['Y','N']);
  IF CH = 'N' THEN EXIT(CHANGE_AMPLIFIER_GAIN);
  SC_CLR_SCREEN;
  FOR I:= 1 TO 5 DO WRITELN;
  WRITELN ('N.B. BOTH gains should be changed to same value');
  REPEAT
   WRITELN ('Gain is ',GAIN_AMP);
   CH := PROMPT ('Change gain ?',['Y','N']);
   IF CH = 'Y' THEN
    BEGIN
     WRITE ('New gain :');
     READ_INTEGER (TEMP);
     IF (TEMP<>1) AND (TEMP<>10) AND(TEMP<>100) THEN WRITELN ('1,10 or 100!')
     ELSE GAIN_AMP := TEMP;
    END;
  UNTIL CH = 'N';
  SC_CLR_SCREEN;

 END; {of Change_Amplifier_Gain}

{-------------------------------------------------------------------------------}

 SEGMENT PROCEDURE CHANGE_ADC_GAIN;

 CONST  WARNING  = 'ADC reading getting low please increase amplifier gains';

 VAR  TOO_MUCH : BOOLEAN;

 BEGIN
   TOO_MUCH := FALSE;
   IF NO_GAIN_CHANGES AND NOT ADC_SATURATED THEN EXIT (CHANGE_ADC_GAIN);

   IF GAIN_UP AND (GAIN_ADC<>1000) THEN
         WRITE (CHR(7),CHR(7),' ADC gain increased to ');
   IF GAIN_DOWN AND (GAIN_ADC<>1) THEN
         WRITE (CHR(7),CHR(7),' ADC gain decreased to ');
   IF GAIN_DOWN AND (GAIN_ADC=1) THEN TOO_MUCH := TRUE;
   IF GAIN_DOWN THEN
        CASE GAIN OF
         GAIN_10  : GAIN := GAIN_1;
         GAIN_100 : GAIN := GAIN_10;
         GAIN_1000: GAIN := GAIN_100;
        END;
   IF GAIN_UP THEN
        CASE GAIN OF
         GAIN_1   : GAIN := GAIN_10;
         GAIN_10  : GAIN := GAIN_100;
         GAIN_100 : GAIN := GAIN_1000;
         GAIN_1000: BEGIN
                     TOO_MUCH := TRUE;
                     IF GAIN_AMP <> 100 THEN WRITELN (WARNING);
                    END;
        END;
   {Assign actual gain of ADC}
   CASE GAIN OF
```

```
    GAIN_1   : GANN_ADC:= 1;
    GAIN_10  : GAIN_ADC:= 10;
    GAIN_100 : GAIN_ADC:= 100;
    GAIN_1000: GAIN_ADC:= 1000;
   END;

  IF NOT TOO_MUCH THEN WRITELN (GAIN_ADC);

 END; {of Change_ADC_GAIN}

{-------------------------------------------------------------------------}

 SEGMENT PROCEDURE CHECK_ADC_GAIN; {Checks whether or not
                                              gain change is necessary}
  CONST  REDUCE_1 = -0.40;
         REDUCE_2 =  0.40;
         TURN_UP1 =  4.90;        {Note slight overlap so}
         TURN_UP2 = -4.90;                    {it's not constantly changing}

  VAR LO,HI :INTEGER;

  BEGIN

    LO := 0;
    HI := 0;
    GAIN_UP := FALSE;
    GAIN_DOWN := FALSE;

    FOR J := 1 TO 6 DO
     BEGIN
      FOR I:= 1 TO 2 DO
        BEGIN
         IF  (MEANS[J,I]> (TURN_UP1/GAIN_ADC/GAIN_AMP))
         OR  (MEANS[J,I]< (TURN_UP2/GAIN_ADC/GAIN_AMP)) THEN HI:=HI+1;
         IF  (MEANS[J,I]< (REDUCE_2/GAIN_ADC/GAIN_AMP))
         AND (MEANS[J,I]> (REDUCE_1/GAIN_ADC/GAIN_AMP)) THEN LO:=LO+1;
        END;
     END;

    IF (HI>0) THEN GAIN_DOWN := TRUE; {If ANY reading has saturated}
    IF (LO=12) THEN GAIN_UP := TRUE;  {If ALL readings are too low}

  END; {of Check_ADC_Gain}

{-------------------------------------------------------------------------}

 SEGMENT PROCEDURE NEW_GAINS;

 VAR CHG : CHAR;

 BEGIN
  SET_YES_NO;
  CHG := PROMPT ('Change ADC Gain? ',['Y','N']);
  GAIN_UP := FALSE;
  GAIN_DOWN := FALSE;
  IF CHG = 'N' THEN CHANGE_AMPLIFIER_GAIN
  ELSE
   BEGIN
    WRITELN ('ADC Gain will be changed by a factor of 10');
    CHG := PROMPT ('Increase ADC Gain? ',['Y','N']);
```

```
    IF CHG = 'Y' THEN GAIN_UP := TRUE
                 ELSE GAIN_DOWN := TRUE;
    CHANGE_ADC_GAIN;
   END;
 END; {of New_Gains}

{-------------------------------------------------------------------------}

 SEGMENT PROCEDURE LAST_RESULTS;  {Prints the previous result c.f. print_results}

  VAR OSTG : STRING;

  BEGIN

   OSTG := '';
   IF MESSES>1 THEN
    BEGIN
     IF CALCULATED THEN STR (MESSES,OSTG) ELSE STR (MESSES-1,OSTG);
     IF CALCULATED THEN STG := CONCAT ('*',OSTG,'* ')
                   ELSE STG := CONCAT ('C',OSTG,'* ');
    END;

   RESULTS (OSTG,OSAMP_NAME,OLD_INT,OLD_DEC,OLD_INC,ERROR,OV1,OV2,OV3);

  END; {of Last_results}

{-------------------------------------------------------------------------}

  SEGMENT PROCEDURE CALC_HOLDER_MAGN;

  VAR NUMBER_KEPT,TEMP_GAIN,TEMP_ADC_GAIN : INTEGER;
      CH : CHAR;

  BEGIN

    TEMP_GAIN := GAIN;
    TEMP_ADC_GAIN := GAIN_ADC;
    GAIN := GAIN_100;
    GAIN_ADC := 100;

    SET_YES_NO;
    NUMBER_KEPT := 0;
    FOR I:= 1 TO 3 DO HOLDER[I] := 0;
    REPEAT
      MESSES := 1;
      SC_CLR_SCREEN;
      FOR I:= 1 TO 5 DO WRITELN;
      WRITELN ('Empty holder');
      PAUSE;
      ADC_SATURATED := FALSE;
      CALCULATED := FALSE;
      WRITE ('** HOLDER **');
      REMOVE_HOLDER := FALSE;
      MOVE_MEASURE;
      REMOVE_HOLDER := TRUE;
      IF BELL THEN WRITE (CHR(7));
      FOR I:= 1 TO 3 DO
        BEGIN
         WRITE ('    ',CHR(87+I),' = ',VOLTS[I]:10:6);
        END;
```

```
    IF QUANTUM_JUMP THEN WRITELN (CHR(7),' JUMP ? ') ELSE WRITELN;
    IF (GAIN_UP) OR (GAIN_DOWN) THEN CHANGE_ADC_GAIN;
    CH := PROMPT ('Keep ? ',['Y','N']);
    IF CH = 'Y' THEN
     BEGIN
      FOR I:= 1 TO 3 DO HOLDER[I] := ((HOLDER[I]*NUMBER_KEPT) + VOLTS[I])
                                                    /(NUMBER_KEPT+1);
      NUMBER_KEPT := NUMBER_KEPT + 1;
      WRITELN ('Average values using ',NUMBER_KEPT,' values');
      FOR I:= 1 TO 3 DO WRITE ('  ',CHR(87+I),' = ',HOLDER[I]:10:6);
      WRITELN;
     END;
    CH := PROMPT ('Repeat ? ',['Y','N']);
  UNTIL CH = 'N';

  GAIN := TEMP_GAIN;
  GAIN_ADC := TEMP_ADC_GAIN;
  WRITELN;

  CH := PROMPT('Save holder magnetisation values? ',['Y','N']);

  IF (CH = 'N') THEN EXIT(CALC_HOLDER_MAGNETISATION)
  ELSE
   BEGIN
    FOR I:= 1 TO 5 DO WRITELN (P_TEXT);
    WRITE (P_TEXT,'**HOLDER MAGNETISATION**');
    FOR I:= 1 TO 3 DO
      BEGIN
       HOLDER[I] := VOLTS[I];
       WRITE (P_TEXT,'   ',CHR(87+I),' = ',HOLDER[I]:10:6);
      END;
    FOR I:= 1 TO 5 DO WRITELN (P_TEXT);
   END;

END; {of Calc_Holder_Magnetisation}
```

```
{-------------------------------------------------------------------------}

                    (**** SEGMENT ROUTINES 3 ****)


   (* Contains the following procedures

            a) CALC_MAGNETIC_VECTOR
            b) CALC_NEW_VECTOR
            c) INITIALISE
                                                August 1984 *)

{-------------------------------------------------------------------------}

 SEGMENT PROCEDURE CALC_MAGNETIC_VECTOR ;

                                {Calcs INT,DEC & INC from voltages read}

 CONST DPR = 57.29577951;

 VAR BGD1,BGD2,E,N,Z : REAL;

 BEGIN
   OLD_INT := INT;                          OV1 := VOLTS[1];
   OLD_DEC := DEC;                          OV2 := VOLTS[2];
   OLD_INC := INC;                          OV3 := VOLTS[3];

   IF NOT CALCULATED THEN
     BEGIN

       {Calc mean voltages}

       BGD1 := (MEANS[1,1] + MEANS[6,1])/2.0;
       BGD2 := (MEANS[1,2] + MEANS[6,2])/2.0;

       VOLTS[1] := (MEANS[5,1] - MEANS[3,1])/2.0;
       VOLTS[2] := (MEANS[2,1] - MEANS[4,1])/2.0;
       VOLTS[3] := 0.0;
       FOR POSN := 2 TO 5 DO VOLTS[3]:= VOLTS[3] + MEANS[POSN,2];
       VOLTS[3] := VOLTS[3]/4.0;
       VOLTS[3] := -(VOLTS[3]-BGD2);   {Remove bgd field and reverse}

       {Calc measurement error}

       N := 0;
       FOR I:= 1 TO 3 DO N := N + SQR(2.0*VOLTS[I]);

       SUMSQ := 0;
       SUMSQ := SUMSQ + SQR(MEANS[2,1])            {Y axis has no bgd values}
                      + SQR(MEANS[4,1])
                      + SQR((MEANS[3,1]-BGD1))
                      + SQR((MEANS[5,1]-BGD1));   {Remove X & Z axis bgd average}
       SUMSQ := SUMSQ + SQR(((MEANS[2,2]+MEANS[4,2])/2)-BGD2)
                      + SQR(((MEANS[3,2]+MEANS[5,2])/2)-BGD2);

       IF N <> 0 THEN ERROR := 100 * SQRT(ABS((2*SUMSQ/N)-1))
                 ELSE ERROR := 1000;            {Normalised deviation}

       FOR I:= 1 TO 3 DO        {Convert volts to mag moment and remove}
```

```
      BEGIN                                {any holder magnetic moment}
       VOLTS[I] := VOLTS[I]*CALS[I];
       IF REMOVE_HOLDER THEN VOLTS[I] := VOLTS[I] - HOLDER[I]*VOLUME;
      END;
    IF AXIAL_OUT THEN VOLTS[3] := 0;   {Zero moment if a squid has failed}
    IF HORIZ_OUT THEN
     BEGIN
      VOLTS[1] := 0;
      VOLTS[2] := 0;
     END;
    FOR I:= 1 TO 3 DO ALL_VOLTS[MESSES,I] := VOLTS[I];
   END;                                {Save for n-measure calculation}


  FOR I:= 1 TO 3 DO VOLTS[I] := VOLTS[I]/VOLUME; {Moment --> Magnetisation}

  N := VOLTS[1];   E := VOLTS[2];   Z := VOLTS[3];

  {Calculate Declination}

  IF (N <  0.000001) AND (N>-0.000001) THEN IF E > 0 THEN DEC := 90
                                                     ELSE DEC := 270;
  IF (N >= 0.000001) THEN DEC := ATAN(E/N) * DPR;
  IF (N >= 0.000001) AND (E < 0) THEN DEC := DEC + 360;
  IF (N <=-0.000001) THEN DEC := 180 - (ATAN(-E/N)*DPR);

  {Calculate Intensity}

  INT := 0;
  FOR I:= 1 TO 3 DO INT := INT + SQR(VOLTS[I]);
  N := SQRT(INT - SQR(Z));          {Horizontal vector for INC}
  INT := SQRT(INT);

  {Calculate Inclination}

  IF (N>0.000001) OR (N<-0.000001) THEN INC := ATAN (Z/N) * DPR
                          ELSE IF Z>0 THEN INC := 90 ELSE INC := -90;


 END; {of Calc_Magnetic_Vector}

{-------------------------------------------------------------------------}

 SEGMENT PROCEDURE CALC_NEW_VECTOR;  {Calculates mag vector
                                              for multi read samples}

  CONST EXCLAMATION = 'Calculation only possible after 2,3,4 or 6 measurements!';
        AXIAL_EXC   = 'Calculation only possible after 3,4 or 6 measurements!';
        HORIZ_EXC   = 'Calculation only possible after 3,6 measuremnts';

  VAR SUMSQ : REAL;
      ERROR_MESSES : INTEGER;

  BEGIN

    {Check that a calculation is sensible}

    IF (MESSES=0) OR (MESSES=1) OR (MESSES=5) THEN
       BEGIN
        WRITELN(CHR(7),EXCLAMATION);
```

```
        EXIT (CALC_NEW_VECTOR);
       END;

    IF AXIAL_OUT AND (MESSES=2) THEN
       BEGIN
        WRITELN(CHR(7),AXIAL_EXC);
        EXIT (CALC_NEW_VECTOR);
       END;

    IF HORIZ_OUT AND (MESSES<>3) AND (MESSES<>6) THEN
       BEGIN
        WRITELN(CHR(7),HORIZ_EXC);
        EXIT (CALC_NEW_VECTOR);
       END;

    {Set calculated for CALC_MAGNETIC_VECTOR}

    CALCULATED := TRUE;

(*   Orientations set for cubes where the arrow points to the top of the *)
(* core; those for cylindrical samples are the same order with the first *)
(* orientation so that the north direction is parallel to the 180 degree *)
(* measure direction.                                                    *)

    {Set non measured values to zero if squid down}

    IF AXIAL_OUT THEN FOR I:= 1 TO MESSES DO ALL_VOLTS[I,3] := 0;
    IF HORIZ_OUT THEN
      FOR I:= 1 TO MESSES DO
       BEGIN
        ALL_VOLTS[I,1] := 0;
        ALL_VOLTS[I,2] := 0;
       END;

        (* Cube Orientation 1:= Arrow at Front pointing Up  *)
        (*                  2:= Arrow at rhs, pointing Down *)

    IF MESSES >= 2 THEN
      BEGIN
       VOLTS[1] := (ALL_VOLTS[1,1] - ALL_VOLTS[2,2])/2.0;
       VOLTS[2] := (ALL_VOLTS[1,2] - ALL_VOLTS[2,1])/2.0;
       VOLTS[3] := (ALL_VOLTS[1,3] - ALL_VOLTS[2,3])/2.0;
      END;

        (* Cube Orientation 3:= Arrow on lhs pointing In  *)
        (*                  4:= Arrow at top pointing Out *)

    IF MESSES = 3 THEN
      BEGIN
       VOLTS[1] := (VOLTS[1]*2.0 + ALL_VOLTS[3,2])/3.0;
       VOLTS[2] := (VOLTS[2]*2.0 + ALL_VOLTS[3,3])/3.0;
       VOLTS[3] := (VOLTS[3]*2.0 + ALL_VOLTS[3,1])/3.0;
       IF AXIAL_OUT THEN   {Only two values on chan 1 & one on chan 3}
        BEGIN
         VOLTS[1] := VOLTS[1]*3.0/2.0;
         VOLTS[3] := VOLTS[3]*3.0;
         ERROR_MESSES := 2;
        END
       ELSE IF HORIZ_OUT THEN  {New orientation sequence}
        BEGIN
```

```
      VOLTS[3] := ALL_VOLTS[1,3];
      VOLTS[2] := ALL_VOLTS[2,3];
      VOLTS[1] := ALL_VOLTS[3,3];
      ERROR_MESSES := 2;
     END;
   END;

IF MESSES >= 4 THEN
   BEGIN
    VOLTS[1] := (VOLTS[1]*2.0 + ALL_VOLTS[3,2] - ALL_VOLTS[4,3])/4.0;
    VOLTS[2] := (VOLTS[2]*2.0 + ALL_VOLTS[3,3] - ALL_VOLTS[4,2])/4.0;
    VOLTS[3] := (VOLTS[3]*2.0 + ALL_VOLTS[3,1] - ALL_VOLTS[4,1])/4.0;
    IF AXIAL_OUT THEN   {Only two values on chans 1 & 3}
     BEGIN
      VOLTS[1] := VOLTS[1]*2.0;
      VOLTS[3] := VOLTS[3]*2.0;
      ERROR_MESSES := 2;
     END;
   END;

     (* Cube Orientation 5:= Arrow on back pointing left    *)
     (*                  6:= Arrow on bottom pointing right *)

IF MESSES = 6 THEN
   BEGIN
     IF AXIAL_OUT THEN  {Average horiz squid values}
      BEGIN
       VOLTS[1] := (VOLTS[1]*2.0 - ALL_VOLTS[5,1])/3.0;
       VOLTS[2] := (VOLTS[2]*2.0 - ALL_VOLTS[5,2])/3.0;
       VOLTS[3] := (VOLTS[3]*2.0 - ALL_VOLTS[5,2] + ALL_VOLTS[6,2])/4.0;
       ERROR_MESSES := 4;
      END

     ELSE IF HORIZ_OUT THEN  {only use axial squid values}
      BEGIN                          {note different orientation sequence}
       VOLTS[1] := (ALL_VOLTS[3,3] - ALL_VOLTS[6,3])/2.0;
       VOLTS[2] := (ALL_VOLTS[2,3] - ALL_VOLTS[5,3])/2.0;
       VOLTS[3] := (ALL_VOLTS[1,3] - ALL_VOLTS[4,3])/2.0;
       ERROR_MESSES := 2;
      END

     ELSE          {Both squids working}
      BEGIN
       VOLTS[1] := (VOLTS[1]*4.0 - ALL_VOLTS[5,1] + ALL_VOLTS[6,3])/6.0;
       VOLTS[2] := (VOLTS[2]*4.0 - ALL_VOLTS[5,3] + ALL_VOLTS[6,1])/6.0;
       VOLTS[3] := (VOLTS[3]*4.0 - ALL_VOLTS[5,2] + ALL_VOLTS[6,2])/6.0;
      END;

   END;

CALC_MAGNETIC_VECTOR;

{Calculate error}

FOR J := 1 TO MESSES DO
FOR I := 1 TO 3 DO SUMSQ := SUMSQ + SQR (ALL_VOLTS[J,I]);
ERROR := 0;
IF (NOT AXIAL_OUT) AND (NOT HORIZ_OUT) THEN ERROR_MESSES := MESSES;
FOR I := 1 TO 3 DO ERROR := ERROR + SQR(VOLTS[I]*ERROR_MESSES);
ERROR := (ERROR_MESSES*SUMSQ/ERROR) - 1;
```

```
    ERROR := 100 * SQRT(ABS(ERROR));

    WRITE ('*C* ',SAMP_NAME);
    WRITELN('  INT = ',INT:9:3,' DEC =  ',DEC:9:3,
                              ' INC = ',INC:9:3,' ERR =',ERROR:4:1);

    IF VOLTS_OUT THEN
     BEGIN
      FOR I := 1 TO LENGTH(SAMP_NAME)+5 DO WRITE (' ');
      WRITELN('  N  = ',VOLTS[1]:9:3,'  E  = ',VOLTS[2]:9:3,
                                '  Z  = ',VOLTS[3]:9:3);
     END;


  END; {of calc_new_vector}

{-------------------------------------------------------------------------------}

 SEGMENT PROCEDURE INITIALISE;  {Initialise variables and files}

   BEGIN

     REWRITE (P_TEXT,'PRINTER:');
     FOR I:= 1 TO 5 DO WRITELN(P_TEXT);

   (* Title *)

     FOR I:= 1 TO 5 DO WRITELN;
     FOR I:= 1 TO 20 DO WRITE(' ');
     WRITE ('CRYOGENIC CONTROL PROGRAM VERSION 1');
     WRITELN;
     FOR I:= 1 TO 2000 DO CH:='K';       {Delay to show heading}

   (* Sample handler positions *)

     POSITION[1] :=  0;                  {Background}
     POSITION[6] :=  0;                  {Background}
     POSITION[3] :=  1;                  {Measure - 0}
     POSITION[4] :=  3;                  {Measure - 90}
     POSITION[5] := 69;                  {Measure - 180}
     POSITION[2] :=  7;                  {Measure - 270}
     INSERT      :=  8;                  {Insert}

   (* Gains *)

     GAIN := GAIN_1;
     GAIN_AMP := 1;
     GAIN_ADC := 1;

   (* Calibrations *)

     ZERO      := 2047.5;
     FACTOR    := 409.6;
     ADC_READS := 2048;
     CALS[1]   := 1.0;
     CALS[2]   := 1.0;
     CALS[3]   := 1.0;
     VOLUME    := 1.0;  {lcc - INT result gives magnetic moment in micro A/m}

   (* Variables *)
```

```
    INT := 0;
    INC := 0;
    DEC := 0;

    FOR I:= 1 TO 3 DO
     BEGIN
      VOLTS[I] := 0.0;
      HOLDER[I] := 0.0;
     END;

    NO_OF_RESULTS := 0;
    TOTAL_RES := 0;

  (* Booleans *)

    BELL             := TRUE;
    PRINT            := TRUE;
    AUTO_NAME        := FALSE;
    AXIAL_OUT        := FALSE;
    HORIZ_OUT        := FALSE;
    VOLTS_OUT        := FALSE;
    REMOVE_HOLDER    := FALSE;
    NO_GAIN_CHANGES  := FALSE;

  (* Sample name *)

    SAMP_NAME := 'Start';
    OSAMP_NAME := 'Start';
    WITH NAME DO
      BEGIN
        SUFFIX := ' Suffix';
        PREFIX := 'Prefix ';
        NUMBER := 0;
        INC    := 1;
      END;

  (* Information file names *)

    HELPS := 'CRYOGEN:HELP_INFO.TEXT';
    KEYS  := 'CRYOGEN:KEYS_INFO.TEXT';

  (* Move sample handler to insert position *)

    MOVE (INSERT);

  (* Get a file name *)

    OPFILE := '';
    CHANGE_FILES;

  (* Get first sample name from keyboard *)

    SC_CLR_SCREEN;
    GET_NAME;

END;  {of Initialise}
```

```
{------------------------------------------------------------------------------}

                    (**** GENERAL ROUTINES 1 ****)

  (* Contains the following procedures

           a) RESULTS
           b) PRINT_RESULTS
           c) WAIT_FOR_STOP
           d) GET_NAME
           e) CALC_MEAN
           f) CHECK_BACKGROUND
           g) MOVE_MEASURE
           h) DEF_COMMAND_KEYS
           i) MAKE_MEASUREMENT
           j) GET_COMMAND

                                                              *)

{------------------------------------------------------------------------------}

PROCEDURE RESULTS ;          {Prints results to hard copy and disc}

 VAR SPACES : INTEGER;

 BEGIN

   NO_OF_RESULTS := NO_OF_RESULTS + 1;
   TOTAL_RES := TOTAL_RES + 1;

   SPACES := LENGTH(RSTG) + LENGTH(RNAME) + 2;

   {Write to printer}

   IF PRINT THEN
    BEGIN
     WRITELN(P_TEXT,RSTG,RNAME,'  INT = ',RINT:9:3,' DEC = ',RDEC:9:3,
                                ' INC = ',RINC:9:3,' ERR =',RERR:4:1);
     IF VOLTS_OUT THEN
      BEGIN
        FOR I:= 1 TO SPACES DO WRITE (P_TEXT,' ');
        WRITELN (P_TEXT,' N  = ',RV1:9:3,'  E  = ',RV2:9:3,
                                                '  Z  = ',RV3:9:3);
      END;
    END;

   {Save in array}

   WITH THE_RESULTS[NO_OF_RESULTS] DO
     BEGIN
      SAMPLE := CONCAT (RSTG,RNAME);
      INTENSITY := RINT;
      DECLINATION := RDEC;
      INCLINATION := RINC;
      ERROR := RERR;
      NORTH := RV1;
      EAST := RV2;
```

```
      DOWN := RV3;
     END;

  END; {of Results}

{-------------------------------------------------------------------------}

 PROCEDURE PRINT_RESULTS;  {Prints result to hard copy and disc}

  BEGIN
    IF CALCULATED THEN
     BEGIN
      STR (MESSES,STG);
      STG := CONCAT ('C',STG,'* ');
     END;

    RESULTS (STG,SAMP_NAME,INT,DEC,INC,ERROR,VOLTS[1],VOLTS[2],VOLTS[3]);

  END; {of Print_Results}

{-------------------------------------------------------------------------}

 PROCEDURE GET_NAME;  {Gets sample name by prompt or auto_name}

  VAR NUM_ST:STRING[10];

  BEGIN
    MESSES := 0;
    OSAMP_NAME := SAMP_NAME;
    IF NOT AUTONAME THEN
      BEGIN
        WRITE ('Sample name :');
        READLN (SAMP_NAME);
      END
    ELSE
      WITH NAME DO
        BEGIN
          NUMBER := NUMBER + INC;
          STR (NUMBER,NUM_ST);
          SAMP_NAME:= CONCAT (PREFIX,NUM_ST,SUFFIX);
          WRITELN ('Sample name :',SAMP_NAME);
        END;

  END; {of Get_Name}

{-------------------------------------------------------------------------}

  PROCEDURE WAIT_FOR_STOP;  {Waits for stop signal from carriage control (0)}

  VAR STOP_CHAN:INTEGER;

  BEGIN

    FOR I:= 1 TO 1000 DO STOP_CHAN := GAIN_100;   {Delay and assign!}
    REPEAT
      WARNPORT (STOP_CHAN);
      READ_ADC (I,STOP_CHAN);
    UNTIL I < HI_TO_LO;    {Waits for the high-low signal to come low}
    FOR I:= 1 TO 200 DO CH:= 'K';
```

```
  END; {of Wait_for_Stop}

{-------------------------------------------------------------------------------}

 PROCEDURE CALC_MEAN (VAR LPOS:INTEGER);

        {Calcs mean of ADC readings and converts to a voltage}

   BEGIN
     MEANS[LPOS,1] := (HORIZ_B*32768.0 + HORIZ_A)/ADC_READS;
     MEANS[LPOS,2] := (AXIAL_B*32768.0 + AXIAL_A)/ADC_READS;

     FOR I:= 1 TO 2 DO IF (MEANS[LPOS,I] > 4090) OR (MEANS[LPOS,I] < 10) THEN
                                          ADC_SATURATED := TRUE;

     FOR I:= 1 TO 2 DO
      BEGIN
       MEANS[LPOS,I] := (MEANS[LPOS,I]-ZERO)/FACTOR;
       MEANS[LPOS,I] := MEANS[LPOS,I] / GAIN_ADC / GAIN_AMP;
      END;
   END; {of Calc_Mean}

{-------------------------------------------------------------------------------}

 PROCEDURE CHECK_BACKGROUND;  {Checks background values for change >1mV}

  CONST mV = 0.005;

  BEGIN
    QUANTUM_JUMP := FALSE;
    FOR I:= 1 TO 2 DO
      BEGIN
        IF ABS((MEANS[1,I] - MEANS[6,I])) > mV THEN QUANTUM_JUMP := TRUE;
      END;
  END; {of Check_Background}

{-------------------------------------------------------------------------------}

 PROCEDURE MOVE_MEASURE;  {Move and measure in 4 perpendicular positions}

   VAR POSN_LESS_1:INTEGER;

   BEGIN

    MOVE (POSITION[1]);
    FOR POSN := 2 TO 7 DO
     BEGIN
      WAIT_FOR_STOP;
      GET_READING (GAIN,HORIZ_A,HORIZ_B,AXIAL_A,AXIAL_B,ADC_READS);
      IF POSN=7 THEN MOVE(INSERT) ELSE MOVE (POSITION[POSN]);
      POSN_LESS_1 := POSN - 1;
      CALC_MEAN (POSN_LESS_1);
     END;
    CHECK_ADC_GAIN;
    CHECK_BACKGROUND;
    CALC_MAGNETIC_VECTOR;

   END; {of Move_Measure}

{-------------------------------------------------------------------------------}
```

```
PROCEDURE DEF_COMMAND_KEYS;  {Defines the function keys for get command}

 BEGIN
   S1:='  H(elp  ';
   S2:='  F(ile  ';
   S3:='  I(nfo  ';
   S4:=' R(epeat ';
   S5:='  C(alc  ';
   S6:='  P(rint ';
   S7:='  N(ame  ';
   C1:='H';C2:='F';C3:='I';C4:='R';C5:='C';C6:='P';C7:='N';
   SS_FNLABEL (S1,S2,S3,S4,S5,S6,S7);
   SS_FNKEYGEN (FALSE,C1,C2,C3,C4,C5,C6,C7);
 END; {of Def_Command_Keys}

{-------------------------------------------------------------------------------}

 PROCEDURE MAKE_MEASUREMENT;

 BEGIN
 { Set up flags and move }

   ADC_SATURATED := FALSE;
   CALCULATED := FALSE;
   STR (MESSES,STG);
   STG := CONCAT ('*',STG,'* ');
   WRITE(STG,SAMP_NAME);
   MOVE_MEASURE;

 { Output the result to the screen only}

   IF BELL THEN WRITE (CHR(7));    {Sound bell if bell switched on}
   WRITE('  INT = ',INT:9:3,' DEC = ',DEC:9:3,' INC = ',INC:9:3);
   IF (NOT AXIAL_OUT) AND (NOT HORIZ_OUT) THEN WRITE (' ERR =',ERROR:4:1);
   IF QUANTUM_JUMP THEN WRITE (CHR(7),'  JUMP ? ');
   WRITELN;

   IF VOLTS_OUT THEN
    BEGIN
      FOR I:= 1 TO LENGTH(SAMP_NAME)+6 DO WRITE (' ');
      WRITELN (' N  = ',VOLTS[1]:9:3,'  E  = ',VOLTS[2]:9:3,
                                    '  Z  = ',VOLTS[3]:9:3);
    END;

 { Check for ADC adjustments before another measurement}

   IF ADC_SATURATED THEN
        WRITELN (CHR(7),'WARNING- ADC saturated. Repeat reading');
   IF (GAIN_UP) OR (GAIN_DOWN) THEN CHANGE_ADC_GAIN;

 END; {of Make_Measurement}

{-------------------------------------------------------------------------------}

PROCEDURE GET_COMMAND;          {Gets the next command}

 VAR CLEAR_SET,SAME_SET,PROMPT_SET:SUBSET;
     CH1:CHAR;
     LINE : INTEGER;
```

```
BEGIN

 CLEAR_SET := ['A','F','H','I','K','M','Q','W','?','^'];
 SAME_SET := ['B','C','D','E','G','L','N','P','R','S','V','X','Z',' '];
 PROMPT_SET := CLEAR_SET + SAME_SET;

 DEF_COMMAND_KEYS;
 REPEAT
  LINE := SC_FIND_Y;
  SC_GOTOXY(0,LINE);
  CH1:= PROMPT ('GO?:',PROMPT_SET);
  IF CH1 = ' ' THEN MESSES := MESSES + 1;
  IF MESSES > 6 THEN CH1 := 'N';
  CASE CH1 OF
    ' ' : MAKE_MEASUREMENT;

    'A' : BEGIN
           AUTO_NAME := NOT AUTO_NAME;
           IF AUTO_NAME THEN SET_AUTONAME
                        ELSE BEGIN
                               CH1 := 'B';
                               WRITELN ('Auto name off');
                             END;
          END;

    'B' : BEGIN
           BELL := NOT BELL;
           IF BELL THEN WRITELN ('Bell on')
                   ELSE WRITELN ('Bell off');
          END;

    'C' : CALC_NEW_VECTOR;

    'D' : BEGIN
           PRINT := NOT PRINT;
           IF PRINT THEN WRITELN ('Printer on')
                    ELSE WRITELN ('Printer off');
          END;

    'E' : BEGIN
           VOLTS_OUT := NOT VOLTS_OUT;
           IF VOLTS_OUT THEN WRITELN ('Components will now be printed')
                        ELSE WRITELN ('Components will not be printed');
          END;

    'F' : CHANGE_FILES;
    'G' : NEW_GAINS;
    'H' : HELP (HELPS);
    'I' : OUTPUT_DATA;
    'K' : SETUP_CALS;
    'L' : LAST_RESULTS;

    'M' : BEGIN
           REMOVE_HOLDER := NOT REMOVE_HOLDER;
           IF REMOVE_HOLDER THEN CALC_HOLDER_MAGN
           ELSE
            BEGIN
             WRITELN ('Holder magnetisation not being removed');
```

```
            CH1 := 'B';
           END;
         END;

    'N' : GET_NAME;
    'P' : PRINT_RESULTS;
    'Q' : SQUID_CALIB;
    'R' : REPEAT_MEASUREMENT;
    'S' : SQUID_FAILURE;
    'V' : NEW_VOLUME;
    'W' : HELP (KEYS);
    'X' : GET_NEW_ADC_READS;

    'Z' : BEGIN
           NO_GAIN_CHANGES := NOT NO_GAIN_CHANGES;
           IF NO_GAIN_CHANGES THEN WRITELN ('Auto gain off')
                              ELSE WRITELN ('Auto gain on');
         END;

    '?' : HELP (KEYS);
    '^' : EXIT (CONTROL);

  END;
  DEF_COMMAND_KEYS;
  IF (CH1 IN CLEAR_SET) THEN
    BEGIN
      SC_CLR_SCREEN;
      WRITELN;
      WRITELN ('Last sample was ',SAMP_NAME,' measurement ',MESSES);
      WRITELN;
    END;
  IF NO_OF_RESULTS = 50 THEN
    BEGIN
     WRITELN (CHR(7),'50 measurements recorded in array. ',
                                 'Saving in ',OP_FILE);
     SAVE_RESULTS(NO_OF_RESULTS);
    END;
 UNTIL FALSE;
END; {of Get_Command}
```

```
UNIT GENERAL;

INTERFACE

  TYPE CHARSET = SET OF CHAR;

  PROCEDURE GET_IPFILENAME (VAR IPFNAME:STRING);  {Get an input file name}
  PROCEDURE GET_OPFILENAME (VAR OPFNAME:STRING);  {Get an output file name}
  FUNCTION  PROMPT (LINE:STRING;LEGAL_COMS:CHARSET):CHAR; {Get a single char
                                                          response to a prompt}
  PROCEDURE PAUSE; {Create a user ended delay using prompt}
  PROCEDURE HELP (VAR FILE_NAME:STRING); {Output a file a screen at a time}
  PROCEDURE SAFE_OPEN (VAR SAFE_TEXT:TEXT;
                       VAR SAFE_FILE_NAME:STRING; INPUT:BOOLEAN);
                                          {Open with IO checking off}
  PROCEDURE READ_INTEGER (VAR INT:INTEGER); {Reads an integer from the keyboard}
  PROCEDURE READ_REAL (VAR REEL:REAL);   {(real) without i/o format errors}

IMPLEMENTATION

USES SCREENOPS;

VAR I        : INTEGER;
    CH       : CHAR;

{-------------------------------------------------------------------------}

PROCEDURE GET_IPFILENAME;
  {Get_ipfilename returns a name in IPFNAME using prompts for an input file.}

  BEGIN
    SC_CLR_SCREEN;
    FOR I := 1 TO 8 DO WRITELN;
    REPEAT
      WRITE ('Give the name of the input file (disc:filename) :');
      READLN (IPFNAME);
      IF (POS('.TEXT',IPFNAME)=0) AND (POS('.text',IPFNAME)=0) THEN
       BEGIN
         CH := PROMPT ('.text suffix?',['Y','N']);
         IF CH = 'Y' THEN IPFNAME := CONCAT (IPFNAME,'.text');
       END;
      WRITELN ('The input file opened will be ',IPFNAME);
      CH:=PROMPT('Is this O.K.?:',['Y','N']);
    UNTIL CH ='Y';
  END;

{-------------------------------------------------------------------------}

PROCEDURE GET_OPFILENAME;
  {Get_opfilename gets an output file name and returns it in OPFNAME.}

  BEGIN
    SC_CLR_SCREEN;
    FOR I := 1 TO 5 DO WRITELN;
    WRITELN ('Note that a file requires a ".text" suffix in order to be able');
    WRITELN ('to transfer it to the main frame.'); WRITELN;
    REPEAT
      WRITE ('Give the new output filename (disc:filename) :');
      READLN (OPFNAME);
```

```
    IF (POS('.TEXT',OPFNAME)=0) AND (POS('.text',OPFNAME)=0) THEN
     BEGIN
       CH := PROMPT ('.text suffix?',['Y','N']);
       IF CH = 'Y' THEN OPFNAME := CONCAT (OPFNAME,'.text');
     END;
    WRITELN ('The output file opened will be ',OPFNAME);
    CH:=PROMPT('Is this O.K.?:',['Y','N']);
  UNTIL CH ='Y';
END;

{-------------------------------------------------------------------------}


FUNCTION PROMPT;

  {Prompt prints a line, waits for a character in legal_coms then
   returns its UPPERCASE equivalent.}

VAR Y_START : INTEGER;

BEGIN
  Y_START := SC_FIND_Y;
  REPEAT
    SC_GOTO_XY(0,Y_START);
    WRITE(LINE);
    READ (CH);
    IF CH IN ['a'..'z']
      THEN CH := CHR( ORD(CH) - ORD('a') + ORD('A'));
    IF NOT (CH IN LEGAL_COMS) THEN WRITE (CHR(8),' ',CHR(7));
  UNTIL CH IN LEGAL_COMS;
  WRITELN;
  PROMPT:= CH;
END;

{-------------------------------------------------------------------------}


PROCEDURE PAUSE;  {Uses prompt as user ending delay}

BEGIN
   CH := PROMPT('Press <space> to continue',[' ']);
END; {of Pause}

{-------------------------------------------------------------------------}

PROCEDURE HELP;
            {Gets help information and writes a page at a time}

 VAR X:TEXT;
     ST:STRING;

 BEGIN
   RESET (X,FILE_NAME);
   WHILE NOT EOF(X) DO
    BEGIN
     I:= 0;
     SC_CLR_SCREEN;
     REPEAT
        READLN (X,ST);
        WRITELN (ST);
```

```
        I := I + 1;
      UNTIL (I = 23) OR EOF(X);
      CH := PROMPT ('Press <space> to continue, "E" to exit',[' ','E']);
      IF (CH = 'E') THEN EXIT(HELP);
     END;
  END; {of Help}

{-------------------------------------------------------------------------}

 PROCEDURE SAFE_OPEN;

 VAR I : INTEGER;

 BEGIN
  I:=0;
  REPEAT
   IF I>0 THEN
    BEGIN
     WRITELN (CHR(7),SAFE_FILE_NAME,' not found.');
     CASE IORESULT OF
       8 : WRITELN ('No room on disc');
       9 : WRITELN ('Disc not found');
      12 : WRITELN ('File already open');
     END;
     PAUSE;
    END;
   IF INPUT THEN
    BEGIN
     GET_IPFILENAME(SAFE_FILE_NAME);
     {$I-} RESET (SAFE_TEXT,SAFE_FILE_NAME); {$I+}
    END
   ELSE
    BEGIN
     GET_OPFILENAME(SAFE_FILE_NAME);
     {$I-} REWRITE (SAFE_TEXT,SAFE_FILE_NAME); {$I+}
    END;
   I := I + 1;
  UNTIL IORESULT = 0;

 END;

{-------------------------------------------------------------------------}

 PROCEDURE READ_INTEGER;

  VAR TEMP_STRING : STRING;
      X,Y,I       : INTEGER;
      LETTER      : BOOLEAN;
      MINUS       : BOOLEAN;
      CH          : CHAR;

  BEGIN

    X := SC_FINDX;
    Y := SC_FINDY;
    REPEAT
     SC_GOTOXY(X,Y);
     WRITE ('                                                    ');
     SC_GOTOXY(X,Y);
     READLN (TEMP_STRING);
```

```
    {Remove spaces}

    REPEAT
     CH := TEMP_STRING[1];
     IF CH = ' ' THEN DELETE (TEMP_STRING,1,1);
    UNTIL CH <> ' ';

    {Check only integers given}

    MINUS := FALSE;
    LETTER := FALSE;
    FOR I:= 1 TO LENGTH(TEMP_STRING) DO
     BEGIN
      CH := TEMP_STRING[I];
      IF NOT (CH IN ['0'..'9','-']) THEN
       BEGIN
          WRITE (CHR(7));
          LETTER := TRUE;
       END;
      IF (CH='-') AND (I>1) THEN
       BEGIN
        WRITE (CHR(7));
        LETTER := TRUE;
       END
      ELSE IF (CH='-') AND (I=1) THEN MINUS := TRUE;
     END;
   UNTIL NOT LETTER;

   {Calculate value}

   X := 1;
   INT := 0;
   IF MINUS THEN DELETE (TEMP_STRING,1,1);
   FOR I:= LENGTH(TEMP_STRING) DOWNTO 1 DO
    BEGIN
     INT := INT + X*(ORD(TEMP_STRING[I])-48);
     X := X*10;
    END;

   IF MINUS THEN INT := -INT;

 END;

{-------------------------------------------------------------------------}

 PROCEDURE READ_REAL;

  VAR TEMP_STRING : STRING;
      X,Y,I       : INTEGER;
      LETTER      : BOOLEAN;
      MINUS       : BOOLEAN;
      CH          : CHAR;
      R           : REAL;

 BEGIN

   X := SC_FINDX;
   Y := SC_FINDY;
   REPEAT
```

```
 SC_GOTOXY(X,Y);
 WRITE ('                                                    ');
 SC_GOTOXY(X,Y);
 READLN (TEMP_STRING);

 {Remove spaces}

 REPEAT
  CH := TEMP_STRING[1];
  IF CH = ' ' THEN DELETE (TEMP_STRING,1,1);
 UNTIL CH <> ' ';

 {Check only integers given}

 MINUS := FALSE;
 LETTER := FALSE;
 FOR I:= 1 TO LENGTH(TEMP_STRING) DO
  BEGIN
   CH := TEMP_STRING[I];
   IF NOT (CH IN ['0'..'9','-','.']) THEN
    BEGIN
       WRITE (CHR(7));
       LETTER := TRUE;
    END;
   IF (CH='-') AND (I>1) THEN
    BEGIN
     WRITE (CHR(7));
     LETTER := TRUE;
    END
   ELSE IF (CH='-') AND (I=1) THEN MINUS := TRUE;
  END;
UNTIL NOT LETTER;

{Calculate value}

 IF MINUS THEN DELETE(TEMP_STRING,1,1);
 Y := POS('.',TEMP_STRING);
 IF Y = 0 THEN Y := LENGTH(TEMP_STRING)+1;

 X := 1;
 REEL := 0;
 FOR I:= Y-1 DOWNTO 1 DO
  BEGIN
   REEL := REEL + X*(ORD(TEMP_STRING[I])-48);
   X := X*10;
  END;
 R := 0.1;
 IF Y<LENGTH(TEMP_STRING) THEN
  BEGIN
   FOR I:= Y+1 TO LENGTH(TEMP_STRING) DO
    BEGIN
     REEL := REEL + R*(ORD(TEMP_STRING[I])-48);
     R := R/10;
    END;
  END;

 IF MINUS THEN REEL := -REEL;

END;
```

```
{-------------------------------------------------------------------------}

BEGIN
END.
```

```
;-------------------------------------------------------------------------
;
;                       E Q U I V A L E N C E S
;
SETES           .EQU    0E802H      ;Extra-segment value to point to VIAs
DATA            .EQU    01H         ;GPIB data bus. Port A of VIA
DIRCTL          .EQU    02H         ;Data direction register of port B
DIRDAT          .EQU    03H         ;Data direction register of port A
;
;-------------------------------------------------------------------------
;
                            .PROC MOVE,1
;
; This procedure moves the carriage system according to the parameter passed
; to it on the stack. The output is directed to the 6502 VIA controlling the
; parallel port.
;
        MOV     BP,SP                           ; Save stack pointer
        MOV     SI,(BP+4)                       ; Get the control integer
        MOV     AX,SETES                        ; Get address of 6502 port
        MOV     ES,AX                           ; Assign extra segment
        MOV     BX,00H                          ; Clear base register for offset
        MOV     AX,SS:(SI)                      ; Control integer ready to be sent
        MOV     ES:(BX+DATA),AX                 ; Send control integer
        MOV     SP,BP                           ; Restore stack pointer
        RETL    2                               ; Return skipping the integer
;
;-------------------------------------------------------------------------
;
.END


;-------------------------------------------------------------------------
;
;             ANALOGUE TO DIGITAL CONVERTOR CONTROL UNIT
;
;-------------------------------------------------------------------------
;
; These routines control the calls to the 6522 registers to read the ADC;
; they can be called from either UCSD FORTRAN or PASCAL programs
;
;-------------------------------------------------------------------------
;
;       Set up Equivalences.
;
SETADC      .EQU    0E808H                  ; Extra segment points to ADC
CTRL        .EQU    00H                     ; Port B of 6522 - CONTROL
DATA        .EQU    01H                     ; Port A of 6522  - DATA BUS
CTRLDIR     .EQU    02H                     ; Data direction reg. Port B
DATADIR     .EQU    03H                     ; Data direction reg. Port A
PCR         .EQU    0CH                     ; Peripheral control reg.
;
;-------------------------------------------------------------------------
;
                        .MACRO ESADC
;
;       Subroutine to set the extra segment to point to the ADC.
;
        MOV     DX,SETADC                   ; Load 6522 location
```

```
        MOV     ES,DX                           ; Set Extra Seg. to ADC
        MOV     BX,00H                          ; Set offset to zero
;
.ENDM
;
;-------------------------------------------------------------------------
;
;       Configure the ADC.
;
                        .MACRO ADCONFIG
;
        ESADC                                   ; Extra segment --> ADC
        MOVBIM ES:(BX+CTRLDIR),0FFH             ; Control lines --> Output
        MOVBIM ES:(BX+DATADIR),00H              ; Data lines    --> Input
        MOVBIM ES:(BX+PCR),0AAH                 ; Handshake control.
.ENDM
;
;-------------------------------------------------------------------------
;
                        .PROC WARN_PORT,1
;
;    Procedure to warn the ADC port that it is about to be read, the data
;    handed to it on the stack is the gain and the channel. This routine is
;    used before a main set of readings to remove any 'wobbly' readings
;    caused by the reed switching in the gain amps.
;    Write out of Port B. The bit patterns here are very important as
;    the write out initiates the conversion. Bits 0-3 control the channel
;    and bits 4-7 the gain.
;
        MOV     BP,SP                           ; Save stack pointer.
        ADCONFIG                                ; Configure ADC (ES also assigned)
        MOV     SI,(BP+4)                       ; Contents to be sent
        MOVBIM  AL,SS:(SI)                      ; Into the accumulator
        MOVBIM  ES:(BX+CTRL),AL                 ; Send to data port B
        MOV     SP,BP                           ; Restore pointer
        RETL    2
;
;-------------------------------------------------------------------------
;
                        .PROC READ_ADC,2
;
;   This routine writes a byte on to the control line; the byte should be
;   passed to it on the stack. The process starts the conversion with the
;   gain and channel as defined by the data byte. Then the channel is read
;   and the result pushed onto the stack for later recovery.
;
;
;
        MOV     BP,SP                           ; Save stack pointer
        MOV     DI,(BP+6)                       ; Destination address
        MOV     SI,(BP+4)                       ; Get the gain/chan
        MOV     AX,SI                           ; Save gain/channel
        ESADC
        MOVBIM ES:(BX+CTRL),AL                  ; Trigger reading
        MOV     CX,30                           ; Set up short delay
$2      LOOP    $2                              ; Wait about 50usecs
        MOVBIM AH,ES:(BX+DATA)                  ; Read first byte of data
        MOV     CX,10                           ; Even shorter delay
$3      LOOP    $3                              ; Wait about 10usecs
        MOVBIM AL,ES:(BX+DATA)                  ; Read lower nibble
```

```
        MOV     CL,04H                          ; Set up count for rotate
        ROR     AX,CL                           ; Adjust reading
        MOV     SS:(DI),AX                      ; Store result on stack
        MOV     SP,BP                           ; Restore stack pointer
        RETL    4                               ; Return
;
;
.END
;-------------------------------------------------------------------------;
;                                                                         ;
;               CRYOGENIC CONTROL 2 CHANNEL ADC READ UNIT                 ;
;                                                                         ;
;-------------------------------------------------------------------------;
;                                                                         ;
;   This routine is explicitly for the cryogenic control program and      ;
;   performs the "simultaneous" reading of two input channels (3 & 7)     ;
;   corresponding to the horizontal and axial squid outputs.              ;
;                                                                         ;
;-------------------------------------------------------------------------;
;                                                                         ;
;                       Set up Equivalences.                              ;
;                                                                         ;
;-------------------------------------------------------------------------;
;                                                                         ;
MMADC       .EQU    0E808H                  ; Memory map location of ADC  ;
CTRL        .EQU    00H                     ; Port B of 6522 - CONTROL    ;
DATA        .EQU    01H                     ; Port A of 6522 - DATA       ;
HORIZ       .EQU    03H                     ; Channel 3 is Horiz Squid    ;
AXIAL       .EQU    07H                     ; Channel 7 is Axial Squid.   ;
;                                                                         ;
;-------------------------------------------------------------------------;
;                                                                         ;
                            .MACRO ESADC
;                                                                         ;
;-------------------------------------------------------------------------;
;                                                                         ;
;       Subroutine to set the extra segment to point to the ADC.          ;
;                                                                         ;
;-------------------------------------------------------------------------;
;                                                                         ;
        MOV     DX,MMADC                        ; Load ADC 6522 location  ;
        MOV     ES,DX                           ; Set Extra Seg. to ADC   ;
        MOV     BX,00H                          ; Set offset to zero      ;
;
.ENDM                                           ; Of ESADC.               ;
;                                                                         ;
;-------------------------------------------------------------------------;
;                                                                         ;
                            .MACRO ADC_READ
;                                                                         ;
;-------------------------------------------------------------------------;
;                                                                         ;
;      Macro routine to perform the actual adc read; result is returned   ;
;      in AX register.                                                    ;
;                                                                         ;
;-------------------------------------------------------------------------;
;                                                                         ;
        ESADC                                   ; Set ES to point to ADC  ;
        MOVBIM ES:(BX+CTRL),AL                  ; Trigger reading         ;
        MOV     CX,50                           ; Set up short delay      ;
```

```
$2      LOOP    $2                              ; Wait about 50usecs        ;
        MOVBIM  AH,ES:(BX+DATA)                 ; Read first byte of data   ;
        MOV     CX,15                           ; Even shorter delay        ;
$3      LOOP    $3                              ; Wait about 10usecs        ;
        MOVBIM  AL,ES:(BX+DATA)                 ; Read lower nibble         ;
        MOV     CL,04H                          ; Set up count for rotate   ;
        ROR     AX,CL                           ; Adjust reading            ;
;                                                                           ;
.ENDM                                           ; Of ADC_READ.              ;
;                                                                           ;
;---------------------------------------------------------------------------;
;                                                                           ;
                        .PROC GET_READING,6
;                                                                           ;
;---------------------------------------------------------------------------;
;                                                                           ;
;       Procedure to obtain the average value of READS readings on two      ;
;       channels X & Z. The results are passed back on the stack, as        ;
;       is the gain of the ADC.                                             ;
;                                                                           ;
;---------------------------------------------------------------------------;
;                                                                           ;
                MOV     BP,SP               ;Save the stack pointer         ;
                MOV     SI,(BP+14)          ;1st parm in list is gain       ;
                MOV     AX,SS:(SI)
                MOV     GAIN,AX             ;Save gain                      ;
                MOV     DI,(BP+12)          ;Horiz result address A         ;
                MOV     HRESA,DI            ;Save H result address A        ;
                MOV     DI,(BP+10)          ;Get H result address B         ;
                MOV     HRESB,DI            ;Save H result Address B        ;
                MOV     DI,(BP+8)           ;Same for axial addresses       ;
                MOV     ARESA,DI
                MOV     DI,(BP+6)
                MOV     ARESB,DI
                MOV     SI,(BP+4)           ;Last parm = no. of reads       ;
                MOV     CX,SS:(SI)          ;No. of reads into counter      ;
                MOV     HSUMA,0             ;Set sums to zero               ;
                MOV     ASUMA,0
                MOV     HSUMB,0
                MOV     ASUMB,0
TOP_LOOP        MOV     COUNT,CX            ;Save count value               ;
                MOVBIM  AL,GAIN             ;Get gain                       ;
                ADD     AL,HORIZ            ;Set AL for read H channel      ;
                ADC_READ                    ;Macro to read ADC              ;
                MOV     DX,HSUMA            ;Recover H Sum A (running)      ;
                ADC     DX,AX               ;Add ADC read value to DX       ;
                JNS     EMPTY1              ;Is DX full?                    ;
                MOV     BX,HSUMB            ;Yes. Get X counter             ;
                INC     BX                  ;Add one                        ;
                MOV     HSUMB,BX            ;Save it again                  ;
                AND     DX,7FFFH            ;Clear sign overflow            ;
                ADD     DX,0                ;Reset flags                    ;
                CLC                         ;Just in case                   ;
EMPTY1          MOV     HSUMA,DX            ;Save DX                        ;
                JMP     MISS1               ;Miss jmp up for LOOP           ;
LOOP1           JMP     TOP_LOOP            ;Goto top of loop               ;
MISS1           MOV     AL,GAIN             ;Get gain                       ;
                MOV     BL,AXIAL            ;Get axial channel no.          ;
                ADD     AL,BL               ;Set AX for ADC read            ;
                ADC_READ                    ;Macro to read ADC              ;
```

```
                MOV     DX,ASUMA        ;Recover A Sum A (running) ;
                ADC     DX,AX           ;Add ADC read value to DX  ;
                JNS     EMPTY3          ;Is DX full?               ;
                MOV     BX,ASUMB        ;Yes. Get Axial counter    ;
                INC     BX              ;Add one                   ;
                MOV     ASUMB,BX        ;Save it again             ;
                AND     DX,7FFFH        ;Clear sign overflow       ;
                ADD     DX,0            ;Reset flags               ;
                CLC                     ;Just in case              ;
EMPTY3          MOV     ASUMA,DX        ;Save DX                   ;
                MOV     CX,COUNT        ;Restore CX value          ;
                LOOP    LOOP1           ;Until CX=0                ;
;                                                                  ;
;------------------------------------------------------------------;
;                                                                  ;
;   Note that the main loop is acheived by jumping back in 2 stages ;
;   as the assembler can't cope with such a big gap betwen labels.   ;
;                                                                  ;
;   At this stage we have READS readings for each channel with their ;
;   respective sums in two word form A & B. Next put results on the  ;
;   stack as two words - A's are the sum; B's the increment count.   ;
;                                                                  ;
;------------------------------------------------------------------;
;                                                                  ;
                MOV     DI,HRESA        ;Return results on stack   ;
                MOV     AX,HSUMA
                MOV     SS:(DI),AX
                MOV     DI,HRESB
                MOV     AX,HSUMB
                MOV     SS:(DI),AX
                MOV     DI,ARESA
                MOV     AX,ASUMA
                MOV     SS:(DI),AX
                MOV     DI,ARESB
                MOV     AX,ASUMB
                MOV     SS:(DI),AX
                MOV     SP,BP           ;Replace stack pointer     ;
                RETL    12              ;Return skipping results   ;
;                                                                  ;
;------------------------------------------------------------------;
;                                                                  ;
;               Assembler variable store assignments               ;
;                                                                  ;
;------------------------------------------------------------------;
;                                                                  ;
GAIN            .WORD
HRESA           .WORD
HRESB           .WORD
HSUMA           .WORD
HSUMB           .WORD
ARESA           .WORD
ARESB           .WORD
ASUMA           .WORD
ASUMB           .WORD
COUNT           .WORD
.END
;------------------------------------------------------------------;
```

REFERENCES

Alldredge, L.R. and Hurwitz, L., (1964). Radial dipoles as the sources of the Earth's main magnetic field. *J. Geophys. Res.*, 69, 12, 2631-2640.

Andersen, N., (1974). On the calculation of filter coefficients for maximum entropy spectral analysis. *Geophysics*, 39, 69-72.

As, J.A. and Zijderveldt, J.D.A., (1958). Magnetic cleaning of rocks in palaeomagnetic research. *Geophys. J. Roy. astr. Soc.*, 1, 308-319.

Banerjee, S.K., Lund, S.P. and Levi, S., (1979). Geomagnetic record in Minnesota lake sediments - absence of the Gothenburg and Erieau excursions. *Geology*, 7, 585-591.

Banerjee, S.K., King, J. and Marvin, J., (1981). A rapid method for magnetic granulometry with application to environmental studies. *Geophys. Res. Lett.*, 8, 333-336.

Barbetti, M.F. and McElhinny, M.W., (1972). Evidence of a geomagnetic excursion 30,000 years BP. *Nature*, 278, 153.

Barbetti, M.F. and McElhinny, M.W., (1976). The Lake Mungo geomagnetic excursion. *Phil. Trans. Roy. Soc.*, A281, 515.

Bardeen J., Cooper L.N. and Schrieffer J.R., (1957). Theory of Superconductivity. *Phys. Rev.*, (1175-1204).

Barton, C.B. and McElhinny, M.W., (1979). Detrital remanent magnetisation in five slowly redeposited long cores of sediment. *Geophys. Res. Lett.*, 6, 229.

Barton, C.E. and McElhinny, M.W., (1981). A 10,000yr geomagnetic secular variation record from three Australian maars. *Geophys. J. Roy. astr. Soc.*, 67, 465-485.

Barton, C.E. and McElhinny, M.W., (1982). Time series analysis of the 10,000yr geomagnetic secular variation record from SE Australia. *Geophys. J.Roy. astr. Soc.*, 68, 709-724.

Barton, C.E., (1983a). Analysis of palaeomagnetic time series and applications. *Geophysical Surveys*, 5, 335-368.

Barton, C.E., (1983b). Spectrum Analysis - section 4.9 (pp. 262-266) of *'Geomagnetism of Baked Clays and Recent Sediments'*, eds. K.M. Creer, P. Tucholka and C.E. Barton, Elsevier, Amsterdam.

Bauer, L.A., (1899). Remarks upon Prof. Rucker's paper and Wilde's magnetarium. *Terrestrial Magnetism*, 4, 130-132.

Berryman, J.G., (1978). Choice of operator length for Maximum Entropy Method spectral analysis. *Geophysics*, 43, 1384-1391.

Bonhommet, N. and Babkine, J., (1967). Sur la presence d'aimantations inversees dans la Chaine des Puys. *C. R. Acad. Sci.*, 264, 92-94.

Bonhommet, N. and Zahringer, J., (1969). Palaeomagnetism and Potassium Argon age determinations of the Laschamp geomagnetic polarity event. *Earth Planet. Sci. Lett.*, 6, 43-46.

Bonifay, E. and Truze, E., (1984). *10 R.A.S.T. Bordeaux*, April 1984, p. 72.

Bonifay, E. and Truze, E., (1984). *5 Congres de Sedimentologie, Marseille*, April 1984, p. 527.

Bonifay, E., Creer, K.M., de Beaulieu, J.L., Casta, L., Delibrias, G., Permet, G., Pons, A., Reille, M., Servant, S., Smith, G., Thouveny, N., Truze, E. and Tucholka, P. (1985). A study of the recent sediments of Lac du Bouchet (Haute-Loire), France: First results. In Rampino, M.R., Newman, W.S., Sanders J.E. and Konigsson, L.K. eds., (1985). *Climate: History, Periodicity and Predictability.* Stroudsburg, Penn., Van Nostrand Reinhold, in press.

Bout, P., (1978). *Watel Ed.*, Brioude, Fr.

Bray, T., (1985). A comparison of three possible methods of estimating relative palaeointensities using lake sediments. *Final year project, Univ. Edinburgh.*

Burg, J.P., (1967). Maximum entropy spectral analysis. *37th Ann. Int. Meeting, Soc. Explor. Geophys., Oklahoma City.*

Burg, J.P., (1968). A new analysis for time series data. *Adv. Study Inst. on Signal Processing, NATO, Enschede.*

Carruthers, A., (1984). A seismic analysis of Lac du Bouchet, France. *Final year project. Univ. Edinburgh.*

Clark, H.C. and Kennett, J., (1973). Palaeomagnetic excursion recorded in latest deep-sea sediments, Gulf of Mexico. *Earth Planet. Sci. Lett.*, 19, 267.

Clark, R.M., (1977). Non parametric estimation of a smooth regression function. *J. Roy. Statist. Soc. B.*, 39, 107-113.

Clark, R.M. and Thompson R., (1978). An objective method for smoothing palaeomagnetic data. *Geophys. J. Roy. astr. Soc.*, 52, 205-213.

Clark, R.M. and Thompson R., (1979). A new statistical approach to the alignment of time series. *Geophys. J. Roy. astr. Soc.*, 58, 593-607.

Clark, R.M. and Thompson R., (1984). Statistical comparison of palaeomagnetic directional records from lake sediments. *Geophys. J. Roy. astr. Soc.*, 76, 337-368.

Collinson, D.W., (1983). *Methods in Rock Magnetism and Palaeomagnetism. Techniques and instrumentation.* Chapman and Hall (Pub). 503 pps.

Condomines, M., (1978). Age of Olby-Laschamp geomagnetic polarity event. *Nature*, 269, 49.

Constable, C.G. and McElhinny, M.W., (1985). Holocene geomagnetic secular variation records from north eastern Australian lake sediments. *Geophys. J. Roy. astr. Soc.*, 81, 121-130.

Cooley, J.W. and Tukey, J.W., (1965). An algorithm for the machine calculation of complex Fourier series. *Mathematics of Computation*, 19, 297-301.

Creer, K.M., Thompson, R., Molyneux, L. and Mackereth, F.J.H., (1972) Geomagnetic secular variation recorded in the stable magnetic remanence of recent

sediments. *Earth Planet. Sci. Lett.*, 14, 115-127.

Creer, K.M. (1974), Geomagnetic variations for the interval 7000 - 25000 bp as recorded in a core of sediment from station 1474 of the Black Sea cruise of "Atlantis II". *Earth Planet. Sci. Lett.*, 23, 34-42.

Creer, K.M., Anderson, T.W. and Lewis, C.M.F., (1976a). Late Quaternary geomagnetic stratigraphy recorded in Lake Erie sediments. *Earth Planet. Sci. Lett.*, 31, 37-47.

Creer, K.M., Gross, D.L. and Lineback, J.A., (1976b). Origin of regional geomagnetic variations recorded by Wisconsinan and Holocene sediments from Lake Michigan, U.S.A. and Lake Windermere, England. *Bull. Geol. Soc. Am.*, 87, 531-540.

Creer, K.M., Hogg, T.E., Malkowski, Z., Mojski, J.E., Niedziolka-Krol, E., Readman, P.W. and Tucholka, P., (1979). Palaeomagnetism of Holocene lake sediments from North Poland. *Geophys. J. Roy. astr. Soc.*, 59, 287-314.

Creer, K.M., Hogg, T.E., Readman, P.W. and Reynaud, C., (1980). Palaeomagnetic secular variation curves extending back to 13 400 B.P. recorded in Lac de Joux, Switzerland. *J. Geophys.*, 48, 139-147.

Creer, K.M., Readman, P.W. and Papamarinopolous, S., (1981). Geomagnetic secular variations in Greece through the last 6,000 years obtained from lake sediment studies.. *Geophys. J. Roy. astr. Soc.*, 66, 193-219.

Creer, K.M. and Tucholka, P., (1982). Secular variation as recorded in lake sediments: a discussion of North American and European results. *Phil. Trans. R. Soc. Lond.*, A306, 87-102.

Creer, K.M., (1983). Computer synthesis of geomagnetic palaeosecular variations, *Nature*, 304, 695-699.

Creer, K.M., Valencio, D.A., Sinito, A.M., Tucholka, P and Vilas, J.F.A., (1983). Geomagnetic secular variations 0-14,000 yr BP as recorded by lake sediments from Argentina. *Geophys. J. Roy. astr. Soc.*, 74, 199-221.

Creer, K.M. and Tucholka, P., (1983a). On the current state of lake sediment palaeomagnetic research. *Geophys. J. Roy. astr. Soc.*, 74, 223- 238.

Creer, K.M. and Tucholka, P., (1983b). Epilogue - chapter 5 (pp. 273-305) of *'Geomagnetism of Baked Clays and Recent Sediments'*, eds. K.M. Creer, P. Tucholka and C.E. Barton, Elsevier, Amsterdam.

Creer, K.M., (1985). Review of lake sediment palaeomagnetic data (Part I), *Geophysical Surveys*, 7, 125-160.

Creer, K.M., Smith, G., Tucholka, P., Bonifay, E., Thouveny, N. and Truze, E., (1985). A preliminary palaeomagnetic study of the Holocene and Late Wurmian sediments of Lac du Bouchet (Haute Loire), France. *Earth Planet. Sci. Lett.*, (In press).

Denham, C.R., (1975), Spectral analysis of palaeomagnetic time series. *J. Geophys. Res.*, 80, 1897-1901.

Denham, C.R. and Cox, A., (1971). Evidence that the Laschamp event did not occur 13 300 - 30 400 years ago. *Earth Planet. Sci. Lett.*, 13, 181.

Dodson, R.E., Fuller, M.D. and Kean, W.F., (1977). Palaeomagnetic secular variations from Lake Michigan sediment cores. *Earth Planet. Sci. Lett.*, 34, 387-395.

Dodson, R.E., (1979). Counterclockwise precession of the geomagnetic field vector and westward drift of the non-dipole field. *J. Geophys. Res.*, 85, 2625-2637.

Dunlop, D.J., (1981). The rock magnetism of fine particles. *Phys. Earth Planet. Int.*, 26, 1-26.

Fisher, R.A., (1953). Dispersion on a sphere. *Proc. R. Soc. (London)*, A217, 295-305.

Fougere, P.F., Zawalick, E.J. and Radoski, H.R., (1976). Spontaneous line splitting in maximum entropy power spectrum analysis. *Phys. Earth Planet. Int.*, 2,201-207.

Fowler, A. (1984). PhD Thesis Univ. Oxford.

Freed, W.K. and Healy, N., (1974). Excursions of the Pleistocene geomagnetic field recorded in Gulf of Mexico sediments. *Earth Planet. Sci. Lett.*, 24, 99.

Gauss, C.F., (1839). Allgemeine theorie des erdmagnetismus. Leipzig.

Gillot, P.Y., Labeyrie, J., Laj, C., Valladas, G., Guerin, G., Poupeau, G. and Delibrias, G., (1979). Age of the Laschamp polarity palaeomagnetic excursion revisited. *Earth Planet. Sci. Lett.*, 24, 99.

Goree, W.S. and Fuller, M., (1976). Magnetometers using RF-driven squids and their applications in rock magnetism and palaeomagnetism. *Rev. Geophys. Space Phys.*, 14, 4, 591-608.

Guerin, G., and Valladas, G., (1980). Thermoluminescence dating of volcanic plagioclases. *Nature*, 286, 697.

Guerin, G., Gillot, P.Y., Reyss, J.L. and Valladas, G., (1984). Datation par thermoluminescence et Potassium-Argon de coulees volcaniques recents. Application a la Chaine des Puys. *Earth Planet. Sci. Lett.*, in press.

Hall, C.M. and York, D., (1978). K - Ar and $^{40}Ar/^{39}Ar$ age of the Laschamp geomagnetic polarity reversal. *Nature*, 274, 462.

Hamano, Y., (1980). An experiment on the post-depositional remanent magnetisation in artificial and natural sediments. *Earth Planet. Sci. Lett.*, 51, 221.

Hedges, R.E.M., (1981). Radiocarbon dating with an accelerator: Review and Preview. *Archaeometry*, 23, 3-18.

Hedges, R.E.M., (1983). Radiocarbon dating of sediments. Section 2.3 (pp. 37-44) of 'Geomagnetism of Baked Clays and Recent Sediments, eds. K.M. Creer, P. Tucholka and C.E. Barton, Elsevier, Amsterdam.

Heller, F., (1980). Self reversal of the natural remanent magnetization of the Olby-Laschamp lavas. *Nature*, 284, 334-335.

Heller, F. and Petersen, N., (1982). The Laschamp excursion. *Phil. Trans. Roy. Soc.*, A306, 169-177.

Hurwitz, L., (1960). Eccentric dipoles and Spherical Harmonic Analysis. *J. Geophys. Res.*, 65, 8, 2555-2556.

Huxtable, J., Aitken, M.J. and Bonhommet, N., (1978). Thermoluminescence dating of sediment baked by lava flows of the Chaine des Puys. *Nature*, 275, 207.

Hyodo, M., (1984). Possibility of reconstruction of the past geomagnetic field from homogeneous sediments. *J. Geomag. Geoelectr.*, 36, 45-62.

Ising, G., (1943). On magnetic properties of varved clay. *Ark. Mat. Astron. Fys.*, 29A, 1-37.

Jacobs, J.A., (1984). *Reversals of the Earth's magnetic field.* Adam Hilger Ltd., Bristol.

Johnson, E.A., Murphy, T. and Torreson, O.W., (1948), The prehistory of the earth's magnetic field. *Terr. Magn. Atmos. Elec.*, 53, 349-372.

Johnson, H.P., Lowrie, W. and Kent, D.V., (1974). Stability of anhysteretic remanent magnetisation in fine and coarse magnetite and maghemite particles. *Geophys. J. Roy. astr. Soc.*, 41, 1-10.

Jones, R.H., (1965). A reappraisal of the periodogram in spectral analysis. *Technometrics*, 7, 531-532.

Josephson, B.D., (1962). Possible new effects in superconductive tunnelling, *Phys. Lett.*, 1, 251-253.

Kent, D.V. (1973). Post-depositional remanent magnetisation in deep-sea sediment. *Nature*, 246, 32.

King, J.W., Banerjee, S.K., Marvin, J. and Holschuh, N., (1981). A critical evaluation of a method: the NRM/ARM ratio of lake sediments as an estimate of relative geomagnetic field intensity. *Eos*, 62, 272.

King, J.W., Banerjee, S.K., Marvin, J. and Ozdemir, 0., (1982). A comparison of different magnetic methods of determining relative grain size of magnetite in natural materials: some results from lake sediments. *Earth Planet. Sci. Lett.*, 59, 404-419.

King, J.W., Banerjee, S.K. and Marvin, J., (1983). A new rock magnetic approach to selecting sediments for geomagnetic palaeointensity studies: application to palaeointensity for the last 4000 years. *J. Geophys. Res.*, 88, 5911-5921.

King, R.F., (1955), Remanent magnetism of artificially deposited sediments, *Monthly Notices Roy. Astron. Soc., Geophys. Suppl.*, 7, 115–134.

Kovacheva, M., (1980). Summarised results of the archaeomagnetic investigation of the geomagnetic field variation for the last 8000 years in south-eastern Europe. *Geophys. J. Roy. astr. Soc.*, 61, 57–64.

Konigsberger, J.G., (1938). Natural residual magnetism of eruptive rocks, I. *Terr. Magn. Atmos. Electr.*, 43, 119–127.

Lederer, C.M., Hollander, J.M. and Perlman, I., (1967). *Table of Isotopes, 6th ed.*, John Wiley, New York.

Libby, W.F., (1955). *Radiocarbon dating. 2nd Ed.*, Univ. Chicago Press, Chicago.

Levi, S. and Banerjee, S.K., (1976). On the possibility of obtaining relative palaeointensities from lake sediments. *Earth Planet. Sci. Lett.*, 29, 219–226.

Liddicoat, J.C. and Coe, R.S. (1979). Mono Lake geomagnetic excursion. *J. Geophys. Res.*, 84, 261.

Lovlie, R., (1974). Post-depositional remanent magnetisation in a redeposited deep-sea sediment. *Earth Planet. Sci. Lett.*, 21, 315.

Lowrie, W. and Fuller, M. (1971). On the alternating field demagnetisation characteristics of multidomain thermoremanent magnetisation in magnetite. *J. Geophys. Res.*, 76, 6339–6349.

Lund, S.P. and Banerjee, S.K., (1985). The palaeomagnetic record of late Quaternary secular variation from Anderson Pond, Tennessee. *Earth Planet. Sci. Lett.*, 72, 219–237.

McNish, A.G. and Johnson, E.A., (1938). Magnetisation of unmetamorphosed varves and marine sediments, *Terr. Magn. Atmos. Elec.*, 53, 349–360.

Mackereth, F.J.H., (1958). A portable core sampler for lake deposits. *Limnol. Oceanog.*, 3, 181–191.

Mackereth, F.J.H., (1971). On the variation in the direction of the horizontal component of the magnetisation in lake sediments. *Earth Planet. Sci. Lett.*, 12,

332-338.

Meissner W. and Ochsenfeld R., (1933), Ein neuer effekt bei Eintritt der Supraleitfuhigkeit. *Naturwissenschaften*, 21, 787-788.

Merrill, R.T., (1970). Low-temperature treatments of magnetite and magnetite-bearing rocks. *J. Geophys. Res.*, 75, 3343-3349.

Molyneux, L., (1971). A complete results magnetometer for measuring the remanent magnetisation of rocks. *Geophys. J. Roy. astr. Soc.*, 24, 429-433.

Morner, N.A., Lanser, J.P. and Hospers, J., (1971). Late Weichselian palaeomagnetic reversal. *Nature Phys. Sci.*, 234, 173.

Morner, N.A. and Lanser, J.P., (1974). The Gothenburg magnetic excursion. *Quat. Res.*, 7, 413.

Mothersill, J.S., (1979). The palaeomagnetic records of the late Quaternary sediments of Thunder bay. *Can. J. Earth Sci.*, 16, 1016-1023.

Mothersill, J.S., (1981). Late Quaternary palaeomagnetic record of the Goderich Basin, Lake Huron. *Can. J. Earth Sci.*, 18, 448-456.

Neel, L., (1949). Theorie du trainage magnetique des ferromagnetiques en grains fins avec application aux terres caites. *Ann. Geophys.*, 5, 99-136.

Neel, L., (1955). Some theoretical aspects of rock magnetism. *Adv. Phys.*, 4, 191-243.

Otofuji, Y. and Sasajima, S., (1981). A magnetisation process of sediments: a laboratory experiment on post-depositional magnetisation. *Geophys. J. Roy. astr. Soc.*, 66, 241.

Ozima, M. and Ozima, M., (1964). Acquisition mechanism of TRM - Low temperature characteristics of TRM and magnetisation of some granites. *1964 Ann. Prog. Rep. Rock Magn. Res. Group, Japan*, 21-29.

Papamarinopolous, S. (1978). Limnomagnetic studies on Greek sediments. Thesis. Univ. Edinburgh.

Rees, A.I., (1965), The use of anisotropy of magnetic susceptibility in the estimation of sedimentary fabric. *Sedimentology*, 4, 257-271.

Runcorn, S.K., (1959). On the theory of geomagnetic secular variation. *Ann. de Geophys.*, 15, 87-92.

Schuster, A., (1898). Investigation of hidden periodicities. *Terrestrial Magnetism*, 3, 13-41.

Singleton, R.C., (1968). Algorithm 339. An ALGOL procedure for the fast Fourier transform with arbitrary factors (C6). *Communications of the ACM*, 11, 776-782.

Skiles, D.D., (1970). A method of inferring the direction of drift of the geomagnetic field from palaeomagnetic data. *J. Geomag. Geoelectr.*, 22, 441-461.

Smylie, D.E., Clark, G.K.C. and Ulrych, T.J., (1973). Analysis of irregularities in the Earths rotation. In: *Methods of computational physics*, 13, 391-340. Academic press. New York.

Snape, C. (1971). An example of anhysteretic moments being induced by alternating field demagnetisation apparatus. *Geophys. J. Roy. astr. Soc.*, 23, 361-364.

Stacey, F.D., (1963). The physical theory of rock magnetism. *Adv. Phys.*, 12, 46-133.

Stober, J.C. and Thompson, R., (1979). An investigation into the source of magnetic minerals in some Finnish lake sediments. *Earth Planet. Sci. Lett.*, 45, 464-474.

Swingler, D.N., (1980). Burg's maximum entropy algorithm versus the discrete Fourier transform as a frequency estimator for uncoded real sinsusoids. *J. Geophys. Res.*, 83, 1435-1438.

Thellier, E. and Thellier, O., (1959). Sur l'intensitie du champ magnetique terrestre dans la passe historique et geologique. *Ann. Geophys.*, 15, 285-376.

Thomas, R.C., (1981). Archaeomagnetism of Greek pottery and Cretan kilns. *Phd. Thesis, Univ. Edinburgh.*

Thompson, R. and Kelts, K., (1974). Holocene sediments and magnetic stratigraphy from Lakes Zug and Zurich, Switzerland. *Sedimentology*, 21, 577-596.

Thompson, R. (1982). A comparison of geomagnetic secular variation as recorded by historical, archaeomagnetic and palaeomagnetic measurements. *Phil. Trans. R. Soc. Lond.*, A306, 103-112.

Thouveny, N., (1983). Etude paleomagnetique de formations du Plio- Pleistocene et de l'Holocene du Massif Central et de ses abords. These de Doctorat de 3 eme cycle, Universite d'Aix-Marseille II, Vol.I (texte) and II (Figures).

Truze, E., (1983). Etude preliminaire de la sedimentation dans les lacs de maars du Deves. Le Lac du Bouchet. Memoire de D.E.A. Universite d'Aix - Marseille II.

Truze, E. and Bonifay, E., (1984). *10 R.A.S.T., Bordeaux*, April 1984.

Tucholka, P., (1980). Short-period secular variations (SPSV) of the geomagnetic field recorded in highly scattered palaeomagnetic records of Holocene sediments from North Poland. *Earth Planet. Sci. Lett.*, 48, 379-384.

Tucker, P., (1979). Selective post-depositional realignment in a synthetic sediment. *Phys. Earth Planet. Inter.*, 20, 11-14.

Tucker, P., (1980). A grain mobility model for post-depositional realignment. *Geophys. J. Roy. astr. Soc.*, 63, 149-163.

Turner, G.M. and Thompson, R., (1979). The behaviour of the Earth's magnetic field as recorded in the sediments of Loch Lomond. *Earth Planet. Sci. Lett.*, 42, 412-426.

Turner, G.M. and Thompson, R., (1981). Lake sediment record of the geomagnetic secular variation in Britain during Holocene times. *Geophys. J. Roy. astr. Soc.*, 65, 703-725.

Turner, G.M., Evans, M.E. and Hussin, I.B., (1982). A geomagnetic secular variation study (31,000 - 19,500 bp) in Western Canada. *Geophys. J. Roy. astr. Soc.*, 71, 159-171.

Ulrych, T.J. and Bishop, T.N., (1975). Maximum entropy spectral analysis and autoregressive decomposition. *Rev. Geophys. Space Phys.*, 13, 183-200.

Valladas, G., Gillot, P.Y., Poupeau, G. and Reyss, J.L., (1977). *5th Eur. Conf. Geochronology, Pisa.*

Verosub, K.L., (1977). The absence of the Mono Lake excursion from the palaeomagnetic record of Clear Lake California. *Earth Planet. Sci. Lett.*, 36, 219-230.

Verosub, K.L. and Banerjee, S.K., (1977). Geomagnetic excursions and their palaeomagnetic record. *Revs. Geophys. Space Phys.*, 15, 145-155.

Vitorello, I. and Van der Voo, R., (1977). Magnetic stratigraphy of Lake Michigan sediments obtained from cores of lacustrine clay. *Quaternary Research*, 7, 398-412.

Vivier, P., (1964). Imprimerie ancienne, Le Puy-en-Velay, Fr.

Walton, D. (1979). Geomagnetic intensities in Athens between 2000 BC and 400 AD. *Nature*, 277, 643-644.

Wand, J.O., Gillespie, R. and Hedges, R.E.M., (1984). Sample preparation for accelerator based radiocarbon dating. *J. Archeo. Sci.*, 10, 159-163.

Wintle, A. (1973). Anomalous fading of thermoluminescence in mineral samples. *Nature*, 245, 143.

Wintle, A., (1983). Thermoluminescence - section 2.6 (pp. 63-71) of *'Geomagnetism of Baked Clays and Recent Sediments'*, eds. K.M. Creer, P. Tucholka and C.E. Barton, Elsevier, Amsterdam.

Yaskawa, K., Nakajima, T., Kawai, N., Torii, M., Notsuhara, N. and Horie, S., (1973). Palaeomagnetism from a core from Lake Biwa (I). *J. Geomag. Geoelec.*, 25, 447.

Yukutake, T. and Tachinaka, H., (1968). The non-dipole part of the Earth's magnetic field. *Bull. Earthqu. Res. Inst.*, 46, 1027-1062.

Yule, G.U., (1927). On a method of investigating periodicities in disturbed series, with special reference to Wolfer's sunspot numbers. *Phil. Trans. Roy. Soc. London. Ser.*, A226, 267-298.